

PUBLISHED BY

INTECH

open science | open minds

World's largest Science,
Technology & Medicine
Open Access book publisher




105,000+
INTERNATIONAL
AUTHORS AND EDITORS


111+ MILLION
DOWNLOADS


BOOKS
DELIVERED TO
151 COUNTRIES

AUTHORS AMONG
TOP 1%
MOST CITED SCIENTIST


12.2%
AUTHORS AND EDITORS
FROM TOP 500 UNIVERSITIES



Selection of our books indexed in the
Book Citation Index in Web of Science™
Core Collection (BKCI)

WEB OF SCIENCE™

Chapter from the book *Handbook of Stillinger-Weber Potential Parameters for Two-Dimensional Atomic Crystals*
Downloaded from: <http://www.intechopen.com/books/handbook-of-stillinger-weber-potential-parameters-for-two-dimensional-atomic-crystals>

Interested in publishing with InTechOpen?
Contact us at book.department@intechopen.com

Parameterization of Stillinger-Weber Potential for Two-Dimensional Atomic Crystals

Jin-Wu Jiang and Yu-Ping Zhou

Additional information is available at the end of the chapter

<http://dx.doi.org/10.5772/intechopen.71929>

Abstract

We parametrize the Stillinger-Weber potential for 156 two-dimensional atomic crystals (TDACs). Parameters for the Stillinger-Weber potential are obtained from the valence force field (VFF) model following the analytic approach (*Nanotechnology*. 2015;26:315706), in which the valence force constants are determined by the phonon spectrum. The Stillinger-Weber potential is an efficient nonlinear interaction and is applicable for numerical simulations of nonlinear physical or mechanical processes. The supplemental resources for all simulations in the present work are available online in <http://jiangjinwu.org/sw>, including a Fortran code to generate crystals' structures, files for molecular dynamics simulations using LAMMPS, files for phonon calculations with the Stillinger-Weber potential using GULP, and files for phonon calculations with the valence force field model using GULP.

Keywords: layered crystal, Stillinger-Weber potential, molecular dynamics simulation, empirical potential

PACS: 78.20.Bh, 63.22.-m, 62.25.-g

1. Introduction

The atomic interaction is of essential importance in the numerical investigation of most physical or mechanical processes [1]. The present work provides parameters for the Stillinger-Weber (SW) empirical potential for 156 two-dimensional atomic crystals (TDACs). In practical applications, these layered materials are usually played as Lego on atomic scale to construct the van der Waals heterostructures with comprehensive properties [2]. The computational cost of *ab initio* for the heterostructure will be substantially increased as compared with one individual atomic layer, because the unit cell for the heterostructure is typically very large resulting from the mismatch of the lattice constants of different layered components. The empirical potential will be a competitive alternative to help out this difficult situation, considering their high efficiency.



In the early stage before 1980s, the computation ability of the scientific community was quite limited. At that time, the valence force field (VFF) model was one popular empirical potential for the description of the atomic interaction, since the VFF model is linear and can be applied in the analytic derivation of most elastic quantities [3]. In this model, each VFF term corresponds to a particular motion style in the crystal. Hence, each parameter in the VFF model usually has clear physical essence, which is beneficial for the parameterization of this model. For instance, the bond stretching term in the VFF model is directly related to the frequency of the longitudinal optical phonon modes, so the force constant of the bond stretching term can be determined from the frequencies of the longitudinal optical phonon modes. The VFF model can thus serve as the starting point for developing atomic empirical potentials for different crystals.

While the VFF model is beneficial for the fastest numerical simulation, its strong limitation is the absence of nonlinear effect. Due to this limitation, the VFF model is not applicable to nonlinear phenomena, for which other potential models with nonlinear components are required. Some representative potential models are (in the order of their simulation costs) SW potential [4], Tersoff potential [5], Brenner potential [6], *ab initio* approaches, etc. The SW potential is one of the simplest potential forms with nonlinear effects included. An advanced feature for the SW potential is that it includes the nonlinear effect, and keeps the numerical simulation at a very fast level.

Considering its distinct advantages, the present article aims at providing the SW potential for 156 TDACs. We will determine parameters for the SW potential from the VFF model, following the analytic approach proposed by one of the present authors (JWJ) [7]. The VFF constants are fitted to the phonon spectrum or the elastic properties in the TDACs.

In this paper, we parametrize the SW potential for 156 TDACs. All structures discussed in the present work are listed in **Tables 1–9**. The supplemental materials are freely available online

1H-ScO ₂	1H-ScS ₂	1H-ScSe ₂	1H-ScTe ₂	1H-TiTe ₂	1H-VO ₂	1H-VS ₂	1H-VSe ₂	1H-VTe ₂
1H-CrO ₂	1H-CrS ₂	1H-CrSe ₂	1H-CrTe ₂	1H-MnO ₂	1H-FeO ₂	1H-FeS ₂	1H-FeSe ₂	1H-FeTe ₂
1H-CoTe ₂	1H-NiS ₂	1H-NiSe ₂	1H-NiTe ₂	1H-NbS ₂	1H-NbSe ₂	1H-MoO ₂	1H-MoS ₂	1H-MoSe ₂
1H-MoTe ₂	1H-TaS ₂	1H-TaSe ₂	1H-WO ₂	1H-WS ₂	1H-WSe ₂	1H-WTe ₂		

The structure is shown in **Figure 1**.

Table 1. 1H-MX₂, with M as the transition metal and X as oxygen or dichalcogenide.

1T-ScO ₂	1T-ScS ₂	1T-ScSe ₂	1T-ScTe ₂	1T-TiS ₂	1T-TiSe ₂	1T-TiTe ₂	1T-VS ₂	1T-VSe ₂
1T-VTe ₂	1T-MnO ₂	1T-MnS ₂	1T-MnSe ₂	1T-MnTe ₂	1T-CoTe ₂	1T-NiO ₂	1T-NiS ₂	1T-NiSe ₂
1T-NiTe ₂	1T-ZrS ₂	1T-ZrSe ₂	1T-ZrTe ₂	1T-NbS ₂	1T-NbSe ₂	1T-NbTe ₂	1T-MoS ₂	1T-MoSe ₂
1T-MoTe ₂	1T-TcS ₂	1T-TcSe ₂	1T-TcTe ₂	1T-RhTe ₂	1T-PdS ₂	1T-PdSe ₂	1T-PdTe ₂	1T-SnS ₂
1T-SnSe ₂	1T-HfS ₂	1T-HfSe ₂	1T-HfTe ₂	1T-TaS ₂	1T-TaSe ₂	1T-TaTe ₂	1T-WS ₂	1T-WSe ₂
1T-WTe ₂	1T-ReS ₂	1T-ReSe ₂	1T-ReTe ₂	1T-IrTe ₂	1T-PtS ₂	1T-PtSe ₂	1T-PtTe ₂	

The structure is shown in **Figure 71**.

Table 2. 1T-MX₂, with M as the transition metal and X as oxygen or dichalcogenide.

Black phosphorus	p-Arsenene	p-Antimonene	p-Bismuthene
------------------	------------	--------------	--------------

The structure is shown in **Figures 178 or 183**.

Table 3. Puckered (p-) M, with M from group V.

	p-SiO	p-GeO	p-SnO
p-CS	p-SiS	p-GeS	p-SnS
p-CSe	p-SiSe	p-GeSe	p-SnSe
p-CTe	p-SiTe	p-GeTe	p-SnTe

The structure is shown in **Figure 189**, and particularly **Figure 191** for p-MX with X = O.

Table 4. Puckered MX, with M from group IV and X from group VI.

Silicene	Germanene	Stanene	Indiene
Blue phosphorus	b-Arsenene	b-Antimonene	b-Bismuthene

The structure is shown in **Figure 222**.

Table 5. Buckled (b-) M, with M from group IV or V.

b-CO	b-SiO	b-GeO	b-SnO
b-CS	b-SiS	b-GeS	b-SnS
b-CSe	b-SiSe	b-GeSe	b-SnSe
b-CTe	b-SiTe	b-GeTe	b-SnTe

The structure is shown in **Figure 239**.

Table 6. Buckled MX, with M from group IV and X from group VI.

b-SnGe	b-SiGe	b-SnSi	b-InP	b-InAs	b-InSb	b-GaAs	b-GaP	b-AlSb
--------	--------	--------	-------	--------	--------	--------	-------	--------

The structure is shown in **Figure 239**.

Table 7. Buckled MX, with both M and X from group IV or M from group III and X from group V.

BO	AlO	GaO	InO
BS	AlS	GaS	InS
BSe	AlSe	GaSe	InSe
BTe	AlTe	GaTe	InTe

The structure is shown in **Figure 290**.

Table 8. Bi-buckled MX, with M from group III and X from group VI.

Borophene

Table 9. The structure is shown in [Figure 323](#).

in [1], including a Fortran code to generate crystals' structures, files for molecular dynamics simulations using LAMMPS, files for phonon calculations with the SW potential using GULP, and files for phonon calculations with the valence force field model using GULP.

2. VFF model and SW potential

2.1. VFF model

The VFF model is one of the most widely used linear models for the description of atomic interactions [3]. The bond stretching and the angle bending are two typical motion styles for most covalent bonding materials. The bond stretching describes the energy variation for a bond due to a bond variation $\Delta r = r - r_0$, with r_0 as the initial bond length. The angle bending gives the energy increment for an angle resulting from an angle variation $\Delta\theta = \theta - \theta_0$, with θ_0 as the initial angle. In the VFF model, the energy variations for the bond stretching and the angle bending are described by the following quadratic forms,

$$V_r = \frac{1}{2}K_r(\Delta r)^2, \quad (1)$$

$$V_\theta = \frac{1}{2}K_\theta(\Delta\theta)^2, \quad (2)$$

where K_r and K_θ are two force constant parameters. These two potential expressions in Eqs. (1) and (2) are directly related to the optical phonon modes in the crystal. Hence, their force constant parameters K_r and K_θ are usually determined by fitting to the phonon dispersion.

2.2. SW potential

In the SW potential, energy increments for the bond stretching and angle bending are described by the following two-body and three-body forms,

$$V_2(r_{ij}) = A(B/r_{ij} - 1)e^{[\rho/(r_{ij}-r_{max})]}, \quad (3)$$

$$V_3(\theta_{ijk}) = Ke^{[\rho_1/(r_{ij}-r_{max12})+\rho_2/(r_{ik}-r_{max13})]} \\ (\cos\theta_{ijk} - \cos\theta_0)^2 \quad (4)$$

where V_2 corresponds to the bond stretching and V_3 associates with the angle bending. The cut-offs r_{max} , r_{max12} , and r_{max13} are geometrically determined by the material's structure. There are five unknown geometrical parameters, i.e., ρ and B in the two-body V_2 term and ρ_1 , ρ_2 , and θ_0 in the three-body V_3 term, and two energy parameters A and K . There is a constraint among these parameters due to the equilibrium condition [7],

$$\rho = \frac{-4B(d - r_{max})^2}{(Bd - d^5)}, \quad (5)$$

where d is the equilibrium bond length from experiments. Eq. (5) ensures that the bond has an equilibrium length d and the V_2 interaction for this bond is at the energy minimum state at the equilibrium configuration.

The energy parameters A and K in the SW potential can be analytically derived from the VFF model as follows,

$$A = \frac{K_r}{\alpha e^{[\rho/(d-r_{max})]}}, \quad (6)$$

$$K = \frac{K_\theta}{2 \sin^2 \theta_0 e^{[\rho_1/(d_1-r_{max12}) + \rho_2/(d_2-r_{max13})]}}, \quad (7)$$

where the coefficient α in Eq. (6) is,

$$\begin{aligned} \alpha &= \left[\frac{\rho}{(d - r_{max})^2} \right]^2 (B/d^4 - 1) \\ &+ \left[\frac{2\rho}{(d - r_{max})^3} \right] (B/d^4 - 1) \\ &+ \left[\frac{\rho}{(d - r_{max})^2} \right] \left(\frac{8B}{d^5} \right) + \left(\frac{20B}{d^6} \right). \end{aligned} \quad (8)$$

In some situations, the SW potential is also written into the following form,

$$V_2(r_{ij}) = \epsilon A_L (B_L \sigma^p r_{ij}^{-p} - \sigma^q r_{ij}^{-q}) e^{[\sigma/(r_{ij}-a\sigma)]}, \quad (9)$$

$$\begin{aligned} V_3(\theta_{ijk}) &= \epsilon \lambda e^{[\gamma\sigma/(r_{ij}-a\sigma) + \gamma\sigma/(r_{jk}-a\sigma)]} \\ &(\cos\theta_{ijk} - \cos\theta_0)^2. \end{aligned} \quad (10)$$

The parameters here can be determined by comparing the SW potential forms in Eqs. (9) and (10) with Eqs. (3) and (4). It is obvious that $p = 4$ and $q = 0$. Eqs. (9) and (10) have two more parameters than Eqs. (3) and (4), so we can set $\epsilon = 1.0$ eV and $\gamma = 1.0$. The other parameters in Eqs. (9) and (10) are related to these parameters in Eqs. (3) and (4) by the following equations

$$A_L = A, \quad (11)$$

$$\sigma = \rho, \quad (12)$$

$$B_L = B/\rho^4, \quad (13)$$

$$a = r_{max}/\rho, \quad (14)$$

$$\lambda = K. \quad (15)$$

The SW potential is implemented in GULP using Eqs. (3) and (4). The SW potential is implemented in LAMMPS using Eqs. (9) and (10).

In the rest of this article, we will develop the VFF model and the SW potential for layered crystals. The VFF model will be developed by fitting to the phonon dispersion from experiments or first-principles calculations. The SW potential will be developed following the above analytic parameterization approach. In this work, GULP [8] is used for the calculation of phonon dispersion and the fitting process, while LAMMPS [9] is used for molecular dynamics simulations. The OVITO [10] and XCRYSDEN [11] packages are used for visualization. All simulation scripts for GULP and LAMMPS are available online in [1].

3. 1H- ScO_2

Most existing theoretical studies on the single-layer 1H- ScO_2 are based on the first-principles calculations. In this section, we will develop the SW potential for the single-layer 1H- ScO_2 .

The structure for the single-layer 1H- ScO_2 is shown in **Figure 1** (with M = Sc and X = O). Each Sc atom is surrounded by six O atoms. These O atoms are categorized into the top group (e.g.,

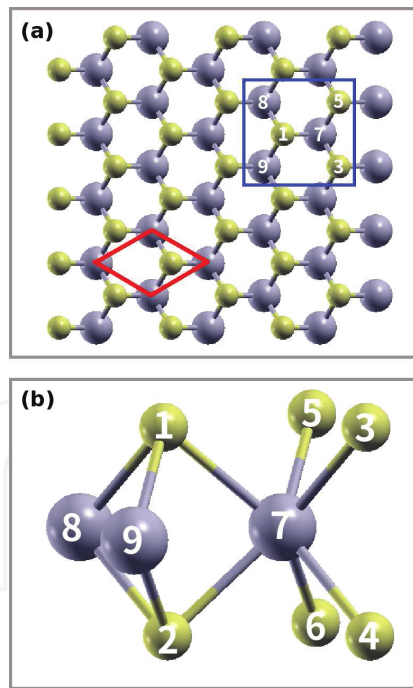


Figure 1. Configuration of the 1H-MX₂ in the 1H phase. (a) Top view. The unit cell is highlighted by a red parallelogram. (b) Enlarged view of atoms in the blue box in (a). Each M atom is surrounded by six X atoms, which are categorized into the top and bottom groups. Atoms X 1, 3, and 5 are from the top group, while atoms X 2, 4, and 6 are from the bottom group. M atoms are represented by larger gray balls. X atoms are represented by smaller yellow balls.

atoms 1, 3, and 5) and bottom group (e.g., atoms 2, 4, and 6). Each O atom is connected to three Sc atoms. The structural parameters are from the first-principles calculations [12], including the lattice constant $a = 3.16 \text{ \AA}$ and the bond length $d_{\text{Sc}-\text{O}} = 2.09 \text{ \AA}$. The resultant angles are $\theta_{\text{ScOO}} = \theta_{\text{OSeSc}} = 98.222^\circ$ and $\theta_{\text{ScOO}'} = 58.398^\circ$, in which atoms O and O' are from different (top or bottom) groups.

Table 10 shows four VFF terms for the single-layer 1H-ScO₂; one of which is the bond stretching interaction shown by Eq. (1), while the other three terms are the angle bending interaction shown by Eq. (2). These force constant parameters are determined by fitting to the acoustic branches in the phonon dispersion along ΓM as shown in **Figure 2(a)**. The *ab initio* calculations for the phonon dispersion are from [12]. **Figure 2(b)** shows that the VFF model and the SW potential give exactly the same phonon dispersion, as the SW potential is derived from the VFF model.

The parameters for the two-body SW potential used by GULP are shown in **Table 11**. The parameters for the three-body SW potential used by GULP are shown in **Table 12**. Some representative parameters for the SW potential used by LAMMPS are listed in **Table 13**. We note that 12 atom types have been introduced for the simulation of the single-layer 1H-ScO₂ using LAMMPS, because the angles around atom Sc in **Figure 1** (with M = Sc and X = O) are not distinguishable in LAMMPS. We have suggested two options to differentiate these angles by implementing some additional constraints in LAMMPS, which can be accomplished by modifying the source file of LAMMPS [13, 14]. According to our experience, it is not so convenient for some users to implement these constraints and recompile the LAMMPS package. Hence, in the present work, we differentiate the angles by introducing more atom types, so it is not necessary to modify the LAMMPS package. **Figure 3** (with M = Sc and X = O) shows that, for 1H-ScO₂, we can differentiate these angles around the Sc atom by assigning these six neighboring O atoms with different atom types. It can be found that twelve atom types are necessary for the purpose of differentiating all six neighbors around one Sc atom.

We use LAMMPS to perform MD simulations for the mechanical behavior of the single-layer 1H-ScO₂ under uniaxial tension at 1 and 300 K. **Figure 4** shows the stress-strain curve for the tension of a single-layer 1H-ScO₂ of dimension $100 \times 100 \text{ \AA}$. Periodic boundary conditions are applied in both armchair and zigzag directions. The single-layer 1H-ScO₂ is stretched uniaxially along the armchair or zigzag direction. The stress is calculated without involving the actual thickness of the quasi-two-dimensional structure of the single-layer 1H-ScO₂. The

VFF type	Bond stretching	Angle bending		
Expression	$\frac{1}{2}K_{\text{Sc}-\text{O}}(\Delta r)^2$	$\frac{1}{2}K_{\text{Sc}-\text{O}-\text{O}}(\Delta\theta)^2$	$\frac{1}{2}K_{\text{Sc}-\text{O}'-\text{O}'}(\Delta\theta)^2$	$\frac{1}{2}K_{\text{O}-\text{Sc}-\text{Sc}}(\Delta\theta)^2$
Parameter	9.417	4.825	4.825	4.825
r_0 or θ_0	2.090	98.222	58.398	98.222

The second line gives an explicit expression for each VFF term. The third line is the force constant parameters. Parameters are in the unit of $\text{ev}/\text{\AA}^2$ for the bond stretching interaction and in the unit of eV for the angle bending interaction. The fourth line gives the initial bond length (in the unit of \AA) for the bond stretching interaction and the initial angle (in the unit of degrees) for the angle bending interaction. The angle θ_{ijk} has atom i as the apex.

Table 10. The VFF model for single-layer 1H-ScO₂.

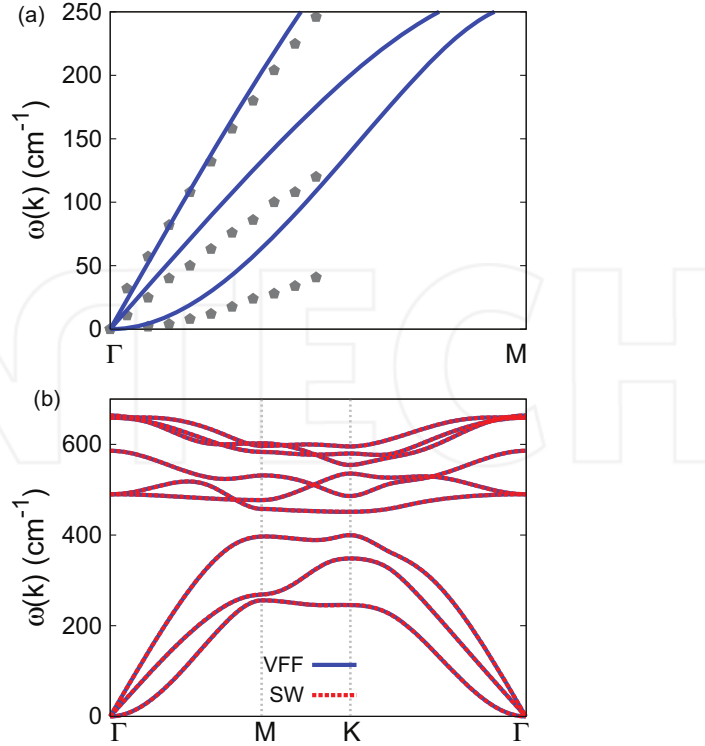


Figure 2. Phonon spectrum for single-layer 1H-ScO₂. (a) Phonon dispersion along the direction Γ M in the Brillouin zone. The results from the VFF model (lines) are comparable with the *ab initio* results (pentagons) from [12]. (b) The phonon dispersion from the SW potential is exactly the same as that from the VFF model.

	A (eV)	ρ (Å)	B (Å ⁴)	r_{\min} (Å)	r_{\max} (Å)
Sc-O	7.506	1.380	9.540	0.0	2.939

Table 11. Two-body SW potential parameters for single-layer 1H-ScO₂ used by GULP [8] as expressed in Eq. (3).

	K (eV)	θ_0 (°)	ρ_1 (Å)	ρ_2 (Å)	$r_{\min 12}$ (Å)	$r_{\max 12}$ (Å)	$r_{\min 13}$ (Å)	$r_{\max 13}$ (Å)	$r_{\min 23}$ (Å)	$r_{\max 23}$ (Å)
$\theta_{\text{Sc}-\text{O}-\text{O}}$	63.576	98.222	1.380	1.380	0.0	2.939	0.0	2.939	0.0	3.460
$\theta_{\text{Sc}-\text{O}-\text{O}'}$	85.850	58.398	1.380	1.380	0.0	2.939	0.0	2.939	0.0	3.460
$\theta_{\text{O}-\text{Sc}-\text{Sc}}$	63.576	98.222	1.380	1.380	0.0	2.939	0.0	2.939	0.0	3.460

The angle θ_{ijk} in the first line indicates the bending energy for the angle with atom i as the apex.

Table 12. Three-body SW potential parameters for single-layer 1H-ScO₂ used by GULP [8] as expressed in Eq. (4).

	ϵ (eV)	σ (Å)	a	λ	γ	$\cos \theta_0$	A_L	B_L	p	q	Tol
Sc ₁ —O ₁ —O ₁	1.000	1.380	2.129	0.000	1.000	0.000	7.506	2.627	4	0	0.0
Sc ₁ —O ₁ —O ₃	1.000	0.000	0.000	63.576	1.000	-0.143	0.000	0.000	4	0	0.0
Sc ₁ —O ₁ —O ₂	1.000	0.000	0.000	85.850	1.000	0.524	0.000	0.000	4	0	0.0
O ₁ —Sc ₁ —Sc ₃	1.000	0.000	0.000	63.576	1.000	-0.143	0.000	0.000	4	0	0.0

Table 13. SW potential parameters for single-layer 1H-ScO₂ used by LAMMPS [9] as expressed in Eqs. (9) and (10).

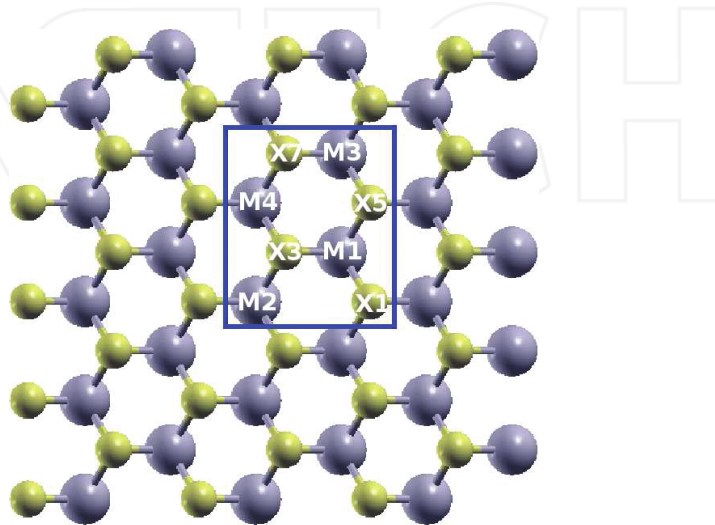


Figure 3. Twelve atom types are introduced to distinguish angles around each M atom for the single-layer 1H-MX₂. Atoms X₁, X₃, X₅, and X₇ are from the top layer. The other four atoms X₂, X₄, X₆, and X₈ are from the bottom layer, which are not displayed in the figure.

Young's modulus can be obtained by a linear fitting of the stress-strain relation in the small strain range of [0, 0.01]. The Young's modulus is 126.3 and 125.4 N/m along the armchair and zigzag directions, respectively. The Young's modulus is essentially isotropic in the armchair and zigzag directions. The Poisson's ratio from the VFF model and the SW potential is $\nu_{xy} = \nu_{yx} = 0.16$.

There is no available value for nonlinear quantities in the single-layer 1H-ScO₂. We have thus used the nonlinear parameter $B = 0.5d^4$ in Eq. (5), which is close to the value of B in most materials. The value of the third-order nonlinear elasticity D can be extracted by fitting the stress-strain relation to the function $\sigma = E\epsilon + \frac{1}{2}D\epsilon^2$ with E as the Young's modulus. The values of D from the present SW potential are -652.8 and -683.3 N/m along the armchair and zigzag directions, respectively. The ultimate stress is about 12.2 N/m at the ultimate strain of 0.19 in the armchair direction at the low temperature of 1 K. The ultimate stress is about 11.7 N/m at the ultimate strain of 0.23 in the zigzag direction at the low temperature of 1 K.

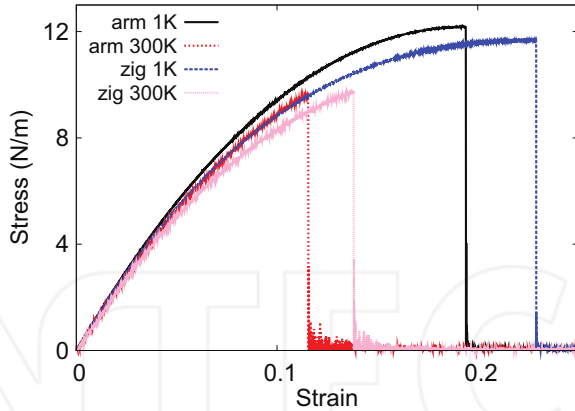


Figure 4. Stress-strain for single-layer 1H-ScO₂ of dimension 100 × 100 Å along the armchair and zigzag directions.

4. 1H-SCS₂

Most existing theoretical studies on the single-layer 1H-ScS₂ are based on the first-principles calculations. In this section, we will develop the SW potential for the single-layer 1H-ScS₂.

The structure for the single-layer 1H-ScS₂ is shown in **Figure 1** (with M = Sc and X = S). Each Sc atom is surrounded by six S atoms. These S atoms are categorized into the top group (e.g., atoms 1, 3, and 5) and bottom group (e.g., atoms 2, 4, and 6). Each S atom is connected to three Sc atoms. The structural parameters are from the first-principles calculations [12], including the lattice constant $a = 3.70$ Å and the bond length $d_{\text{Sc-S}} = 2.52$ Å. The resultant angles are $\theta_{\text{ScSS}} = \theta_{\text{SScS}} = 94.467^\circ$ and $\theta_{\text{ScSS'}} = 64.076^\circ$, in which atoms S and S' are from different (top or bottom) groups.

Table 14 shows four VFF terms for the single-layer 1H-ScS₂; one of which is the bond stretching interaction shown by Eq. (1), while the other three terms are the angle bending interaction shown by Eq. (2). These force constant parameters are determined by fitting to the acoustic branches in the phonon dispersion along the ΓM as shown in **Figure 5(a)**. The *ab initio* calculations for the phonon dispersion are from [12]. **Figure 5(b)** shows that the VFF model

VFF type	Bond stretching	Angle bending	
Expression	$\frac{1}{2} K_{\text{Sc-S}}(\Delta r)^2$	$\frac{1}{2} K_{\text{Sc-S-S}}(\Delta\theta)^2$	$\frac{1}{2} K_{\text{Sc-S-S'}}(\Delta\theta)^2$
Parameter	5.192	2.027	2.027
r_0 or θ_0	2.520	94.467	64.076

The second line gives an explicit expression for each VFF term. The third line is the force constant parameters. Parameters are in the unit of eV/Å² for the bond stretching interaction and in the unit of eV for the angle bending interaction. The fourth line gives the initial bond length (in the unit of Å) for the bond stretching interaction and the initial angle (in the unit of degrees) for the angle bending interaction. The angle θ_{ijk} has atom i as the apex.

Table 14. The VFF model for single-layer 1H-ScS₂.

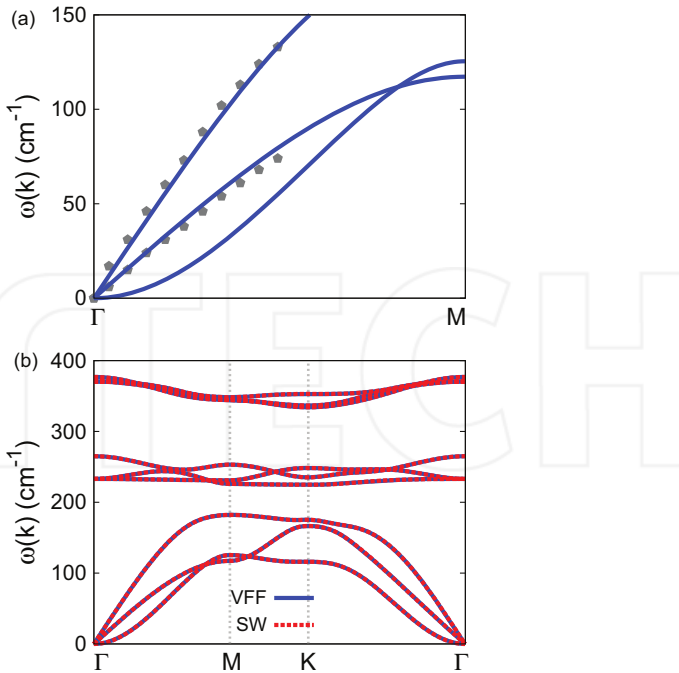


Figure 5. Phonon spectrum for single-layer 1H-ScS₂. (a) Phonon dispersion along the GM direction in the Brillouin zone. The results from the VFF model (lines) are comparable with the *ab initio* results (pentagons) from [12]. (b) The phonon dispersion from the SW potential is exactly the same as that from the VFF model.

and the SW potential give exactly the same phonon dispersion, as the SW potential is derived from the VFF model.

The parameters for the two-body SW potential used by GULP are shown in **Table 15**. The parameters for the three-body SW potential used by GULP are shown in **Table 16**. Some representative parameters for the SW potential used by LAMMPS are listed in **Table 17**. We note that 12 atom types have been introduced for the simulation of the single-layer 1H-ScS₂ using LAMMPS, because the angles around atom Sc in **Figure 1** (with M = Sc and X = S) are not distinguishable in LAMMPS. We have suggested two options to differentiate these angles by implementing some additional constraints in LAMMPS, which can be accomplished by modifying the source file of LAMMPS [13, 14]. According to our experience, it is not so convenient for some users to implement these constraints and recompile the LAMMPS package. Hence, in the present work, we differentiate the angles by introducing more atom types, so it is not necessary to modify the LAMMPS package. **Figure 2** (with M = Sc and X = S) shows that, for

	A (eV)	ρ (Å)	B (Å ⁴)	r_{min} (Å)	r_{max} (Å)
Sc—S	5.505	1.519	20.164	0.0	3.498

Table 15. Two-body SW potential parameters for single-layer 1H-ScS₂ used by GULP [8] as expressed in Eq. (3).

	K (eV)	θ_0 ($^\circ$)	ρ_1 (\AA)	ρ_2 (\AA)	$r_{\min\ 12}$ (\AA)	$r_{\max\ 12}$ (\AA)	$r_{\min\ 13}$ (\AA)	$r_{\max\ 13}$ (\AA)	$r_{\min\ 23}$ (\AA)	$r_{\max\ 23}$ (\AA)
$\theta_{\text{Sc}-\text{S}-\text{S}}$	22.768	94.467	1.519	1.519	0.0	3.498	0.0	3.498	0.0	4.132
$\theta_{\text{Sc}-\text{S}-\text{S}'}$	27.977	64.076	1.519	1.519	0.0	3.498	0.0	3.498	0.0	4.132
$\theta_{\text{S}-\text{Sc}-\text{Sc}}$	22.768	94.467	1.519	1.519	0.0	3.498	0.0	3.498	0.0	4.132

The angle θ_{ijk} in the first line indicates the bending energy for the angle with atom i as the apex.

Table 16. Three-body SW potential parameters for single-layer 1H-ScS₂ used by GULP [8] as expressed in Eq. (4).

	ϵ (eV)	σ (\AA)	a	λ	γ	$\cos \theta_0$	A_L	B_L	p	q	Tol
Sc ₁ -S ₁ -S ₁	1.000	1.519	2.303	0.000	1.000	0.000	5.505	3.784	4	0	0.0
Sc ₁ -S ₁ -S ₃	1.000	0.000	0.000	22.768	1.000	-0.078	0.000	0.000	4	0	0.0
Sc ₁ -S ₁ -S ₂	1.000	0.000	0.000	27.977	1.000	0.437	0.000	0.000	4	0	0.0
S ₁ -Sc ₁ -Sc ₃	1.000	0.000	0.000	22.768	1.000	-0.078	0.000	0.000	4	0	0.0

Table 17. SW potential parameters for single-layer 1H-ScS₂ used by LAMMPS [9] as expressed in Eqs. (9) and (10).

1H-ScS₂, we can differentiate these angles around the Sc atom by assigning these six neighboring S atoms with different atom types. It can be found that twelve atom types are necessary for the purpose of differentiating all six neighbors around one Sc atom.

We use LAMMPS to perform MD simulations for the mechanical behavior of the single-layer 1H-ScS₂ under uniaxial tension at 1 and 300 K. **Figure 6** shows the stress-strain curve for the tension of a single-layer 1H-ScS₂ of dimension 100 × 100 Å. Periodic boundary conditions are applied in both armchair and zigzag directions. The single-layer 1H-ScS₂ is stretched uniaxially along the armchair or zigzag direction. The stress is calculated without involving the actual thickness of the quasi-two-dimensional structure of the single-layer 1H-ScS₂. The Young's modulus can be obtained by a linear fitting of the stress-strain relation in the small strain range of [0, 0.01]. The

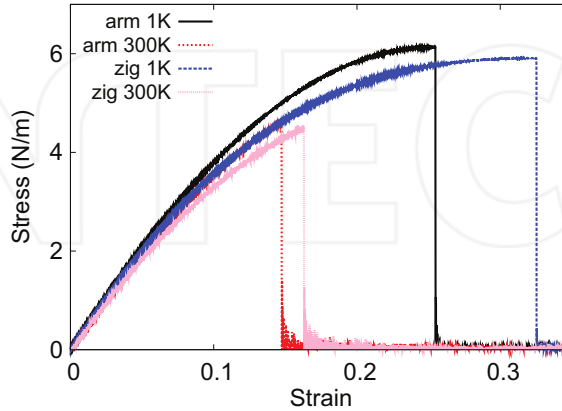


Figure 6. Stress-strain for single-layer 1H-ScS₂ of dimension 100 × 100 Å along the armchair and zigzag directions.

Young's modulus is 43.8 and 43.2 N/m along the armchair and zigzag directions, respectively. The Young's modulus is essentially isotropic in the armchair and zigzag directions. The Poisson's ratio from the VFF model and the SW potential is $\nu_{xy} = \nu_{yx} = 0.30$.

There is no available value for nonlinear quantities in the single-layer 1H-ScS₂. We have thus used the nonlinear parameter $B = 0.5d^4$ in Eq. (5), which is close to the value of B in most materials. The value of the third-order nonlinear elasticity D can be extracted by fitting the stress-strain relation to the function $\sigma = E\epsilon + \frac{1}{2}D\epsilon^2$ with E as the Young's modulus. The values of D from the present SW potential are -146.9 and -159.1 N/m along the armchair and zigzag directions, respectively. The ultimate stress is about 6.1 N/m at the ultimate strain of 0.25 in the armchair direction at the low temperature of 1 K. The ultimate stress is about 5.9 N/m at the ultimate strain of 0.32 in the zigzag direction at the low temperature of 1 K.

5. 1H-SCSe₂

Most existing theoretical studies on the single-layer 1H-ScSe₂ are based on the first-principles calculations. In this section, we will develop the SW potential for the single-layer 1H-ScSe₂.

The structure for the single-layer 1H-ScSe₂ is shown in **Figure 1** (with M = Sc and X = Se). Each Sc atom is surrounded by six Se atoms. These Se atoms are categorized into the top group (e.g., atoms 1, 3, and 5) and bottom group (e.g., atoms 2, 4, and 6). Each Se atom is connected to three Sc atoms. The structural parameters are from the first-principles calculations [12], including the lattice constant $a = 3.38$ Å and the bond length $d_{Sc-Se} = 2.65$ Å. The resultant angles are $\theta_{ScSeSe} = \theta_{SeScSe} = 92.859^\circ$ and $\theta_{ScSeSe'} = 66.432^\circ$, in which atoms Se and Se' are from different (top or bottom) groups.

Table 18 shows four VFF terms for the single-layer 1H-ScSe₂; one of which is the bond stretching interaction shown by Eq. (1), while the other three terms are the angle bending interaction shown by Eq. (2). These force constant parameters are determined by fitting to the acoustic branches in the phonon dispersion along the Γ M as shown in **Figure 7(a)**. The *ab initio* calculations for the phonon dispersion are from [12]. **Figure 7(b)** shows that the VFF model and the SW potential give exactly the same phonon dispersion, as the SW potential is derived from the VFF model.

VFF type	Bond stretching	Angle bending		
Expression	$\frac{1}{2}K_{Sc-Se}(\Delta r)^2$	$\frac{1}{2}K_{Sc-Se-Se}(\Delta\theta)^2$	$\frac{1}{2}K_{Sc-Se-Se'}(\Delta\theta)^2$	$\frac{1}{2}K_{Se-Sc-Sc}(\Delta\theta)^2$
Parameter	5.192	2.027	2.027	2.027
r_0 or θ_0	2.650	92.859	66.432	92.859

The second line gives an explicit expression for each VFF term. The third line is the force constant parameters. Parameters are in the unit of eV/Å² for the bond stretching interaction and in the unit of eV for the angle bending interaction. The fourth line gives the initial bond length (in the unit of Å) for the bond stretching interaction and the initial angle (in the unit of degrees) for the angle bending interaction. The angle θ_{ijk} has atom i as the apex.

Table 18. The VFF model for single-layer 1H-ScSe₂.

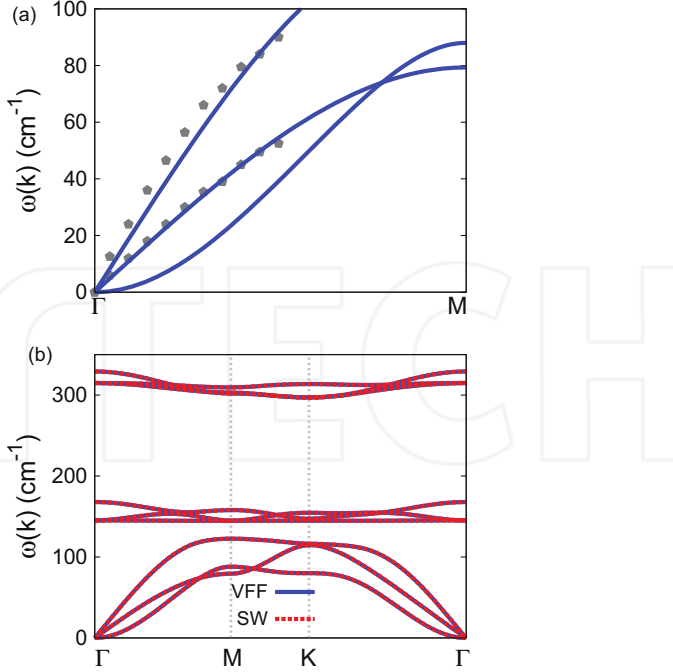


Figure 7. Phonon spectrum for single-layer 1H-ScSe₂. (a) Phonon dispersion along the Γ M direction in the Brillouin zone. The results from the VFF model (lines) are comparable with the *ab initio* results (pentagons) from [12]. (b) The phonon dispersion from the SW potential is exactly the same as that from the VFF model.

The parameters for the two-body SW potential used by GULP are shown in **Table 19**. The parameters for the three-body SW potential used by GULP are shown in **Table 20**. Some representative parameters for the SW potential used by LAMMPS are listed in **Table 21**. We note that 12 atom types have been introduced for the simulation of the single-layer 1H-ScSe₂

	A (eV)	ρ (Å)	B (Å ⁴)	r_{\min} (Å)	r_{\max} (Å)
Sc-Se	5.853	1.533	24.658	0.0	3.658

Table 19. Two-body SW potential parameters for single-layer 1H-ScSe₂ used by GULP [8] as expressed in Eq. (3).

	K (eV)	θ_0 (°)	ρ_1 (Å)	ρ_2 (Å)	$r_{\min 12}$ (Å)	$r_{\max 12}$ (Å)	$r_{\min 13}$ (Å)	$r_{\max 13}$ (Å)	$r_{\min 23}$ (Å)	$r_{\max 23}$ (Å)
$\theta_{\text{Sc}-\text{Se}-\text{Se}}$	21.292	92.859	1.533	1.533	0.0	3.658	0.0	3.658	0.0	4.327
$\theta_{\text{Sc}-\text{Se}-\text{Se}'}$	25.280	66.432	1.533	1.533	0.0	3.658	0.0	3.658	0.0	4.327
$\theta_{\text{Se}-\text{Sc}-\text{Sc}}$	21.292	92.859	1.533	1.533	0.0	3.658	0.0	3.658	0.0	4.327

The angle θ_{ijk} in the first line indicates the bending energy for the angle with atom i as the apex.

Table 20. Three-body SW potential parameters for single-layer 1H-ScSe₂ used by GULP [8] as expressed in Eq. (4).

using LAMMPS, because the angles around atom Sc in **Figure 1** (with M = Sc and X = Se) are not distinguishable in LAMMPS. We have suggested two options to differentiate these angles by implementing some additional constraints in LAMMPS, which can be accomplished by modifying the source file of LAMMPS [13, 14]. According to our experience, it is not so convenient for some users to implement these constraints and recompile the LAMMPS package. Hence, in the present work, we differentiate the angles by introducing more atom types, so it is not necessary to modify the LAMMPS package. **Figure 2** (with M = Sc and X = Se) shows that, for 1H-ScSe₂, we can differentiate these angles around the Sc atom by assigning these six neighboring Se atoms with different atom types. It can be found that twelve atom types are necessary for the purpose of differentiating all six neighbors around one Sc atom.

We use LAMMPS to perform MD simulations for the mechanical behavior of the single-layer 1H-ScSe₂ under uniaxial tension at 1 and 300 K. **Figure 8** shows the stress-strain curve for the tension of a single-layer 1H-ScSe₂ of dimension 100 × 100 Å. Periodic boundary conditions are applied in both armchair and zigzag directions. The single-layer 1H-ScSe₂ is stretched uniaxially along the armchair or zigzag direction. The stress is calculated without involving the actual thickness of the quasi-two-dimensional structure of the single-layer 1H-ScSe₂. The Young's modulus can be obtained by a linear fitting of the stress-strain relation in the small strain range of [0, 0.01]. The Young's modulus is 39.4 and 39.9 N/m along the armchair and zigzag directions, respectively.

	ϵ (eV)	σ (Å)	a	λ	γ	$\cos \theta_0$	A_L	B_L	p	q	Tol
Sc ₁ —Se ₁ —Se ₁	1.000	1.533	2.386	0.000	1.000	0.000	5.853	4.464	4	0	0.0
Sc ₁ —Se ₁ —Se ₃	1.000	0.000	0.000	21.292	1.000	-0.050	0.000	0.000	4	0	0.0
Sc ₁ —Se ₁ —Se ₂	1.000	0.000	0.000	25.280	1.000	0.400	0.000	0.000	4	0	0.0
Se ₁ —Sc ₁ —Sc ₃	1.000	0.000	0.000	21.292	1.000	-0.050	0.000	0.000	4	0	0.0

Table 21. SW potential parameters for single-layer 1H-ScSe₂ used by LAMMPS [9] as expressed in Eqs. (9) and (10).

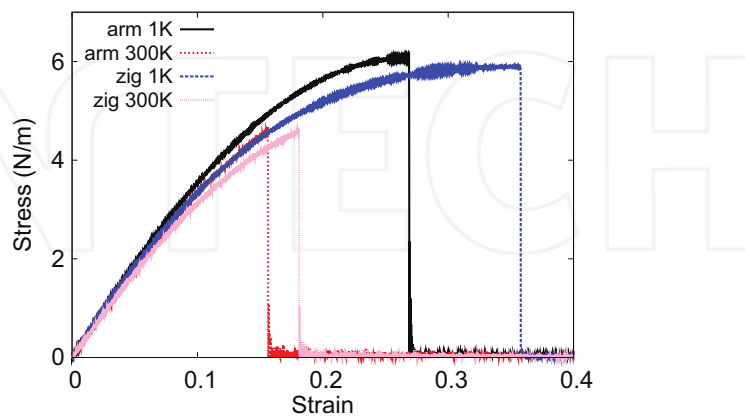


Figure 8. Stress-strain for single-layer 1H-ScSe₂ of dimension 100 × 100 Å along the armchair and zigzag directions.

The Young's modulus is essentially isotropic in the armchair and zigzag directions. The Poisson's ratio from the VFF model and the SW potential is $\nu_{xy} = \nu_{yx} = 0.32$.

There is no available value for nonlinear quantities in the single-layer 1H-ScSe₂. We have thus used the nonlinear parameter $B = 0.5d^4$ in Eq. (5), which is close to the value of B in most materials. The value of the third-order nonlinear elasticity D can be extracted by fitting the stress-strain relation to the function $\sigma = E\epsilon + \frac{1}{2}D\epsilon^2$ with E as the Young's modulus. The values of D from the present SW potential are -115.7 and -135.7 N/m along the armchair and zigzag directions, respectively. The ultimate stress is about 6.1 N/m at the ultimate strain of 0.27 in the armchair direction at the low temperature of 1 K. The ultimate stress is about 5.9 N/m at the ultimate strain of 0.35 in the zigzag direction at the low temperature of 1 K.

6. 1H-ScTe₂

Most existing theoretical studies on the single-layer 1H-ScTe₂ are based on the first-principles calculations. In this section, we will develop the SW potential for the single-layer 1H-ScTe₂.

The structure for the single-layer 1H-ScTe₂ is shown in **Figure 1** (with M = Sc and X = Te). Each Sc atom is surrounded by six Te atoms. These Te atoms are categorized into the top group (e.g., atoms 1, 3, and 5) and bottom group (e.g., atoms 2, 4, and 6). Each Te atom is connected to three Sc atoms. The structural parameters are from the first-principles calculations [12], including the lattice constant $a = 3.62$ Å and the bond length $d_{\text{Sc}-\text{Te}} = 2.89$ Å. The resultant angles are $\theta_{\text{ScTeTe}} = \theta_{\text{TeScSc}} = 77.555^\circ$ and $\theta_{\text{ScTeTe}'} = 87.364^\circ$, in which atoms Te and Te' are from different (top or bottom) groups.

Table 22 shows four VFF terms for the single-layer 1H-ScTe₂; one of which is the bond stretching interaction shown by Eq. (1), while the other three terms are the angle bending interaction shown by Eq. (2). These force constant parameters are determined by fitting to the acoustic branches in the phonon dispersion along the ΓM as shown in **Figure 9(a)**. The *ab initio* calculations for the phonon dispersion are from [12]. There is only one (longitudinal) acoustic branch available. We find that the VFF parameters can be chosen to be the same as that of the 1H-ScSe₂, from which the longitudinal acoustic branch agrees with the *ab initio* results as shown in **Figure 9(a)**. It has also been shown that the VFF parameters can be the same for TaSe₂ and NbSe₂ of similar

VFF type	Bond stretching	Angle bending		
Expression	$\frac{1}{2}K_{\text{Sc}-\text{Te}}(\Delta r)^2$	$\frac{1}{2}K_{\text{Sc}-\text{Te}-\text{Te}}(\Delta\theta)^2$	$\frac{1}{2}K_{\text{Sc}-\text{Te}-\text{Te}'}(\Delta\theta)^2$	$\frac{1}{2}K_{\text{Te}-\text{Sc}-\text{Sc}}(\Delta\theta)^2$
Parameter	5.192	2.027	2.027	2.027
r_0 or θ_0	2.890	77.555	87.364	87.364

The second line gives an explicit expression for each VFF term. The third line is the force constant parameters. Parameters are in the unit of eV/Å² for the bond stretching interaction and in the unit of eV for the angle bending interaction. The fourth line gives the initial bond length (in the unit of Å) for the bond stretching interaction and the initial angle (in the unit of degrees) for the angle bending interaction. The angle θ_{ijk} has atom i as the apex.

Table 22. The VFF model for single-layer 1H-ScTe₂.

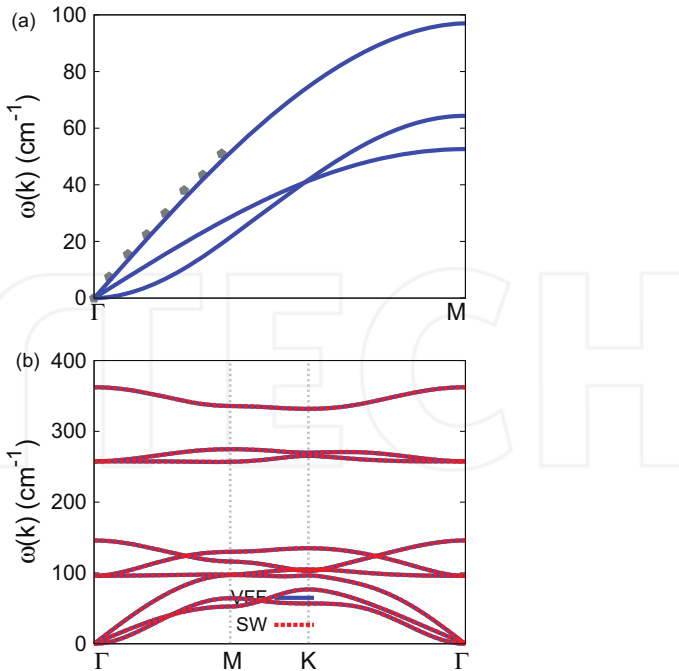


Figure 9. Phonon spectrum for single-layer 1H-ScTe₂. (a) Phonon dispersion along the Γ M direction in the Brillouin zone. The results from the VFF model (lines) are comparable with the *ab initio* results (pentagons) from [12]. (b) The phonon dispersion from the SW potential is exactly the same as that from the VFF model.

structure [15]. **Figure 9(b)** shows that the VFF model and the SW potential give exactly the same phonon dispersion, as the SW potential is derived from the VFF model.

The parameters for the two-body SW potential used by GULP are shown in **Table 23**. The parameters for the three-body SW potential used by GULP are shown in **Table 24**. Some representative parameters for the SW potential used by LAMMPS are listed in **Table 25**. We note that 12 atom types have been introduced for the simulation of the single-layer 1H-ScTe₂ using LAMMPS, because the angles around atom Sc in **Figure 1** (with M = Sc and X = Te) are not distinguishable in LAMMPS. We have suggested two options to differentiate these angles by implementing some additional constraints in LAMMPS, which can be accomplished by modifying the source file of LAMMPS [13, 14]. According to our experience, it is not so convenient for some users to implement these constraints and recompile the LAMMPS package. Hence, in the present work, we differentiate the angles by introducing more atom types, so it is not necessary to modify the LAMMPS package. **Figure 2** (with M = Sc and X = Te) shows

	A (eV)	ρ (Å)	B (Å ⁴)	r_{\min} (Å)	r_{\max} (Å)
Sc-Te	4.630	1.050	34.879	0.0	3.761

Table 23. Two-body SW potential parameters for single-layer 1H-ScTe₂ used by GULP [8] as expressed in Eq. (3).

	K (eV)	θ_0 ($^\circ$)	ρ_1 (\AA)	ρ_2 (\AA)	$r_{\min\ 12}$ (\AA)	$r_{\max\ 12}$ (\AA)	$r_{\min\ 13}$ (\AA)	$r_{\max\ 13}$ (\AA)	$r_{\min\ 23}$ (\AA)	$r_{\max\ 23}$ (\AA)
$\theta_{\text{Sc}-\text{Te}-\text{Te}}$	11.848	77.555	1.050	1.050	0.0	3.761	0.0	3.761	0.0	4.504
$\theta_{\text{Sc}-\text{Te}-\text{Te}'}$	11.322	87.364	1.050	1.050	0.0	3.761	0.0	3.761	0.0	4.504
$\theta_{\text{Te}-\text{Sc}-\text{Sc}}$	11.848	77.555	1.050	1.050	0.0	3.761	0.0	3.761	0.0	4.504

The angle θ_{ijk} in the first line indicates the bending energy for the angle with atom i as the apex.

Table 24. Three-body SW potential parameters for single-layer 1H-ScTe₂ used by GULP [8] as expressed in Eq. (4).

	ϵ (eV)	σ (\AA)	a	λ	γ	$\cos \theta_0$	A_L	B_L	p	q	Tol
Sc ₁ —Te ₁ —Te ₁	1.000	1.050	3.581	0.000	1.000	0.000	4.630	28.679	4	0	0.0
Sc ₁ —Te ₁ —Te ₃	1.000	0.000	0.000	11.848	1.000	0.216	0.000	0.000	4	0	0.0
Sc ₁ —Te ₁ —Te ₂	1.000	0.000	0.000	11.322	1.000	0.046	0.000	0.000	4	0	0.0
Te ₁ —Sc ₁ —Sc ₃	1.000	0.000	0.000	11.848	1.000	0.216	0.000	0.000	4	0	0.0

Table 25. SW potential parameters for single-layer 1H-ScTe₂ used by LAMMPS [9] as expressed in Eqs. (9) and (10).

that, for 1H-ScTe₂, we can differentiate these angles around the Sc atom by assigning these six neighboring Te atoms with different atom types. It can be found that twelve atom types are necessary for the purpose of differentiating all six neighbors around one Sc atom.

We use LAMMPS to perform MD simulations for the mechanical behavior of the single-layer 1H-ScTe₂ under uniaxial tension at 1 and 300 K. **Figure 10** shows the stress-strain curve for the tension of a single-layer 1H-ScTe₂ of dimension 100 × 100 Å. Periodic boundary conditions are applied in both armchair and zigzag directions. The single-layer 1H-ScTe₂ is stretched uniaxially along the armchair or zigzag direction. The stress is calculated without involving the actual thickness of the quasi-two-dimensional structure of the single-layer 1H-ScTe₂. The Young's modulus can be obtained by a linear fitting of the stress-strain relation in the small

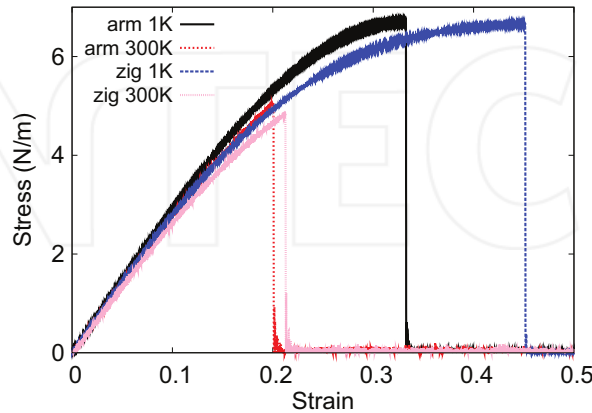


Figure 10. Stress-strain for single-layer 1H-ScTe₂ of dimension 100 × 100 Å along the armchair and zigzag directions.

strain range of [0, 0.01]. The Young's modulus is 29.3 and 28.8 N/m along the armchair and zigzag directions, respectively. The Young's modulus is essentially isotropic in the armchair and zigzag directions. The Poisson's ratio from the VFF model and the SW potential is $\nu_{xy} = \nu_{yx} = 0.38$.

There is no available value for nonlinear quantities in the single-layer 1H-ScTe₂. We have thus used the nonlinear parameter $B = 0.5d^4$ in Eq. (5), which is close to the value of B in most materials. The value of the third-order nonlinear elasticity D can be extracted by fitting the stress-strain relation to the function $\sigma = E\epsilon + \frac{1}{2}D\epsilon^2$ with E as the Young's modulus. The values of D from the present SW potential are -43.2 and -59.3 N/m along the armchair and zigzag directions, respectively. The ultimate stress is about 6.7 N/m at the ultimate strain of 0.33 in the armchair direction at the low temperature of 1 K. The ultimate stress is about 6.7 N/m at the ultimate strain of 0.45 in the zigzag direction at the low temperature of 1 K.

7. 1H-TiTe₂

Most existing theoretical studies on the single-layer 1H-TiTe₂ are based on the first-principles calculations. In this section, we will develop both VFF model and the SW potential for the single-layer 1H-TiTe₂.

The structure for the single-layer 1H-TiTe₂ is shown in **Figure 1** (with M = Ti and X = Se). Each Ti atom is surrounded by six Te atoms. These Te atoms are categorized into the top group (e.g., atoms 1, 3, and 5) and bottom group (e.g., atoms 2, 4, and 6). Each Te atom is connected to three Ti atoms. The structural parameters are from [12], including the lattice constant $a = 3.62$ Å and the bond length $d_{Ti-Te} = 2.75$ Å. The resultant angles are $\theta_{TiTeTe} = \theta_{TeTiTi} = 82.323^\circ$ and $\theta_{TiTeTe'} = 81.071^\circ$, in which atoms Te and Te' are from different (top or bottom) groups.

Table 26 shows the VFF terms for the 1H-TiTe₂; one of which is the bond stretching interaction shown by Eq. (1), while the other terms are the angle bending interaction shown by Eq. (2). These force constant parameters are determined by fitting to the three acoustic branches in the phonon dispersion along the Γ M as shown in **Figure 11(a)**. The *ab initio* calculations for the

VFF type	Bond stretching	Angle bending	
Expression	$\frac{1}{2}K_{Ti-Te}(\Delta r)^2$	$\frac{1}{2}K_{Ti-Te-Te}(\Delta\theta)^2$	$\frac{1}{2}K_{Ti-Te-Te'}(\Delta\theta)^2$
Parameter	4.782	3.216	3.216
r_0 or θ_0	2.750	82.323	81.071
			82.323

The second line gives an explicit expression for each VFF term. The third line is the force constant parameters. Parameters are in the unit of eV/Å² for the bond stretching interaction and in the unit of eV for the angle bending interaction. The fourth line gives the initial bond length (in the unit of Å) for the bond stretching interaction and the initial angle (in the unit of degrees) for the angle bending interaction. The angle θ_{ijk} has atom i as the apex.

Table 26. The VFF model for single-layer 1H-TiTe₂.

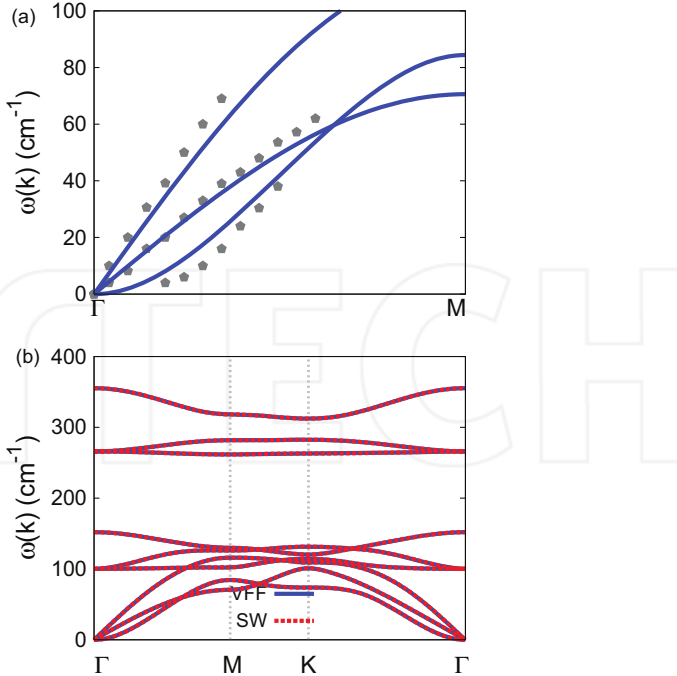


Figure 11. Phonon dispersion for single-layer 1H-TiTe₂. (a) The VFF model is fitted to the three acoustic branches in the long wave limit along the Γ M direction. The *ab initio* results (gray pentagons) are from Ref. [12]. (b) The VFF model (blue lines) and the SW potential (red lines) give the same phonon dispersion for single-layer 1H-TiTe₂ along Γ MK Γ .

phonon dispersion are from [12]. **Figure 11(b)** shows that the VFF model and the SW potential give exactly the same phonon dispersion, as the SW potential is derived from the VFF model.

The parameters for the two-body SW potential used by GULP are shown in **Table 27**. The parameters for the three-body SW potential used by GULP are shown in **Table 28**. Parameters for the SW potential used by LAMMPS are listed in **Table 29**. We note that 12 atom types have been introduced for the simulation of the single-layer 1H-TiTe₂ using LAMMPS, because the angles around atom Ti in **Figure 1** (with M = Ti and X = Te) are not distinguishable in LAMMPS. We have suggested two options to differentiate these angles by implementing some additional constraints in LAMMPS, which can be accomplished by modifying the source file of LAMMPS [13, 14]. According to our experience, it is not so convenient for some users to implement these constraints and recompile the LAMMPS package. Hence, in the present work, we differentiate the angles by introducing more atom types, so it is not necessary to modify the LAMMPS package. **Figure 2** (with M = Ti and X = Te) shows that, for 1H-TiTe₂, we

	A (eV)	ρ (\AA)	B (\AA^4)	r_{\min} (\AA)	r_{\max} (\AA)
Ti-Te	4.414	1.173	28.596	0.0	3.648

Table 27. Two-body SW potential parameters for single-layer 1H-TiTe₂ used by GULP [8] as expressed in Eq. (3).

	K (eV)	θ_0 ($^\circ$)	ρ_1 (\AA)	ρ_2 (\AA)	$r_{\min 12}$ (\AA)	$r_{\max 12}$ (\AA)	$r_{\min 13}$ (\AA)	$r_{\max 13}$ (\AA)	$r_{\min 23}$ (\AA)	$r_{\max 23}$ (\AA)
$\theta_{\text{Ti}-\text{Te}-\text{Te}}$	22.321	82.323	1.173	1.173	0.0	3.648	0.0	3.648	0.0	4.354
$\theta_{\text{Ti}-\text{Te}-\text{Te}'}$	22.463	81.071	1.173	1.173	0.0	3.648	0.0	3.648	0.0	4.354
$\theta_{\text{Te}-\text{Ti}-\text{Ti}}$	11.321	82.323	1.173	1.173	0.0	3.648	0.0	3.648	0.0	4.354

The angle θ_{ijk} in the first line indicates the bending energy for the angle with atom i as the apex.

Table 28. Three-body SW potential parameters for single-layer 1H-TiTe₂ used by GULP [8] as expressed in Eq. (4).

	ϵ (eV)	σ (\AA)	a	λ	γ	$\cos \theta_0$	A_L	B_L	p	q	Tol
Ti ₁ -Te ₁ -Te ₁	1.000	1.173	3.110	0.000	1.000	0.000	4.414	15.100	4	0	0.0
Ti ₁ -Te ₁ -Te ₃	1.000	0.000	0.000	22.321	1.000	0.134	0.000	0.000	4	0	0.0
Ti ₁ -Te ₁ -Te ₂	1.000	0.000	0.000	22.463	1.000	0.155	0.000	0.000	4	0	0.0
Te ₁ -Ti ₁ -Ti ₃	1.000	0.000	0.000	22.321	1.000	0.134	0.000	0.000	4	0	0.0

Atom types in the first column are displayed in **Figure 2** (with M = Ti and X = Te).

Table 29. SW potential parameters for single-layer 1H-TiTe₂ used by LAMMPS [9] as expressed in Eqs. (9) and (10).

can differentiate these angles around the Ti atom by assigning these six neighboring Te atoms with different atom types. It can be found that twelve atom types are necessary for the purpose of differentiating all six neighbors around one Ti atom.

We use LAMMPS to perform MD simulations for the mechanical behavior of the single-layer 1H-TiTe₂ under uniaxial tension at 1 and 300 K. **Figure 12** shows the stress-strain curve for the tension of a single-layer 1H-TiTe₂ of dimension 100 × 100 Å. Periodic boundary conditions are applied in both armchair and zigzag directions. The single-layer 1H-TiTe₂ is stretched uniaxially along the armchair or zigzag direction. The stress is calculated without involving the actual

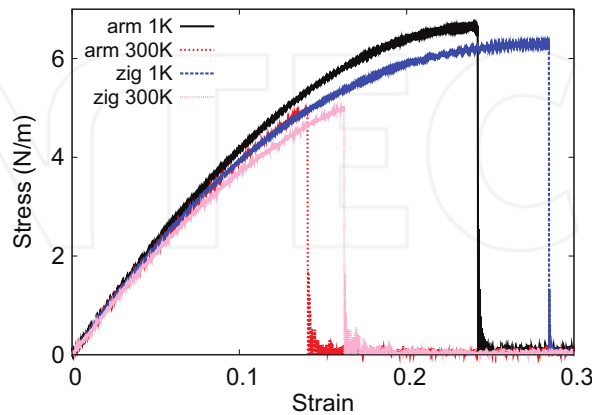


Figure 12. Stress-strain for single-layer 1H-TiTe₂ of dimension 100 × 100 Å along the armchair and zigzag directions.

thickness of the quasi-two-dimensional structure of the single-layer 1H-TiTe₂. The Young's modulus can be obtained by a linear fitting of the stress-strain relation in the small strain range of [0, 0.01]. The Young's modulus is 47.9 and 47.1 N/m along the armchair and zigzag directions, respectively. The Young's modulus is essentially isotropic in the armchair and zigzag directions. The Poisson's ratio from the VFF model and the SW potential is $\nu_{xy} = \nu_{yx} = 0.29$.

There is no available value for the nonlinear quantities in the single-layer 1H-TiTe₂. We have thus used the nonlinear parameter $B = 0.5d^4$ in Eq. (5), which is close to the value of B in most materials. The value of the third-order nonlinear elasticity D can be extracted by fitting the stress-strain relation to the function $\sigma = E\epsilon + \frac{1}{2}D\epsilon^2$ with E as the Young's modulus. The values of D from the present SW potential are -158.6 and -176.3 N/m along the armchair and zigzag directions, respectively. The ultimate stress is about 6.6 N/m at the ultimate strain of 0.24 in the armchair direction at the low temperature of 1 K. The ultimate stress is about 6.3 N/m at the ultimate strain of 0.28 in the zigzag direction at the low temperature of 1 K.

8. 1H-VO₂

Most existing theoretical studies on the single-layer 1H-VO₂ are based on the first-principles calculations. In this section, we will develop the SW potential for the single-layer 1H-VO₂.

The structure for the single-layer 1H-VO₂ is shown in **Figure 1** (with M = V and X = O). Each V atom is surrounded by six O atoms. These O atoms are categorized into the top group (e.g., atoms 1, 3, and 5) and bottom group (e.g., atoms 2, 4, and 6). Each O atom is connected to three V atoms. The structural parameters are from the first-principles calculations [12], including the lattice constant $a = 2.70$ Å and the bond length $d_{V-O} = 1.92$ Å. The resultant angles are $\theta_{VOO} = \theta_{OVV} = 89.356^\circ$ and $\theta_{VOO'} = 71.436^\circ$, in which atoms O and O' are from different (top or bottom) groups.

Table 30 shows four VFF terms for the single-layer 1H-VO₂; one of which is the bond stretching interaction shown by Eq. (1), while the other three terms are the angle bending interaction shown by Eq. (2). These force constant parameters are determined by fitting to the acoustic branches in the phonon dispersion along the TM as shown in **Figure 13(a)**. The *ab initio* calculations for the phonon dispersion are from [12]. **Figure 13(b)** shows that the VFF

VFF type	Bond stretching	Angle bending		
Expression	$\frac{1}{2}K_{V-O}(\Delta r)^2$	$\frac{1}{2}K_{V-O-O}(\Delta\theta)^2$	$\frac{1}{2}K_{V-O-O'}(\Delta\theta)^2$	$\frac{1}{2}K_{O-V-V}(\Delta\theta)^2$
Parameter	9.417	4.825	4.825	4.825
r_0 or θ_0	1.920	89.356	71.436	89.356

The second line gives an explicit expression for each VFF term. The third line is the force constant parameters. Parameters are in the unit of eV/Å² for the bond stretching interaction and in the unit of eV for the angle bending interaction. The fourth line gives the initial bond length (in the unit of Å) for the bond stretching interaction and the initial angle (in the unit of degrees) for the angle bending interaction. The angle θ_{ijk} has atom i as the apex.

Table 30. The VFF model for single-layer 1H-VO₂.

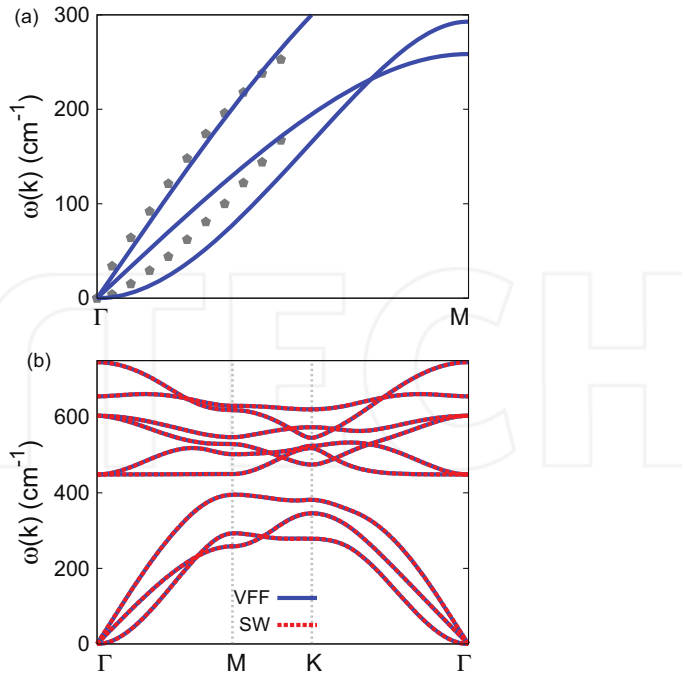


Figure 13. Phonon spectrum for single-layer 1H-VO₂. (a) Phonon dispersion along the Γ M direction in the Brillouin zone. The results from the VFF model (lines) are comparable with the *ab initio* results (pentagons) from [12]. (b) The phonon dispersion from the SW potential is exactly the same as that from the VFF model.

model and the SW potential give exactly the same phonon dispersion, as the SW potential is derived from the VFF model.

The parameters for the two-body SW potential used by GULP are shown in **Table 31**. The parameters for the three-body SW potential used by GULP are shown in **Table 32**. Some representative

	A (eV)	ρ (Å)	B (Å ⁴)	r_{\min} (Å)	r_{\max} (Å)
V-O	5.105	1.011	6.795	0.0	2.617

Table 31. Two-body SW potential parameters for single-layer 1H-VO₂ used by GULP [8] as expressed in Eq. (3).

	K (eV)	θ_0 (°)	ρ_1 (Å)	ρ_2 (Å)	$r_{\min 12}$ (Å)	$r_{\max 12}$ (Å)	$r_{\min 13}$ (Å)	$r_{\max 13}$ (Å)	$r_{\min 23}$ (Å)	$r_{\max 23}$ (Å)
θ_{V-O-O}	43.951	89.356	1.011	1.011	0.0	2.617	0.0	2.617	0.0	3.105
$\theta_{V-O-O'}$	48.902	71.436	1.011	1.011	0.0	2.617	0.0	2.617	0.0	3.105
θ_{O-V-V}	43.951	89.356	1.011	1.011	0.0	2.617	0.0	2.617	0.0	3.105

The angle θ_{ijk} in the first line indicates the bending energy for the angle with atom *i* as the apex.

Table 32. Three-body SW potential parameters for single-layer 1H-VO₂ used by GULP [8] as expressed in Eq. (4).

	ϵ (eV)	σ (Å)	a	λ	γ	$\cos \theta_0$	A_L	B_L	p	q	Tol
V ₁ -O ₁ -O ₁	1.000	1.011	2.589	0.000	1.000	0.000	5.105	6.509	4	0	0.0
V ₁ -O ₁ -O ₃	1.000	0.000	0.000	43.951	1.000	0.011	0.000	0.000	4	0	0.0
V ₁ -O ₁ -O ₂	1.000	0.000	0.000	48.902	1.000	0.318	0.000	0.000	4	0	0.0
O ₁ -V ₁ -V ₃	1.000	0.000	0.000	43.951	1.000	0.011	0.000	0.000	4	0	0.0

Table 33. SW potential parameters for single-layer 1H-VO₂ used by LAMMPS [9] as expressed in Eqs. (9) and (10).

parameters for the SW potential used by LAMMPS are listed in **Table 33**. We note that 12 atom types have been introduced for the simulation of the single-layer 1H-VO₂ using LAMMPS, because the angles around atom V in **Figure 1** (with M = V and X = O) are not distinguishable in LAMMPS. We have suggested two options to differentiate these angles by implementing some additional constraints in LAMMPS, which can be accomplished by modifying the source file of LAMMPS [13, 14]. According to our experience, it is not so convenient for some users to implement these constraints and recompile the LAMMPS package. Hence, in the present work, we differentiate the angles by introducing more atom types, so it is not necessary to modify the LAMMPS package. **Figure 2** (with M = V and X = O) shows that, for 1H-VO₂, we can differentiate these angles around the V atom by assigning these six neighboring O atoms with different atom types. It can be found that twelve atom types are necessary for the purpose of differentiating all six neighbors around one V atom.

We use LAMMPS to perform MD simulations for the mechanical behavior of the single-layer 1H-VO₂ under uniaxial tension at 1 and 300 K. **Figure 14** shows the stress-strain curve for the tension of a single-layer 1H-VO₂ of dimension 100 × 100 Å. Periodic boundary conditions are applied in both armchair and zigzag directions. The single-layer 1H-VO₂ is stretched uniaxially along the armchair or zigzag direction. The stress is calculated without involving the actual thickness of the quasi-two-dimensional structure of the single-layer 1H-VO₂. The Young's modulus can be obtained by a linear fitting of the stress-strain relation in the

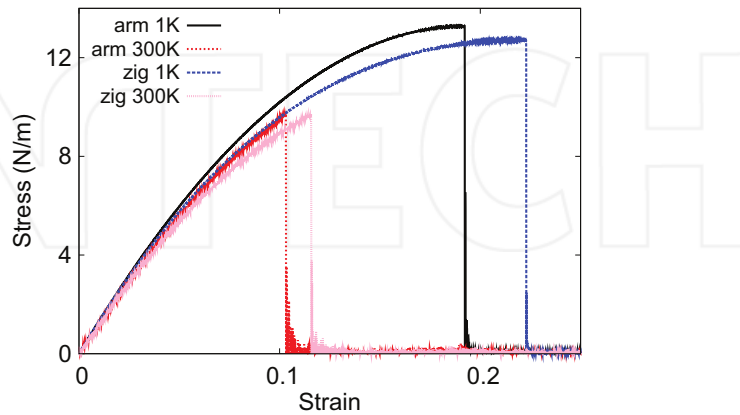


Figure 14. Stress-strain for single-layer 1H-VO₂ of dimension 100 × 100 Å along the armchair and zigzag directions.

small strain range of [0, 0.01]. The Young's modulus is 133.0 and 132.9 N/m along the armchair and zigzag directions, respectively. The Young's modulus is essentially isotropic in the armchair and zigzag directions. The Poisson's ratio from the VFF model and the SW potential is $\nu_{xy} = \nu_{yx} = 0.17$.

There is no available value for nonlinear quantities in the single-layer 1H-VO₂. We have thus used the nonlinear parameter $B = 0.5d^4$ in Eq. (5), which is close to the value of B in most materials. The value of the third-order nonlinear elasticity D can be extracted by fitting the stress-strain relation to the function $\sigma = E\epsilon + \frac{1}{2}D\epsilon^2$ with E as the Young's modulus. The values of D from the present SW potential are -652.3 and -705.8 N/m along the armchair and zigzag directions, respectively. The ultimate stress is about 13.3 N/m at the ultimate strain of 0.19 in the armchair direction at the low temperature of 1 K. The ultimate stress is about 12.7 N/m at the ultimate strain of 0.22 in the zigzag direction at the low temperature of 1 K.

9. 1H-VS₂

Most existing theoretical studies on the single-layer 1H-VS₂ are based on the first-principles calculations. In this section, we will develop both VFF model and the SW potential for the single-layer 1H-VS₂.

The structure for the single-layer 1H-VS₂ is shown in **Figure 1** (with M = V and X = S). Each V atom is surrounded by six S atoms. These S atoms are categorized into the top group (e.g., atoms 1, 3, and 5) and bottom group (e.g., atoms 2, 4, and 6). Each S atom is connected to three V atoms. The structural parameters are from [12], including the lattice constant $a = 3.09$ Å and the bond length $d_{V-S} = 2.31$ Å. The resultant angles are $\theta_{VSS} = \theta_{SVV} = 83.954^\circ$ and $\theta_{VSS'} = 78.878^\circ$, in which atoms S and S' are from different (top or bottom) groups.

Table 34 shows the VFF terms for the 1H-VS₂; one of which is the bond stretching interaction shown by Eq. (1), while the other terms are the angle bending interaction shown by Eq. (2). These force constant parameters are determined by fitting to the three acoustic branches in the phonon dispersion along the Γ M as shown in **Figure 15(a)**. The *ab initio* calculations for the phonon dispersion are from [16]. The phonon dispersion can also be found in other *ab initio*

VFF type	Bond stretching	Angle bending		
Expression	$\frac{1}{2}K_{V-S}(\Delta r)^2$	$\frac{1}{2}K_{V-S-S}(\Delta\theta)^2$	$\frac{1}{2}K_{V-S-S'}(\Delta\theta)^2$	$\frac{1}{2}K_{S-V-V}(\Delta\theta)^2$
Parameter	8.392	4.074	4.074	4.074
r_0 or θ_0	2.310	83.954	78.878	83.954

The second line gives an explicit expression for each VFF term. The third line is the force constant parameters. Parameters are in the unit of eV/Å² for the bond stretching interaction and in the unit of eV for the angle bending interaction. The fourth line gives the initial bond length (in the unit of Å) for the bond stretching interaction and the initial angle (in the unit of degrees) for the angle bending interaction. The angle θ_{ijk} has atom *i* as the apex.

Table 34. The VFF model for single-layer 1H-VS₂.

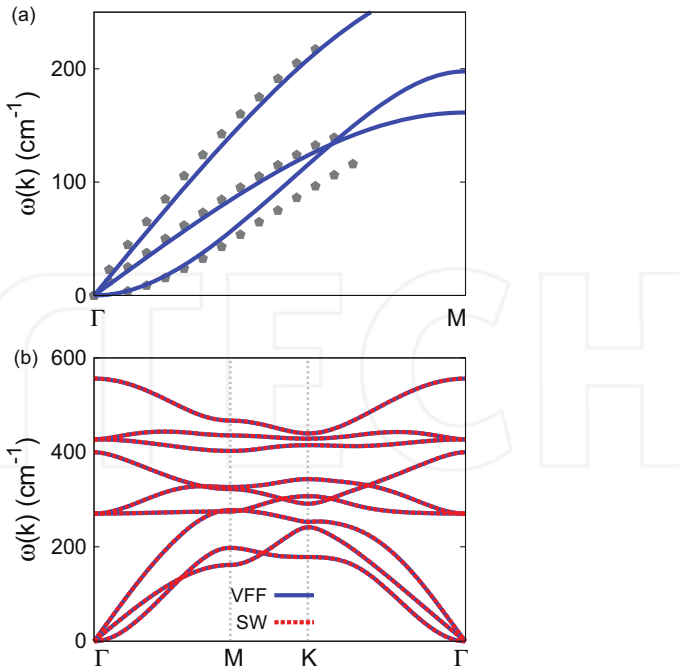


Figure 15. Phonon dispersion for single-layer 1H-VS₂. (a) The VFF model is fitted to the three acoustic branches in the long wave limit along the Γ M direction. The *ab initio* results (gray pentagons) are from [16]. (b) The VFF model (blue lines) and the SW potential (red lines) give the same phonon dispersion for single-layer 1H-VS₂ along Γ MK Γ .

calculations [12]. **Figure 15(b)** shows that the VFF model and the SW potential give exactly the same phonon dispersion, as the SW potential is derived from the VFF model.

The parameters for the two-body SW potential used by GULP are shown in **Table 35**. The parameters for the three-body SW potential used by GULP are shown in **Table 36**. Parameters

	A (eV)	ρ (\AA)	B (\AA^4)	r_{\min} (\AA)	r_{\max} (\AA)
V-S	5.714	1.037	14.237	0.0	3.084

Table 35. Two-body SW potential parameters for single-layer 1H-VS₂ used by GULP [8] as expressed in Eq. (3).

	K (eV)	θ_0 (°)	ρ_1 (\AA)	ρ_2 (\AA)	$r_{\min 12}$ (\AA)	$r_{\max 12}$ (\AA)	$r_{\min 13}$ (\AA)	$r_{\max 13}$ (\AA)	$r_{\min 23}$ (\AA)	$r_{\max 23}$ (\AA)
θ_{V-S-S}	30.059	83.954	1.037	1.037	0.0	3.084	0.0	3.084	0.0	3.676
$\theta_{V-S-S'}$	30.874	78.878	1.037	1.037	0.0	3.084	0.0	3.084	0.0	3.676
θ_{S-V-V}	30.059	83.954	1.037	1.037	0.0	3.084	0.0	3.084	0.0	3.676

The angle θ_{ijk} in the first line indicates the bending energy for the angle with atom i as the apex.

Table 36. Three-body SW potential parameters for single-layer 1H-VS₂ used by GULP [8] as expressed in Eq. (4).

	ϵ (eV)	σ (Å)	a	λ	γ	$\cos \theta_0$	A_L	B_L	p	q	Tol
V ₁ —S ₁ —S ₁	1.000	1.037	2.973	0.000	1.000	0.000	5.714	12.294	4	0	0.0
V ₁ —S ₁ —S ₃	1.000	0.000	0.000	30.059	1.000	0.105	0.000	0.000	4	0	0.0
V ₁ —S ₁ —S ₂	1.000	0.000	0.000	30.874	1.000	0.193	0.000	0.000	4	0	0.0
S ₁ —V ₁ —V ₃	1.000	0.000	0.000	30.059	1.000	0.105	0.000	0.000	4	0	0.0

Atom types in the first column are displayed in **Figure 2** (with M = V and X = S).

Table 37. SW potential parameters for single-layer 1H-VS₂ used by LAMMPS [9] as expressed in Eqs. (9) and (10).

for the SW potential used by LAMMPS are listed in **Table 37**. We note that 12 atom types have been introduced for the simulation of the single-layer 1H-VS₂ using LAMMPS, because the angles around atom V in **Figure 1** (with M = V and X = S) are not distinguishable in LAMMPS. We have suggested two options to differentiate these angles by implementing some additional constraints in LAMMPS, which can be accomplished by modifying the source file of LAMMPS [13, 14]. According to our experience, it is not so convenient for some users to implement these constraints and recompile the LAMMPS package. Hence, in the present work, we differentiate the angles by introducing more atom types, so it is not necessary to modify the LAMMPS package. **Figure 2** (with M = V and X = S) shows that, for 1H-VS₂, we can differentiate these angles around the V atom by assigning these six neighboring S atoms with different atom types. It can be found that twelve atom types are necessary for the purpose of differentiating all six neighbors around one V atom.

We use LAMMPS to perform MD simulations for the mechanical behavior of the single-layer 1H-VS₂ under uniaxial tension at 1 and 300 K. **Figure 16** shows the stress-strain curve for the tension of a single-layer 1H-VS₂ of dimension 100 × 100 Å. Periodic boundary conditions are applied in both armchair and zigzag directions. The single-layer 1H-VS₂ is stretched uniaxially along the armchair or zigzag direction. The stress is calculated without involving the actual

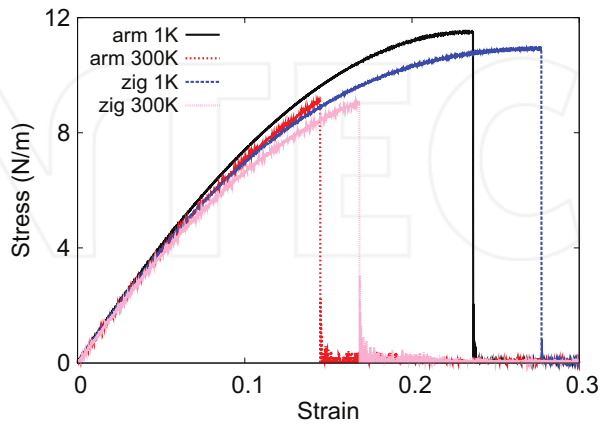


Figure 16. Stress-strain for single-layer 1H-VS₂ of dimension 100 × 100 Å along the armchair and zigzag directions.

thickness of the quasi-two-dimensional structure of the single-layer 1H-VSe₂. The Young's modulus can be obtained by a linear fitting of the stress-strain relation in the small strain range of [0, 0.01]. The Young's modulus is 86.5 and 85.3 N/m along the armchair and zigzag directions, respectively. The Young's modulus is essentially isotropic in the armchair and zigzag directions. The Poisson's ratio from the VFF model and the SW potential is $\nu_{xy} = \nu_{yx} = 0.28$.

There is no available value for the nonlinear quantities in the single-layer 1H-VSe₂. We have thus used the nonlinear parameter $B = 0.5d^4$ in Eq. (5), which is close to the value of B in most materials. The value of the third-order nonlinear elasticity D can be extracted by fitting the stress-strain relation to the function $\sigma = E\epsilon + \frac{1}{2}D\epsilon^2$ with E as the Young's modulus. The values of D from the present SW potential are -302.0 and -334.7 N/m along the armchair and zigzag directions, respectively. The ultimate stress is about 11.5 N/m at the ultimate strain of 0.23 in the armchair direction at the low temperature of 1 K. The ultimate stress is about 10.9 N/m at the ultimate strain of 0.27 in the zigzag direction at the low temperature of 1 K.

10. 1H-VSe₂

Most existing theoretical studies on the single-layer 1H-VSe₂ are based on the first-principles calculations. In this section, we will develop both VFF model and the SW potential for the single-layer 1H-VSe₂.

The structure for the single-layer 1H-VSe₂ is shown in **Figure 1** (with M = V and X = Se). Each V atom is surrounded by six Se atoms. These Se atoms are categorized into the top group (e.g., atoms 1, 3, and 5) and bottom group (e.g., atoms 2, 4, and 6). Each Se atom is connected to three V atoms. The structural parameters are from [12], including the lattice constant $a = 3.24 \text{ \AA}$ and the bond length $d_{V-Se} = 2.45 \text{ \AA}$. The resultant angles are $\theta_{VSeSe} = \theta_{SeVv} = 82.787^\circ$ and $\theta_{VSeSe'} = 80.450^\circ$, in which atoms Se and Se' are from different (top or bottom) groups.

Table 38 shows the VFF terms for the 1H-VSe₂; one of which is the bond stretching interaction shown by Eq. (1), while the other terms are the angle bending interaction shown by Eq. (2). These force constant parameters are determined by fitting to the three acoustic branches in the phonon dispersion along the Γ M as shown in **Figure 17(a)**. The *ab initio* calculations for the

VFF type	Bond stretching	Angle bending		
Expression	$\frac{1}{2}K_{V-Se}(\Delta r)^2$	$\frac{1}{2}K_{V-Se-Se}(\Delta\theta)^2$	$\frac{1}{2}K_{V-Se-Se'}(\Delta\theta)^2$	$\frac{1}{2}K_{Se-V-V}(\Delta\theta)^2$
Parameter	6.492	4.716	4.716	4.716
r_0 or θ_0	2.450	82.787	80.450	82.787

The second line gives an explicit expression for each VFF term. The third line is the force constant parameters. Parameters are in the unit of eV/ \AA^2 for the bond stretching interaction and in the unit of eV for the angle bending interaction. The fourth line gives the initial bond length (in the unit of \AA) for the bond stretching interaction and the initial angle (in the unit of degrees) for the angle bending interaction. The angle θ_{ijk} has atom i as the apex.

Table 38. The VFF model for single-layer 1H-VSe₂.

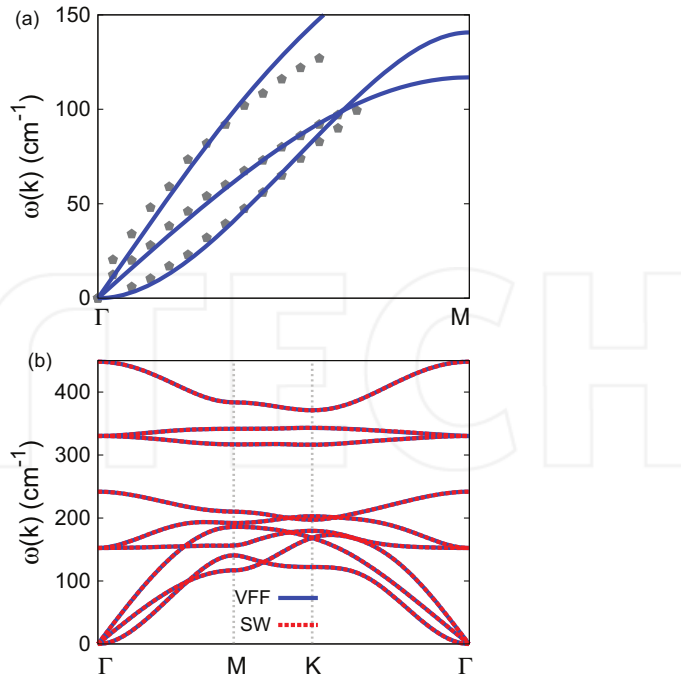


Figure 17. Phonon dispersion for single-layer 1H-VSe₂. (a) The VFF model is fitted to the three acoustic branches in the long wave limit along the Γ M direction. The *ab initio* results (gray pentagons) are from [12]. (b) The VFF model (blue lines) and the SW potential (red lines) give the same phonon dispersion for single-layer 1H-VSe₂ along Γ MKT.

phonon dispersion are from [12]. **Figure 17(b)** shows that the VFF model and the SW potential give exactly the same phonon dispersion, as the SW potential is derived from the VFF model.

The parameters for the two-body SW potential used by GULP are shown in **Table 39**. The parameters for the three-body SW potential used by GULP are shown in **Table 40**. Parameters

	$A(\text{eV})$	$\rho(\text{\AA})$	$B(\text{\AA}^4)$	$r_{\min}(\text{\AA})$	$r_{\max}(\text{\AA})$
V—Se	4.817	1.061	18.015	0.0	3.256

Table 39. Two-body SW potential parameters for single-layer 1H-VSe₂ used by GULP [8] as expressed in Eq. (3).

	$K(\text{eV})$	$\theta_0(\text{^\circ})$	$\rho_1(\text{\AA})$	$\rho_2(\text{\AA})$	$r_{\min12}(\text{\AA})$	$r_{\max12}(\text{\AA})$	$r_{\min13}(\text{\AA})$	$r_{\max13}(\text{\AA})$	$r_{\min23}(\text{\AA})$	$r_{\max23}(\text{\AA})$
$\theta_{\text{V—Se—Se}}$	33.299	82.787	1.061	1.061	0.0	3.256	0.0	3.256	0.0	3.884
$\theta_{\text{V—Se—Se}'}$	33.702	80.450	1.061	1.061	0.0	3.256	0.0	3.256	0.0	3.884
$\theta_{\text{Se—V—V}}$	33.299	82.787	1.061	1.061	0.0	3.256	0.0	3.256	0.0	3.884

The angle θ_{ijk} in the first line indicates the bending energy for the angle with atom i as the apex.

Table 40. Three-body SW potential parameters for single-layer 1H-VSe₂ used by GULP [8] as expressed in Eq. (4).

for the SW potential used by LAMMPS are listed in **Table 41**. We note that 12 atom types have been introduced for the simulation of the single-layer 1H-VSe₂ using LAMMPS, because the angles around atom V in **Figure 1** (with M = V and X = Se) are not distinguishable in LAMMPS. We have suggested two options to differentiate these angles by implementing some additional constraints in LAMMPS, which can be accomplished by modifying the source file of LAMMPS [13, 14]. According to our experience, it is not so convenient for some users to implement these constraints and recompile the LAMMPS package. Hence, in the present work, we differentiate the angles by introducing more atom types, so it is not necessary to modify the LAMMPS package. **Figure 2** (with M = V and X = Se) shows that, for 1H-VSe₂, we can differentiate these angles around the V atom by assigning these six neighboring Se atoms with different atom types. It can be found that 12 atom types are necessary for the purpose of differentiating all 6 neighbors around 1 V atom.

We use LAMMPS to perform MD simulations for the mechanical behavior of the single-layer 1H-VSe₂ under uniaxial tension at 1 and 300 K. **Figure 18** shows the stress-strain curve for the tension of a single-layer 1H-VSe₂ of dimension 100×100 Å. Periodic boundary conditions are applied in both armchair and zigzag directions. The single-layer 1H-VSe₂ is stretched uniaxially along the armchair or zigzag direction. The stress is calculated without involving

	ϵ (eV)	σ (Å)	α	λ	γ	$\cos \theta_0$	A_L	B_L	p	q	Tol
V ₁ —Se ₁ —Se ₁	1.000	1.061	3.070	0.000	1.000	0.000	4.817	14.236	4	0	0.0
V ₁ —Se ₁ —Se ₃	1.000	0.000	0.000	33.299	1.000	0.126	0.000	0.000	4	0	0.0
V ₁ —Se ₁ —Se ₂	1.000	0.000	0.000	33.702	1.000	0.166	0.000	0.000	4	0	0.0
Se ₁ —V ₁ —V ₃	1.000	0.000	0.000	33.299	1.000	0.126	0.000	0.000	4	0	0.0

Atom types in the first column are displayed in **Figure 2** (with M = V and X = Se).

Table 41. SW potential parameters for single-layer 1H-VSe₂ used by LAMMPS [9] as expressed in Eqs. (9) and (10).

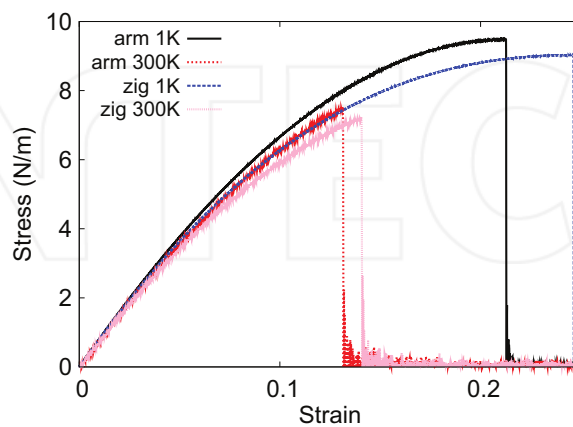


Figure 18. Stress-strain for single-layer 1H-VSe₂ of dimension 100×100 Å along the armchair and zigzag directions.

the actual thickness of the quasi-two-dimensional structure of the single-layer 1H-VSe₂. The Young's modulus can be obtained by a linear fitting of the stress-strain relation in the small strain range of [0, 0.01]. The Young's modulus is 81.7 and 80.6 N/m along the armchair and zigzag directions, respectively. The Young's modulus is essentially isotropic in the armchair and zigzag directions. The Poisson's ratio from the VFF model and the SW potential is $\nu_{xy} = \nu_{yx} = 0.23$.

There is no available value for the nonlinear quantities in the single-layer 1H-VSe₂. We have thus used the nonlinear parameter $B = 0.5d^4$ in Eq. (5), which is close to the value of B in most materials. The value of the third-order nonlinear elasticity D can be extracted by fitting the stress-strain relation to the function $\sigma = E\epsilon + \frac{1}{2}D\epsilon^2$ with E as the Young's modulus. The values of D from the present SW potential are -335.2 and -363.3 N/m along the armchair and zigzag directions, respectively. The ultimate stress is about 9.5 N/m at the ultimate strain of 0.21 in the armchair direction at the low temperature of 1 K. The ultimate stress is about 9.0 N/m at the ultimate strain of 0.24 in the zigzag direction at the low temperature of 1 K.

11. 1H-VTe₂

Most existing theoretical studies on the single-layer 1H-VTe₂ are based on the first-principles calculations. In this section, we will develop both VFF model and the SW potential for the single-layer 1H-VTe₂.

The structure for the single-layer 1H-VTe₂ is shown in **Figure 1** (with M = V and X = Te). Each V atom is surrounded by six Te atoms. These Te atoms are categorized into the top group (e.g., atoms 1, 3, and 5) and bottom group (e.g., atoms 2, 4, and 6). Each Te atom is connected to three V atoms. The structural parameters are from [12], including the lattice constant $a = 3.48$ Å and the bond length $d_{V-Te} = 2.66$ Å. The resultant angles are $\theta_{VTeTe} = \theta_{TeV} = 81.708^\circ$ and $\theta_{VTeTe'} = 81.891^\circ$, in which atoms Te and Te' are from different (top or bottom) groups.

Table 42 shows the VFF terms for the 1H-VTe₂; one of which is the bond stretching interaction shown by Eq. (1), while the other terms are the angle bending interaction shown by Eq. (2). These force constant parameters are determined by fitting to the three acoustic branches in the phonon dispersion along the Γ M as shown in **Figure 19(a)**. The *ab initio* calculations for the

VFF type	Bond stretching	Angle bending		
Expression	$\frac{1}{2}K_{V-Te}(\Delta r)^2$	$\frac{1}{2}K_{V-Te-Te}(\Delta\theta)^2$	$\frac{1}{2}K_{V-Te-Te'}(\Delta\theta)^2$	$\frac{1}{2}K_{Te-V-V}(\Delta\theta)^2$
Parameter	6.371	4.384	4.384	4.384
r_0 or θ_0	2.660	81.708	81.891	81.708

The second line gives an explicit expression for each VFF term. The third line is the force constant parameters. Parameters are in the unit of eV/Å² for the bond stretching interaction and in the unit of eV for the angle bending interaction. The fourth line gives the initial bond length (in the unit of Å) for the bond stretching interaction and the initial angle (in the unit of degrees) for the angle bending interaction. The angle θ_{ijk} has atom i as the apex.

Table 42. The VFF model for single-layer 1H-VTe₂.

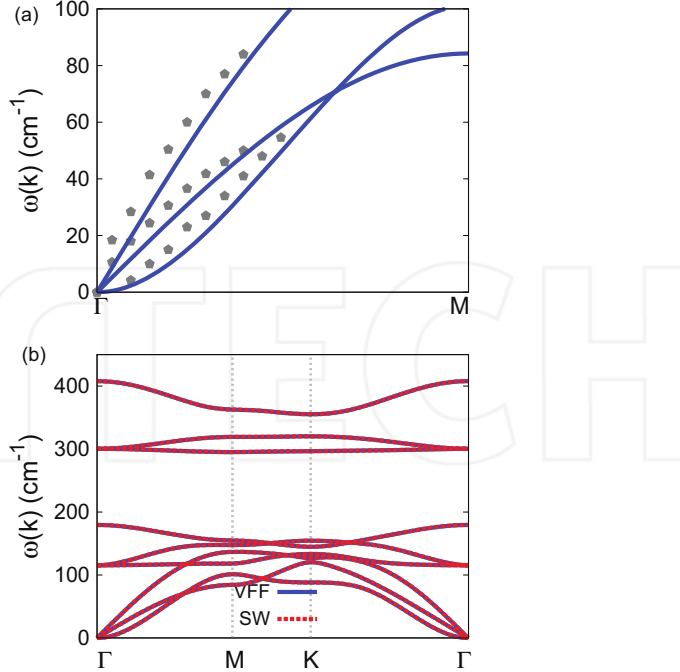


Figure 19. Phonon dispersion for single-layer 1H-VTe₂. (a) The VFF model is fitted to the three acoustic branches in the long wave limit along the Γ M direction. The *ab initio* results (gray pentagons) are from [12]. (b) The VFF model (blue lines) and the SW potential (red lines) give the same phonon dispersion for single-layer 1H-VTe₂ along Γ MK Γ .

phonon dispersion are from [12]. **Figure 19(b)** shows that the VFF model and the SW potential give exactly the same phonon dispersion, as the SW potential is derived from the VFF model.

The parameters for the two-body SW potential used by GULP are shown in **Table 43**. The parameters for the three-body SW potential used by GULP are shown in **Table 44**. Parameters

	A (eV)	ρ (\AA)	B (\AA^4)	r_{\min} (\AA)	r_{\max} (\AA)
V—Te	5.410	1.112	25.032	0.0	3.520

Table 43. Two-body SW potential parameters for single-layer 1H-VTe₂ used by GULP [8] as expressed in Eq. (3).

	K (eV)	θ_0 ($^\circ$)	ρ_1 (\AA)	ρ_2 (\AA)	$r_{\min 12}$ (\AA)	$r_{\max 12}$ (\AA)	$r_{\min 13}$ (\AA)	$r_{\max 13}$ (\AA)	$r_{\min 23}$ (\AA)	$r_{\max 23}$ (\AA)
$\theta_{\text{V—Te—Te}}$	29.743	81.708	1.112	1.112	0.0	3.520	0.0	3.520	0.0	4.203
$\theta_{\text{V—Te—Te}'}$	29.716	81.891	1.112	1.112	0.0	3.520	0.0	3.520	0.0	4.203
$\theta_{\text{Te—V—V}}$	29.743	81.708	1.112	1.112	0.0	3.520	0.0	3.520	0.0	4.203

The angle θ_{ijk} in the first line indicates the bending energy for the angle with atom i as the apex.

Table 44. Three-body SW potential parameters for single-layer 1H-VTe₂ used by GULP [8] as expressed in Eq. (4).

	ϵ (eV)	σ (\AA)	a	λ	γ	$\cos \theta_0$	A_L	B_L	p	q	Tol
V ₁ —Te ₁ —Te ₁	1.000	1.112	3.164	0.000	1.000	0.000	5.410	16.345	4	0	0.0
V ₁ —Te ₁ —Te ₃	1.000	0.000	0.000	29.743	1.000	0.144	0.000	0.000	4	0	0.0
V ₁ —Te ₁ —Te ₂	1.000	0.000	0.000	29.716	1.000	0.141	0.000	0.000	4	0	0.0
Te ₁ —V ₁ —V ₃	1.000	0.000	0.000	29.743	1.000	0.144	0.000	0.000	4	0	0.0

Atom types in the first column are displayed in **Figure 2** (with M = V and X = Te).

Table 45. SW potential parameters for single-layer 1H-VTe₂ used by LAMMPS [9] as expressed in Eqs. (9) and (10).

for the SW potential used by LAMMPS are listed in **Table 45**. We note that 12 atom types have been introduced for the simulation of the single-layer 1H-VTe₂ using LAMMPS, because the angles around atom V in **Figure 1** (with M = V and X = Te) are not distinguishable in LAMMPS. We have suggested two options to differentiate these angles by implementing some additional constraints in LAMMPS, which can be accomplished by modifying the source file of LAMMPS [13, 14]. According to our experience, it is not so convenient for some users to implement these constraints and recompile the LAMMPS package. Hence, in the present work, we differentiate the angles by introducing more atom types, so it is not necessary to modify the LAMMPS package. **Figure 2** (with M = V and X = Te) shows that, for 1H-VTe₂, we can differentiate these angles around the V atom by assigning these six neighboring Te atoms with different atom types. It can be found that 12 atom types are necessary for the purpose of differentiating all 6 neighbors around 1 V atom.

We use LAMMPS to perform MD simulations for the mechanical behavior of the single-layer 1H-VTe₂ under uniaxial tension at 1 and 300 K. **Figure 20** shows the stress-strain curve for the tension of a single-layer 1H-VTe₂ of dimension 100 × 100 Å. Periodic boundary conditions are applied in both armchair and zigzag directions. The single-layer 1H-VTe₂ is stretched uniaxially along the armchair or zigzag direction. The stress is calculated without involving the actual thickness of the quasi-two-dimensional structure of the single-layer 1H-VTe₂. The

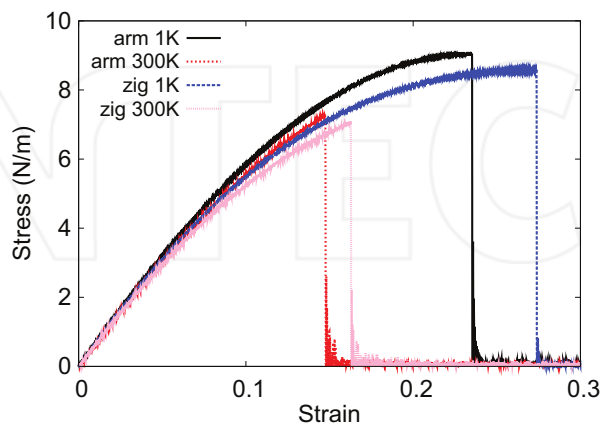


Figure 20. Stress-strain for single-layer 1H-VTe₂ of dimension 100×100 Å along the armchair and zigzag directions.

Young's modulus can be obtained by a linear fitting of the stress-strain relation in the small strain range of [0, 0.01]. The Young's modulus is 68.1 and 66.8 N/m along the armchair and zigzag directions, respectively. The Young's modulus is essentially isotropic in the armchair and zigzag directions. The Poisson's ratio from the VFF model and the SW potential is $\nu_{xy} = \nu_{yx} = 0.28$.

There is no available value for the nonlinear quantities in the single-layer 1H-VTe₂. We have thus used the nonlinear parameter $B = 0.5d^4$ in Eq. (5), which is close to the value of B in most materials. The value of the third-order nonlinear elasticity D can be extracted by fitting the stress-strain relation to the function $\sigma = E\epsilon + \frac{1}{2}D\epsilon^2$ with E as the Young's modulus. The values of D from the present SW potential are -237.4 and -260.4 N/m along the armchair and zigzag directions, respectively. The ultimate stress is about 9.0 N/m at the ultimate strain of 0.23 in the armchair direction at the low temperature of 1 K. The ultimate stress is about 8.6 N/m at the ultimate strain of 0.27 in the zigzag direction at the low temperature of 1 K.

12. 1H-CrO₂

Most existing theoretical studies on the single-layer 1H-CrO₂ are based on the first-principles calculations. In this section, we will develop the SW potential for the single-layer 1H-CrO₂.

The structure for the single-layer 1H-CrO₂ is shown in **Figure 1** (with M = Cr and X = O). Each Cr atom is surrounded by six O atoms. These O atoms are categorized into the top group (e.g., atoms 1, 3, and 5) and bottom group (e.g., atoms 2, 4, and 6). Each O atom is connected to three Cr atoms. The structural parameters are from the first-principles calculations [12], including the lattice constant $a = 2.58$ Å and the bond length $d_{Cr-O} = 1.88$ Å. The resultant angles are $\theta_{CrOO} = \theta_{OCrCr} = 86.655^\circ$ and $\theta_{CrOO'} = 75.194^\circ$, in which atoms O and O' are from different (top or bottom) groups.

Table 46 shows four VFF terms for the single-layer 1H-CrO₂; one of which is the bond stretching interaction shown by Eq. (1), while the other three terms are the angle bending interaction shown by Eq. (2). These force constant parameters are determined by fitting to the acoustic branches in the phonon dispersion along the Γ M as shown in **Figure 21(a)**. The *ab initio* calculations for the phonon dispersion are from [12]. **Figure 21(b)** shows that the VFF

VFF type	Bond stretching		Angle bending	
Expression	$\frac{1}{2}K_{Cr-O}(\Delta r)^2$	$\frac{1}{2}K_{Cr-O-O}(\Delta\theta)^2$	$\frac{1}{2}K_{Cr-O-O'}(\Delta\theta)^2$	$\frac{1}{2}K_{O-Cr-Cr}(\Delta\theta)^2$
Parameter	12.881	8.039	8.039	8.039
r_0 or θ_0	1.880	86.655	75.194	86.655

The second line gives an explicit expression for each VFF term. The third line is the force constant parameters. Parameters are in the unit of eV/Å² for the bond stretching interaction and in the unit of eV for the angle bending interaction. The fourth line gives the initial bond length (in the unit of Å) for the bond stretching interaction and the initial angle (in the unit of degrees) for the angle bending interaction. The angle θ_{ijk} has atom *i* as the apex.

Table 46. The VFF model for single-layer 1H-CrO₂.

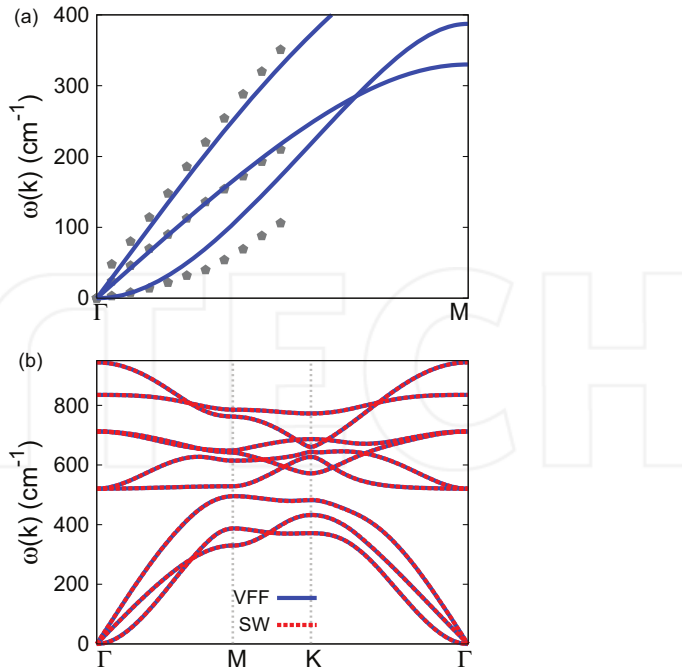


Figure 21. Phonon spectrum for single-layer 1H-CrO₂. (a) Phonon dispersion along the Γ M direction in the Brillouin zone. The results from the VFF model (lines) are comparable with the *ab initio* results (pentagons) from [12]. (b) The phonon dispersion from the SW potential is exactly the same as that from the VFF model.

model and the SW potential give exactly the same phonon dispersion, as the SW potential is derived from the VFF model.

The parameters for the two-body SW potential used by GULP are shown in **Table 47**. The parameters for the three-body SW potential used by GULP are shown in **Table 48**. Some representative parameters for the SW potential used by LAMMPS are listed in **Table 49**. We

	A (eV)	ρ (Å)	B (Å ⁴)	r_{\min} (Å)	r_{\max} (Å)
Cr—O	6.343	0.916	6.246	0.0	2.536

Table 47. Two-body SW potential parameters for single-layer 1H-CrO₂ used by GULP [8] as expressed in Eq. (3).

	K (eV)	θ_0 (°)	ρ_1 (Å)	ρ_2 (Å)	$r_{\min 12}$ (Å)	$r_{\max 12}$ (Å)	$r_{\min 13}$ (Å)	$r_{\max 13}$ (Å)	$r_{\min 23}$ (Å)	$r_{\max 23}$ (Å)
$\theta_{\text{Cr—O—O}}$	65.805	86.655	0.916	0.916	0.0	2.536	0.0	2.536	0.0	3.016
$\theta_{\text{Cr—O—O'}}$	70.163	75.194	0.916	0.916	0.0	2.536	0.0	2.536	0.0	3.016
$\theta_{\text{O—Cr—Cr}}$	65.805	86.655	0.916	0.916	0.0	2.536	0.0	2.536	0.0	3.016

The angle θ_{ijk} in the first line indicates the bending energy for the angle with atom i as the apex.

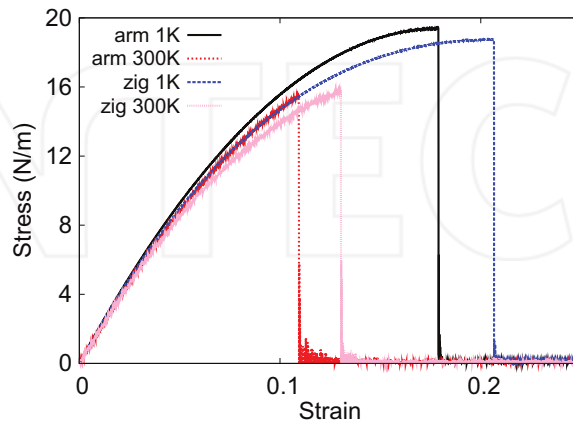
Table 48. Three-body SW potential parameters for single-layer 1H-CrO₂ used by GULP [8] as expressed in Eq. (4).

	ϵ (eV)	σ (\AA)	a	λ	γ	$\cos \theta_0$	A_L	B_L	p	q	Tol
$\text{Cr}_1-\text{O}_1-\text{O}_1$	1.000	0.916	2.769	0.000	1.000	0.000	6.242	8.871	4	0	0.0
$\text{Cr}_1-\text{O}_1-\text{O}_3$	1.000	0.000	0.000	65.805	1.000	0.058	0.000	0.000	4	0	0.0
$\text{Cr}_1-\text{O}_1-\text{O}_2$	1.000	0.000	0.000	70.163	1.000	0.256	0.000	0.000	4	0	0.0
$\text{O}_1-\text{Cr}_1-\text{Cr}_3$	1.000	0.000	0.000	65.805	1.000	0.058	0.000	0.000	4	0	0.0

Table 49. SW potential parameters for single-layer 1H-CrO₂ used by LAMMPS [9] as expressed in Eqs. (9) and (10).

note that 12 atom types have been introduced for the simulation of the single-layer 1H-CrO₂ using LAMMPS, because the angles around atom Cr in **Figure 1** (with M = Cr and X = O) are not distinguishable in LAMMPS. We have suggested two options to differentiate these angles by implementing some additional constraints in LAMMPS, which can be accomplished by modifying the source file of LAMMPS [13, 14]. According to our experience, it is not so convenient for some users to implement these constraints and recompile the LAMMPS package. Hence, in the present work, we differentiate the angles by introducing more atom types, so it is not necessary to modify the LAMMPS package. **Figure 2** (with M = Cr and X = O) shows that, for 1H-CrO₂, we can differentiate these angles around the Cr atom by assigning these six neighboring O atoms with different atom types. It can be found that 12 atom types are necessary for the purpose of differentiating all 6 neighbors around 1 Cr atom.

We use LAMMPS to perform MD simulations for the mechanical behavior of the single-layer 1H-CrO₂ under uniaxial tension at 1 and 300 K. **Figure 22** shows the stress-strain curve for the tension of a single-layer 1H-CrO₂ of dimension 100 × 100 Å. Periodic boundary conditions are applied in both armchair and zigzag directions. The single-layer 1H-CrO₂ is stretched uniaxially along the armchair or zigzag direction. The stress is calculated without involving the actual thickness of the quasi-two-dimensional structure of the single-layer 1H-CrO₂. The Young's modulus can be obtained by a linear fitting of the stress-strain relation in the small strain range of [0, 0.01]. The Young's modulus is 210.6 and 209.0 N/m along the armchair and

**Figure 22.** Stress-strain for single-layer 1H-CrO₂ of dimension 100×100 Å along the armchair and zigzag directions.

zigzag directions, respectively. The Young's modulus is essentially isotropic in the armchair and zigzag directions. The Poisson's ratio from the VFF model and the SW potential is $\nu_{xy} = \nu_{yx} = 0.13$.

There is no available value for nonlinear quantities in the single-layer 1H-CrO₂. We have thus used the nonlinear parameter $B = 0.5d^4$ in Eq. (5), which is close to the value of B in most materials. The value of the third-order nonlinear elasticity D can be extracted by fitting the stress-strain relation to the function $\sigma = E\epsilon + \frac{1}{2}D\epsilon^2$ with E as the Young's modulus. The values of D from the present SW potential are -1127.7 and -1185.8 N/m along the armchair and zigzag directions, respectively. The ultimate stress is about 19.4 N/m at the ultimate strain of 0.18 in the armchair direction at the low temperature of 1 K. The ultimate stress is about 18.7 N/m at the ultimate strain of 0.20 in the zigzag direction at the low temperature of 1 K.

13. 1H-CrS₂

Most existing theoretical studies on the single-layer 1H-CrS₂ are based on the first-principles calculations. In this section, we will develop both VFF model and the SW potential for the single-layer 1H-CrS₂.

The structure for the single-layer 1H-CrS₂ is shown in **Figure 1** (with M = Cr and X = S). Each Cr atom is surrounded by six S atoms. These S atoms are categorized into the top group (e.g., atoms 1, 3, and 5) and bottom group (e.g., atoms 2, 4, and 6). Each S atom is connected to three Cr atoms. The structural parameters are from [17], including the lattice constant $a = 2.99$ Å and the bond length $d_{Cr-S} = 2.254$ Å. The resultant angles are $\theta_{CrSS} = \theta_{SCrCr} = 83.099^\circ$ and $\theta_{CrSS'} = 80.031^\circ$, in which atoms S and S' are from different (top or bottom) groups.

Table 50 shows four VFF terms for the 1H-CrS₂; one of which is the bond stretching interaction shown by Eq. (1), while the other three terms are the angle bending interaction shown by Eq. (2). These force constant parameters are determined by fitting to the three acoustic branches in the phonon dispersion along the TM as shown in **Figure 23(a)**. The *ab initio* calculations for the phonon dispersion are from [17]. Similar phonon dispersion can also be found in other *ab initio*

VFF type	Bond stretching	Angle bending		
Expression	$\frac{1}{2}K_{Cr-S}(\Delta r)^2$	$\frac{1}{2}K_{Cr-S-S}(\Delta\theta)^2$	$\frac{1}{2}K_{Cr-S-S'}(\Delta\theta)^2$	$\frac{1}{2}K_{S-Cr-Cr}(\Delta\theta)^2$
Parameter	8.752	4.614	4.614	4.614
r_0 or θ_0	2.254	83.099	80.031	83.099

The second line gives an explicit expression for each VFF term. The third line is the force constant parameters. Parameters are in the unit of eV/Å² for the bond stretching interaction and in the unit of eV for the angle bending interaction. The fourth line gives the initial bond length (in the unit of Å) for the bond stretching interaction and the initial angle (in the unit of degrees) for the angle bending interaction. The angle θ_{ijk} has atom i as the apex.

Table 50. The VFF model for single-layer 1H-CrS₂.

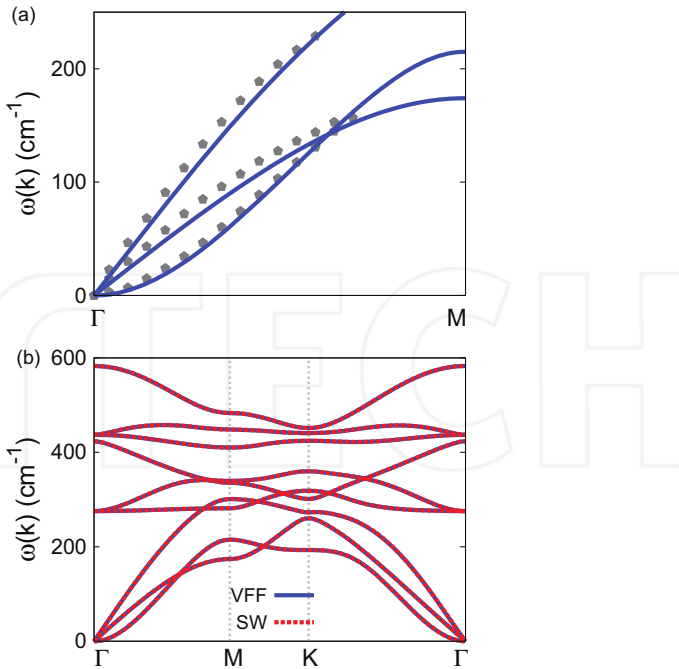


Figure 23. Phonon dispersion for single-layer 1H-CrS₂. (a) The VFF model is fitted to the three acoustic branches in the long wave limit along the Γ M direction. The *ab initio* results (gray pentagons) are from [17]. (b) The VFF model (blue lines) and the SW potential (red lines) give the same phonon dispersion for single-layer 1H-CrS₂ along Γ MK Γ .

calculations [12]. **Figure 23(b)** shows that the VFF model and the SW potential give exactly the same phonon dispersion, as the SW potential is derived from the VFF model.

The parameters for the two-body SW potential used by GULP are shown in **Table 51**. The parameters for the three-body SW potential used by GULP are shown in **Table 52**. Parameters

	A (eV)	ρ (\AA)	B (\AA^4)	r_{\min} (\AA)	r_{\max} (\AA)
Cr—S	5.544	0.985	12.906	0.0	2.999

Table 51. Two-body SW potential parameters for single-layer 1HCrS₂ used by GULP [8] as expressed in Eq. (3).

	K (eV)	θ_0 (°)	ρ_1 (\AA)	ρ_2 (\AA)	$r_{\min 12}$ (\AA)	$r_{\max 12}$ (\AA)	$r_{\min 13}$ (\AA)	$r_{\max 13}$ (\AA)	$r_{\min 23}$ (\AA)	$r_{\max 23}$ (\AA)
$\theta_{\text{Cr-S-S}}$	32.963	83.099	0.985	0.985	0.0	2.999	0.0	2.999	0.0	3.577
$\theta_{\text{Cr-S-S'}}$	33.491	80.031	0.985	0.985	0.0	2.999	0.0	2.999	0.0	3.577
$\theta_{\text{S-Cr-Cr}}$	32.963	83.099	0.985	0.985	0.0	2.999	0.0	2.999	0.0	3.577

The angle θ_{ijk} in the first line indicates the bending energy for the angle with atom i as the apex.

Table 52. Three-body SW potential parameters for single-layer 1H-CrS₂ used by GULP [8] as expressed in Eq. (4).

	ϵ (eV)	σ (\AA)	a	λ	γ	$\cos \theta_0$	A_L	B_L	p	q	Tol
Cr ₁ —S ₁ —S ₁	1.000	0.985	3.043	0.000	1.000	0.000	5.544	13.683	4	0	0.0
Cr ₁ —S ₁ —S ₃	1.000	0.000	0.000	32.963	1.000	0.120	0.000	0.000	4	0	0.0
Cr ₁ —S ₁ —S ₂	1.000	0.000	0.000	33.491	1.000	0.173	0.000	0.000	4	0	0.0
S ₁ —Cr ₁ —Cr ₃	1.000	0.000	0.000	32.963	1.000	0.120	0.000	0.000	4	0	0.0

Atom types in the first column are displayed in **Figure 2** (with M = Cr and X = S).

Table 53. SW potential parameters for single-layer 1H-CrS₂ used by LAMMPS [9] as expressed in Eqs. (9) and (10).

for the SW potential used by LAMMPS are listed in **Table 53**. We note that 12 atom types have been introduced for the simulation of the single-layer 1H-CrS₂ using LAMMPS, because the angles around atom Cr in **Figure 1** (with M = Cr and X = S) are not distinguishable in LAMMPS. We have suggested two options to differentiate these angles by implementing some additional constraints in LAMMPS, which can be accomplished by modifying the source file of LAMMPS [13, 14]. According to our experience, it is not so convenient for some users to implement these constraints and recompile the LAMMPS package. Hence, in the present work, we differentiate the angles by introducing more atom types, so it is not necessary to modify the LAMMPS package. **Figure 2** (with M = Cr and X = S) shows that, for 1H-CrS₂, we can differentiate these angles around the Cr atom by assigning these six neighboring S atoms with different atom types. It can be found that 12 atom types are necessary for the purpose of differentiating all 6 neighbors around 1 Cr atom.

We use LAMMPS to perform MD simulations for the mechanical behavior of the single-layer 1H-CrS₂ under uniaxial tension at 1 and 300 K. **Figure 24** shows the stress-strain curve for the tension of a single-layer 1H-CrS₂ of dimension 100 × 100 Å. Periodic boundary conditions are applied in both armchair and zigzag directions. The single-layer 1H-CrS₂ is stretched uniaxially along the armchair or zigzag direction. The stress is calculated without involving the actual thickness of the quasi-two-dimensional structure of the single-layer 1H-CrS₂. The

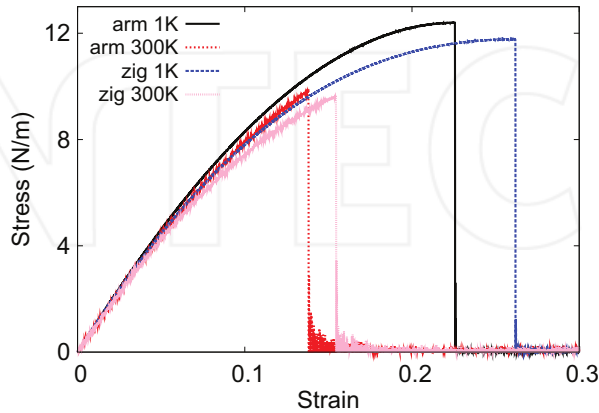


Figure 24. Stress-strain for single-layer 1H-CrS₂ of dimension 100 × 100 Å along the armchair and zigzag directions.

Young's modulus can be obtained by a linear fitting of the stress-strain relation in the small strain range of [0, 0.01]. The Young's modulus is 98.4 and 97.8 N/m along the armchair and zigzag directions, respectively. The Young's modulus is essentially isotropic in the armchair and zigzag directions. These values are in reasonably agreement with the *ab initio* results, e.g., 112.0 N/m from [18], or 111.9 N/m from [19]. The Poisson's ratio from the VFF model and the SW potential is $\nu_{xy} = \nu_{yx} = 0.26$, which agrees with the *ab initio* value of 0.27 [18, 19].

There is no available value for the nonlinear quantities in the single-layer 1H-CrS₂. We have thus used the nonlinear parameter $B = 0.5d^4$ in Eq. (5), which is close to the value of B in most materials. The value of the third-order nonlinear elasticity D can be extracted by fitting the stress-strain relation to the function $\sigma = E\epsilon + \frac{1}{2}D\epsilon^2$ with E as the Young's modulus. The values of D from the present SW potential are -364.8 and -409.3 N/m along the armchair and zigzag directions, respectively. The ultimate stress is about 12.4 N/m at the ultimate strain of 0.22 in the armchair direction at the low temperature of 1 K. The ultimate stress is about 11.8 N/m at the ultimate strain of 0.26 in the zigzag direction at the low temperature of 1 K.

14. 1H-CrSe₂

Most existing theoretical studies on the single-layer 1H-CrSe₂ are based on the first-principles calculations. In this section, we will develop both VFF model and the SW potential for the single-layer 1H-CrSe₂.

The structure for the single-layer 1H-CrSe₂ is shown in **Figure 1** (with M = Cr and X = Se). Each Cr atom is surrounded by six Se atoms. These Se atoms are categorized into the top group (e.g., atoms 1, 3, and 5) and bottom group (e.g., atoms 2, 4, and 6). Each Se atom is connected to three Cr atoms. The structural parameters are from [12], including the lattice constant $a = 3.13$ Å and the bond length $d_{Cr-Se} = 2.38$ Å. The resultant angles are $\theta_{CrSeSe} = \theta_{SeCrCr} = 82.229^\circ$ and $\theta_{CrSeSe'} = 81.197^\circ$, in which atoms Se and Se' are from different (top or bottom) groups.

Table 54 shows four VFF terms for the 1H-CrSe₂; one of which is the bond stretching interaction shown by Eq. (1), while the other three terms are the angle bending interaction shown by Eq. (2). These force constant parameters are determined by fitting to the three acoustic

VFF type	Bond stretching	Angle bending		
Expression	$\frac{1}{2}K_{Cr-Se}(\Delta r)^2$	$\frac{1}{2}K_{Cr-Se-Se}(\Delta\theta)^2$	$\frac{1}{2}K_{Cr-Se-Se'}(\Delta\theta)^2$	$\frac{1}{2}K_{Se-Cr-Cr}(\Delta\theta)^2$
Parameter	9.542	4.465	4.465	4.465
r_0 or θ_0	2.380	82.229	81.197	82.229

The second line gives an explicit expression for each VFF term. The third line is the force constant parameters. Parameters are in the unit of eV/Å² for the bond stretching interaction and in the unit of eV for the angle bending interaction. The fourth line gives the initial bond length (in the unit of Å) for the bond stretching interaction and the initial angle (in the unit of degrees) for the angle bending interaction. The angle θ_{ijk} has atom i as the apex.

Table 54. The VFF model for single-layer 1H-CrSe₂.

branches in the phonon dispersion along the Γ M as shown in **Figure 25(a)**. The *ab initio* calculations for the phonon dispersion are from [12]. **Figure 25(b)** shows that the VFF model and the SW potential give exactly the same phonon dispersion, as the SW potential is derived from the VFF model.

The parameters for the two-body SW potential used by GULP are shown in **Table 55**. The parameters for the three-body SW potential used by GULP are shown in **Table 56**. Parameters for the SW potential used by LAMMPS are listed in **Table 57**. We note that 12 atom types have been introduced for the simulation of the single-layer 1H-CrSe₂ using LAMMPS, because the angles around atom Cr in **Figure 1** (with M = Cr and X = Se) are not distinguishable in LAMMPS. We have suggested two options to differentiate these angles by implementing some additional constraints in LAMMPS, which can be accomplished by modifying the source file of LAMMPS [13, 14]. According to our experience, it is not so convenient for some users to

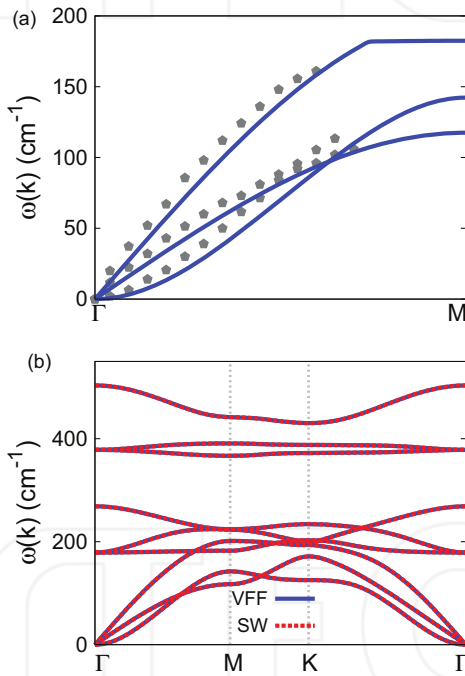


Figure 25. Phonon dispersion for single-layer 1H-CrSe₂. (a) The VFF model is fitted to the three acoustic branches in the long wave limit along the Γ M direction. The *ab initio* results (gray pentagons) are from [21]. (b) The VFF model (blue lines) and the SW potential (red lines) give the same phonon dispersion for single-layer 1H-CrSe₂ along Γ MKG.

	A (eV)	ρ (\AA)	B (\AA^4)	r_{\min} (\AA)	r_{\max} (\AA)
Cr—Se	6.581	1.012	16.043	0.0	3.156

Table 55. Two-body SW potential parameters for single-layer 1H-CrSe₂ used by GULP [8] as expressed in Eq. (3).

	K (eV)	θ_0 ($^\circ$)	ρ_1 (\AA)	ρ_2 (\AA)	$r_{\min 12}$ (\AA)	$r_{\max 12}$ (\AA)	$r_{\min 13}$ (\AA)	$r_{\max 13}$ (\AA)	$r_{\min 23}$ (\AA)	$r_{\max 23}$ (\AA)
$\theta_{\text{Cr--Se--Se}}$	30.881	82.229	1.012	1.012	0.0	3.156	0.0	3.156	0.0	3.767
$\theta_{\text{Cr--Se--Se'}}$	31.044	81.197	1.012	1.012	0.0	3.156	0.0	3.156	0.0	3.767
$\theta_{\text{Se--Cr--Cr}}$	30.881	82.229	1.012	1.012	0.0	3.156	0.0	3.156	0.0	3.767

The angle θ_{ijk} in the first line indicates the bending energy for the angle with atom i as the apex.

Table 56. Three-body SW potential parameters for single-layer 1H-CrSe₂ used by GULP [8] as expressed in Eq. (4).

	ϵ (eV)	σ (\AA)	a	λ	γ	$\cos \theta_0$	A_L	B_L	p	q	Tol
Cr ₁ --Se ₁ --Se ₁	1.000	1.012	3.118	0.000	1.000	0.000	6.581	15.284	4	0	0.0
Cr ₁ --Se ₁ --Se ₃	1.000	0.000	0.000	30.881	1.000	0.135	0.000	0.000	4	0	0.0
Cr ₁ --Se ₁ --Se ₂	1.000	0.000	0.000	31.044	1.000	0.153	0.000	0.000	4	0	0.0
Se ₁ --Cr ₁ --Cr ₃	1.000	0.000	0.000	30.881	1.000	0.135	0.000	0.000	4	0	0.0

Atom types in the first column are displayed in Figure 2 (with M = Cr and X = Se).

Table 57. SW potential parameters for single-layer 1H-CrSe₂ used by LAMMPS [9] as expressed in Eqs. (9) and (10).

implement these constraints and recompile the LAMMPS package. Hence, in the present work, we differentiate the angles by introducing more atom types, so it is not necessary to modify the LAMMPS package. **Figure 2** (with M = Cr and X = Se) shows that, for 1H-CrSe₂, we can differentiate these angles around the Cr atom by assigning these six neighboring Se atoms with different atom types. It can be found that 12 atom types are necessary for the purpose of differentiating all 6 neighbors around 1 Cr atom.

We use LAMMPS to perform MD simulations for the mechanical behavior of the single-layer 1H-CrSe₂ under uniaxial tension at 1 and 300 K. **Figure 26** shows the stress-strain curve for the

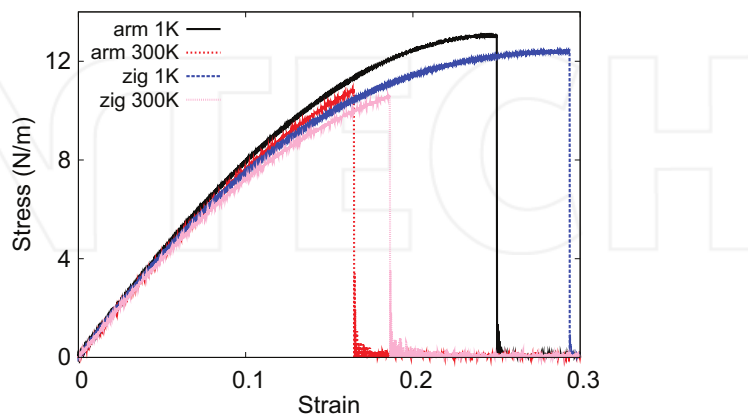


Figure 26. Stress-strain for single-layer 1H-CrSe₂ of dimension 100 × 100 \AA along the armchair and zigzag directions.

tension of a single-layer 1H-CrSe₂ of dimension 100 × 100 Å. Periodic boundary conditions are applied in both armchair and zigzag directions. The single-layer 1H-CrSe₂ is stretched uniaxially along the armchair or zigzag direction. The stress is calculated without involving the actual thickness of the quasi-two-dimensional structure of the single-layer 1H-CrSe₂. The Young's modulus can be obtained by a linear fitting of the stress-strain relation in the small strain range of [0, 0.01]. The Young's modulus is 90.0 and 89.0 N/m along the armchair and zigzag directions, respectively. The Young's modulus is essentially isotropic in the armchair and zigzag directions. These values are in reasonably agreement with the *ab initio* results, e.g., 88.0 N/m from [18], or 87.9 N/m from [19]. The Poisson's ratio from the VFF model and the SW potential is $\nu_{xy} = \nu_{yx} = 0.30$, which agrees with the *ab initio* value of 0.30 [18, 19].

There is no available value for the nonlinear quantities in the single-layer 1H-CrSe₂. We have thus used the nonlinear parameter $B = 0.5d^4$ in Eq. (5), which is close to the value of B in most two-dimensional atomic layered materials. The value of the third-order nonlinear elasticity D can be extracted by fitting the stress-strain relation to the function $\sigma = E\epsilon + \frac{1}{2}D\epsilon^2$ with E as the Young's modulus. The values of D from the present SW potential are -279.6 and -318.8 N/m along the armchair and zigzag directions, respectively. The ultimate stress is about 13.0 N/m at the ultimate strain of 0.25 in the armchair direction at the low temperature of 1 K. The ultimate stress is about 12.4 N/m at the ultimate strain of 0.29 in the zigzag direction at the low temperature of 1 K.

15. 1H-CrTe₂

Most existing theoretical studies on the single-layer 1H-CrTe₂ are based on the first-principles calculations. In this section, we will develop both VFF model and the SW potential for the single-layer 1H-CrTe₂.

The structure for the single-layer 1H-CrTe₂ is shown in **Figure 1** (with M = Cr and X = Te). Each Cr atom is surrounded by six Te atoms. These Te atoms are categorized into the top group (e.g., atoms 1, 3, and 5) and bottom group (e.g., atoms 2, 4, and 6). Each Te atom is connected to three Cr atoms. The structural parameters are from [12], including the lattice constant $a = 3.39$ Å and the bond length $d_{Cr-Te} = 2.58$ Å. The resultant angles are $\theta_{CrTeTe} = \theta_{TeCrCr} = 82.139^\circ$ and $\theta_{CrTeTe'} = 81.316^\circ$, in which atoms Te and Te' are from different (top or bottom) groups.

Table 58 shows three VFF terms for the 1H-CrTe₂; one of which is the bond stretching interaction shown by Eq. (1), while the other two terms are the angle bending interaction shown by Eq. (2). These force constant parameters are determined by fitting to the three acoustic branches in the phonon dispersion along the ΓM as shown in **Figure 27(a)**. The *ab initio* calculations for the phonon dispersion are from [12]. **Figure 27(b)** shows that the VFF model and the SW potential give exactly the same phonon dispersion, as the SW potential is derived from the VFF model.

The parameters for the two-body SW potential used by GULP are shown in **Table 59**. The parameters for the three-body SW potential used by GULP are shown in **Table 60**. Parameters for the SW potential used by LAMMPS are listed in **Table 61**. We note that 12 atom types have

VFF type	Bond stretching	Angle bending	
Expression	$\frac{1}{2}K_{\text{Cr}-\text{Te}}(\Delta r)^2$	$\frac{1}{2}K_{\text{Cr}-\text{Te}-\text{Te}}(\Delta\theta)^2$	$\frac{1}{2}K_{\text{Cr}-\text{Te}-\text{Te}'}(\Delta\theta)^2$
Parameter	8.197	4.543	4.543
r_0 or θ_0	2.580	82.139	81.316

The second line gives an explicit expression for each VFF term. The third line is the force constant parameters. Parameters are in the unit of eV/Å² for the bond stretching interaction and in the unit of eV for the angle bending interaction. The fourth line gives the initial bond length (in the unit of Å) for the bond stretching interaction and the initial angle (in the unit of degrees) for the angle bending interaction. The angle θ_{ijk} has atom i as the apex.

Table 58. The VFF model for single-layer 1H-CrTe₂.

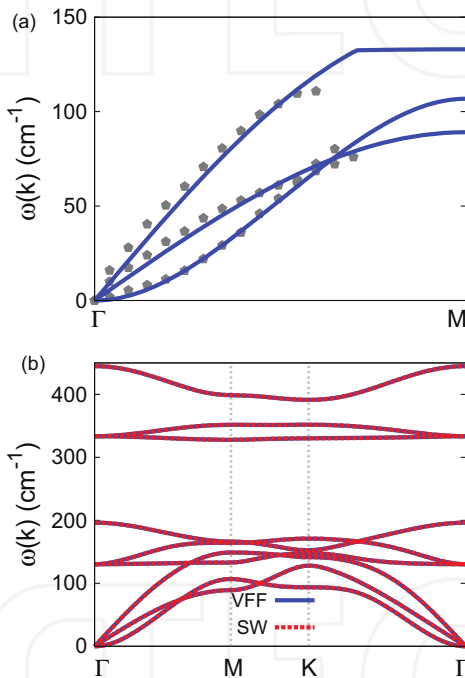


Figure 27. Phonon dispersion for single-layer 1H-CrTe₂. (a) The VFF model is fitted to the three acoustic branches in the long wave limit along the Γ M direction. The *ab initio* results (gray pentagons) are from [12]. (b) The VFF model (blue lines) and the SW potential (red lines) give the same phonon dispersion for single-layer 1H-CrTe₂ along Γ MK Γ .

	A (eV)	ρ (Å)	B (Å ⁴)	r_{\min} (Å)	r_{\max} (Å)
Cr—Te	6.627	1.094	22.154	0.0	3.420

Table 59. Two-body SW potential parameters for single-layer 1H-CrTe₂ used by GULP [8] as expressed in Eq. (3).

	K (eV)	θ_0 ($^{\circ}$)	ρ_1 (\AA)	ρ_2 (\AA)	$r_{\min 12}$ (\AA)	$r_{\max 12}$ (\AA)	$r_{\min 13}$ (\AA)	$r_{\max 13}$ (\AA)	$r_{\min 23}$ (\AA)	$r_{\max 23}$ (\AA)
$\theta_{\text{Cr}-\text{Te}-\text{Te}}$	31.316	82.139	1.094	1.094	0.0	3.420	0.0	3.420	0.0	4.082
$\theta_{\text{Cr}-\text{Te}-\text{Te}'}$	31.447	81.316	1.094	1.094	0.0	3.420	0.0	3.420	0.0	4.082
$\theta_{\text{Te}-\text{Cr}-\text{Cr}}$	31.316	82.139	1.094	1.094	0.0	3.420	0.0	3.420	0.0	4.082

The angle θ_{ijk} in the first line indicates the bending energy for the angle with atom i as the apex.

Table 60. Three-body SW potential parameters for single-layer 1H-CrTe₂ used by GULP [8] as expressed in Eq. (4).

	ϵ (eV)	σ (\AA)	a	λ	γ	$\cos \theta_0$	A_L	B_L	p	q	Tol
Cr ₁ —Te ₁ —Te ₁	1.000	1.094	3.126	0.000	1.000	0.000	6.627	15.461	4	0	0.0
Cr ₁ —Te ₁ —Te ₃	1.000	0.000	0.000	31.316	1.000	0.137	0.000	0.000	4	0	0.0
Cr ₁ —Te ₁ —Te ₂	1.000	0.000	0.000	31.447	1.000	0.151	0.000	0.000	4	0	0.0
Te ₁ —Cr ₁ —Cr ₃	1.000	0.000	0.000	31.316	1.000	0.137	0.000	0.000	4	0	0.0

Atom types in the first column are displayed in **Figure 2** (with M = Cr and X = Te).

Table 61. SW potential parameters for single-layer 1H-CrTe₂ used by LAMMPS [9] as expressed in Eqs. (9) and (10).

been introduced for the simulation of the single-layer 1H-CrTe₂ using LAMMPS, because the angles around atom Cr in **Figure 1** (with M = Cr and X = Te) are not distinguishable in LAMMPS. We have suggested two options to differentiate these angles by implementing some additional constraints in LAMMPS, which can be accomplished by modifying the source file of LAMMPS [13, 14]. According to our experience, it is not so convenient for some users to implement these constraints and recompile the LAMMPS package. Hence, in the present work, we differentiate the angles by introducing more atom types, so it is not necessary to modify the LAMMPS package. **Figure 2** (with M = Cr and X = Te) shows that, for 1H-CrTe₂, we can differentiate these angles around the Cr atom by assigning these six neighboring Te atoms with different atom types. It can be found that 12 atom types are necessary for the purpose of differentiating all 6 neighbors around 1 Cr atom.

We use LAMMPS to perform MD simulations for the mechanical behavior of the single-layer 1H-CrTe₂ under uniaxial tension at 1 and 300 K. **Figure 28** shows the stress-strain curve for the tension of a single-layer 1H-CrTe₂ of dimension 100 × 100 \AA . Periodic boundary conditions are applied in both armchair and zigzag directions. The single-layer 1H-CrTe₂ is stretched uniaxially along the armchair or zigzag direction. The stress is calculated without involving the actual thickness of the quasi-two-dimensional structure of the single-layer 1H-CrTe₂. The Young's modulus can be obtained by a linear fitting of the stress-strain relation in the small strain range of [0, 0.01]. The Young's modulus is 77.2 and 76.4 N/m along the armchair and zigzag directions, respectively. The Young's modulus is essentially isotropic in the armchair and zigzag directions. These values are in reasonably agreement with the *ab initio* results, e.g., 63.9 N/m from [18, 19]. The Poisson's ratio from the VFF model and the SW potential is $\nu_{xy} = \nu_{yx} = 0.30$, which agrees with the *ab initio* value of 0.30 [18, 19].

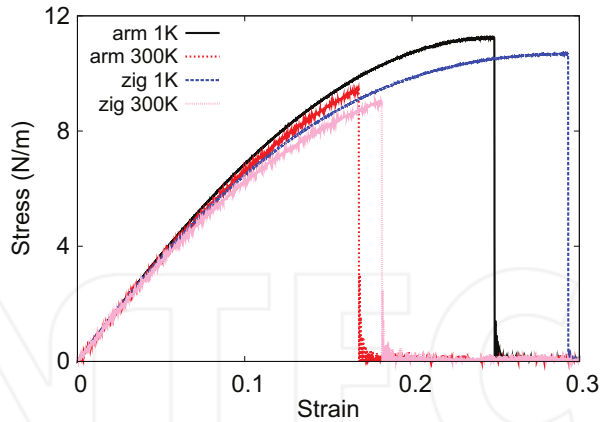


Figure 28. Stress-strain for single-layer 1H-CrTe₂ of dimension 100 × 100 Å along the armchair and zigzag directions.

There is no available value for the nonlinear quantities in the single-layer 1H-CrTe₂. We have thus used the nonlinear parameter $B = 0.5d^4$ in Eq. (5), which is close to the value of B in most two-dimensional atomic layered materials. The value of the third-order nonlinear elasticity D can be extracted by fitting the stress-strain relation to the function $\sigma = E\epsilon + \frac{1}{2}D\epsilon^2$ with E as the Young's modulus. The values of D from the present SW potential are -237.1 and -280.8 N/m along the armchair and zigzag directions, respectively. The ultimate stress is about 11.2 N/m at the ultimate strain of 0.25 in the armchair direction at the low temperature of 1 K. The ultimate stress is about 10.7 N/m at the ultimate strain of 0.29 in the zigzag direction at the low temperature of 1 K.

16. 1H-MnO₂

Most existing theoretical studies on the single-layer 1H-MnO₂ are based on the first-principles calculations. In this section, we will develop the SW potential for the single-layer 1H-MnO₂.

The structure for the single-layer 1H-MnO₂ is shown in **Figure 1** (with M = Mn and X = O). Each Mn atom is surrounded by six O atoms. These O atoms are categorized into the top group (e.g., atoms 1, 3, and 5) and bottom group (e.g., atoms 2, 4, and 6). Each O atom is connected to three Mn atoms. The structural parameters are from the first-principles calculations [12], including the lattice constant $a = 2.61$ Å and the bond length $d_{\text{Mn}-\text{O}} = 1.87$ Å. The resultant angles are $\theta_{\text{MnOO}} = \theta_{\text{OMnMn}} = 88.511^\circ$ and $\theta_{\text{MnOO'}} = 72.621^\circ$, in which atoms O and O' are from different (top or bottom) groups.

Table 62 shows four VFF terms for the single-layer 1H-MnO₂; one of which is the bond stretching interaction shown by Eq. (1), while the other three terms are the angle bending interaction shown by Eq. (2). These force constant parameters are determined by fitting to the acoustic branches in the phonon dispersion along the Γ M as shown in **Figure 29(a)**. The *ab*

initio calculations for the phonon dispersion are from [12]. Typically, the transverse acoustic branch has a linear dispersion, so is higher than the flexural branch. However, it can be seen that the transverse acoustic branch is close to the flexural branch, which should be due to the underestimation from the *ab initio* calculations. **Figure 29(b)** shows that the VFF model and the SW potential give exactly the same phonon dispersion, as the SW potential is derived from the VFF model.

VFF type	Bond stretching	Angle bending	
Expression	$\frac{1}{2}K_{\text{Mn}-\text{O}}(\Delta r)^2$	$\frac{1}{2}K_{\text{Mn}-\text{O}-\text{O}}(\Delta\theta)^2$	$\frac{1}{2}K_{\text{Mn}-\text{O}-\text{O}}(\Delta\theta)^2$
Parameter	9.382	6.253	6.253
r_0 or θ_0	1.870	88.511	72.621
			88.511

The second line gives an explicit expression for each VFF term. The third line is the force constant parameters. Parameters are in the unit of eV/Å² for the bond stretching interaction and in the unit of eV for the angle bending interaction. The fourth line gives the initial bond length (in the unit of Å) for the bond stretching interaction and the initial angle (in the unit of degrees) for the angle bending interaction. The angle θ_{ijk} has atom i as the apex.

Table 62. The VFF model for single-layer 1H-MnO₂.

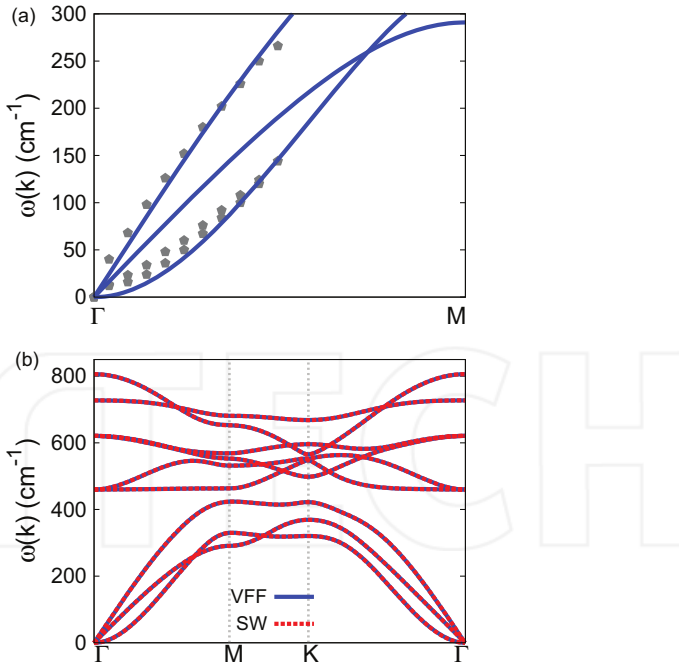


Figure 29. Phonon spectrum for single-layer 1H-MnO₂. (a) Phonon dispersion along the Γ M direction in the Brillouin zone. The results from the VFF model (lines) are comparable with the *ab initio* results (pentagons) from [12]. (b) The phonon dispersion from the SW potential is exactly the same as that from the VFF model.

The parameters for the two-body SW potential used by GULP are shown in **Table 63**. The parameters for the three-body SW potential used by GULP are shown in **Table 64**. Some representative parameters for the SW potential used by LAMMPS are listed in **Table 65**. We note that 12 atom types have been introduced for the simulation of the single-layer 1H-MnO₂ using LAMMPS, because the angles around atom Mn in **Figure 1** (with M = Mn and X = O) are not distinguishable in LAMMPS. We have suggested two options to differentiate these angles by implementing some additional constraints in LAMMPS, which can be accomplished by modifying the source file of LAMMPS [13, 14]. According to our experience, it is not so convenient for some users to implement these constraints and recompile the LAMMPS package. Hence, in the present work, we differentiate the angles by introducing more atom types, so it is not necessary to modify the LAMMPS package. **Figure 2** (with M = Mn and X = O) shows that, for 1H-MnO₂, we can differentiate these angles around the Mn atom by assigning these six neighboring O atoms with different atom types. It can be found that 12 atom types are necessary for the purpose of differentiating all 6 neighbors around 1 Mn atom.

We use LAMMPS to perform MD simulations for the mechanical behavior of the single-layer 1H-MnO₂ under uniaxial tension at 1 and 300 K. **Figure 30** shows the stress-strain curve for the tension of a single-layer 1H-MnO₂ of dimension 100 × 100 Å. Periodic boundary conditions are applied in both armchair and zigzag directions. The single-layer 1H-MnO₂ is stretched uniaxially

	<i>A</i> (eV)	<i>ρ</i> (Å)	<i>B</i> (Å ⁴)	<i>r</i> _{min} (Å)	<i>r</i> _{max} (Å)
Mn—O	4.721	0.961	6.114	0.0	2.540

Table 63. Two-body SW potential parameters for single-layer 1H-MnO₂ used by GULP [8] as expressed in Eq. (3).

	<i>K</i> (eV)	<i>θ</i> ₀ (°)	<i>ρ</i> ₁ (Å)	<i>ρ</i> ₂ (Å)	<i>r</i> _{min12} (Å)	<i>r</i> _{max12} (Å)	<i>r</i> _{min13} (Å)	<i>r</i> _{max13} (Å)	<i>r</i> _{min23} (Å)	<i>r</i> _{max23} (Å)
θ _{Mn—O—O}	55.070	88.511	0.961	0.961	0.0	2.540	0.0	2.540	0.0	3.016
θ _{Mn—O—O'}	60.424	72.621	0.961	0.961	0.0	2.540	0.0	2.540	0.0	3.016
θ _{O—Mn—Mn}	55.070	88.511	0.961	0.961	0.0	2.540	0.0	2.540	0.0	3.016

The angle θ_{ijk} in the first line indicates the bending energy for the angle with atom *i* as the apex.

Table 64. Three-body SW potential parameters for single-layer 1H-MnO₂ used by GULP [8] as expressed in Eq. (4).

	<i>ε</i> (eV)	<i>σ</i> (Å)	<i>a</i>	<i>λ</i>	<i>γ</i>	$\cos \theta_0$	<i>A</i> _L	<i>B</i> _L	<i>p</i>	<i>q</i>	Tol
Mn ₁ —O ₁ —O ₁	1.000	0.961	2.643	0.000	1.000	0.000	4.721	7.158	4	0	0.0
Mn ₁ —O ₁ —O ₃	1.000	0.000	0.000	55.070	1.000	0.026	0.000	0.000	4	0	0.0
Mn ₁ —O ₁ —O ₂	1.000	0.000	0.000	60.424	1.000	0.299	0.000	0.000	4	0	0.0
O ₁ —Mn ₁ —Mn ₃	1.000	0.000	0.000	55.070	1.000	0.026	0.000	0.000	4	0	0.0

Table 65. SW potential parameters for single-layer 1H-MnO₂ used by LAMMPS [9] as expressed in Eqs. (9) and (10).

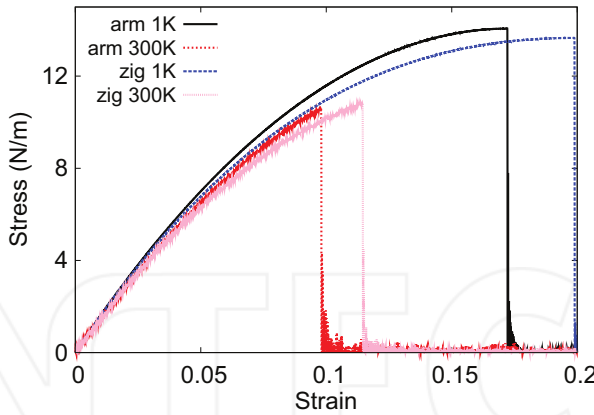


Figure 30. Stress-strain for single-layer 1H-MnO₂ of dimension 100 × 100 Å along the armchair and zigzag directions.

along the armchair or zigzag direction. The stress is calculated without involving the actual thickness of the quasi-two-dimensional structure of the single-layer 1H-MnO₂. The Young's modulus can be obtained by a linear fitting of the stress-strain relation in the small strain range of [0, 0.01]. The Young's modulus is 161.1 and 160.2 N/m along the armchair and zigzag directions, respectively. The Young's modulus is essentially isotropic in the armchair and zigzag directions. The Poisson's ratio from the VFF model and the SW potential is $\nu_{xy} = \nu_{yx} = 0.10$.

There is no available value for nonlinear quantities in the single-layer 1H-MnO₂. We have thus used the nonlinear parameter $B = 0.5d^4$ in Eq. (5), which is close to the value of B in most materials. The value of the third-order nonlinear elasticity D can be extracted by fitting the stress-strain relation to the function $\sigma = E\epsilon + \frac{1}{2}D\epsilon^2$ with E as the Young's modulus. The values of D from the present SW potential are -915.9 and -957.1 N/m along the armchair and zigzag directions, respectively. The ultimate stress is about 14.1 N/m at the ultimate strain of 0.17 in the armchair direction at the low temperature of 1 K. The ultimate stress is about 13.7 N/m at the ultimate strain of 0.20 in the zigzag direction at the low temperature of 1 K.

17. 1H-FeO₂

Most existing theoretical studies on the single-layer 1H-FeO₂ are based on the first-principles calculations. In this section, we will develop the SW potential for the single-layer 1H-FeO₂.

The structure for the single-layer 1H-FeO₂ is shown in Figure 1 (with M = Fe and X = O). Each Fe atom is surrounded by six O atoms. These O atoms are categorized into the top group (e.g., atoms 1, 3, and 5) and bottom group (e.g., atoms 2, 4, and 6). Each O atom is connected to three Fe atoms. The structural parameters are from the first-principles calculations [12], including the lattice constant $a = 2.62$ Å and the bond length $d_{\text{Fe}-\text{O}} = 1.88$ Å. The resultant angles are $\theta_{\text{FeOO}} = \theta_{\text{OFeFe}} = 88.343^\circ$ and $\theta_{\text{FeOO'}} = 72.856^\circ$, in which atoms O and O' are from different (top or bottom) groups.

Table 66 shows four VFF terms for the single-layer 1H-FeO₂; one of which is the bond stretching interaction shown by Eq. (1), while the other three terms are the angle bending interaction shown by Eq. (2). These force constant parameters are determined by fitting to the three acoustic branches in the phonon dispersion along the Γ M as shown in **Figure 31(a)**. The *ab initio* calculations for the phonon dispersion are from [12]. **Figure 31(b)** shows that the VFF

VFF type	Bond stretching	Angle bending		
Expression	$\frac{1}{2}K_{\text{Fe}-\text{O}}(\Delta r)^2$	$\frac{1}{2}K_{\text{Fe}-\text{O}-\text{O}}(\Delta\theta)^2$	$\frac{1}{2}K_{\text{Fe}-\text{O}-\text{O}'}(\Delta\theta)^2$	$\frac{1}{2}K_{\text{O}-\text{Fe}-\text{Fe}}(\Delta\theta)^2$
Parameter	8.377	3.213	3.213	3.213
r_0 or θ_0	1.880	88.343	72.856	88.343

The second line gives an explicit expression for each VFF term. The third line is the force constant parameters. Parameters are in the unit of eV/ \AA^2 for the bond stretching interaction and in the unit of eV for the angle bending interaction. The fourth line gives the initial bond length (in the unit of \AA) for the bond stretching interaction and the initial angle (in the unit of degrees) for the angle bending interaction. The angle θ_{ijk} has atom i as the apex.

Table 66. The VFF model for single-layer 1H-FeO₂.

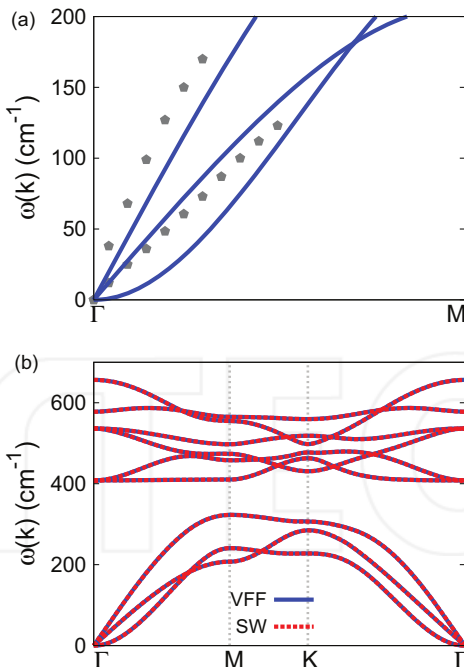


Figure 31. Phonon spectrum for single-layer 1H-FeO₂. (a) Phonon dispersion along the Γ M direction in the Brillouin zone. The results from the VFF model (lines) are comparable with the *ab initio* results (pentagons) from [12]. (b) The phonon dispersion from the SW potential is exactly the same as that from the VFF model.

model and the SW potential give exactly the same phonon dispersion, as the SW potential is derived from the VFF model.

The parameters for the two-body SW potential used by GULP are shown in **Table 67**. The parameters for the three-body SW potential used by GULP are shown in **Table 68**. Some representative parameters for the SW potential used by LAMMPS are listed in **Table 69**. We note that 12 atom types have been introduced for the simulation of the single-layer 1H-FeO₂ using LAMMPS, because the angles around atom Fe in **Figure 1** (with M = Fe and X = O) are not distinguishable in LAMMPS. We have suggested two options to differentiate these angles by implementing some additional constraints in LAMMPS, which can be accomplished by modifying the source file of LAMMPS [13, 14]. According to our experience, it is not so convenient for some users to implement these constraints and recompile the LAMMPS package. Hence, in the present work, we differentiate the angles by introducing more atom types, so it is not necessary to modify the LAMMPS package. **Figure 2** (with M = Fe and X = O) shows that, for 1H-FeO₂, we can differentiate these angles around the Fe atom by assigning these six neighboring O atoms with different atom types. It can be found that 12 atom types are necessary for the purpose of differentiating all 6 neighbors around 1 Fe atom.

We use LAMMPS to perform MD simulations for the mechanical behavior of the single-layer 1H-FeO₂ under uniaxial tension at 1 and 300 K. **Figure 32** shows the stress-strain curve for the tension of a single-layer 1H-FeO₂ of dimension 100×100 Å. Periodic boundary conditions are applied in both armchair and zigzag directions. The single-layer 1H-FeO₂ is stretched

	<i>A</i> (eV)	<i>ρ</i> (Å)	<i>B</i> (Å ⁴)	<i>r</i> _{min} (Å)	<i>r</i> _{max} (Å)
Fe—O	4.242	0.962	6.246	0.0	2.552

Table 67. Two-body SW potential parameters for single-layer 1H-FeO₂ used by GULP [8] as expressed in Eq. (3).

	<i>K</i> (eV)	<i>θ</i> ₀ (°)	<i>ρ</i> ₁ (Å)	<i>ρ</i> ₂ (Å)	<i>r</i> _{min12} (Å)	<i>r</i> _{max12} (Å)	<i>r</i> _{min13} (Å)	<i>r</i> _{max13} (Å)	<i>r</i> _{min23} (Å)	<i>r</i> _{max23} (Å)
θ _{Fe—O—O}	28.105	88.343	0.962	0.962	0.0	2.552	0.0	2.552	0.0	3.031
θ _{Fe—O—O'}	30.754	72.856	0.962	0.962	0.0	2.552	0.0	2.552	0.0	3.031
θ _{O—Fe—Fe}	28.105	88.343	0.962	0.962	0.0	2.552	0.0	2.552	0.0	3.031

The angle θ_{ijk} in the first line indicates the bending energy for the angle with atom *i* as the apex.

Table 68. Three-body SW potential parameters for single-layer 1H-FeO₂ used by GULP [8] as expressed in Eq. (4).

	<i>ε</i> (eV)	<i>σ</i> (Å)	<i>a</i>	<i>λ</i>	<i>γ</i>	$\cos \theta_0$	<i>A</i> _L	<i>B</i> _L	<i>p</i>	<i>q</i>	Tol
Fe ₁ —O ₁ —O ₁	1.000	0.962	2.654	0.000	1.000	0.000	4.242	7.298	4	0	0.0
Fe ₁ —O ₁ —O ₃	1.000	0.000	0.000	28.105	1.000	0.029	0.000	0.000	4	0	0.0
Fe ₁ —O ₁ —O ₂	1.000	0.000	0.000	30.754	1.000	0.295	0.000	0.000	4	0	0.0
O ₁ —Fe ₁ —Fe ₃	1.000	0.000	0.000	28.105	1.000	0.029	0.000	0.000	4	0	0.0

Table 69. SW potential parameters for single-layer 1H-FeO₂ used by LAMMPS [9] as expressed in Eqs. (9) and (10).

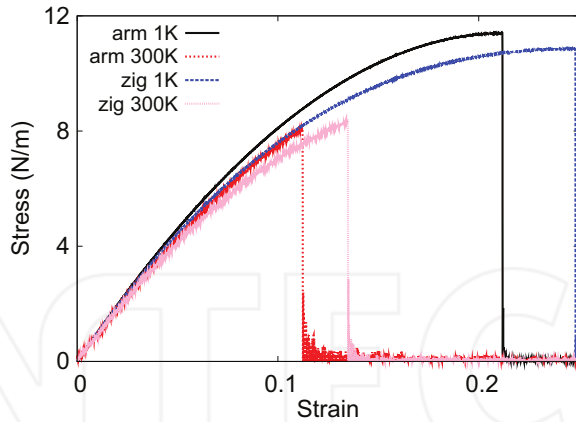


Figure 32. Stress-strain for single-layer 1H-FeO₂ of dimension 100 × 100 Å along the armchair and zigzag directions.

uniaxially along the armchair or zigzag direction. The stress is calculated without involving the actual thickness of the quasi-two-dimensional structure of the single-layer 1H-FeO₂. The Young's modulus can be obtained by a linear fitting of the stress-strain relation in the small strain range of [0, 0.01]. The Young's modulus is 100.2 and 99.3 N/m along the armchair and zigzag directions, respectively. The Young's modulus is essentially isotropic in the armchair and zigzag directions. The Poisson's ratio from the VFF model and the SW potential is $\nu_{xy} = \nu_{yx} = 0.23$.

There is no available value for nonlinear quantities in the single-layer 1H-FeO₂. We have thus used the nonlinear parameter $B = 0.5d^4$ in Eq. (5), which is close to the value of B in most materials. The value of the third-order nonlinear elasticity D can be extracted by fitting the stress-strain relation to the function $\sigma = E\epsilon + \frac{1}{2}D\epsilon^2$ with E as the Young's modulus. The values of D from the present SW potential are -423.4 and -460.2 N/m along the armchair and zigzag directions, respectively. The ultimate stress is about 11.4 N/m at the ultimate strain of 0.21 in the armchair direction at the low temperature of 1 K. The ultimate stress is about 10.9 N/m at the ultimate strain of 0.25 in the zigzag direction at the low temperature of 1 K.

18 1H-FES₂

Most existing theoretical studies on the single-layer 1H-FeS₂ are based on the first-principles calculations. In this section, we will develop the SW potential for the single-layer 1H-FeS₂.

The structure for the single-layer 1H-FeS₂ is shown in **Figure 1** (with M=Fe and X=S). Each Fe atom is surrounded by six S atoms. These S atoms are categorized into the top group (e.g., atoms 1, 3, and 5) and bottom group (e.g., atoms 2, 4, and 6). Each S atom is connected to three Fe atoms. The structural parameters are from the first-principles calculations [12], including the lattice constant $a = 3.06$ Å and the bond length $d_{\text{Fe-S}} = 2.22$ Å. The resultant angles are

$\theta_{\text{FeSS}} = \theta_{\text{SFeFe}} = 87.132^\circ$ and $\theta_{\text{FeSS'}} = 74.537^\circ$, in which atoms S and S' are from different (top or bottom) groups.

Table 70 shows four VFF terms for the single-layer 1H-FeS₂; one of which is the bond stretching interaction shown by Eq. (1), while the other three terms are the angle bending interaction shown by Eq. (2). These force constant parameters are determined by fitting to the three acoustic branches in the phonon dispersion along the Γ M as shown in **Figure 33(a)**. The *ab initio* calculations for the phonon dispersion are from Ref. [12]. **Figure 33(b)** shows that the

VFF type	Bond stretching	Angle bending		
Expression	$\frac{1}{2}K_{\text{Fe-S}}(\Delta r)^2$	$\frac{1}{2}K_{\text{Fe-S-S}}(\Delta\theta)^2$	$\frac{1}{2}K_{\text{Fe-S-S}}(\Delta\theta)^2$	$\frac{1}{2}K_{\text{S-Fe-Fe}}(\Delta\theta)^2$
Parameter	6.338	3.964	3.964	3.964
r_0 or θ_0	2.220	87.132	74.537	87.132

The second line gives an explicit expression for each VFF term. The third line is the force constant parameters. Parameters are in the unit of eV/Å² for the bond stretching interaction and in the unit of eV for the angle bending interaction. The fourth line gives the initial bond length (in the unit of Å) for the bond stretching interaction and the initial angle (in the unit of degrees) for the angle bending interaction. The angle θ_{ijk} has atom *i* as the apex.

Table 70. The VFF model for single-layer 1H-FeS₂.

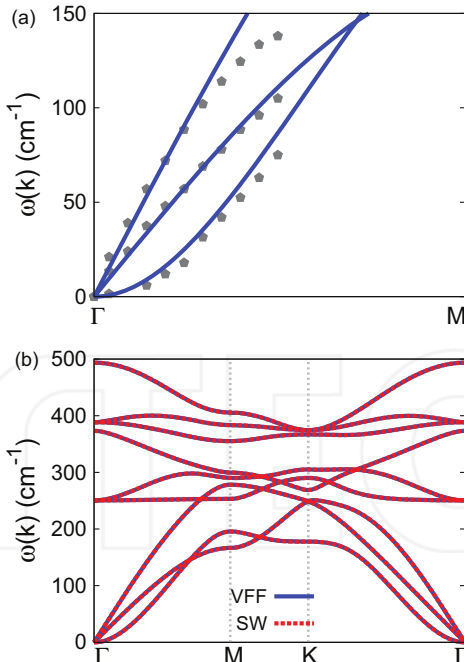


Figure 33. Phonon spectrum for single-layer 1H-FeS₂. (a) Phonon dispersion along the Γ M direction in the Brillouin zone. The results from the VFF model (lines) are comparable with the *ab initio* results (pentagons) from Ref. [12]. (b) The phonon dispersion from the SW potential is exactly the same as that from the VFF model.

VFF model and the SW potential give exactly the same phonon dispersion, as the SW potential is derived from the VFF model.

The parameters for the two-body SW potential used by GULP are shown in **Table 71**. The parameters for the three-body SW potential used by GULP are shown in **Table 72**. Some representative parameters for the SW potential used by LAMMPS are listed in **Table 73**. We note that 12 atom types have been introduced for the simulation of the single-layer 1H-FeS₂ using LAMMPS, because the angles around atom Fe in **Figure 1** (with M=Fe and X=S) are not distinguishable in LAMMPS. We have suggested two options to differentiate these angles by implementing some additional constraints in LAMMPS, which can be accomplished by modifying the source file of LAMMPS [13, 14]. According to our experience, it is not so convenient for some users to implement these constraints and recompile the LAMMPS package. Hence, in the present work, we differentiate the angles by introducing more atom types, so it is not necessary to modify the LAMMPS package. **Figure 2** (with M=Fe and X=S) shows that, for 1H-FeS₂, we can differentiate these angles around the Fe atom by assigning these six neighboring S atoms with different atom types. It can be found that 12 atom types are necessary for the purpose of differentiating all 6 neighbors around 1 Fe atom.

We use LAMMPS to perform MD simulations for the mechanical behavior of the single-layer 1H-FeS₂ under uniaxial tension at 1 and 300 K. **Figure 34** shows the stress-strain curve for the tension of a single-layer 1H-FeS₂ of dimension 100 × 100 Å. Periodic boundary conditions are applied in both armchair and zigzag directions. The single-layer 1H-FeS₂ is stretched

	<i>A</i> (eV)	<i>ρ</i> (Å)	<i>B</i> (Å ⁴)	<i>r</i> _{min} (Å)	<i>r</i> _{max} (Å)
Fe—S	4.337	1.097	12.145	0.0	3.000

Table 71. Two-body SW potential parameters for single-layer 1H-FeS₂ used by GULP [8] as expressed in Eq. (3).

	<i>K</i> (eV)	<i>θ</i> ₀ (°)	<i>ρ</i> ₁ (Å)	<i>ρ</i> ₂ (Å)	<i>r</i> _{min12} (Å)	<i>r</i> _{max12} (Å)	<i>r</i> _{min13} (Å)	<i>r</i> _{max13} (Å)	<i>r</i> _{min23} (Å)	<i>r</i> _{max23} (Å)
θ _{Fe—S—S}	33.060	87.132	1.097	1.097	0.0	3.000	0.0	3.000	0.0	3.567
θ _{Fe—S—S'}	35.501	74.537	1.097	1.097	0.0	3.000	0.0	3.000	0.0	3.567
θ _{S—Fe—Fe}	33.060	87.132	1.097	1.097	0.0	3.000	0.0	3.000	0.0	3.567

The angle θ_{ijk} in the first line indicates the bending energy for the angle with atom *i* as the apex.

Table 72. Three-body SW potential parameters for single-layer 1H-FeS₂ used by GULP [8] as expressed in Eq. (4).

	<i>ε</i> (eV)	<i>σ</i> (Å)	<i>a</i>	<i>λ</i>	<i>γ</i>	<i>cos θ</i> ₀	<i>A</i> _L	<i>B</i> _L	<i>p</i>	<i>q</i>	Tol
Fe ₁ —S ₁ —S ₁	1.000	1.097	2.735	0.000	1.000	0.000	4.337	8.338	4	0	0.0
Fe ₁ —S ₁ —S ₃	1.000	0.000	0.000	33.060	1.000	0.050	0.000	0.000	4	0	0.0
Fe ₁ —S ₁ —S ₂	1.000	0.000	0.000	35.501	1.000	0.267	0.000	0.000	4	0	0.0
S ₁ —Fe ₁ —Fe ₃	1.000	0.000	0.000	33.060	1.000	0.050	0.000	0.000	4	0	0.0

Table 73. SW potential parameters for single-layer 1H-FeS₂ used by LAMMPS [9] as expressed in Eqs. (9) and (10).

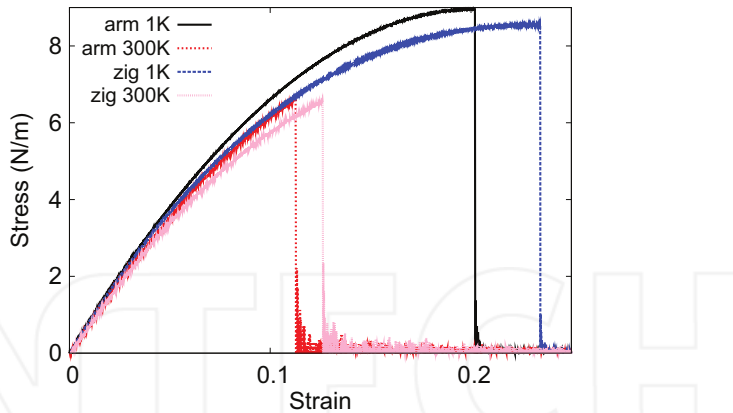


Figure 34. Stress-strain for single-layer 1H-FeS₂ of dimension 100 × 100 Å along the armchair and zigzag directions.

uniaxially along the armchair or zigzag direction. The stress is calculated without involving the actual thickness of the quasi-two-dimensional structure of the single-layer 1H-FeS₂. The Young's modulus can be obtained by a linear fitting of the stress-strain relation in the small strain range of [0, 0.01]. The Young's modulus is 83.6 and 83.4 N/m along the armchair and zigzag directions, respectively. The Young's modulus is essentially isotropic in the armchair and zigzag directions. The Poisson's ratio from the VFF model and the SW potential is $\nu_{xy} = \nu_{yx} = 0.20$.

There is no available value for nonlinear quantities in the single-layer 1H-FeS₂. We have thus used the nonlinear parameter $B = 0.5d^4$ in Eq. (5), which is close to the value of B in most materials. The value of the third-order nonlinear elasticity D can be extracted by fitting the stress-strain relation to the function $\sigma = E\epsilon + \frac{1}{2}D\epsilon^2$ with E as the Young's modulus. The values of D from the present SW potential are -377.5 and -412.7 N/m along the armchair and zigzag directions, respectively. The ultimate stress is about 9.0 N/m at the ultimate strain of 0.20 in the armchair direction at the low temperature of 1 K. The ultimate stress is about 8.6 N/m at the ultimate strain of 0.23 in the zigzag direction at the low temperature of 1 K.

19. 1H-FeSe₂

Most existing theoretical studies on the single-layer 1H-FeSe₂ are based on the first-principles calculations. In this section, we will develop the SW potential for the single-layer 1H-FeSe₂.

The structure for the single-layer 1H-FeSe₂ is shown in **Figure 1** (with M=Fe and X=Se). Each Fe atom is surrounded by six Se atoms. These Se atoms are categorized into the top group (e.g., atoms 1, 3, and 5) and bottom group (e.g., atoms 2, 4, and 6). Each Se atom is connected to three Fe atoms. The structural parameters are from the first-principles calculations [12], including the lattice constant $a = 3.22$ Å and the bond length $d_{Fe-Se} = 2.35$ Å. The resultant angles are

$\theta_{\text{FeSeSe}} = \theta_{\text{SeFeFe}} = 86.488^\circ$ and $\theta_{\text{FeSeSe}'} = 75.424^\circ$, in which atoms Se and Se' are from different (top or bottom) groups.

Table 74 shows four VFF terms for the single-layer 1H-FeSe₂; one of which is the bond stretching interaction shown by Eq. (1), while the other three terms are the angle bending interaction shown by Eq. (2). These force constant parameters are determined by fitting to the three acoustic branches in the phonon dispersion along the Γ M as shown in **Figure 35(a)**. The

VFF type	Bond stretching	Angle bending		
Expression	$\frac{1}{2}K_{\text{Fe}-\text{Se}}(\Delta r)^2$	$\frac{1}{2}K_{\text{Fe}-\text{Se}-\text{Se}}(\Delta\theta)^2$	$\frac{1}{2}K_{\text{Fe}-\text{Se}-\text{Se}'}(\Delta\theta)^2$	$\frac{1}{2}K_{\text{Se}-\text{Fe}-\text{Fe}}(\Delta\theta)^2$
Parameter	6.338	3.964	3.964	3.964
r_0 or θ_0	2.350	86.488	75.424	86.488

The second line gives an explicit expression for each VFF term. The third line is the force constant parameters. Parameters are in the unit of eV/Å² for the bond stretching interaction and in the unit of eV for the angle bending interaction. The fourth line gives the initial bond length (in the unit of Å) for the bond stretching interaction and the initial angle (in the unit of degrees) for the angle bending interaction. The angle θ_{ijk} has atom *i* as the apex.

Table 74. The VFF model for single-layer 1H-FeSe₂.

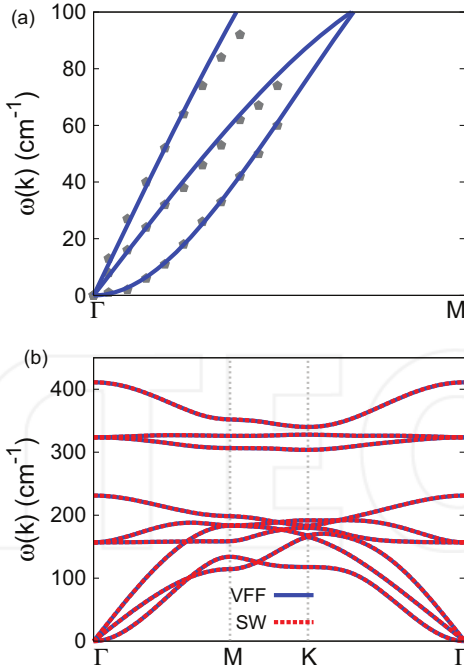


Figure 35. Phonon spectrum for single-layer 1H-FeSe₂. (a) Phonon dispersion along the Γ M direction in the Brillouin zone. The results from the VFF model (lines) are comparable with the *ab initio* results (pentagons) from Ref. [12]. (b) The phonon dispersion from the SW potential is exactly the same as that from the VFF model.

ab initio calculations for the phonon dispersion are from Ref. [12]. **Figure 35(b)** shows that the VFF model and the SW potential give exactly the same phonon dispersion, as the SW potential is derived from the VFF model.

The parameters for the two-body SW potential used by GULP are shown in **Table 75**. The parameters for the three-body SW potential used by GULP are shown in **Table 76**. Some representative parameters for the SW potential used by LAMMPS are listed in **Table 77**. We note that 12 atom types have been introduced for the simulation of the single-layer 1H-FeSe₂ using LAMMPS, because the angles around atom Fe in **Figure 1** (with M=Fe and X=Se) are not distinguishable in LAMMPS. We have suggested two options to differentiate these angles by implementing some additional constraints in LAMMPS, which can be accomplished by modifying the source file of LAMMPS [13, 14]. According to our experience, it is not so convenient for some users to implement these constraints and recompile the LAMMPS package. Hence, in the present work, we differentiate the angles by introducing more atom types, so it is not necessary to modify the LAMMPS package. **Figure 2** (with M=Fe and X=Se) shows that, for 1H-FeSe₂, we can differentiate these angles around the Fe atom by assigning these six neighboring Se atoms with different atom types. It can be found that 12 atom types are necessary for the purpose of differentiating all 6 neighbors around 1 Fe atom.

We use LAMMPS to perform MD simulations for the mechanical behavior of the single-layer 1H-FeSe₂ under uniaxial tension at 1 and 300 K. **Figure 36** shows the stress-strain curve for the tension of a single-layer 1H-FeSe₂ of dimension 100 × 100 Å. Periodic boundary conditions are

	A (eV)	ρ (Å)	B (Å ⁴)	r_{\min} (Å)	r_{\max} (Å)
Fe-Se	4.778	1.139	15.249	0.0	3.168

Table 75. Two-body SW potential parameters for single-layer 1H-FeSe₂ used by GULP [8] as expressed in Eq. (3).

	K (eV)	θ_0 (°)	ρ_1 (Å)	ρ_2 (Å)	$r_{\min 12}$ (Å)	$r_{\max 12}$ (Å)	$r_{\min 13}$ (Å)	$r_{\max 13}$ (Å)	$r_{\min 23}$ (Å)	$r_{\max 23}$ (Å)
$\theta_{\text{Fe}-\text{Se}-\text{Se}}$	32.235	86.488	1.139	1.139	0.0	3.168	0.0	3.168	0.0	3.768
$\theta_{\text{Fe}-\text{Se}-\text{Se}'}$	34.286	75.424	1.139	1.139	0.0	3.168	0.0	3.168	0.0	3.768
$\theta_{\text{Se}-\text{Fe}-\text{Fe}}$	32.235	86.488	1.139	1.139	0.0	3.168	0.0	3.168	0.0	3.768

The angle θ_{ijk} in the first line indicates the bending energy for the angle with atom *i* as the apex.

Table 76. Three-body SW potential parameters for single-layer 1H-FeSe₂ used by GULP [8] as expressed in Eq. (4).

	ϵ (eV)	σ (Å)	a	λ	γ	$\cos \theta_0$	A_L	B_L	p	q	Tol
Fe ₁ —Se ₁ —Se ₁	1.000	1.139	2.781	0.000	1.000	0.000	4.778	9.049	4	0	0.0
Fe ₁ —Se ₁ —Se ₃	1.000	0.000	0.000	32.235	1.000	0.061	0.000	0.000	4	0	0.0
Fe ₁ —Se ₁ —Se ₂	1.000	0.000	0.000	34.286	1.000	0.252	0.000	0.000	4	0	0.0
Se ₁ —Fe ₁ —Fe ₃	1.000	0.000	0.000	32.235	1.000	0.061	0.000	0.000	4	0	0.0

Table 77. SW potential parameters for single-layer 1H-FeSe₂ used by LAMMPS [9] as expressed in Eqs. (9) and (10).

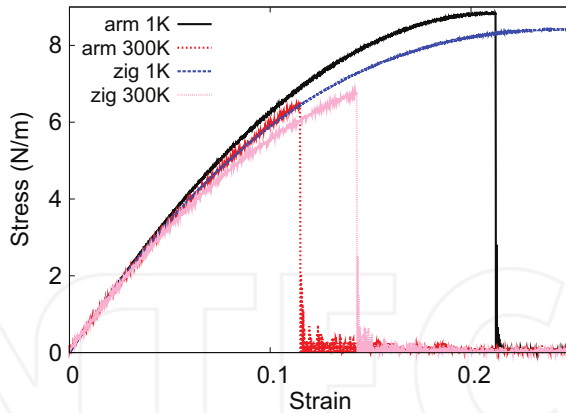


Figure 36. Stress-strain for single-layer 1H-FeSe₂ of dimension 100 × 100 Å along the armchair and zigzag directions.

applied in both armchair and zigzag directions. The single-layer 1H-FeSe₂ is stretched uniaxially along the armchair or zigzag direction. The stress is calculated without involving the actual thickness of the quasi-two-dimensional structure of the single-layer 1H-FeSe₂. The Young's modulus can be obtained by a linear fitting of the stress-strain relation in the small strain range of [0, 0.01]. The Young's modulus is 77.3 and 77.4 N/m along the armchair and zigzag directions, respectively. The Young's modulus is essentially isotropic in the armchair and zigzag directions. The Poisson's ratio from the VFF model and the SW potential is $\nu_{xy} = \nu_{yx} = 0.23$.

There is no available value for nonlinear quantities in the single-layer 1H-FeSe₂. We have thus used the nonlinear parameter $B = 0.5d^4$ in Eq. (5), which is close to the value of B in most materials. The value of the third-order nonlinear elasticity D can be extracted by fitting the stress-strain relation to the function $\sigma = E\epsilon + \frac{1}{2}D\epsilon^2$ with E as the Young's modulus. The values of D from the present SW potential are -323.8 and -360.8 N/m along the armchair and zigzag directions, respectively. The ultimate stress is about 8.8 N/m at the ultimate strain of 0.21 in the armchair direction at the low temperature of 1 K. The ultimate stress is about 8.4 N/m at the ultimate strain of 0.25 in the zigzag direction at the low temperature of 1 K.

20. 1H-FeTe₂

Most existing theoretical studies on the single-layer 1H-FeTe₂ are based on the first-principles calculations. In this section, we will develop the SW potential for the single-layer 1H-FeTe₂.

The structure for the single-layer 1H-FeTe₂ is shown in **Figure 1** (with M=Fe and X=Te). Each Fe atom is surrounded by six Te atoms. These Te atoms are categorized into the top group (e.g., atoms 1, 3, and 5) and bottom group (e.g., atoms 2, 4, and 6). Each Te atom is connected to three Fe atoms. The structural parameters are from the first-principles calculations [12],

including the lattice constant $a = 3.48 \text{ \AA}$ and the bond length $d_{\text{Fe}-\text{Te}} = 2.53 \text{ \AA}$. The resultant angles are $\theta_{\text{FeTeTe}} = \theta_{\text{TeFeFe}} = 86.904^\circ$ and $\theta_{\text{FeTeTe}'} = 74.851^\circ$, in which atoms Te and Te' are from different (top or bottom) groups.

Table 78 shows four VFF terms for the single-layer 1H-FeTe₂; one of which is the bond stretching interaction shown by Eq. (1), while the other three terms are the angle bending interaction shown by Eq. (2). These force constant parameters are determined by fitting to the two in-plane acoustic branches in the phonon dispersion along the ΓM as shown in **Figure 37(a)**. The *ab initio* calculations for the phonon dispersion are from Ref. [12]. **Figure 37(b)** shows that the VFF model and the SW potential give exactly the same phonon dispersion, as the SW potential is derived from the VFF model.

The parameters for the two-body SW potential used by GULP are shown in **Table 79**. The parameters for the three-body SW potential used by GULP are shown in **Table 80**. Some representative parameters for the SW potential used by LAMMPS are listed in **Table 81**. We note that 12 atom types have been introduced for the simulation of the single-layer 1H-FeTe₂ using LAMMPS, because the angles around atom Fe in **Figure 1** (with M=Fe and X=Te) are not distinguishable in LAMMPS. We have suggested two options to differentiate these angles by implementing some additional constraints in LAMMPS, which can be accomplished by modifying the source file of LAMMPS [13, 14]. According to our experience, it is not so convenient for some users to implement these constraints and recompile the LAMMPS package. Hence, in the present work, we differentiate the angles by introducing more atom types, so it is not necessary to modify the LAMMPS package. **Figure 2** (with M=Fe and X=Te) shows that, for 1H-FeTe₂, we can differentiate these angles around the Fe atom by assigning these six neighboring Te atoms with different atom types. It can be found that 12 atom types are necessary for the purpose of differentiating all 6 neighbors around 1 Fe atom.

We use LAMMPS to perform MD simulations for the mechanical behavior of the single-layer 1H-FeTe₂ under uniaxial tension at 1 and 300 K. **Figure 38** shows the stress-strain curve for the tension of a single-layer 1H-FeTe₂ of dimension $100 \times 100 \text{ \AA}$. Periodic boundary conditions are applied in both armchair and zigzag directions. The single-layer 1H-FeTe₂ is stretched uniaxially along the armchair or zigzag direction. The stress is calculated without involving the actual thickness of the quasi-two-dimensional structure of the single-layer 1H-FeTe₂. The Young's modulus can be obtained by a linear fitting of the stress-strain relation in the small

VFF type	Bond stretching	Angle bending		
Expression	$\frac{1}{2}K_{\text{Fe}-\text{Te}}(\Delta r)^2$	$\frac{1}{2}K_{\text{Fe}-\text{Te}-\text{Te}}(\Delta\theta)^2$	$\frac{1}{2}K_{\text{Fe}-\text{Te}-\text{Te}'}(\Delta\theta)^2$	$\frac{1}{2}K_{\text{Te}-\text{Fe}-\text{Fe}}(\Delta\theta)^2$
Parameter	6.338	3.964	3.964	3.964
r_0 or θ_0	2.530	86.904	74.851	86.904

The second line gives an explicit expression for each VFF term. The third line is the force constant parameters. Parameters are in the unit of eV/ \AA^2 for the bond stretching interaction and in the unit of eV for the angle bending interaction. The fourth line gives the initial bond length (in the unit of \AA) for the bond stretching interaction and the initial angle (in the unit of degrees) for the angle bending interaction. The angle θ_{ijk} has atom i as the apex.

Table 78. The VFF model for single-layer 1H-FeTe₂.

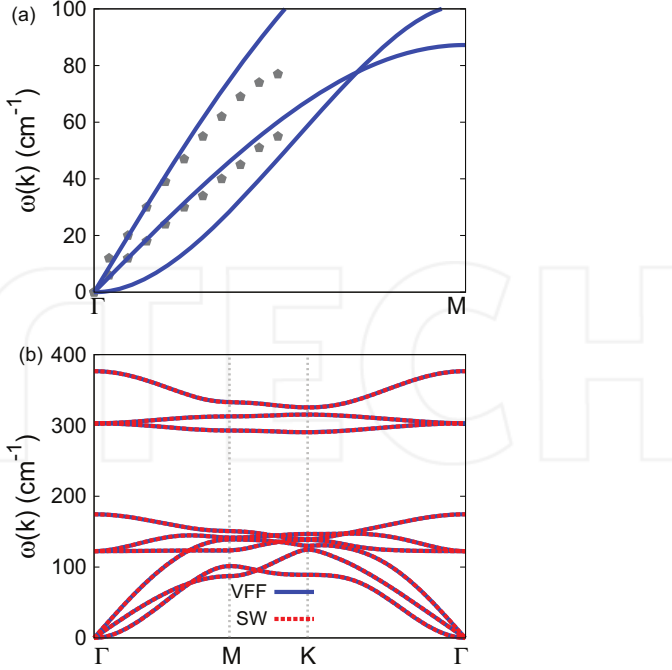


Figure 37. Phonon spectrum for single-layer 1H-FeTe₂. (a) Phonon dispersion along the Γ M direction in the Brillouin zone. The results from the VFF model (lines) are comparable with the *ab initio* results (pentagons) from Ref. [12]. (b) The phonon dispersion from the SW potential is exactly the same as that from the VFF model.

	A (eV)	ρ (Å)	B (Å ⁴)	r_{\min} (Å)	r_{\max} (Å)
Fe—Te	5.599	1.242	20.486	0.0	3.416

Table 79. Two-body SW potential parameters for single-layer 1H-FeTe₂ used by GULP [8] as expressed in Eq. (3).

	K (eV)	θ_0 (°)	ρ_1 (Å)	ρ_2 (Å)	$r_{\min 12}$ (Å)	$r_{\max 12}$ (Å)	$r_{\min 13}$ (Å)	$r_{\max 13}$ (Å)	$r_{\min 23}$ (Å)	$r_{\max 23}$ (Å)
$\theta_{\text{Fe}-\text{Te}-\text{Te}}$	32.766	86.904	1.242	1.242	0.0	3.416	0.0	3.416	0.0	4.062
$\theta_{\text{Fe}-\text{Te}-\text{Te}'}$	35.065	74.851	1.242	1.242	0.0	3.416	0.0	3.416	0.0	4.062
$\theta_{\text{Te}-\text{Fe}-\text{Fe}}$	32.766	86.904	1.242	1.242	0.0	3.416	0.0	3.416	0.0	4.062

The angle θ_{ijk} in the first line indicates the bending energy for the angle with atom i as the apex.

Table 80. Three-body SW potential parameters for single-layer 1H-FeTe₂ used by GULP [8] as expressed in Eq. (4).

strain range of [0, 0.01]. The Young's modulus is 69.6 and 69.8 N/m along the armchair and zigzag directions, respectively. The Young's modulus is essentially isotropic in the armchair and zigzag directions. The Poisson's ratio from the VFF model and the SW potential is $\nu_{xy} = \nu_{yx} = 0.25$.

	ϵ (eV)	σ (Å)	a	λ	γ	$\cos \theta_0$	A_L	B_L	p	q	Tol
Fe ₁ —Te ₁ —Te ₁	1.000	1.242	2.751	0.000	1.000	0.000	5.599	8.615	4	0	0.0
Fe ₁ —Te ₁ —Te ₃	1.000	0.000	0.000	32.766	1.000	0.054	0.000	0.000	4	0	0.0
Fe ₁ —Te ₁ —Te ₂	1.000	0.000	0.000	35.065	1.000	0.261	0.000	0.000	4	0	0.0
Te ₁ —Fe ₁ —Fe ₃	1.000	0.000	0.000	32.766	1.000	0.054	0.000	0.000	4	0	0.0

Table 81. SW potential parameters for single-layer 1H-FeTe₂ used by LAMMPS [9] as expressed in Eqs. (9) and (10).

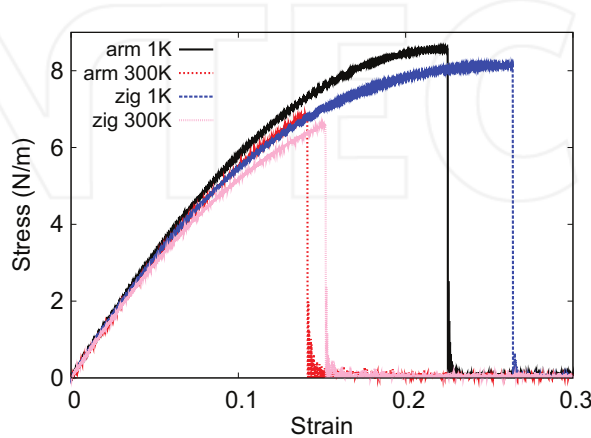


Figure 38. Stress-strain for single-layer 1H-FeTe₂ of dimension 100 × 100 Å along the armchair and zigzag directions.

There is no available value for nonlinear quantities in the single-layer 1H-FeTe₂. We have thus used the nonlinear parameter $B = 0.5d^4$ in Eq. (5), which is close to the value of B in most materials. The value of the third-order nonlinear elasticity D can be extracted by fitting the stress-strain relation to the function $\sigma = E\epsilon + \frac{1}{2}D\epsilon^2$ with E as the Young's modulus. The values of D from the present SW potential are -267.5 and -302.8 N/m along the armchair and zigzag directions, respectively. The ultimate stress is about 8.6 N/m at the ultimate strain of 0.22 in the armchair direction at the low temperature of 1 K. The ultimate stress is about 8.1 N/m at the ultimate strain of 0.26 in the zigzag direction at the low temperature of 1 K.

21. 1H-COTE₂

Most existing theoretical studies on the single-layer 1H-CoTe₂ are based on the first-principles calculations. In this section, we will develop the SW potential for the single-layer 1H-CoTe₂.

The structure for the single-layer 1H-CoTe₂ is shown in Figure 1 (with M=Co and X=Te). Each Co atom is surrounded by six Te atoms. These Te atoms are categorized into the top group (e.g., atoms 1, 3, and 5) and bottom group (e.g., atoms 2, 4, and 6). Each Te atom is connected to

three Co atoms. The structural parameters are from the first-principles calculations [12], including the lattice constant $a = 3.52 \text{ \AA}$ and the bond length $d_{\text{Co}-\text{Te}} = 2.51 \text{ \AA}$. The resultant angles are $\theta_{\text{CoTeTe}} = \theta_{\text{TeCoCo}} = 89.046^\circ$ and $\theta_{\text{CoTeTe}'} = 71.873^\circ$, in which atoms Te and Te' are from different (top or bottom) groups.

Table 82 shows four VFF terms for the single-layer 1H-CoTe₂; one of which is the bond stretching interaction shown by Eq. (1), while the other three terms are the angle bending interaction shown by Eq. (2). These force constant parameters are determined by fitting to the acoustic branches in the phonon dispersion along the ΓM as shown in **Figure 39(a)**. The *ab initio* calculations for the phonon dispersion are from Ref. [12]. **Figure 39(b)** shows that the VFF model and the SW potential give exactly the same phonon dispersion, as the SW potential is derived from the VFF model.

The parameters for the two-body SW potential used by GULP are shown in **Table 83**. The parameters for the three-body SW potential used by GULP are shown in **Table 84**. Some representative parameters for the SW potential used by LAMMPS are listed in **Table 85**. We note that 12 atom types have been introduced for the simulation of the single-layer 1H-CoTe₂ using LAMMPS, because the angles around atom Co in **Figure 1** (with M=Co and X=Te) are not distinguishable in LAMMPS. We have suggested two options to differentiate these angles by implementing some additional constraints in LAMMPS, which can be accomplished by modifying the source file of LAMMPS [13, 14]. According to our experience, it is not so convenient for some users to implement these constraints and recompile the LAMMPS package. Hence, in the present work, we differentiate the angles by introducing more atom types, so it is not necessary to modify the LAMMPS package. **Figure 2** (with M=Co and X=Te) shows that, for 1H-CoTe₂, we can differentiate these angles around the Co atom by assigning these six neighboring Te atoms with different atom types. It can be found that 12 atom types are necessary for the purpose of differentiating all 6 neighbors around 1 Co atom.

We use LAMMPS to perform MD simulations for the mechanical behavior of the single-layer 1H-CoTe₂ under uniaxial tension at 1 and 300 K. **Figure 40** shows the stress-strain curve for the tension of a single-layer 1H-CoTe₂ of dimension $100 \times 100 \text{ \AA}$. Periodic boundary conditions are applied in both armchair and zigzag directions. The single-layer 1H-CoTe₂ is stretched uniaxially along the armchair or zigzag direction. The stress is calculated without involving

VFF type	Bond stretching	Angle bending		
Expression	$\frac{1}{2}K_{\text{Co}-\text{Te}}(\Delta r)^2$	$\frac{1}{2}K_{\text{Co}-\text{Te}-\text{Te}}(\Delta\theta)^2$	$\frac{1}{2}K_{\text{Co}-\text{Te}-\text{Te}'}(\Delta\theta)^2$	$\frac{1}{2}K_{\text{Te}-\text{Co}-\text{Co}}(\Delta\theta)^2$
Parameter	6.712	2.656	2.656	2.656
r_0 or θ_0	2.510	89.046	71.873	89.046

The second line gives an explicit expression for each VFF term. The third line is the force constant parameters. Parameters are in the unit of eV/ \AA^2 for the bond stretching interaction and in the unit of eV for the angle bending interaction. The fourth line gives the initial bond length (in the unit of \AA^2) for the bond stretching interaction and the initial angle (in the unit of degrees) for the angle bending interaction. The angle θ_{ijk} has atom i as the apex.

Table 82. The VFF model for single-layer 1H-CoTe₂.

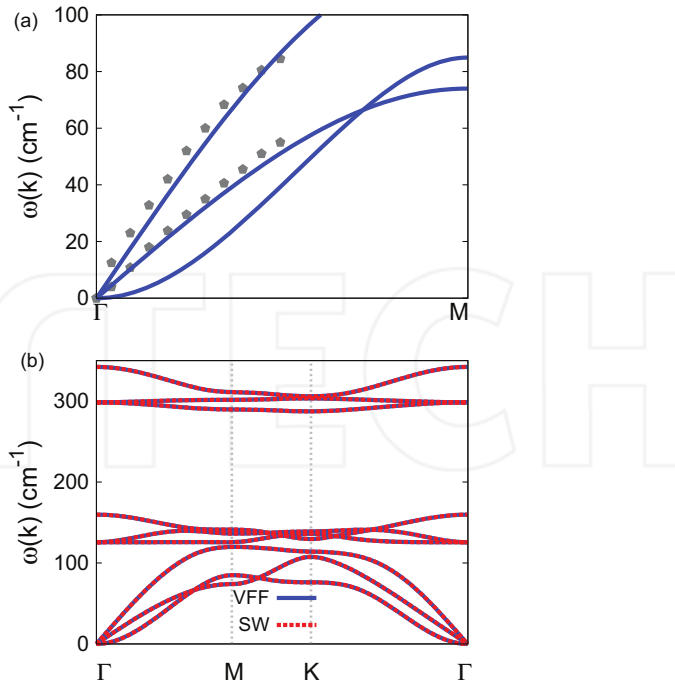


Figure 39. Phonon spectrum for single-layer 1H-CoTe₂. (a) Phonon dispersion along the Γ M direction in the Brillouin zone. The results from the VFF model (lines) are comparable with the *ab initio* results (pentagons) from Ref. [12]. (b) The phonon dispersion from the SW potential is exactly the same as that from the VFF model.

	A (eV)	ρ (\AA)	B (\AA^4)	r_{\min} (\AA)	r_{\max} (\AA)
Co—Te	6.169	1.310	19.846	0.0	3.417

Table 83. Two-body SW potential parameters for single-layer 1H-CoTe₂ used by GULP [8] as expressed in Eq. (3).

	K (eV)	θ_0 (°)	ρ_1 (\AA)	ρ_2 (\AA)	$r_{\min 12}$ (\AA)	$r_{\max 12}$ (\AA)	$r_{\min 13}$ (\AA)	$r_{\max 13}$ (\AA)	$r_{\min 23}$ (\AA)	$r_{\max 23}$ (\AA)
$\theta_{\text{Co}-\text{Te}-\text{Te}}$	23.895	89.046	1.310	1.310	0.0	3.417	0.0	3.417	0.0	4.055
$\theta_{\text{Co}-\text{Te}-\text{Te}'}$	26.449	71.873	1.310	1.310	0.0	3.417	0.0	3.417	0.0	4.055
$\theta_{\text{Te}-\text{Co}-\text{Co}}$	23.895	89.046	1.310	1.310	0.0	3.417	0.0	3.417	0.0	4.055

The angle θ_{ijk} in the first line indicates the bending energy for the angle with atom i as the apex.

Table 84. Three-body SW potential parameters for single-layer 1H-CoTe₂ used by GULP [8] as expressed in Eq. (4).

the actual thickness of the quasi-two-dimensional structure of the single-layer 1H-CoTe₂. The Young's modulus can be obtained by a linear fitting of the stress-strain relation in the small strain range of [0, 0.01]. The Young's modulus is 53.7 and 54.3 N/m along the armchair and

	ϵ (eV)	σ (\AA)	a	λ	γ	$\cos \theta_0$	A_L	B_L	p	q	Tol
Co ₁ —Te ₁ —Te ₁	1.000	1.310	2.608	0.000	1.000	0.000	6.169	6.739	4	0	0.0
Co ₁ —Te ₁ —Te ₃	1.000	0.000	0.000	23.895	1.000	0.017	0.000	0.000	4	0	0.0
Co ₁ —Te ₁ —Te ₂	1.000	0.000	0.000	26.449	1.000	0.311	0.000	0.000	4	0	0.0
Te ₁ —Co ₁ —Co ₃	1.000	0.000	0.000	23.895	1.000	0.017	0.000	0.000	4	0	0.0

Table 85. SW potential parameters for single-layer 1H-CoTe₂ used by LAMMPS [9] as expressed in Eqs. (9) and (10).

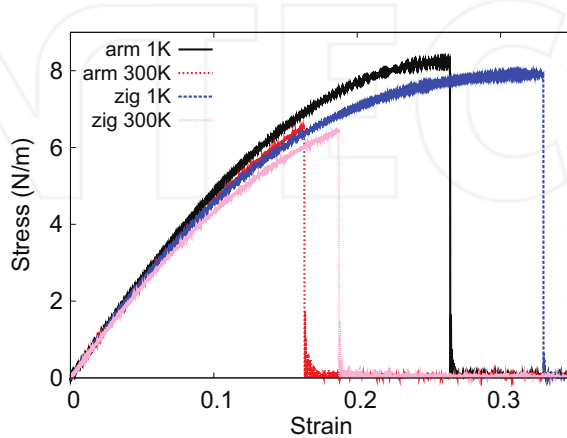


Figure 40. Stress-strain for single-layer 1H-CoTe₂ of dimension 100 × 100 \AA along the armchair and zigzag directions.

zigzag directions, respectively. The Young's modulus is essentially isotropic in the armchair and zigzag directions. The Poisson's ratio from the VFF model and the SW potential is $\nu_{xy} = \nu_{yx} = 0.32$.

There is no available value for nonlinear quantities in the single-layer 1H-CoTe₂. We have thus used the nonlinear parameter $B = 0.5d^4$ in Eq. (5), which is close to the value of B in most materials. The value of the third-order nonlinear elasticity D can be extracted by fitting the stress-strain relation to the function $\sigma = E\epsilon + \frac{1}{2}D\epsilon^2$ with E as the Young's modulus. The values of D from the present SW potential are -157.2 and -187.9 N/m along the armchair and zigzag directions, respectively. The ultimate stress is about 8.2 N/m at the ultimate strain of 0.26 in the armchair direction at the low temperature of 1 K. The ultimate stress is about 7.9 N/m at the ultimate strain of 0.33 in the zigzag direction at the low temperature of 1 K.

22. 1H-NiS₂

Most existing theoretical studies on the single-layer 1H-NiS₂ are based on the first-principles calculations. In this section, we will develop the SW potential for the single-layer 1H-NiS₂.

The structure for the single-layer 1H-NiS₂ is shown in **Figure 1** (with M=Ni and X=S). Each Ni atom is surrounded by six S atoms. These S atoms are categorized into the top group (e.g., atoms 1, 3, and 5) and bottom group (e.g., atoms 2, 4, and 6). Each S atom is connected to three Ni atoms. The structural parameters are from the first-principles calculations [12], including the lattice constant $a = 3.40 \text{ \AA}$ and the bond length $d_{\text{Ni-S}} = 2.24 \text{ \AA}$. The resultant angles are $\theta_{\text{NiSS}} = \theta_{\text{SNiNi}} = 98.740^\circ$ and $\theta_{\text{NiSS'}} = 57.593^\circ$, in which atoms S and S' are from different (top or bottom) groups.

Table 86 shows four VFF terms for the single-layer 1H-NiS₂; one of which is the bond stretching interaction shown by Eq. (1), while the other three terms are the angle bending interaction shown by Eq. (2). These force constant parameters are determined by fitting to the acoustic branches in the phonon dispersion along the TM as shown in **Figure 41(a)**. The *ab initio* calculations for the phonon dispersion are from Ref. [12]. **Figure 41(b)** shows that the VFF model and the SW potential give exactly the same phonon dispersion, as the SW potential is derived from the VFF model.

The parameters for the two-body SW potential used by GULP are shown in **Table 87**. The parameters for the three-body SW potential used by GULP are shown in **Table 88**. Some representative parameters for the SW potential used by LAMMPS are listed in **Table 89**. We note that 12 atom types have been introduced for the simulation of the single-layer 1H-NiS₂ using LAMMPS, because the angles around atom Ni in **Figure 1** (with M=Ni and X=S) are not distinguishable in LAMMPS. We have suggested two options to differentiate these angles by implementing some additional constraints in LAMMPS, which can be accomplished by modifying the source file of LAMMPS [13, 14]. According to our experience, it is not so convenient for some users to implement these constraints and recompile the LAMMPS package. Hence, in the present work, we differentiate the angles by introducing more atom types, so it is not necessary to modify the LAMMPS package. **Figure 2** (with M=Ni and X=S) shows that, for 1H-NiS₂, we can differentiate these angles around the Ni atom by assigning these six neighboring S atoms with different atom types. It can be found that 12 atom types are necessary for the purpose of differentiating all 6 neighbors around 1 Ni atom.

We use LAMMPS to perform MD simulations for the mechanical behavior of the single-layer 1H-NiS₂ under uniaxial tension at 1 and 300 K. **Figure 42** shows the stress-strain curve for the tension of a single-layer 1H-NiS₂ of dimension $100 \times 100 \text{ \AA}$. Periodic boundary conditions are

VFF type	Bond stretching	Angle bending		
Expression	$\frac{1}{2}K_{\text{Ni-S}}(\Delta r)^2$	$\frac{1}{2}K_{\text{Ni-S-S}}(\Delta\theta)^2$	$\frac{1}{2}K_{\text{Ni-S-S'}}(\Delta\theta)^2$	$\frac{1}{2}K_{\text{S-Ni-Ni}}(\Delta\theta)^2$
Parameter	6.933	3.418	3.418	3.418
r_0 or θ_0	2.240	98.740	57.593	98.740

The second line gives an explicit expression for each VFF term. The third line is the force constant parameters. Parameters are in the unit of eV/ \AA^2 for the bond stretching interaction and in the unit of eV for the angle bending interaction. The fourth line gives the initial bond length (in the unit of \AA) for the bond stretching interaction and the initial angle (in the unit of degrees) for the angle bending interaction. The angle θ_{ijk} has atom i as the apex.

Table 86. The VFF model for single-layer 1H-NiS₂.

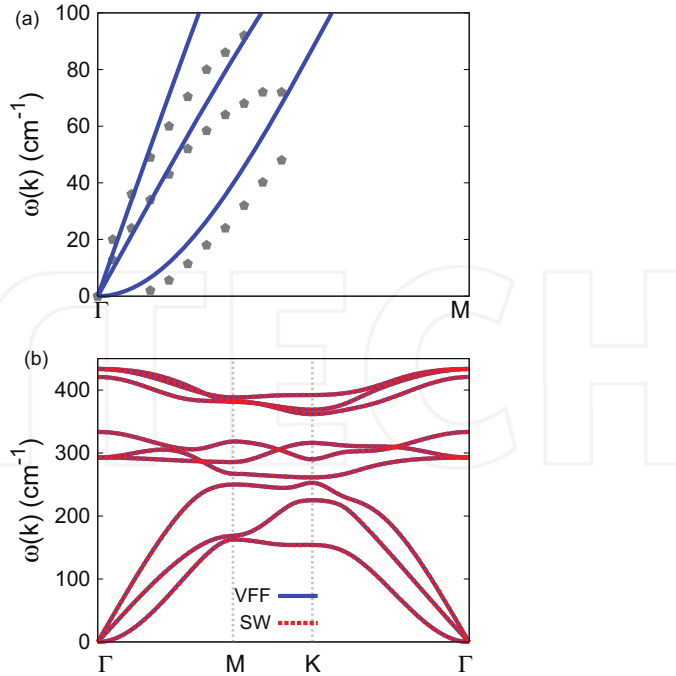


Figure 41. Phonon spectrum for single-layer 1H-NiS₂. (a) Phonon dispersion along the Γ M direction in the Brillouin zone. The results from the VFF model (lines) are comparable with the *ab initio* results (pentagons) from Ref. [12]. (b) The phonon dispersion from the SW potential is exactly the same as that from the VFF model.

	A (eV)	ρ (\AA)	B (\AA^4)	r_{\min} (\AA)	r_{\max} (\AA)
Ni-S	6.425	1.498	12.588	0.0	3.156

Table 87. Two-body SW potential parameters for single-layer 1H-NiS₂ used by GULP [8] as expressed in Eq. (3).

	K (eV)	θ_0 (°)	ρ_1 (\AA)	ρ_2 (\AA)	$r_{\min 12}$ (\AA)	$r_{\max 12}$ (\AA)	$r_{\min 13}$ (\AA)	$r_{\max 13}$ (\AA)	$r_{\min 23}$ (\AA)	$r_{\max 23}$ (\AA)
$\theta_{\text{Ni-S-S}}$	46.062	98.740	1.498	1.498	0.0	3.156	0.0	3.156	0.0	3.713
$\theta_{\text{Ni-S-S'}}$	63.130	57.593	1.498	1.498	0.0	3.156	0.0	3.156	0.0	3.713
$\theta_{\text{S-Ni-Ni}}$	46.062	98.740	1.498	1.498	0.0	3.156	0.0	3.156	0.0	3.713

The angle θ_{ijk} in the first line indicates the bending energy for the angle with atom i as the apex.

Table 88. Three-body SW potential parameters for single-layer 1H-NiS₂ used by GULP [8] as expressed in Eq. (4).

applied in both armchair and zigzag directions. The single-layer 1H-NiS₂ is stretched uniaxially along the armchair or zigzag direction. The stress is calculated without involving the actual thickness of the quasi-two-dimensional structure of the single-layer 1H-NiS₂. The Young's modulus can be obtained by a linear fitting of the stress-strain relation in the small

	ϵ (eV)	σ (\AA)	a	λ	γ	$\cos \theta_0$	A_L	B_L	p	q	Tol
Ni ₁ —S ₁ —S ₁	1.000	1.498	2.107	0.000	1.000	0.000	6.425	2.502	4	0	0.0
Ni ₁ —S ₁ —S ₃	1.000	0.000	0.000	46.062	1.000	-0.152	0.000	0.000	4	0	0.0
Ni ₁ —S ₁ —S ₂	1.000	0.000	0.000	63.130	1.000	0.536	0.000	0.000	4	0	0.0
S ₁ —Ni ₁ —Ni ₃	1.000	0.000	0.000	46.062	1.000	-0.152	0.000	0.000	4	0	0.0

Table 89. SW potential parameters for single-layer 1H-NiS₂ used by LAMMPS [9] as expressed in Eqs. (9) and (10).

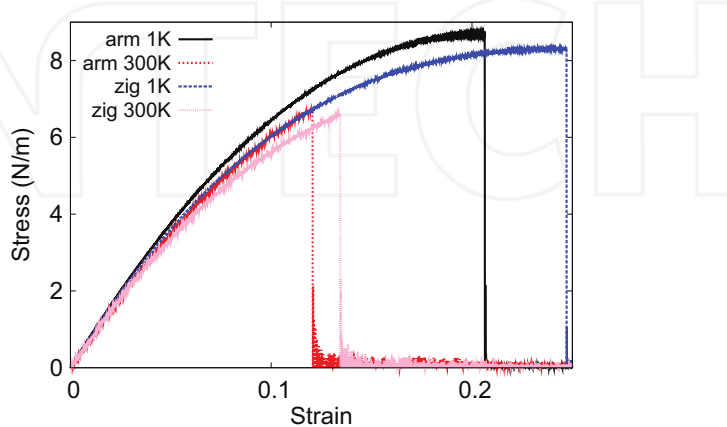


Figure 42. Stress-strain for single-layer 1H-NiS₂ of dimension $100 \times 100 \text{ \AA}$ along the armchair and zigzag directions.

strain range of $[0, 0.01]$. The Young's modulus is 84.0 and 82.5 N/m along the armchair and zigzag directions, respectively. The Young's modulus is essentially isotropic in the armchair and zigzag directions. The Poisson's ratio from the VFF model and the SW potential is $\nu_{xy} = \nu_{yx} = 0.19$.

There is no available value for nonlinear quantities in the single-layer 1H-NiS₂. We have thus used the nonlinear parameter $B = 0.5d^4$ in Eq. (5), which is close to the value of B in most materials. The value of the third-order nonlinear elasticity D can be extracted by fitting the stress-strain relation to the function $\sigma = E\epsilon + \frac{1}{2}D\epsilon^2$ with E as the Young's modulus. The values of D from the present SW potential are -403.2 and -414.8 N/m along the armchair and zigzag directions, respectively. The ultimate stress is about 8.7 N/m at the ultimate strain of 0.20 in the armchair direction at the low temperature of 1 K. The ultimate stress is about 8.3 N/m at the ultimate strain of 0.24 in the zigzag direction at the low temperature of 1 K.

23. 1H-NiSe₂

Most existing theoretical studies on the single-layer 1H-NiSe₂ are based on the first-principles calculations. In this section, we will develop the SW potential for the single-layer 1H-NiSe₂.

The structure for the single-layer 1H-NiSe₂ is shown in **Figure 1** (with M=Ni and X=Se). Each Ni atom is surrounded by six Se atoms. These Se atoms are categorized into the top group (e.g., atoms 1, 3, and 5) and bottom group (e.g., atoms 2, 4, and 6). Each Se atom is connected to three Ni atoms. The structural parameters are from the first-principles calculations [12], including the lattice constant $a = 3.33 \text{ \AA}$ and the bond length $d_{\text{Ni-Se}} = 2.35 \text{ \AA}$. The resultant angles are $\theta_{\text{NiSeSe}} = \theta_{\text{SeNiNi}} = 90.228^\circ$ and $\theta_{\text{NiSeSe}'} = 70.206^\circ$, in which atoms Se and Se' are from different (top or bottom) groups.

Table 90 shows four VFF terms for the single-layer 1H-NiSe₂; one of which is the bond stretching interaction shown by Eq. (1), while the other three terms are the angle bending interaction shown by Eq. (2). These force constant parameters are determined by fitting to the acoustic branches in the phonon dispersion along the ΓM as shown in **Figure 43(a)**. The *ab initio* calculations for the phonon dispersion are from Ref. [12]. The lowest acoustic branch (flexural mode) is almost linear in the *ab initio* calculations, which may be due to the violation of the rigid rotational invariance [20]. **Figure 43(b)** shows that the VFF model and the SW potential give exactly the same phonon dispersion, as the SW potential is derived from the VFF model.

The parameters for the two-body SW potential used by GULP are shown in **Table 91**. The parameters for the three-body SW potential used by GULP are shown in **Table 92**. Some representative parameters for the SW potential used by LAMMPS are listed in **Table 93**. We note that 12 atom types have been introduced for the simulation of the single-layer 1H-NiSe₂ using LAMMPS, because the angles around atom Ni in **Figure 1** (with M=Ni and X=Se) are not distinguishable in LAMMPS. We have suggested two options to differentiate these angles by implementing some additional constraints in LAMMPS, which can be accomplished by modifying the source file of LAMMPS [13, 14]. According to our experience, it is not so convenient for some users to implement these constraints and recompile the LAMMPS package. Hence, in the present work, we differentiate the angles by introducing more atom types, so it is not necessary to modify the LAMMPS package. **Figure 2** (with M=Ni and X=Se) shows that, for 1H-NiSe₂, we can differentiate these angles around the Ni atom by assigning these six neighboring Se atoms with different atom types. It can be found that 12 atom types are necessary for the purpose of differentiating all 6 neighbors around 1 Ni atom.

We use LAMMPS to perform MD simulations for the mechanical behavior of the single-layer 1H-NiSe₂ under uniaxial tension at 1 and 300 K. **Figure 44** shows the stress-strain curve for the

VFF type	Bond stretching	Angle bending		
Expression	$\frac{1}{2}K_{\text{Ni-Se}}(\Delta r)^2$	$\frac{1}{2}K_{\text{Ni-Se-Se}}(\Delta\theta)^2$	$\frac{1}{2}K_{\text{Ni-Se-Se}'}(\Delta\theta)^2$	$\frac{1}{2}K_{\text{Se-Ni-Ni}}(\Delta\theta)^2$
Parameter	4.823	2.171	2.171	2.171
r_0 or θ_0	2.350	90.228	70.206	90.228

The second line gives an explicit expression for each VFF term. The third line is the force constant parameters. Parameters are in the unit of eV/c² for the bond stretching interaction and in the unit of eV for the angle bending interaction. The fourth line gives the initial bond length (in the unit of eV/Å²) for the bond stretching interaction and the initial angle (in the unit of degrees) for the angle bending interaction. The angle θ_{ijk} has atom *i* as the apex.

Table 90. The VFF model for single-layer 1H-NiSe₂.

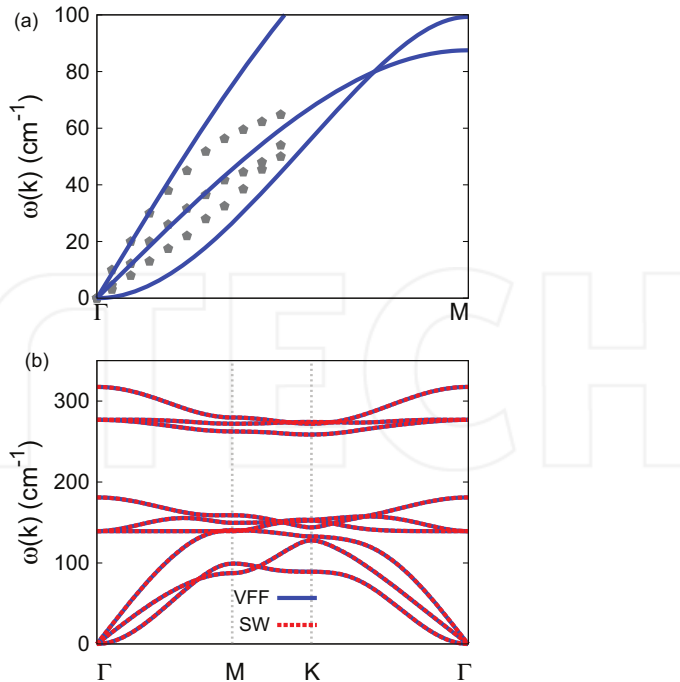


Figure 43. Phonon spectrum for single-layer 1H-NiSe₂. (a) Phonon dispersion along the Γ M direction in the Brillouin zone. The results from the VFF model (lines) are comparable with the *ab initio* results (pentagons) from Ref. [12]. (b) The phonon dispersion from the SW potential is exactly the same as that from the VFF model.

	A (eV)	ρ (Å)	B (Å ⁴)	r_{\min} (Å)	r_{\max} (Å)
Ni–Se	4.004	1.267	15.249	0.0	3.213

Table 91. Two-body SW potential parameters for single-layer 1H-NiSe₂ used by GULP [8] as expressed in Eq. (3).

	K (eV)	θ_0 (°)	ρ_1 (Å)	ρ_2 (Å)	$r_{\min 12}$ (Å)	$r_{\max 12}$ (Å)	$r_{\min 13}$ (Å)	$r_{\max 13}$ (Å)	$r_{\min 23}$ (Å)	$r_{\max 23}$ (Å)
$\theta_{\text{Ni–Se–Se}}$	20.479	90.228	1.267	1.267	0.0	3.213	0.0	3.213	0.0	3.809
$\theta_{\text{Ni–Se–Se'}}$	23.132	70.206	1.267	1.267	0.0	3.213	0.0	3.213	0.0	3.809
$\theta_{\text{Se–Ni–Ni}}$	20.479	90.228	1.267	1.267	0.0	3.213	0.0	3.213	0.0	3.809

The angle θ_{ijk} in the first line indicates the bending energy for the angle with atom i as the apex.

Table 92. Three-body SW potential parameters for single-layer 1H-NiSe₂ used by GULP [8] as expressed in Eq. (4).

tension of a single-layer 1H-NiSe₂ of dimension 100 × 100 Å. Periodic boundary conditions are applied in both armchair and zigzag directions. The single-layer 1H-NiSe₂ is stretched uniaxially along the armchair or zigzag direction. The stress is calculated without involving the actual thickness of the quasi-two-dimensional structure of the single-layer 1H-NiSe₂. The

	ϵ (eV)	σ (\AA)	a	λ	γ	$\cos \theta_0$	A_L	B_L	p	q	Tol
Ni ₁ —Se ₁ —Se ₁	1.000	1.267	2.535	0.000	1.000	0.000	4.004	5.913	4	0	0.0
Ni ₁ —Se ₁ —Se ₃	1.000	0.000	0.000	20.479	1.000	-0.004	0.000	0.000	4	0	0.0
Ni ₁ —Se ₁ —Se ₂	1.000	0.000	0.000	23.132	1.000	0.339	0.000	0.000	4	0	0.0
Se ₁ —Ni ₁ —Ni ₃	1.000	0.000	0.000	20.479	1.000	-0.004	0.000	0.000	4	0	0.0

Table 93. SW potential parameters for single-layer 1H-NiSe₂ used by LAMMPS [9] as expressed in Eqs. (9) and (10).

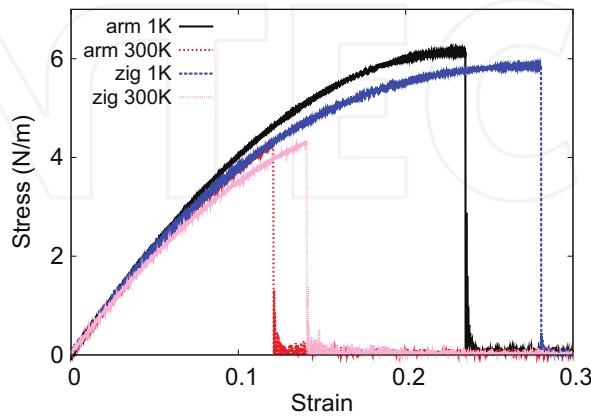


Figure 44. Stress-strain for single-layer 1H-NiSe₂ of dimension 100 × 100 Å along the armchair and zigzag directions

Young's modulus can be obtained by a linear fitting of the stress-strain relation in the small strain range of [0, 0.01]. The Young's modulus is 47.6 and 47.8 N/m along the armchair and zigzag directions, respectively. The Young's modulus is essentially isotropic in the armchair and zigzag directions. The Poisson's ratio from the VFF model and the SW potential is $\nu_{xy} = \nu_{yx} = 0.27$.

There is no available value for nonlinear quantities in the single-layer 1H-NiSe₂. We have thus used the nonlinear parameter $B = 0.5d^4$ in Eq. (5), which is close to the value of B in most materials. The value of the third-order nonlinear elasticity D can be extracted by fitting the stress-strain relation to the function $\sigma = E\epsilon + \frac{1}{2}D\epsilon^2$ with E as the Young's modulus. The values of D from the present SW potential are -173.9 and -197.6 N/m along the armchair and zigzag directions, respectively. The ultimate stress is about 6.1 N/m at the ultimate strain of 0.23 in the armchair direction at the low temperature of 1 K. The ultimate stress is about 5.9 N/m at the ultimate strain of 0.28 in the zigzag direction at the low temperature of 1 K.

24. 1H-NiTe₂

Most existing theoretical studies on the single-layer 1H-NiTe₂ are based on the first-principles calculations. In this section, we will develop the SW potential for the single-layer 1H-NiTe₂.

The structure for the single-layer 1H-NiTe₂ is shown in **Figure 1** (with M=Ni and X=Te). Each Ni atom is surrounded by six Te atoms. These Te atoms are categorized into the top group (e.g., atoms 1, 3, and 5) and bottom group (e.g., atoms 2, 4, and 6). Each Te atom is connected to three Ni atoms. The structural parameters are from the first-principles calculations [12], including the lattice constant $a = 3.59 \text{ \AA}$ and the bond length $d_{\text{Ni}-\text{Te}} = 2.54 \text{ \AA}$. The resultant angles are $\theta_{\text{NiTeTe}} = \theta_{\text{TeNiNi}} = 89.933^\circ$ and $\theta_{\text{NiTeTe}'} = 70.624^\circ$, in which atoms Te and Te' are from different (top or bottom) groups.

Table 94 shows four VFF terms for the single-layer 1H-NiTe₂; one of which is the bond stretching interaction shown by Eq. (1), while the other three terms are the angle bending interaction shown by Eq. (2). These force constant parameters are determined by fitting to the acoustic branches in the phonon dispersion along the FM as shown in **Figure 45(a)**. The *ab initio* calculations for the phonon dispersion are from Ref. [12]. The lowest acoustic branch (flexural mode) is almost linear in the *ab initio* calculations, which may be due to the violation of the rigid rotational invariance [20]. The transverse acoustic branch is very close to the longitudinal acoustic branch in the *ab initio* calculations. **Figure 45(b)** shows that the VFF model and the SW potential give exactly the same phonon dispersion, as the SW potential is derived from the VFF model.

The parameters for the two-body SW potential used by GULP are shown in **Table 95**. The parameters for the three-body SW potential used by GULP are shown in **Table 96**. Some representative parameters for the SW potential used by LAMMPS are listed in **Table 97**. We note that 12 atom types have been introduced for the simulation of the single-layer 1H-NiTe₂ using LAMMPS, because the angles around atom Ni in **Figure 1** (with M=Ni and X=Te) are not distinguishable in LAMMPS. We have suggested two options to differentiate these angles by implementing some additional constraints in LAMMPS, which can be accomplished by modifying the source file of LAMMPS [13, 14]. According to our experience, it is not so convenient for some users to implement these constraints and recompile the LAMMPS package. Hence, in the present work, we differentiate the angles by introducing more atom types, so it is not necessary to modify the LAMMPS package. **Figure 2** (with M=Ni and X=Te) shows that, for 1H-NiTe₂, we can differentiate these angles around the Ni atom by assigning these six neighboring Te atoms with different atom types. It can be found that 12 atom types are necessary for the purpose of differentiating all 6 neighbors around 1 Ni atom.

VFF type	Bond stretching	Angle bending		
Expression	$\frac{1}{2}K_{\text{Ni}-\text{Te}}(\Delta r)^2$	$\frac{1}{2}K_{\text{Ni}-\text{Te}-\text{Te}}(\Delta\theta)^2$	$\frac{1}{2}K_{\text{Ni}-\text{Te}-\text{Te}'}(\Delta\theta)^2$	$\frac{1}{2}K_{\text{Te}-\text{Ni}-\text{Ni}}(\Delta\theta)^2$
Parameter	6.712	2.656	2.656	2.656
r_0 or θ_0	2.540	89.933	70.624	89.933

The second line gives an explicit expression for each VFF term. The third line is the force constant parameters. Parameters are in the unit of eV/\text{\AA}^2 for the bond stretching interaction and in the unit of eV for the angle bending interaction. The fourth line gives the initial bond length (in the unit of \text{\AA}) for the bond stretching interaction and the initial angle (in the unit of degrees) for the angle bending interaction. The angle θ_{ijk} has atom i as the apex.

Table 94. The VFF model for single-layer 1H-NiTe₂.

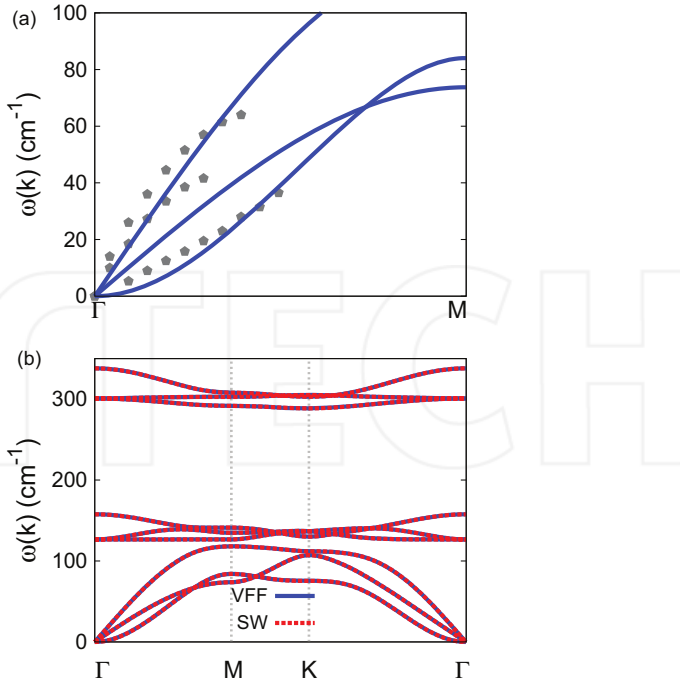


Figure 45. Phonon spectrum for single-layer 1H-NiTe₂. (a) Phonon dispersion along the Γ M direction in the Brillouin zone. The results from the VFF model (lines) are comparable with the *ab initio* results (pentagons) from Ref. [12]. (b) The phonon dispersion from the SW potential is exactly the same as that from the VFF model.

	A (eV)	ρ (Å)	B (Å ⁴)	r_{\min} (Å)	r_{\max} (Å)
Ni—Te	6.461	1.359	20.812	0.0	3.469

Table 95. Two-body SW potential parameters for single-layer 1H-NiTe₂ used by GULP [8] as expressed in Eq. (3).

	K (eV)	θ_0 (°)	ρ_1 (Å)	ρ_2 (Å)	$r_{\min 12}$ (Å)	$r_{\max 12}$ (Å)	$r_{\min 13}$ (Å)	$r_{\max 13}$ (Å)	$r_{\min 23}$ (Å)	$r_{\max 23}$ (Å)
$\theta_{\text{Ni—Te—Te}}$	24.759	89.933	1.359	1.359	0.0	3.469	0.0	3.469	0.0	4.114
$\theta_{\text{Ni—Te—Te'}}$	27.821	70.624	1.359	1.359	0.0	3.469	0.0	3.469	0.0	4.114
$\theta_{\text{Te—Ni—Ni}}$	24.759	89.933	1.359	1.359	0.0	3.469	0.0	3.469	0.0	4.114

The angle θ_{ijk} in the first line indicates the bending energy for the angle with atom i as the apex.

Table 96. Three-body SW potential parameters for single-layer 1H-NiTe₂ used by GULP [8] as expressed in Eq. (4).

We use LAMMPS to perform MD simulations for the mechanical behavior of the single-layer 1H-NiTe₂ under uniaxial tension at 1 and 300 K. **Figure 46** shows the stress-strain curve for the tension of a single-layer 1H-NiTe₂ of dimension 100 × 100 Å. Periodic boundary conditions are

	ϵ (eV)	σ (\AA)	a	λ	γ	$\cos \theta_0$	A_L	B_L	p	q	Tol
Ni ₁ —Te ₁ —Te ₁	1.000	1.359	2.553	0.000	1.000	0.000	6.461	6.107	4	0	0.0
Ni ₁ —Te ₁ —Te ₃	1.000	0.000	0.000	24.759	1.000	0.001	0.000	0.000	4	0	0.0
Ni ₁ —Te ₁ —Te ₂	1.000	0.000	0.000	27.821	1.000	0.332	0.000	0.000	4	0	0.0
Te ₁ —Ni ₁ —Ni ₃	1.000	0.000	0.000	24.759	1.000	0.001	0.000	0.000	4	0	0.0

Table 97. SW potential parameters for single-layer 1H-NiTe₂ used by LAMMPS [9] as expressed in Eqs. (9) and (10).

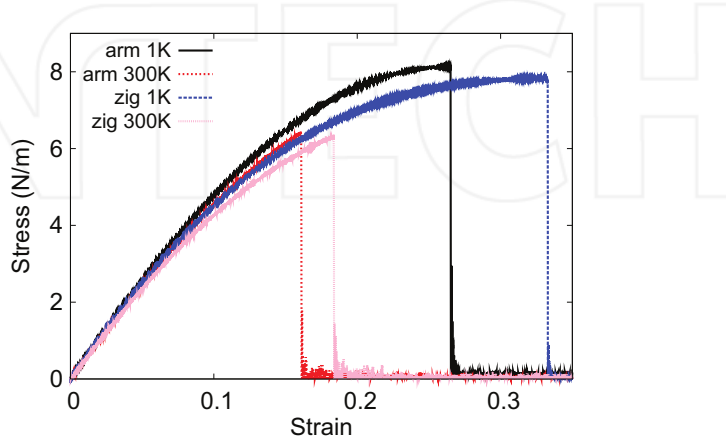


Figure 46. Stress-strain for single-layer 1H-NiTe₂ of dimension $100 \times 100 \text{ \AA}$ along the armchair and zigzag directions.

applied in both armchair and zigzag directions. The single-layer 1H-NiTe₂ is stretched uniaxially along the armchair or zigzag direction. The stress is calculated without involving the actual thickness of the quasi-two-dimensional structure of the single-layer 1H-NiTe₂. The Young's modulus can be obtained by a linear fitting of the stress-strain relation in the small strain range of [0, 0.01]. The Young's modulus is 53.2 and 53.6 N/m along the armchair and zigzag directions, respectively. The Young's modulus is essentially isotropic in the armchair and zigzag directions. The Poisson's ratio from the VFF model and the SW potential is $\nu_{xy} = \nu_{yx} = 0.32$.

There is no available value for nonlinear quantities in the single-layer 1H-NiTe₂. We have thus used the nonlinear parameter $B = 0.5d^4$ in Eq. (5), which is close to the value of B in most materials. The value of the third-order nonlinear elasticity D can be extracted by fitting the stress-strain relation to the function $\sigma = E\epsilon + \frac{1}{2}D\epsilon^2$ with E as the Young's modulus. The values of D from the present SW potential are -156.6 and -184.8 N/m along the armchair and zigzag directions, respectively. The ultimate stress is about 8.1 N/m at the ultimate strain of 0.26 in the armchair direction at the low temperature of 1 K. The ultimate stress is about 7.8 N/m at the ultimate strain of 0.33 in the zigzag direction at the low temperature of 1 K.

25. 1H-NbS₂

In 1983, the VFF model was developed to investigate the lattice dynamical properties in the bulk 2H-NbS₂ [21]. In this section, we will develop the SW potential for the single-layer 1H-NbS₂.

The structure for the single-layer 1H-NbS₂ is shown in **Figure 1** (with M=Nb and X=S). Each Nb atom is surrounded by six S atoms. These S atoms are categorized into the top group (e.g., atoms 1, 3, and 5) and bottom group (e.g., atoms 2, 4, and 6). Each S atom is connected to three Nb atoms. The structural parameters are from Ref. [21], including the lattice constant $a = 3.31 \text{ \AA}$ and the bond length $d_{\text{Nb-S}} = 2.47 \text{ \AA}$. The resultant angles are $\theta_{\text{NbSS}} = \theta_{\text{SnbNb}} = 84.140^\circ$ and $\theta_{\text{NbSS'}} = 78.626^\circ$, in which atoms S and S' are from different (top or bottom) groups.

Table 98 shows four VFF terms for the 1H-NbS₂; one of which is the bond stretching interaction shown by Eq. (1), while the other three terms are the angle bending interaction shown by Eq. (2). These force constant parameters are determined by fitting to the three acoustic branches in the phonon dispersion along the ΓM as shown in **Figure 47(a)**. The theoretical phonon frequencies (gray pentagons) are from Ref. [21], which are the phonon dispersion of bulk 2H-NbS₂. We have used these phonon frequencies as the phonon dispersion of the single-layer 1H-NbS₂, as the interlayer interaction in the bulk 2H-NbS₂ only induces weak effects on the two in-plane acoustic branches. The interlayer coupling will strengthen the out-of-plane acoustic branch (flexural branch), so the flexural branch from the present VFF model (blue line) is lower than the theoretical results for bulk 2H-NbS₂ (gray pentagons). **Figure 47(b)** shows that the VFF model and the SW potential give exactly the same phonon dispersion, as the SW potential is derived from the VFF model.

The parameters for the two-body SW potential used by GULP are shown in **Table 99**. The parameters for the three-body SW potential used by GULP are shown in **Table 100**. Parameters for the SW potential used by LAMMPS are listed in **Table 101**. We note that 12 atom types have been introduced for the simulation of the single-layer 1H-NbS₂ using LAMMPS, because the angles around atom Nb in **Figure 1** (with M=Nb and X=S) are not distinguishable in LAMMPS. We have suggested two options to differentiate these angles by implementing some additional constraints in LAMMPS, which can be accomplished by modifying the source file of LAMMPS [13, 14]. According to our experience, it is not so convenient for some users to implement these constraints and recompile the LAMMPS package. Hence, in the present work,

VFF type	Bond stretching	Angle bending		
Expression	$\frac{1}{2}K_{\text{Nb-S}}(\Delta r)^2$	$\frac{1}{2}K_{\text{Nb-S-S}}(\Delta\theta)^2$	$\frac{1}{2}K_{\text{Nb-S-S'}}(\Delta\theta)^2$	$\frac{1}{2}K_{\text{S-Nb-Nb}}(\Delta\theta)^2$
Parameter	8.230	4.811	4.811	4.811
r_0 or θ_0	2.470	84.140	78.626	84.140

The second line gives an explicit expression for each VFF term. The third line is the force constant parameters. Parameters are in the unit of eV/ \AA^2 for the bond stretching interaction and in the unit of eV for the angle bending interaction. The fourth line gives the initial bond length (in the unit of \AA) for the bond stretching interaction and the initial angle (in the unit of degrees) for the angle bending interaction. The angle θ_{ijk} has atom i as the apex.

Table 98. The VFF model for single-layer 1H-NbS₂.

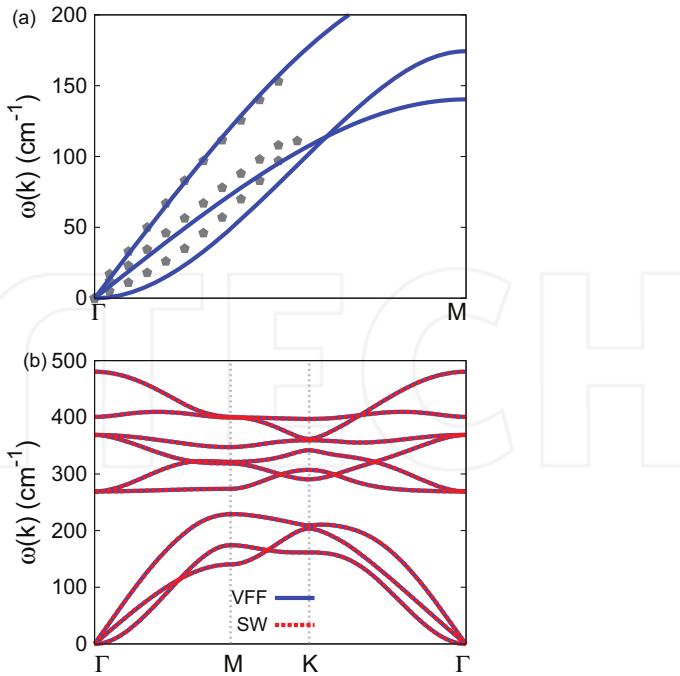


Figure 47. Phonon dispersion for single-layer 1H-NbS₂. (a) The VFF model is fitted to the three acoustic branches in the long wave limit along the Γ M direction. The theoretical results (gray pentagons) are from Ref. [21]. The blue lines are from the present VFF model. (b) The VFF model (blue lines) and the SW potential (red lines) give the same phonon dispersion for single-layer 1H-NbS₂ along Γ MKT.

	A (eV)	ρ (\AA)	B (\AA^4)	r_{\min} (\AA)	r_{\max} (\AA)
Nb—S	6.439	1.116	18.610	0.0	3.300

Table 99. Two-body SW potential parameters for single-layer 1H-NbS₂ used by GULP [8] as expressed in Eq. (3).

	K (eV)	θ_0 (°)	ρ_1 (\AA)	ρ_2 (\AA)	$r_{\min 12}$ (\AA)	$r_{\max 12}$ (\AA)	$r_{\min 13}$ (\AA)	$r_{\max 13}$ (\AA)	$r_{\min 23}$ (\AA)	$r_{\max 23}$ (\AA)
$\theta_{\text{Nb-S-S}}$	35.748	84.140	1.116	1.116	0.0	3.300	0.0	3.300	0.0	3.933
$\theta_{\text{Nb-S-S}'}$	36.807	78.626	1.116	1.116	0.0	3.300	0.0	3.300	0.0	3.933
$\theta_{\text{S-Nb-Nb}}$	35.748	84.140	1.116	1.116	0.0	3.300	0.0	3.300	0.0	3.933

The angle θ_{ijk} in the first line indicates the bending energy for the angle with atom i as the apex.

Table 100. Three-body SW potential parameters for single-layer 1H-NbS₂ used by GULP [8] as expressed in Eq. (4).

we differentiate the angles by introducing more atom types, so it is not necessary to modify the LAMMPS package. **Figure 2** (with M=Nb and X=S) shows that, for 1H-NbS₂, we can differentiate these angles around the Nb atom by assigning these six neighboring S atoms with

	ϵ (eV)	σ (\AA)	a	λ	γ	$\cos \theta_0$	A_L	B_L	p	q	Tol
Nb ₁ —S ₁ —S ₁	1.000	1.116	2.958	0.000	1.000	0.000	6.439	12.014	4	0	0.0
Nb ₁ —S ₁ —S ₃	1.000	0.000	0.000	35.748	1.000	0.102	0.000	0.000	4	0	0.0
Nb ₁ —S ₁ —S ₂	1.000	0.000	0.000	36.807	1.000	0.197	0.000	0.000	4	0	0.0
S ₁ —Nb ₁ —Nb ₃	1.000	0.000	0.000	35.748	1.000	0.102	0.000	0.000	4	0	0.0

Atom types in the first column are displayed in Figure 2 (with M=Nb and X=S).

Table 101. SW potential parameters for single-layer 1H-NbS₂ used by LAMMPS [9] as expressed in Eqs. (9) and (10).

different atom types. It can be found that 12 atom types are necessary for the purpose of differentiating all 6 neighbors around 1 Nb atom.

We use LAMMPS to perform MD simulations for the mechanical behavior of the single-layer 1H-NbS₂ under uniaxial tension at 1 and 300 K. Figure 48 shows the stress-strain curve for the tension of a single-layer 1H-NbS₂ of dimension 100 × 100 Å. Periodic boundary conditions are applied in both armchair and zigzag directions. The single-layer 1H-NbS₂ is stretched uniaxially along the armchair or zigzag direction. The stress is calculated without involving the actual thickness of the quasi-two-dimensional structure of the single-layer 1H-NbS₂. The Young's modulus can be obtained by a linear fitting of the stress-strain relation in the small strain range of [0, 0.01]. The Young's modulus is 87.7 and 87.2 N/m along the armchair and zigzag directions, respectively. The Young's modulus is essentially isotropic in the armchair and zigzag directions. The Poisson's ratio from the VFF model and the SW potential is $\nu_{xy} = \nu_{yx} = 0.27$.

There is no available value for the nonlinear quantities in the single-layer 1H-NbS₂. We have thus used the nonlinear parameter $B = 0.5d^4$ in Eq. (5), which is close to the value of B in most materials. The value of the third-order nonlinear elasticity D can be extracted by fitting the

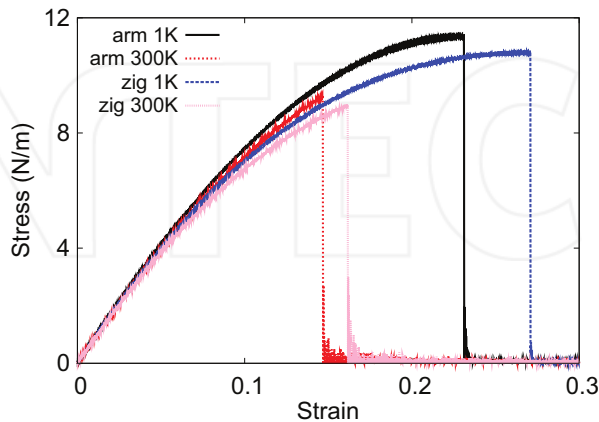


Figure 48. Stress-strain for single-layer 1H-NbS₂ of dimension 100 × 100 Å along the armchair and zigzag directions.

stress-strain relation to the function $\sigma = E\epsilon + \frac{1}{2}D\epsilon^2$ with E as the Young's modulus. The values of D from the present SW potential are -315.3 and -355.1 N/m along the armchair and zigzag directions, respectively. The ultimate stress is about 11.4 N/m at the ultimate strain of 0.23 in the armchair direction at the low temperature of 1 K. The ultimate stress is about 10.8 N/m at the ultimate strain of 0.27 in the zigzag direction at the low temperature of 1 K.

26. 1H-NbSe₂

In 1983, the VFF model was developed to investigate the lattice dynamical properties in the bulk 2H-NbSe₂ [15, 21]. In this section, we will develop the SW potential for the single-layer 1H-NbSe₂.

The structure for the single-layer 1H-NbSe₂ is shown in **Figure 1** (with M=Nb and X=Se). Each Nb atom is surrounded by six Se atoms. These Se atoms are categorized into the top group (e.g., atoms 1, 3, and 5) and bottom group (e.g., atoms 2, 4, and 6). Each Se atom is connected to three Nb atoms. The structural parameters are from Ref. [21], including the lattice constant $a = 3.45$ Å and the bond length $d_{Nb-Se} = 2.60$ Å. The resultant angles are $\theta_{NbSeSe} = \theta_{SNbNb} = 83.129^\circ$ and $\theta_{NbSeSe'} = 79.990^\circ$, in which atoms Se and Se' are from different (top or bottom) groups.

Table 102 shows four VFF terms for the 1H-NbSe₂; one of which is the bond stretching interaction shown by Eq. (1), while the other three terms are the angle bending interaction shown by Eq. (2). These force constant parameters are determined by fitting to the three acoustic branches in the phonon dispersion along the Γ M as shown in **Figure 49(a)**. The theoretical phonon frequencies (gray pentagons) are from Ref. [21], which are the phonon dispersion of bulk 2H-NbSe₂. We have used these phonon frequencies as the phonon dispersion of the single-layer 1H-NbSe₂, as the interlayer interaction in the bulk 2H-NbSe₂ only induces weak effects on the two in-plane acoustic branches. The interlayer coupling will strengthen the out-of-plane acoustic branch (flexural branch), so the flexural branch from the present VFF model (blue line) is lower than the theoretical results for bulk 2H-NbSe₂ (gray pentagons). It turns out that the VFF parameters for the single-layer 1H-NbSe₂ are the same as the single-layer NbS₂. The phonon dispersion for single-layer 1H-NbSe₂ was also shown in

VFF type	Bond stretching	Angle bending		
Expression	$\frac{1}{2}K_{Nb-Se}(\Delta r)^2$	$\frac{1}{2}K_{Nb-Se-Se}(\Delta\theta)^2$	$\frac{1}{2}K_{Nb-Se-Se'}(\Delta\theta)^2$	$\frac{1}{2}K_{Se-Nb-Nb}(\Delta\theta)^2$
Parameter	8.230	4.811	4.811	4.811
r_0 or θ_0	2.600	83.129	79.990	83.129

The second line gives an explicit expression for each VFF term. The third line is the force constant parameters. Parameters are in the unit of eV/Å² for the bond stretching interaction and in the unit of eV for the angle bending interaction. The fourth line gives the initial bond length (in the unit of Å) for the bond stretching interaction and the initial angle (in the unit of degrees) for the angle bending interaction. The angle θ_{ijk} has atom i as the apex.

Table 102. The VFF model for single-layer 1H-NbSe₂.

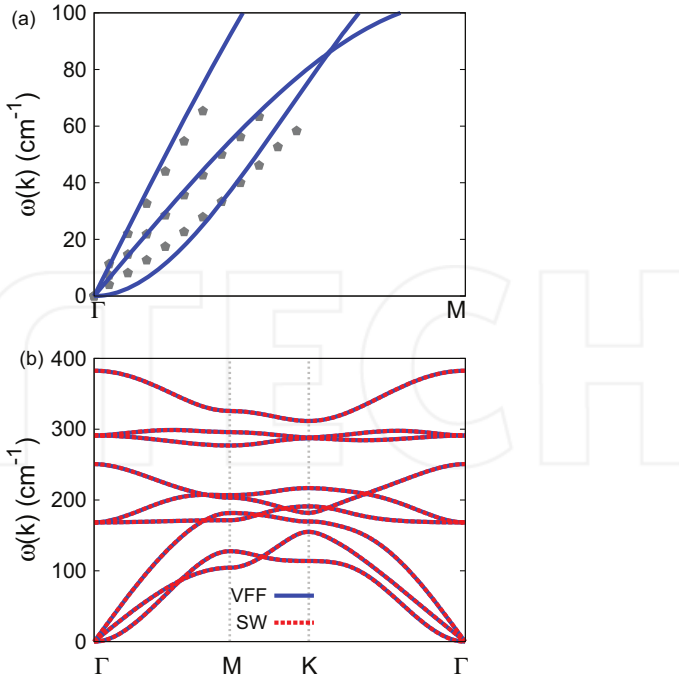


Figure 49. Phonon dispersion for single-layer 1H-NbSe₂. (a) The VFF model is fitted to the three acoustic branches in the long wave limit along the Γ M direction. The theoretical results (gray pentagons) are from Ref. [15]. The blue lines are from the present VFF model. (b) The VFF model (blue lines) and the SW potential (red lines) give the same phonon dispersion for single-layer 1H-NbSe₂ along Γ MK Γ .

Ref. [12]. **Figure 49(b)** shows that the VFF model and the SW potential give exactly the same phonon dispersion, as the SW potential is derived from the VFF model.

The parameters for the two-body SW potential used by GULP are shown in **Table 103**. The parameters for the three-body SW potential used by GULP are shown in **Table 104**. Parameters for the SW potential used by LAMMPS are listed in **Table 105**. We note that 12 atom types have been introduced for the simulation of the single-layer 1H-NbSe₂ using LAMMPS, because the angles around atom Nb in **Figure 1** (with M=Nb and X=Se) are not distinguishable in LAMMPS. We have suggested two options to differentiate these angles by implementing some additional constraints in LAMMPS, which can be accomplished by modifying the source file of LAMMPS [13, 14]. According to our experience, it is not so convenient for some users to implement these constraints and recompile the LAMMPS package. Hence, in the present work,

	A (eV)	ρ (\AA)	B (\AA^4)	r_{\min} (\AA)	r_{\max} (\AA)
Nb-Se	6.942	1.138	22.849	0.0	3.460

Table 103. Two-body SW potential parameters for single-layer 1H-NbSe₂ used by GULP [8] as expressed in Eq. (3).

	K (eV)	θ_0 ($^\circ$)	ρ_1 (\AA)	ρ_2 (\AA)	$r_{\min 12}$ (\AA)	$r_{\max 12}$ (\AA)	$r_{\min 13}$ (\AA)	$r_{\max 13}$ (\AA)	$r_{\min 23}$ (\AA)	$r_{\max 23}$ (\AA)
$\theta_{\text{Nb}-\text{Se}-\text{Se}}$	34.409	83.129	1.138	1.138	0.0	3.460	0.0	3.460	0.0	4.127
$\theta_{\text{Nb}-\text{Se}-\text{Se}'}$	34.973	79.990	1.138	1.138	0.0	3.460	0.0	3.460	0.0	4.127
$\theta_{\text{Se}-\text{Nb}-\text{Nb}}$	34.409	83.129	1.138	1.138	0.0	3.460	0.0	3.460	0.0	4.127

The angle θ_{ijk} in the first line indicates the bending energy for the angle with atom i as the apex.

Table 104. Three-body SW potential parameters for single-layer 1H-NbSe₂ used by GULP [8] as expressed in Eq. (4).

	ϵ (eV)	σ (\AA)	a	λ	γ	$\cos \theta_0$	A_L	B_L	p	q	Tol
Nb ₁ —Se ₁ —Se ₁	1.000	1.138	3.041	0.000	1.000	0.000	6.942	13.631	4	0	0.0
Nb ₁ —Se ₁ —Se ₃	1.000	0.000	0.000	34.409	1.000	0.120	0.000	0.000	4	0	0.0
Nb ₁ —Se ₁ —Se ₂	1.000	0.000	0.000	34.973	1.000	0.174	0.000	0.000	4	0	0.0
Se ₁ —Nb ₁ —Nb ₃	1.000	0.000	0.000	34.409	1.000	0.120	0.000	0.000	4	0	0.0

Atom types in the first column are displayed in **Figure 2** (with M=Nb and X=Se).

Table 105. SW potential parameters for single-layer 1H-NbSe₂ used by LAMMPS [9] as expressed in Eqs. (9) and (10).

we differentiate the angles by introducing more atom types, so it is not necessary to modify the LAMMPS package. **Figure 2** (with M=Nb and X=Se) shows that, for 1H-NbSe₂, we can differentiate these angles around the Nb atom by assigning these six neighboring Se atoms with different atom types. It can be found that 12 atom types are necessary for the purpose of differentiating all 6 neighbors around 1 Nb atom.

We use LAMMPS to perform MD simulations for the mechanical behavior of the single-layer 1H-NbSe₂ under uniaxial tension at 1 and 300 K. **Figure 50** shows the stress-strain curve for the tension of a single-layer 1H-NbSe₂ of dimension 100 × 100 Å. Periodic boundary conditions

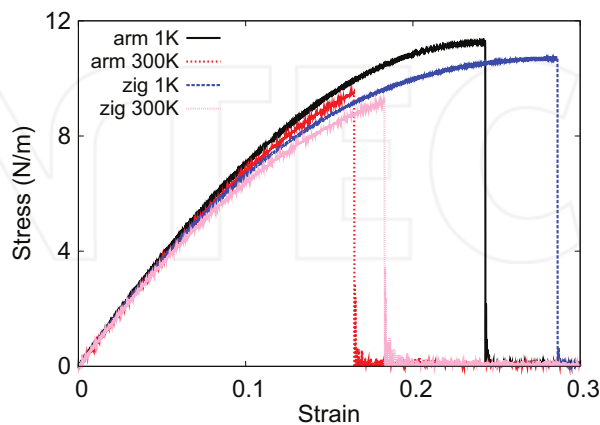


Figure 50. Stress-strain for single-layer 1H-NbSe₂ of dimension 100 × 100 Å along the armchair and zigzag directions.

are applied in both armchair and zigzag directions. The single-layer 1H-NbSe₂ is stretched uniaxially along the armchair or zigzag direction. The stress is calculated without involving the actual thickness of the quasi-two-dimensional structure of the single-layer 1H-NbSe₂. The Young's modulus can be obtained by a linear fitting of the stress-strain relation in the small strain range of [0, 0.01]. The Young's modulus is 80.2 and 80.7 N/m along the armchair and zigzag directions, respectively. The Young's modulus is essentially isotropic in the armchair and zigzag directions. The Poisson's ratio from the VFF model and the SW potential is $\nu_{xy} = \nu_{yx} = 0.29$.

There is no available value for the nonlinear quantities in the single-layer 1H-NbSe₂. We have thus used the nonlinear parameter $B = 0.5d^4$ in Eq. (5), which is close to the value of B in most materials. The value of the third-order nonlinear elasticity D can be extracted by fitting the stress-strain relation to the function $\sigma = E\epsilon + \frac{1}{2}D\epsilon^2$ with E as the Young's modulus. The values of D from the present SW potential are -258.8 and -306.1 N/m along the armchair and zigzag directions, respectively. The ultimate stress is about 11.2 N/m at the ultimate strain of 0.24 in the armchair direction at the low temperature of 1 K. The ultimate stress is about 10.7 N/m at the ultimate strain of 0.28 in the zigzag direction at the low temperature of 1 K.

27. 1H-MoO₂

Most existing theoretical studies on the single-layer 1H-MoO₂ are based on the first-principles calculations. In this section, we will develop the SW potential for the single-layer 1H-MoO₂.

The structure for the single-layer 1H-MoO₂ is shown in **Figure 1** (with M = Mo and X = O). Each Mo atom is surrounded by six O atoms. These O atoms are categorized into the top group (e.g., atoms 1, 3, and 5) and bottom group (e.g., atoms 2, 4, and 6). Each O atom is connected to three Mo atoms. The structural parameters are from the first-principles calculations [12], including the lattice constant $a = 2.78$ Å and the bond length $d_{\text{Mo}-\text{O}} = 2.00$ Å. The resultant angles are $\theta_{\text{MoOO}} = \theta_{\text{OMoMo}} = 88.054^\circ$ and $\theta_{\text{MoOO}'} = 73.258^\circ$, in which atoms O and O' are from different (top or bottom) groups.

Table 106 shows four VFF terms for the single-layer 1H-MoO₂; one of which is the bond stretching interaction shown by Eq. (1), while the other three terms are the angle bending

VFF type	Bond stretching	Angle bending		
Expression	$\frac{1}{2}K_{\text{Mo}-\text{O}}(\Delta r)^2$	$\frac{1}{2}K_{\text{Mo}-\text{O}-\text{O}}(\Delta\theta)^2$	$\frac{1}{2}K_{\text{Mo}-\text{O}-\text{O}'}(\Delta\theta)^2$	$\frac{1}{2}K_{\text{O}-\text{Mo}-\text{Mo}}(\Delta\theta)^2$
Parameter	14.622	8.410	8.410	8.410
r_0 or θ_0	2.000	88.054	73.258	88.054

The second line gives an explicit expression for each VFF term. The third line is the force constant parameters. Parameters are in the unit of eV/Å² for the bond stretching interaction and in the unit of eV for the angle bending interaction. The fourth line gives the initial bond length (in the unit of Å) for the bond stretching interaction and the initial angle (in the unit of degrees) for the angle bending interaction. The angle θ_{ijk} has atom i as the apex.

Table 106. The VFF model for single-layer 1H-MoO₂.

interaction shown by Eq. (2). These force constant parameters are determined by fitting to the acoustic branches in the phonon dispersion along the Γ M as shown in **Figure 51(a)**. The *ab initio* calculations for the phonon dispersion are from Ref. [12]. **Figure 51(b)** shows that the VFF model and the SW potential give exactly the same phonon dispersion, as the SW potential is derived from the VFF model.

The parameters for the two-body SW potential used by GULP are shown in **Table 107**. The parameters for the three-body SW potential used by GULP are shown in **Table 108**. Some representative parameters for the SW potential used by LAMMPS are listed in **Table 109**. We note that 12 atom types have been introduced for the simulation of the single-layer 1H-MoO₂ using LAMMPS, because the angles around atom Mo in **Figure 1** (with M = Mo and X = O) are not distinguishable in LAMMPS. We have suggested two options to differentiate these angles by implementing some additional constraints in LAMMPS, which can be accomplished by modifying the source file of LAMMPS [13, 14]. According to our experience, it is not so

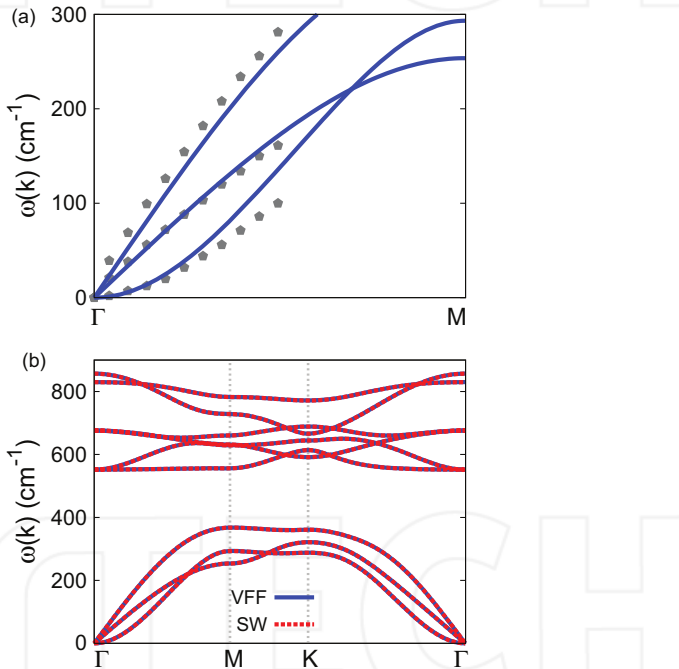


Figure 51. Phonon spectrum for single-layer 1H-MoO₂. (a) Phonon dispersion along the Γ M direction in the Brillouin zone. The results from the VFF model (lines) are comparable with the *ab initio* results (pentagons) from Ref. [12]. (b) The phonon dispersion from the SW potential is exactly the same as that from the VFF model.

	A (eV)	ρ (\AA)	B (\AA^4)	r_{\min} (\AA)	r_{\max} (\AA)
Mo-O	8.317	1.015	8.000	0.0	2.712

Table 107. Two-body SW potential parameters for single-layer 1H-MoO₂ used by GULP [8] as expressed in Eq. (3).

	K (eV)	θ_0 ($^\circ$)	ρ_1 (\AA)	ρ_2 (\AA)	$r_{\min 12}$ (\AA)	$r_{\max 12}$ (\AA)	$r_{\min 13}$ (\AA)	$r_{\max 13}$ (\AA)	$r_{\min 23}$ (\AA)	$r_{\max 23}$ (\AA)
$\theta_{\text{Mo}-\text{O}-\text{O}}$	72.735	88.054	1.015	1.015	0.0	2.712	0.0	2.712	0.0	3.222
$\theta_{\text{Mo}-\text{O}-\text{O}'}$	79.226	73.258	1.015	1.015	0.0	2.712	0.0	2.712	0.0	3.222
$\theta_{\text{O}-\text{Mo}-\text{Mo}}$	72.735	88.054	1.015	1.015	0.0	2.712	0.0	2.712	0.0	3.222

The angle θ_{ijk} in the first line indicates the bending energy for the angle with atom i as the apex.

Table 108. Three-body SW potential parameters for single-layer 1H-MoO₂ used by GULP [8] as expressed in Eq. (4).

	ϵ (eV)	σ (\AA)	a	λ	γ	$\cos \theta_0$	A_L	B_L	p	q	Tol
Mo ₁ —O ₁ —O ₁	1.000	1.015	2.673	0.000	1.000	0.000	8.317	7.541	4	0	0.0
Mo ₁ —O ₁ —O ₃	1.000	0.000	0.000	72.735	1.000	0.034	0.000	0.000	4	0	0.0
Mo ₁ —O ₁ —O ₂	1.000	0.000	0.000	79.226	1.000	0.288	0.000	0.000	4	0	0.0
O ₁ —Mo ₁ —Mo ₃	1.000	0.000	0.000	72.735	1.000	0.034	0.000	0.000	4	0	0.0

Table 109. SW potential parameters for single-layer 1H-MoO₂ used by LAMMPS [9] as expressed in Eqs. (9) and (10).

convenient for some users to implement these constraints and recompile the LAMMPS package. Hence, in the present work, we differentiate the angles by introducing more atom types, so it is not necessary to modify the LAMMPS package. **Figure 2** (with M = Mo and X = O) shows that, for 1H-MoO₂, we can differentiate these angles around the Mo atom by assigning these six neighboring O atoms with different atom types. It can be found that 12 atom types are necessary for the purpose of differentiating all 6 neighbors around 1 Mo atom.

We use LAMMPS to perform MD simulations for the mechanical behavior of the single-layer 1H-MoO₂ under uniaxial tension at 1 and 300 K. **Figure 52** shows the stress-strain curve for the tension of a single-layer 1H-MoO₂ of dimension 100 × 100 Å. Periodic boundary conditions are

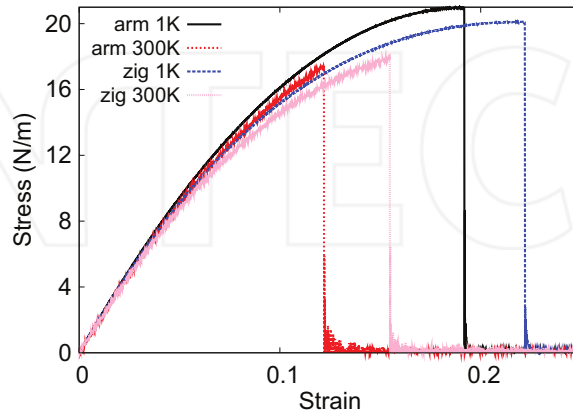


Figure 52. Stress-strain for single-layer 1H-MoO₂ of dimension 100 × 100 Å along the armchair and zigzag directions.

applied in both armchair and zigzag directions. The single-layer 1H-MoO₂ is stretched uniaxially along the armchair or zigzag direction. The stress is calculated without involving the actual thickness of the quasi-two-dimensional structure of the single-layer 1H-MoO₂. The Young's modulus can be obtained by a linear fitting of the stress-strain relation in the small strain range of [0, 0.01]. The Young's modulus is 210.0 and 209.3 N/m along the armchair and zigzag directions, respectively. The Young's modulus is essentially isotropic in the armchair and zigzag directions. The Poisson's ratio from the VFF model and the SW potential is $\nu_{xy} = \nu_{yx} = 0.17$.

There is no available value for nonlinear quantities in the single-layer 1H-MoO₂. We have thus used the nonlinear parameter $B = 0.5d^4$ in Eq. (5), which is close to the value of B in most materials. The value of the third-order nonlinear elasticity D can be extracted by fitting the stress-strain relation to the function $\sigma = E\epsilon + \frac{1}{2}D\epsilon^2$ with E as the Young's modulus. The values of D from the present SW potential are -1027.8 and -1106.8 N/m along the armchair and zigzag directions, respectively. The ultimate stress is about 21.0 N/m at the ultimate strain of 0.19 in the armchair direction at the low temperature of 1 K. The ultimate stress is about 20.1 N/m at the ultimate strain of 0.22 in the zigzag direction at the low temperature of 1 K.

28. 1H-MoS₂

Several potentials have been proposed to describe the interaction for the single-layer 1H-MoS₂. In 1975, Wakabayashi et al. developed a VFF model to calculate the phonon spectrum of the bulk 2H-MoS₂ [22]. In 2009, Liang et al. parameterized a bond-order potential for 1H-MoS₂ [23], which is based on the bond order concept underlying the Brenner potential [6]. A separate force field model was parameterized in 2010 for MD simulations of bulk 2H-MoS₂ [24]. The present author (J.W.J.) and his collaborators parameterized the SW potential for 1H-MoS₂ in 2013 [13], which was improved by one of the present authors (J.W.J.) in 2015 [7]. Recently, another set of parameters for the SW potential were proposed for the single-layer 1H-MoS₂ [25].

We show the VFF model and the SW potential for single-layer 1H-MoS₂ in this section. These potentials have been developed in previous works. The VFF model presented here is from Ref. [22], while the SW potential presented in this section is from Ref. [7].

The structural parameters for the single-layer 1H-MoS₂ are from the first-principles calculations as shown in **Figure 1** (with M = Mo and X = S) [26]. The Mo atom layer in the single-layer 1H-MoS₂ is sandwiched by two S atom layers. Accordingly, each Mo atom is surrounded by six S atoms, while each S atom is connected to three Mo atoms. The bond length between neighboring Mo and S atoms is $d = 2.382$ Å, and the angles are $\theta_{MoSS} = 80.581^\circ$ and $\theta_{SMoMo} = 80.581^\circ$.

The VFF model for single-layer 1H-MoS₂ is from Ref. [22], which is able to describe the phonon spectrum and the sound velocity accurately. We have listed the first three leading force constants for single-layer 1H-MoS₂ in **Table 110**, neglecting other weak interaction terms. The SW potential parameters for single-layer 1H-MoS₂ used by GULP are listed in **Tables 111** and **112**.

VFF type	Bond stretching	Angle bending	
Expression	$\frac{1}{2}K_{Mo-S}(\Delta r_{Mo-S})^2$	$\frac{1}{2}K_{MoSS}(\Delta\theta_{MoSS})^2$	$\frac{1}{2}K_{SMoMo}(\Delta\theta_{SMoMo})^2$
Parameter	8.640	5.316	4.891
r_0 or θ_0	2.382	80.581	80.581

The second line gives the expression for each VFF term. Parameters are in the unit of eV/Å² for the bond stretching interaction and in the unit of eV for the angle bending interaction. The fourth line gives the initial bond length (in the unit of Å) for the bond stretching interaction and the initial angle (in the unit of degrees) for the angle bending interaction. The angle θ_{ijk} has atom i as the apex.

Table 110. The VFF model parameters for single-layer 1H-MoS₂ from Ref. [22].

	A (eV)	ρ (Å)	B (Å ⁴)	r_{min} (Å)	r_{max} (Å)
r_{Mo-S}	6.918	1.252	17.771	0.0	3.16

Table 111. Two-body SW potential parameters for single-layer 1H-MoS₂ used by GULP [8] as expressed in Eq. (3).

	K (eV)	θ_0 (°)	ρ_1 (Å)	ρ_2 (Å)	$r_{min\,12}$ (Å)	$r_{max\,12}$ (Å)	$r_{min\,13}$ (Å)	$r_{max\,13}$ (Å)	$r_{min\,23}$ (Å)	$r_{max\,23}$ (Å)
θ_{MoSS}	67.883	81.788	1.252	1.252	0.0	3.16	0.0	3.16	0.0	3.78
θ_{SMoMo}	62.449	81.788	1.252	1.252	0.0	3.16	0.0	3.16	0.0	4.27

The angle θ_{ijk} in the first line indicates the bending energy for the angle with atom i as the apex.

Table 112. Three-body SW potential parameters for single-layer 1H-MoS₂ used by GULP [8] as expressed in Eq. (4).

The SW potential parameters for single-layer 1H-MoS₂ used by LAMMPS [9] are listed in **Table 113**. We note that 12 atom types have been introduced for the simulation of the single-layer 1H-MoS₂ using LAMMPS, because the angles around atom Mo in **Figure 1** (with M = Mo and X = S) are not distinguishable in LAMMPS. We have suggested two options to differentiate these angles by implementing some additional constraints in LAMMPS, which can be accomplished by modifying the source file of LAMMPS [13, 14]. According to our experience, it is not so convenient for some users to implement these constraints and recompile the LAMMPS package. Hence, in the present work, we differentiate the angles by introducing more atom types, so it is not necessary to modify the LAMMPS package. **Figure 2** (with M = Mo and X = S)

	ϵ (eV)	σ (Å)	a	λ	γ	$\cos\theta_0$	A_L	B_L	p	q	Tol
Mo ₁ —S ₁ —S ₁	1.000	1.252	2.523	0.000	1.000	0.000	6.918	7.223	4	0	0.0
Mo ₁ —S ₁ —S ₃	1.000	0.000	0.000	67.883	1.000	0.143	0.000	0.000	4	0	0.0
S ₁ —Mo ₁ —Mo ₃	1.000	0.000	0.000	62.449	1.000	0.143	0.000	0.000	4	0	0.0

Atom types in the first column are displayed in **Figure 2** (with M = Mo and X = S).

Table 113. SW potential parameters for single-layer 1H-MoS₂ used by LAMMPS 9 as expressed in Eqs. (9) and 10.

shows that, for 1H-MoS₂, we can differentiate these angles around the Mo atom by assigning these six neighboring S atoms with different atom types. It can be found that 12 atom types are necessary for the purpose of differentiating all 6 neighbors around 1 Mo atom.

We use GULP to compute the phonon dispersion for the single-layer 1H-MoS₂ as shown in **Figure 53**. The results from the VFF model are quite comparable with the experiment data. The phonon dispersion from the SW potential is the same as that from the VFF model, which indicates that the SW potential has fully inherited the linear portion of the interaction from the VFF model.

We use LAMMPS to perform MD simulations for the mechanical behavior of the single-layer 1H-MoS₂ under uniaxial tension at 1 and 300 K. **Figure 54** shows the stress-strain curve during

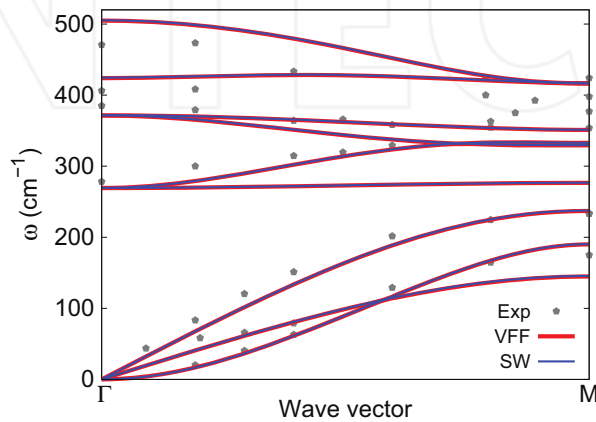


Figure 53. Phonon spectrum for single-layer 1H-MoS₂. Phonon dispersion along the Γ M direction in the Brillouin zone. The results from the VFF model (lines) are comparable with the experiment data (pentagons) from Ref. [22]. The phonon dispersion from the SW potential is exactly the same as that from the VFF model.

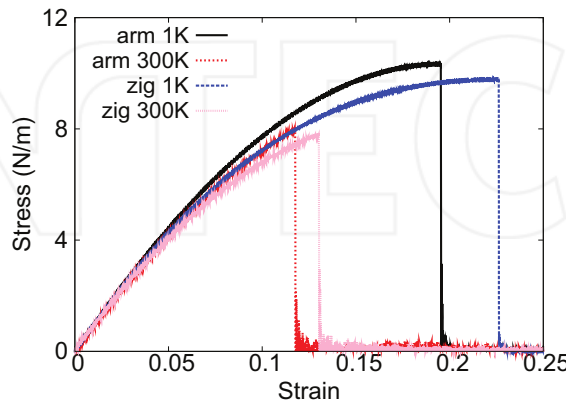


Figure 54. Stress-strain for single-layer 1H-MoS₂ of dimension 100×100 Å along the armchair and zigzag directions.

the tension of a single-layer 1H-MoS₂ of dimension 100 × 100 Å. Periodic boundary conditions are applied in both armchair and zigzag directions. The single-layer 1H-MoS₂ is stretched uniaxially along the armchair or zigzag direction. The stress is calculated without involving the actual thickness of the quasi-two-dimensional structure of the single-layer 1H-MoS₂. The Young's modulus can be obtained by a linear fitting of the stress-strain relation in the small strain range of [0, 0.01]. The Young's modulus is 97 and 96 N/m along the armchair and zigzag directions, respectively. The Young's modulus is isotropic in the armchair and zigzag directions. These values are in considerable agreement with the experimental results, e.g., 120 ± 30 N/m from Refs [27, 28], or 180 ± 60 N/m from Ref. [29]. The third-order nonlinear elastic constant D can be obtained by fitting the stress-strain relation to $\sigma = E\epsilon + \frac{1}{2}D\epsilon^2$ with E as the Young's modulus. The values of D are -418 and -461 N/m along the armchair and zigzag directions, respectively. The Poisson's ratio from the VFF model and the SW potential is $\nu_{xy} = \nu_{yx} = 0.27$.

29. 1H-MoSe₂

There is a recent parameter set for the SW potential in the single-layer 1H-MoSe₂ [25]. In this section, we will develop both VFF model and the SW potential for the single-layer 1H-MoSe₂.

The structure for the single-layer 1H-MoSe₂ is shown in **Figure 1** (with M = Mo and X = Se). Each Mo atom is surrounded by six Se atoms. These Se atoms are categorized into the top group (e.g., atoms 1, 3, and 5) and bottom group (e.g., atoms 2, 4, and 6). Each Se atom is connected to three Mo atoms. The structural parameters are from Ref. [30], including the lattice constant $a = 3.321$ Å and the bond length $d_{Mo-Se} = 2.528$ Å. The resultant angles are $\theta_{MoSeSe} = \theta_{SeMoMo} = 82.119^\circ$ and $\theta_{MoSeSe'} = 81.343^\circ$, in which atoms Se and Se' are from different (top or bottom) groups.

Table 114 shows four VFF terms for the 1H-MoSe₂; one of which is the bond stretching interaction shown by Eq. (1), while the other three terms are the angle bending interaction shown by Eq. (2). These force constant parameters are determined by fitting to the three acoustic branches in the phonon dispersion along the ΓM as shown in **Figure 55(a)**. The *ab initio* calculations for the phonon dispersion are from Ref. [30]. Similar phonon dispersion can

VFF type	Bond stretching	Angle bending	
Expression	$\frac{1}{2}K_{Mo-Se}(\Delta r)^2$	$\frac{1}{2}K_{Mo-Se-Se}(\Delta\theta)^2$	$\frac{1}{2}K_{Mo-Se-Se'}(\Delta\theta)^2$
Parameter	7.928	6.945	6.945
r_0 or θ_0	2.528	82.119	82.119

The second line gives an explicit expression for each VFF term. The third line is the force constant parameters. Parameters are in the unit of eV/Å² for the bond stretching interaction and in the unit of eV for the angle bending interaction. The fourth line gives the initial bond length (in the unit of Å) for the bond stretching interaction and the initial angle (in the unit of degrees) for the angle bending interaction. The angle θ_{ijk} has atom i as the apex.

Table 114. The VFF model for single-layer 1H-MoSe₂.

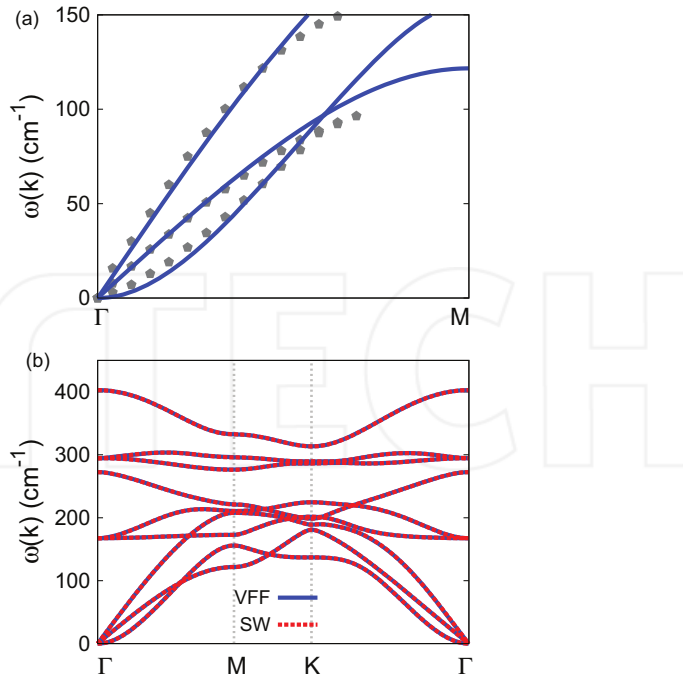


Figure 55. Phonon dispersion for single-layer 1H-MoSe₂. (a) The VFF model is fitted to the three acoustic branches in the long wave limit along the Γ M direction. The *ab initio* results (gray pentagons) are from Ref. [30]. (b) The VFF model (blue lines) and the SW potential (red lines) give the same phonon dispersion for single-layer 1H-MoSe₂ along Γ MK Γ .

also be found in other *ab initio* calculations [12, 31–34]. **Figure 55(b)** shows that the VFF model and the SW potential give exactly the same phonon dispersion, as the SW potential is derived from the VFF model.

The parameters for the two-body SW potential used by GULP are shown in **Table 115**. The parameters for the three-body SW potential used by GULP are shown in **Table 116**. Parameters for the SW potential used by LAMMPS are listed in **Table 117**. We note that 12 atom types have been introduced for the simulation of the single-layer 1H-MoSe₂ using LAMMPS, because the angles around atom Mo in **Figure 1** (with M = Mo and X = Se) are not distinguishable in LAMMPS. We have suggested two options to differentiate these angles by implementing some additional constraints in LAMMPS, which can be accomplished by modifying the source file of LAMMPS [13, 14]. According to our experience, it is not so convenient for some users to implement these constraints and recompile the LAMMPS package. Hence, in the present work,

	A (eV)	ρ (\AA)	B (\AA^4)	r_{\min} (\AA)	r_{\max} (\AA)
Mo-Se	5.737	0.913	18.787	0.0	3.351

Table 115. Two-body SW potential parameters for single-layer 1H-MoSe₂ used by GULP [8] as expressed in Eq. (3).

	K (eV)	θ_0 (°)	ρ_1 (Å)	ρ_2 (Å)	$r_{\min 12}$ (Å)	$r_{\max 12}$ (Å)	$r_{\min 13}$ (Å)	$r_{\max 13}$ (Å)	$r_{\min 23}$ (Å)	$r_{\max 23}$ (Å)
$\theta_{\text{Mo}-\text{Se}-\text{Se}}$	32.526	82.119	0.913	0.913	0.0	3.351	0.0	3.351	0.0	4.000
$\theta_{\text{Mo}-\text{Se}-\text{Se}'}$	32.654	81.343	0.913	0.913	0.0	3.351	0.0	3.351	0.0	4.000
$\theta_{\text{Se}-\text{Mo}-\text{Mo}}$	27.079	82.119	0.913	0.913	0.0	3.351	0.0	3.351	0.0	4.000

The angle θ_{ijk} in the first line indicates the bending energy for the angle with atom i as the apex.

Table 116. Three-body SW potential parameters for single-layer 1H-MoSe₂ used by GULP [8] as expressed in Eq. (4).

	σ (eV)	a (Å)	λ	γ	$\cos \theta_0$	A_L	B_L	p	q	100×100	Tol
Mo ₁ —Se ₁ —Se ₁	1.000	0.913	3.672	0.000	1.000	0.000	5.737	27.084	4	0	0.0
Mo ₁ —Se ₁ —Se ₃	1.000	0.000	0.000	32.526	1.000	0.137	0.000	0.000	4	0	0.0
Mo ₁ —Se ₁ —Se ₂	1.000	0.000	0.000	32.654	1.000	0.151	0.000	0.000	4	0	0.0
Se ₁ —Mo ₁ —Mo ₃	1.000	0.000	0.000	27.079	1.000	0.137	0.000	0.000	4	0	0.0

Atom types in the first column are displayed in **Figure 2** (with M = Mo and X = Se).

Table 117. SW potential parameters for single-layer 1H-MoSe₂ used by LAMMPS [9] as expressed in Eqs. (9) and (10).

we differentiate the angles by introducing more atom types, so it is not necessary to modify the LAMMPS package. **Figure 2** (with M = Mo and X = Se) shows that, for 1H-MoSe₂, we can differentiate these angles around the Mo atom by assigning these six neighboring Se atoms with different atom types. It can be found that 12 atom types are necessary for the purpose of differentiating all 6 neighbors around 1 Mo atom.

We use LAMMPS to perform MD simulations for the mechanical behavior of the single-layer 1H-MoSe₂ under uniaxial tension at 1 and 300 K. **Figure 56** shows the stress-strain curve during the tension of a single-layer 1H-MoSe₂ of dimension 100 × 100 Å. Periodic boundary

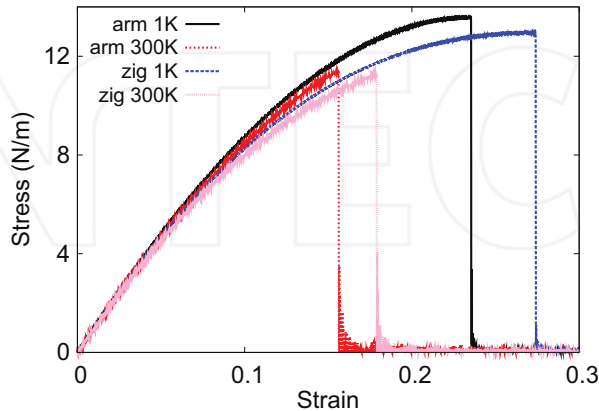


Figure 56. Stress-strain for single-layer 1H-MoSe₂ of dimension 100 × 100 Å along the armchair and zigzag directions.

conditions are applied in both armchair and zigzag directions. The single-layer 1H-MoSe₂ is stretched uniaxially along the armchair or zigzag direction. The stress is calculated without involving the actual thickness of the quasi-two-dimensional structure of the single-layer 1H-MoSe₂. The Young's modulus can be obtained by a linear fitting of the stress-strain relation in the small strain range of [0, 0.01]. The Young's modulus is 103.0 and 101.8 N/m along the armchair and zigzag directions, respectively. The Young's modulus is essentially isotropic in the armchair and zigzag directions. These values are in considerable agreement with the experimental results, e.g., 103.9 N/m from Ref. [18], or 113.9 N/m from Ref. [35]. The Poisson's ratio from the VFF model and the SW potential is $\nu_{xy} = \nu_{yx} = 0.24$, which agrees quite well with the *ab initio* value of 0.23 [18].

We have determined the nonlinear parameter to be $B = 0.46d^4$ in Eq. (5) by fitting to the third-order nonlinear elastic constant D from the *ab initio* calculations [35]. We have extracted the value of $D = -383.7$ N/m by fitting the stress-strain relation along the armchair direction in the *ab initio* calculations to the function $\sigma = E\epsilon + \frac{1}{2}D\epsilon^2$ with E as the Young's modulus. The values of D from the present SW potential are -365.4 and -402.4 N/m along the armchair and zigzag directions, respectively. The ultimate stress is about 13.6 N/m at the ultimate strain of 0.23 in the armchair direction at the low temperature of 1 K. The ultimate stress is about 13.0 N/m at the ultimate strain of 0.27 in the zigzag direction at the low temperature of 1 K.

30. 1H-MoTe₂

Most existing theoretical studies on the single-layer 1H-MoTe₂ are based on the first-principles calculations. In this section, we will develop both VFF model and the SW potential for the single-layer 1H-MoTe₂.

The structure for the single-layer 1H-MoTe₂ is shown in **Figure 1** (with M = Mo and X = Te). Each Mo atom is surrounded by six Te atoms. These Te atoms are categorized into the top group (e.g., atoms 1, 3, and 5) and bottom group (e.g., atoms 2, 4, and 6). Each Te atom is connected to three Mo atoms. The structural parameters are from Ref. [36], including the lattice constant $a = 3.55\text{\AA}$ and the bond length $d_{\text{Mo}-\text{Te}} = 2.73\text{\AA}$. The resultant angles are $\theta_{\text{MoTeTe}} = \theta_{\text{TeMoMo}} = 81.111^\circ$ and $\theta_{\text{MoTeTe}'} = 82.686^\circ$, in which atoms Te and Te' are from different (top or bottom) groups.

Table 118 shows four VFF terms for the 1H-MoTe₂; one of which is the bond stretching interaction shown by Eq. (1), while the other three terms are the angle bending interaction shown by Eq. (2). These force constant parameters are determined by fitting to the three acoustic branches in the phonon dispersion along the TM as shown in **Figure 57(a)**. The *ab initio* calculations for the phonon dispersion are from Ref. [36]. Similar phonon dispersion can also be found in other *ab initio* calculations [12, 34, 37]. **Figure 57(b)** shows that the VFF model and the SW potential give exactly the same phonon dispersion, as the SW potential is derived from the VFF model.

The parameters for the two-body SW potential used by GULP are shown in **Table 119**. The parameters for the three-body SW potential used by GULP are shown in **Table 120**. Parameters

VFF type	Bond stretching	Angle bending	
Expression	$\frac{1}{2}K_{\text{Mo}-\text{Te}}(\Delta r)^2$	$\frac{1}{2}K_{\text{Mo}-\text{Te}-\text{Te}}(\Delta\theta)^2$	$\frac{1}{2}K_{\text{Mo}-\text{Te}-\text{Te}'}(\Delta\theta)^2$
Parameter	6.317	6.184	6.184
r_0 or θ_0	2.730	81.111	82.686

The second line gives an explicit expression for each VFF term. The third line is the force constant parameters. Parameters are in the unit of eV/Å² for the bond stretching interaction and in the unit of eV for the angle bending interaction. The fourth line gives the initial bond length (in the unit of Å) for the bond stretching interaction and the initial angle (in the unit of degrees) for the angle bending interaction. The angle θ_{ijk} has atom i as the apex.

Table 118. The VFF model for single-layer 1H-MoTe₂.

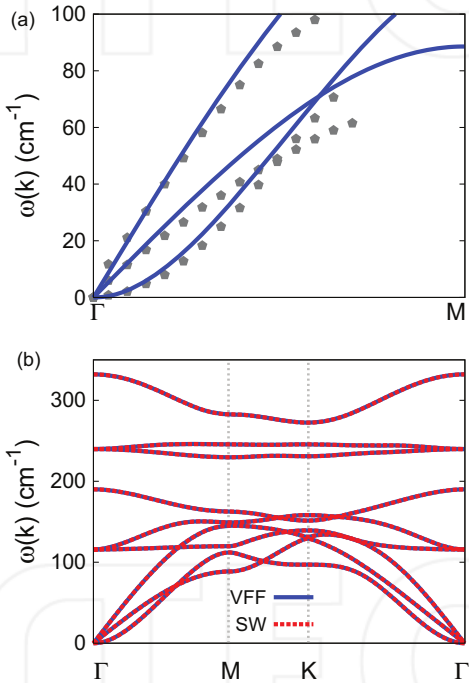


Figure 57. Phonon dispersion for single-layer 1H-MoTe₂. (a) The VFF model is fitted to the three acoustic branches in the long wave limit along the Γ M direction. The *ab initio* results (gray pentagons) are from Ref. [36]. (b) The VFF model (blue lines) and the SW potential (red lines) give the same phonon dispersion for single-layer 1H-MoTe₂ along Γ MKT.

	A (eV)	ρ (Å)	B (Å ⁴)	r_{\min} (Å)	r_{\max} (Å)
Mo-Te	5.086	0.880	24.440	0.0	3.604

Table 119. Two-body SW potential parameters for single-layer 1H-MoTe₂ used by GULP [8] as expressed in Eq. (3).

	K (eV)	θ_0 ($^\circ$)	ρ_1 (\AA)	ρ_2 (\AA)	$r_{\min 12}$ (\AA)	$r_{\max 12}$ (\AA)	$r_{\min 13}$ (\AA)	$r_{\max 13}$ (\AA)	$r_{\min 23}$ (\AA)	$r_{\max 23}$ (\AA)
$\theta_{\text{Mo}-\text{Te}-\text{Te}}$	23.705	81.111	0.880	0.880	0.0	3.604	0.0	3.604	0.0	4.305
$\theta_{\text{Mo}-\text{Te}-\text{Te}'}$	23.520	82.686	0.880	0.880	0.0	3.604	0.0	3.604	0.0	4.305
$\theta_{\text{Te}-\text{Mo}-\text{Mo}}$	20.029	81.111	0.880	0.880	0.0	3.604	0.0	3.604	0.0	4.305

The angle θ_{ijk} in the first line indicates the bending energy for the angle with atom i as the apex.

Table 120. Three-body SW potential parameters for single-layer 1H-MoTe₂ used by GULP [8] as expressed in Eq. (4).

for the SW potential used by LAMMPS are listed in **Table 121**. We note that 12 atom types have been introduced for the simulation of the single-layer 1H-MoTe₂ using LAMMPS, because the angles around atom Mo in **Figure 1** (with M = Mo and X = Te) are not distinguishable in LAMMPS. We have suggested two options to differentiate these angles by implementing some additional constraints in LAMMPS, which can be accomplished by modifying the source file of LAMMPS [13, 14]. According to our experience, it is not so convenient for some users to implement these constraints and recompile the LAMMPS package. Hence, in the present work, we differentiate the angles by introducing more atom types, so it is not necessary to modify the LAMMPS package. **Figure 2** (with M = Mo and X = Te) shows that, for 1H-MoTe₂, we can differentiate these angles around the Mo atom by assigning these six neighboring Te atoms with different atom types. It can be found that 12 atom types are necessary for the purpose of differentiating all 6 neighbors around 1 Mo atom.

We use LAMMPS to perform MD simulations for the mechanical behavior of the single-layer 1H-MoTe₂ under uniaxial tension at 1 and 300 K. **Figure 58** shows the stress-strain curve for the tension of a single-layer 1H-MoTe₂ of dimension 100 × 100 Å. Periodic boundary conditions are applied in both armchair and zigzag directions. The single-layer 1H-MoTe₂ is stretched uniaxially along the armchair or zigzag direction. The stress is calculated without involving the actual thickness of the quasi-two-dimensional structure of the single-layer 1H-MoTe₂. The Young's modulus can be obtained by a linear fitting of the stress-strain relation in the small strain range of [0, 0.01]. The Young's modulus is 79.8 and 78.5 N/m along the armchair and zigzag directions, respectively. The Young's modulus is essentially isotropic in the armchair and zigzag directions. These values are in considerable agreement with the experimental results, e.g., 79.4 N/m from Ref. [18], or 87.0 N/m from Ref. [35]. The Poisson's ratio from the VFF model and the SW potential is $\nu_{xy} = \nu_{yx} = 0.25$, which agrees with the *ab initio* value of 0.24 [18].

	ϵ (eV)	σ (\AA)	a	λ	γ	$\cos \theta_0$	A_L	B_L	p	q	Tol
Mo ₁ —Te ₁ —Te ₁	1.000	0.900	4.016	0.000	1.000	0.000	5.169	37.250	4	0	0.0
Mo ₁ —Te ₁ —Te ₃	1.000	0.000	0.000	24.163	1.000	0.143	0.000	0.000	4	0	0.0
Te ₁ —Mo ₁ —Mo ₃	1.000	0.000	0.000	20.416	1.000	0.143	0.000	0.000	4	0	0.0

Atom types in the first column are displayed in **Figure 2** (with M = Mo and X = Te).

Table 121. SW potential parameters for single-layer 1H-MoTe₂ used by LAMMPS [9] as expressed in Eqs. (9) and (10).

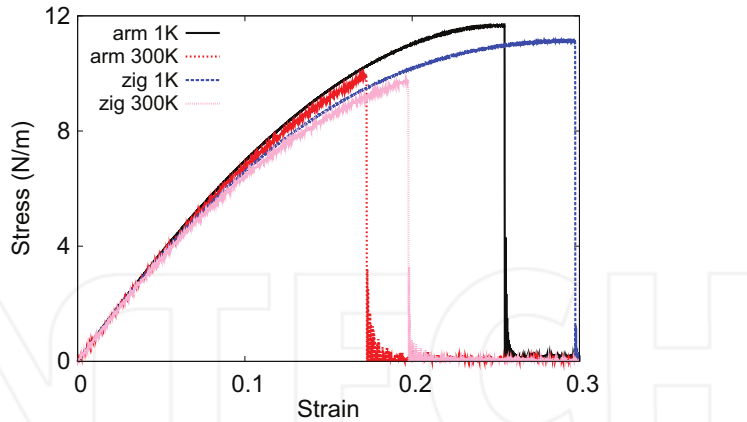


Figure 58. Stress-strain for single-layer 1H-MoTe₂ of dimension θ_0 Å along the armchair and zigzag directions.

We have determined the nonlinear parameter to be $B = 0.44d^4$ in Eq. (5) by fitting to the third-order nonlinear elastic constant D from the *ab initio* calculations [35]. We have extracted the value of $D = -278.2$ N/m by fitting the stress-strain relation along the armchair direction in the *ab initio* calculations to the function $\sigma = E\epsilon + \frac{1}{2}D\epsilon^2$ with E as the Young's modulus. The values of D from the present SW potential are -250.5 and -276.6 N/m along the armchair and zigzag directions, respectively. The ultimate stress is about 11.7 N/m at the ultimate strain of 0.25 in the armchair direction at the low temperature of 1 K. The ultimate stress is about 11.1 N/m at the ultimate strain of 0.29 in the zigzag direction at the low temperature of 1 K.

31. 1H-TaS₂

In 1983, the VFF model was developed to investigate the lattice dynamical properties in the bulk 2H-TaS₂ [21]. In this section, we will develop the SW potential for the single-layer 1H-TaS₂.

The structure for the single-layer 1H-TaS₂ is shown in **Figure 1** (with M = Ta and X = S). Each Ta atom is surrounded by six S atoms. These S atoms are categorized into the top group (e.g., atoms 1, 3, and 5) and bottom group (e.g., atoms 2, 4, and 6). Each S atom is connected to three Ta atoms. The structural parameters are from Ref. [21], including the lattice constant $a = 3.315$ Å and the bond length $d_{\text{Ta-S}} = 2.48$ Å. The resultant angles are $\theta_{\text{TaSS}} = \theta_{\text{STaTa}} = 83.879^\circ$ and $\theta_{\text{TaSS'}} = 78.979^\circ$, in which atoms S and S' are from different (top or bottom) groups.

Table 122 shows the VFF terms for the 1H-TaS₂; one of which is the bond stretching interaction shown by Eq. (1), while the others are the angle bending interaction shown by Eq. (2). These force constant parameters are determined by fitting to the three acoustic branches in the phonon dispersion along the ϵ as shown in **Figure 59(a)**. The theoretical phonon frequencies (gray pentagons) are from Ref. [21], which are the phonon dispersion of bulk 2H-TaS₂. We

VFF type	Bond stretching	Angle bending	
Expression	$\frac{1}{2}K_{\text{Ta-S}}(\Delta r)^2$	$\frac{1}{2}K_{\text{Ta-S-S}}(\Delta\theta)^2$	$\frac{1}{2}K_{\text{Ta-S-S'}}(\Delta\theta)^2$
Parameter	8.230	4.811	4.811
r_0 or θ_0	2.480	83.879	78.979

The second line gives an explicit expression for each VFF term. The third line is the force constant parameters. Parameters are in the unit of eV/Å² for the bond stretching interaction and in the unit of eV for the angle bending interaction. The fourth line gives the initial bond length (in the unit of Å) for the bond stretching interaction and the initial angle (in the unit of degrees) for the angle bending interaction. The angle θ_{ijk} has atom i as the apex.

Table 122. The VFF model for single-layer 1H-TaS₂.

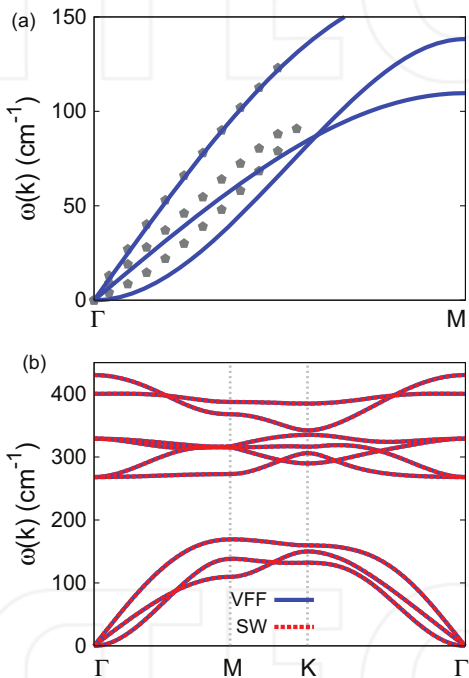


Figure 59. Phonon dispersion for single-layer 1H-TaS₂. (a) The VFF model is fitted to the three acoustic branches in the long wave limit along the Γ M direction. The theoretical results (gray pentagons) are from Ref. [21]. The blue lines are from the present VFF model. (b) The VFF model (blue lines) and the SW potential (red lines) give the same phonon dispersion for single-layer 1H-TaS₂ along Γ MKT.

have used these phonon frequencies as the phonon dispersion of the single-layer 1H-TaS₂, as the interlayer interaction in the bulk 2H-TaS₂ only induces weak effects on the two in-plane acoustic branches. The interlayer coupling will strengthen the out-of-plane acoustic (flexural) branch, so the flexural branch from the present VFF model (blue line) is lower than the theoretical results for bulk 2H-TaS₂ (gray pentagons). **Figure 59(b)** shows that the VFF model

and the SW potential give exactly the same phonon dispersion, as the SW potential is derived from the VFF model.

The parameters for the two-body SW potential used by GULP are shown in **Table 123**. The parameters for the three-body SW potential used by GULP are shown in **Table 124**. Parameters for the SW potential used by LAMMPS are listed in **Table 125**. We note that 12 atom types have been introduced for the simulation of the single-layer 1H-TaS₂ using LAMMPS, because the angles around atom Ta in **Figure 1** (with M = Ta and X = S) are not distinguishable in LAMMPS. We have suggested two options to differentiate these angles by implementing some additional constraints in LAMMPS, which can be accomplished by modifying the source file of LAMMPS [13, 14]. According to our experience, it is not so convenient for some users to implement these constraints and recompile the LAMMPS package. Hence, in the present work, we differentiate the angles by introducing more atom types, so it is not necessary to modify the LAMMPS package. **Figure 2** (with M = Ta and X = S) shows that, for 1H-TaS₂, we can differentiate these angles around the Ta atom by assigning these six neighboring S atoms with different atom types. It can be found that 12 atom types are necessary for the purpose of differentiating all 6 neighbors around 1 Ta atom.

We use LAMMPS to perform MD simulations for the mechanical behavior of the single-layer 1H-TaS₂ under uniaxial tension at 1 and 300 K. **Figure 60** shows the stress-strain curve for the

	A (eV)	ρ (Å)	B (Å ⁴)	r_{\min} (Å)	r_{\max} (Å)
Ta-S	6.446	1.111	18.914	0.0	3.310

Table 123. Two-body SW potential parameters for single-layer 1H-TaS₂ used by GULP [8] as expressed in Eq. (3).

	K (eV)	θ_0 (°)	ρ_1 (Å)	ρ_2 (Å)	$r_{\min\ 12}$ (Å)	$r_{\max\ 12}$ (Å)	$r_{\min\ 13}$ (Å)	$r_{\max\ 13}$ (Å)	$r_{\min\ 23}$ (Å)	$r_{\max\ 23}$ (Å)
$\theta_{\text{Ta}-\text{S}-\text{S}}$	35.396	83.879	1.111	1.111	0.0	3.310	0.0	3.310	0.0	3.945
$\theta_{\text{Ta}-\text{S}-\text{S}'}$	36.321	78.979	1.111	1.111	0.0	3.310	0.0	3.310	0.0	3.945
$\theta_{\text{S}-\text{Ta}-\text{Ta}}$	35.396	83.879	1.111	1.111	0.0	3.310	0.0	3.310	0.0	3.945

The angle θ_{ijk} in the first line indicates the bending energy for the angle with atom i as the apex.

Table 124. Three-body SW potential parameters for single-layer 1H-TaS₂ used by GULP [8] as expressed in Eq. (4).

	ϵ (eV)	σ (Å)	a	λ	γ	$\cos \theta_0$	A_L	B_L	p	q	Tol
Ta ₁ -S ₁ -S ₁	1.000	1.111	2.979	0.000	1.000	0.000	6.446	12.408	4	0	0.0
Ta ₁ -S ₁ -S ₃	1.000	0.000	0.000	35.396	1.000	0.107	0.000	0.000	4	0	0.0
Ta ₁ -S ₁ -S ₂	1.000	0.000	0.000	36.321	1.000	0.191	0.000	0.000	4	0	0.0
S ₁ -Ta ₁ -Ta ₃	1.000	0.000	0.000	35.396	1.000	0.107	0.000	0.000	4	0	0.0

Atom types in the first column are displayed in **Figure 2** (with M = Ta and X = S).

Table 125. SW potential parameters for single-layer 1H-TaS₂ used by LAMMPS [9] as expressed in Eqs. (9) and (10).

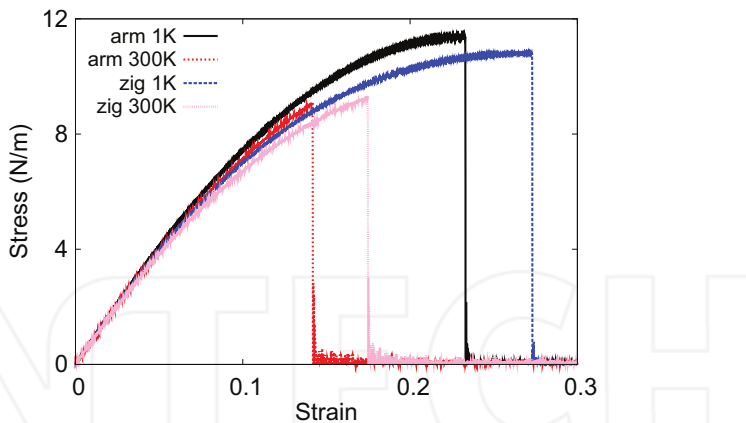


Figure 60. Stress-strain for single-layer 1H-TaS₂ of dimension 100 × 100 Å along the armchair and zigzag directions.

tension of a single-layer 1H-TaS₂ of dimension 100 × 100 Å. Periodic boundary conditions are applied in both armchair and zigzag directions. The single-layer 1H-TaS₂ is stretched uniaxially along the armchair or zigzag direction. The stress is calculated without involving the actual thickness of the quasi-two-dimensional structure of the single-layer 1H-TaS₂. The Young's modulus can be obtained by a linear fitting of the stress-strain relation in the small strain range of [0, 0.01]. The Young's modulus is 87.4 and 86.6 N/m along the armchair and zigzag directions, respectively. The Poisson's ratio from the VFF model and the SW potential is $\nu_{xy} = \nu_{yx} = 0.27$.

There is no available value for the nonlinear quantities in the single-layer 1H-TaS₂. We have thus used the nonlinear parameter $B = 0.5d^4$ in Eq. (5), which is close to the value of B in most materials. The value of the third-order nonlinear elasticity D can be extracted by fitting the stress-strain relation to the function $\sigma = E\epsilon + \frac{1}{2}D\epsilon^2$ with E as the Young's modulus. The values of D from the present SW potential are -313.0 and -349.3 N/m along the armchair and zigzag directions, respectively. The ultimate stress is about 11.4 N/m at the ultimate strain of 0.23 in the armchair direction at the low temperature of 1 K. The ultimate stress is about 10.8 N/m at the ultimate strain of 0.27 in the zigzag direction at the low temperature of 1 K.

32. 1H-TaSe₂

The VFF model was developed to investigate the lattice dynamical properties in the bulk 2H-TaSe₂ [15, 21]. In this section, we will develop the SW potential for the single-layer 1H-TaSe₂.

The structure for the single-layer 1H-TaSe₂ is shown in Figure 1 (with M = Ta and X = Se). Each Ta atom is surrounded by six Se atoms. These Se atoms are categorized into the top group (e.g., atoms 1, 3, and 5) and bottom group (e.g., atoms 2, 4, and 6). Each Se atom is connected to

three Ta atoms. The structural parameters are from Ref. [21], including the lattice constant $a = 3.436\text{\AA}$ and the bond length $d_{\text{Ta}-\text{Se}} = 2.59\text{\AA}$. The resultant angles are $\theta_{\text{TaSeSe}} = \theta_{\text{SeTaTa}} = 83.107^\circ$ and $\theta_{\text{TaSeSe}'} = 80.019^\circ$, in which atoms Se and Se' are from different (top or bottom) groups.

Table 126 shows the VFF terms for the 1H-TaSe₂; one of which is the bond stretching interaction shown by Eq. (1), while the others are the angle bending interaction shown by Eq. (2). These force constant parameters are determined by fitting to the three acoustic branches in the phonon dispersion along the ΓM as shown in **Figure 61(a)**. The theoretical phonon frequencies (gray pentagons) are from Ref. [21], which are the phonon dispersion of bulk 2H-TaSe₂. We have used these phonon frequencies as the phonon dispersion of the single-layer 1H-TaSe₂, as the interlayer interaction in the bulk 2H-TaSe₂ only induces weak effects on the two in-plane acoustic branches. The interlayer coupling will strengthen the out-of-plane acoustic branch (flexural branch), so the flexural branch from the present VFF model (blue line) is lower than the theoretical results for bulk 2H-TaSe₂ (gray pentagons). **Figure 61(b)** shows that the VFF model and the SW potential give exactly the same phonon dispersion, as the SW potential is derived from the VFF model.

The parameters for the two-body SW potential used by GULP are shown in **Table 127**. The parameters for the three-body SW potential used by GULP are shown in **Table 128**. Parameters for the SW potential used by LAMMPS are listed in **Table 129**. We note that 12 atom types have been introduced for the simulation of the single-layer 1H-TaSe₂ using LAMMPS, because the angles around atom Ta in **Figure 1** (with M = Ta and X = Se) are not distinguishable in LAMMPS. We have suggested two options to differentiate these angles by implementing some additional constraints in LAMMPS, which can be accomplished by modifying the source file of LAMMPS [13, 14]. According to our experience, it is not so convenient for some users to implement these constraints and recompile the LAMMPS package. Hence, in the present work, we differentiate the angles by introducing more atom types, so it is not necessary to modify the LAMMPS package. **Figure 2** (with M = Ta and X = Se) shows that, for 1H-TaSe₂, we can differentiate these angles around the Ta atom by assigning these six neighboring Se atoms with different atom types. It can be found that 12 atom types are necessary for the purpose of differentiating all 6 neighbors around 1 Ta atom.

VFF type	Bond stretching	Angle bending		
Expression	$\frac{1}{2}K_{\text{Ta}-\text{Se}}(\Delta r)^2$	$\frac{1}{2}K_{\text{Ta}-\text{Se}-\text{Se}}(\Delta\theta)^2$	$\frac{1}{2}K_{\text{Ta}-\text{Se}-\text{Se}'}(\Delta\theta)^2$	$\frac{1}{2}K_{\text{Se}-\text{Ta}-\text{Ta}}(\Delta\theta)^2$
Parameter	8.230	4.811	4.811	4.811
r_0 or θ_0	2.590	83.107	80.019	83.107

The second line gives an explicit expression for each VFF term. The third line is the force constant parameters. Parameters are in the unit of eV/ \AA^2 for the bond stretching interaction and in the unit of eV for the angle bending interaction. The fourth line gives the initial bond length (in the unit of \AA) for the bond stretching interaction and the initial angle (in the unit of degrees) for the angle bending interaction. The angle θ_{ijk} has atom i as the apex.

Table 126. The VFF model for single-layer 1H-TaSe₂.

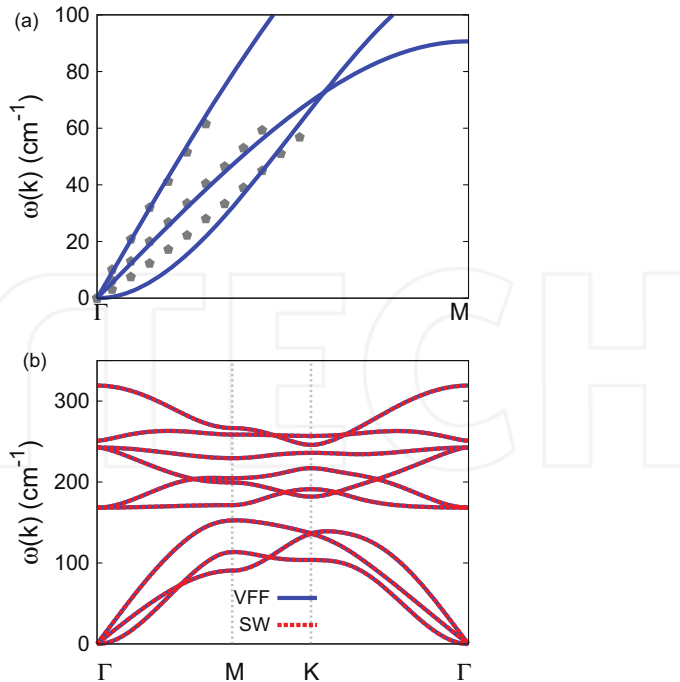


Figure 61. Phonon dispersion for single-layer 1H-TaSe₂. (a) The VFF model is fitted to the three acoustic branches in the long wave limit along the Γ M direction. The theoretical results (gray pentagons) are from Ref. [15]. The blue lines are from the present VFF model. (b) The VFF model (blue lines) and the SW potential (red lines) give the same phonon dispersion for single-layer 1H-TaSe₂ along Γ MK Γ .

	A (eV)	ρ (\AA)	B (\AA^4)	r_{\min} (\AA)	r_{\max} (\AA)
Ta—Se	6.885	1.133	22.499	0.0	3.446

Table 127. Two-body SW potential parameters for single-layer 1H-TaSe₂ used by GULP [8] as expressed in Eq. (3).

	K (eV)	θ_0 (°)	ρ_1 (\AA)	ρ_2 (\AA)	$r_{\min 12}$ (\AA)	$r_{\max 12}$ (\AA)	$r_{\min 13}$ (\AA)	$r_{\max 13}$ (\AA)	$r_{\min 23}$ (\AA)	$r_{\max 23}$ (\AA)
$\theta_{\text{Ta—Se—Se}}$	34.381	83.107	1.133	1.133	0.0	3.446	0.0	3.446	0.0	4.111
$\theta_{\text{Ta—Se—Se'}}$	34.936	80.019	1.133	1.133	0.0	3.446	0.0	3.446	0.0	4.111
$\theta_{\text{Se—Ta—Ta}}$	34.381	83.107	1.133	1.133	0.0	3.446	0.0	3.446	0.0	4.111

The angle θ_{ijk} in the first line indicates the bending energy for the angle with atom i as the apex.

Table 128. Three-body SW potential parameters for single-layer 1H-TaSe₂ used by GULP [8] as expressed in Eq. (4).

We use LAMMPS to perform MD simulations for the mechanical behavior of the single-layer 1H-TaSe₂ under uniaxial tension at 1 and 300 K. **Figure 62** shows the stress-strain curve for the tension of a single-layer 1H-TaSe₂ of dimension $100 \times 100 \text{\AA}$. Periodic boundary conditions are

	ϵ (eV)	σ (\AA)	a	λ	γ	$\cos \theta_0$	A_L	B_L	p	q	Tol
Ta ₁ —Se ₁ —Se ₁	1.000	1.133	3.043	0.000	1.000	0.000	6.885	13.668	4	0	0.0
Ta ₁ —Se ₁ —Se ₃	1.000	0.000	0.000	34.381	1.000	0.120	0.000	0.000	4	0	0.0
Ta ₁ —Se ₁ —Se ₂	1.000	0.000	0.000	34.936	1.000	0.173	0.000	0.000	4	0	0.0
Se ₁ —Ta ₁ —Ta ₃	1.000	0.000	0.000	34.381	1.000	0.120	0.000	0.000	4	0	0.0

Atom types in the first column are displayed in Figure 2 (with M = Ta and X = Se).

Table 129. SW potential parameters for single-layer 1H-TaSe₂ used by LAMMPS [16] as expressed in Eqs. (9) and (10).

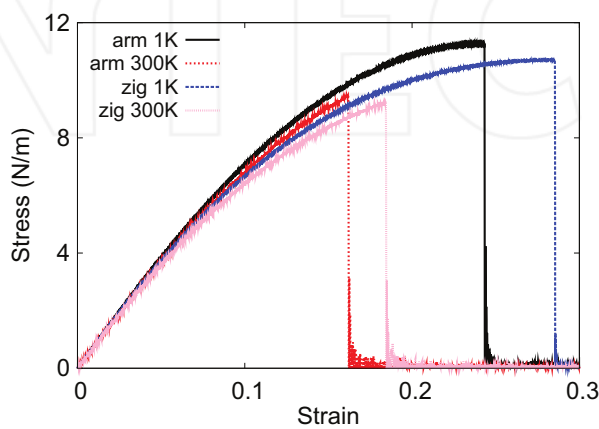


Figure 62. Stress-strain for single-layer 1H-TaSe₂ of dimension 100 × 100 Å along the armchair and zigzag directions.

applied in both armchair and zigzag directions. The single-layer 1H-TaSe₂ is stretched uniaxially along the armchair or zigzag direction. The stress is calculated without involving the actual thickness of the quasi-two-dimensional structure of the single-layer 1H-TaSe₂. The Young's modulus can be obtained by a linear fitting of the stress-strain relation in the small strain range of [0, 0.01]. The Young's modulus is 80.8 and 81.1 N/m along the armchair and zigzag directions, respectively. The Young's modulus is essentially isotropic in the armchair and zigzag directions. The Poisson's ratio from the VFF model and the SW potential is $\nu_{xy} = \nu_{yx} = 0.29$.

There is no available value for the nonlinear quantities in the single-layer 1H-TaSe₂. We have thus used the nonlinear parameter $B = 0.5d^4$ in Eq. (5), which is close to the value of B in most materials. The value of the third-order nonlinear elasticity D can be extracted by fitting the stress-strain relation to the function $\sigma = E\epsilon + \frac{1}{2}D\epsilon^2$ with E as the Young's modulus. The values of D from the present SW potential are -263.3 and -308.6 N/m along the armchair and zigzag directions, respectively. The ultimate stress is about 11.3 N/m at the ultimate strain of 0.24 in the armchair direction at the low temperature of 1 K. The ultimate stress is about 10.7 N/m at the ultimate strain of 0.28 in the zigzag direction at the low temperature of 1 K.

33. 1H-WO₂

Most existing theoretical studies on the single-layer 1H-WO₂ are based on the first-principles calculations. In this section, we will develop the SW potential for the single-layer 1H-WO₂.

The structure for the single-layer 1H-WO₂ is shown in **Figure 1** (with M = W and X = O). Each W atom is surrounded by six O atoms. These O atoms are categorized into the top group (e.g., atoms 1, 3, and 5) and bottom group (e.g., atoms 2, 4, and 6). Each O atom is connected to three W atoms. The structural parameters are from the first-principles calculations [12], including the lattice constant $a = 2.80\text{\AA}$ and the bond length $d_{W-O} = 2.03\text{\AA}$. The resultant angles are $\theta_{WOO} = \theta_{OWW} = 87.206^\circ$ and $\theta_{WOO'} = 74.435^\circ$, in which atoms O and O' are from different (top or bottom) groups.

Table 130 shows four VFF terms for the single-layer 1H-WO₂; one of which is the bond stretching interaction shown by Eq. (1), while the other three terms are the angle bending interaction shown by Eq. (2). These force constant parameters are determined by fitting to the acoustic branches in the phonon dispersion along the Γ M as shown in **Figure 63(a)**. The *ab initio* calculations for the phonon dispersion are from Ref. [12]. **Figure 63(b)** shows that the VFF model and the SW potential give exactly the same phonon dispersion, as the SW potential is derived from the VFF model.

The parameters for the two-body SW potential used by GULP are shown in **Table 131**. The parameters for the three-body SW potential used by GULP are shown in **Table 132**. Some representative parameters for the SW potential used by LAMMPS are listed in **Table 133**. We note that 12 atom types have been introduced for the simulation of the single-layer 1H-WO₂ using LAMMPS, because the angles around atom W in **Figure 1** (with M = W and X = O) are not distinguishable in LAMMPS. We have suggested two options to differentiate these angles by implementing some additional constraints in LAMMPS, which can be accomplished by modifying the source file of LAMMPS [13, 14]. According to our experience, it is not so convenient for some users to implement these constraints and recompile the LAMMPS package. Hence, in the present work, we differentiate the angles by introducing more atom types, so it is not necessary to modify the LAMMPS package. **Figure 2** (with M = W and X = O) shows that, for 1H-WO₂, we can differentiate these angles around the W atom by assigning these six

VFF type	Bond stretching	Angle bending		
Expression	$\frac{1}{2}K_{W-O}(\Delta r)^2$	$\frac{1}{2}K_{W-O-O}(\Delta\theta)^2$	$\frac{1}{2}K_{W-O-O'}(\Delta\theta)^2$	$\frac{1}{2}K_{O-W-W}(\Delta\theta)^2$
Parameter	15.318	10.276	10.276	10.276
r_0 or θ_0	2.030	87.206	74.435	87.206

The second line gives an explicit expression for each VFF term. The third line is the force constant parameters. Parameters are in the unit of eV/ \AA^2 for the bond stretching interaction and in the unit of eV for the angle bending interaction. The fourth line gives the initial bond length (in the unit of \AA) for the bond stretching interaction and the initial angle (in the unit of degrees) for the angle bending interaction. The angle θ_{ijk} has atom *i* as the apex.

Table 130. The VFF model for single-layer 1H-WO₂.

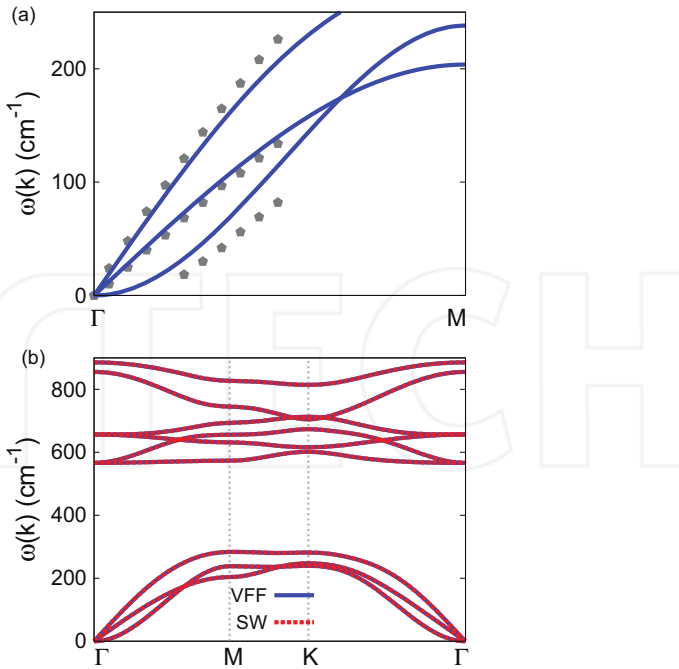


Figure 63. Phonon spectrum for single-layer 1H-WO₂. (a) Phonon dispersion along the $a = 2.80$ direction in the Brillouin zone. The results from the VFF model (lines) are comparable with the *ab initio* results (pentagons) from Ref. [12]. (b) The phonon dispersion from the SW potential is exactly the same as that from the VFF model.

	A (eV)	ρ (Å)	B (Å ⁴)	r_{\min} (Å)	r_{\max} (Å)
W—O	8.781	1.005	8.491	0.0	2.744

Table 131. Two-body SW potential parameters for single-layer 1H-WO₂ used by GULP [8] as expressed in Eq. (3).

	K (eV)	θ_0 (°)	ρ_1 (Å)	ρ_2 (Å)	$r_{\min 12}$ (Å)	$r_{\max 12}$ (Å)	$r_{\min 13}$ (Å)	$r_{\max 13}$ (Å)	$r_{\min 23}$ (Å)	$r_{\max 23}$ (Å)
θ_{W-O-O}	85.955	87.206	1.005	1.005	0.0	2.744	0.0	2.744	0.0	3.262
$\theta_{W-O-O'}$	92.404	74.435	1.005	1.005	0.0	2.744	0.0	2.744	0.0	3.262
θ_{O-W-W}	85.955	87.206	1.005	1.005	0.0	2.744	0.0	2.744	0.0	3.262

The angle θ_{ijk} in the first line indicates the bending energy for the angle with atom i as the apex.

Table 132. Three-body SW potential parameters for single-layer 1H-WO₂ used by GULP [8] as expressed in Eq. (4).

neighboring O atoms with different atom types. It can be found that 12 atom types are necessary for the purpose of differentiating all 6 neighbors around 1 W atom.

We use LAMMPS to perform MD simulations for the mechanical behavior of the single-layer 1H-WO₂ under uniaxial tension at 1 and 300 K. **Figure 64** shows the stress-strain curve for the

	ϵ (eV)	σ (\AA)	a	λ	γ	$\cos \theta_0$	A_L	B_L	p	q	Tol
W ₁ —O ₁ —O ₁	1.000	1.005	2.730	0.000	1.000	0.000	8.781	8.316	4	0	0.0
W ₁ —O ₁ —O ₃	1.000	0.000	0.000	85.955	1.000	0.049	0.000	0.000	4	0	0.0
W ₁ —O ₁ —O ₂	1.000	0.000	0.000	92.404	1.000	0.268	0.000	0.000	4	0	0.0
O ₁ —W ₁ —W ₃	1.000	0.000	0.000	85.955	1.000	0.049	0.000	0.000	4	0	0.0

Table 133. SW potential parameters for single-layer 1H-WO₂ used by LAMMPS [9] as expressed in Eqs. (9) and (10).

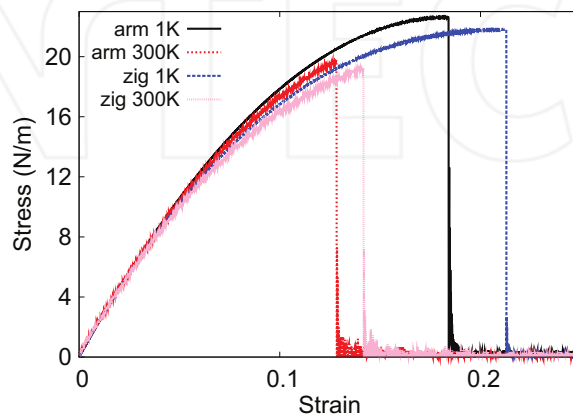


Figure 64. Stress-strain for single-layer 1H-WO₂ of dimension $100 \times 100\text{\AA}$ along the armchair and zigzag directions.

tension of a single-layer 1H-WO₂ of dimension $100 \times 100\text{\AA}$. Periodic boundary conditions are applied in both armchair and zigzag directions. The single-layer 1H-WO₂ is stretched uniaxially along the armchair or zigzag direction. The stress is calculated without involving the actual thickness of the quasi-two-dimensional structure of the single-layer 1H-WO₂. The Young's modulus can be obtained by a linear fitting of the stress-strain relation in the small strain range of [0, 0.01]. The Young's modulus is 237.1 and 237.2 N/m along the armchair and zigzag directions, respectively. The Young's modulus is essentially isotropic in the armchair and zigzag directions. The Poisson's ratio from the VFF model and the SW potential is $\nu_{xy} = \nu_{yx} = 0.15$.

There is no available value for nonlinear quantities in the single-layer 1H-WO₂. We have thus used the nonlinear parameter $B = 0.5d^4$ in Eq. (5), which is close to the value of B in most materials. The value of the third-order nonlinear elasticity D can be extracted by fitting the stress-strain relation to the function $\sigma = E\epsilon + \frac{1}{2}D\epsilon^2$ with E as the Young's modulus. The values of D from the present SW potential are -1218.0 and -1312.9 N/m along the armchair and zigzag directions, respectively. The ultimate stress is about 22.6 N/m at the ultimate strain of 0.18 in the armchair direction at the low temperature of 1 K. The ultimate stress is about 21.8 N/m at the ultimate strain of 0.21 in the zigzag direction at the low temperature of 1 K.

34. 1H-WS₂

Most existing theoretical studies on the single-layer 1H-WS₂ are based on the first-principles calculations. In this section, we will develop both VFF model and the SW potential for the single-layer 1H-WS₂.

Table 134 shows the VFF terms for the 1H-WS₂; one of which is the bond stretching interaction shown by Eq. (1), while the other terms are the angle bending interaction shown by Eq. (2). These force constant parameters are determined by fitting to the three acoustic branches in the phonon dispersion along the Γ M as shown in **Figure 65(a)**. The *ab initio* calculations for the phonon dispersion are from Ref. [31]. Similar phonon dispersion can also be found in other *ab initio* calculations [12, 26, 34, 38, 39]. **Figure 65(b)** shows that the VFF model and the SW potential give exactly the same phonon dispersion, as the SW potential is derived from the VFF model.

The parameters for the two-body SW potential used by GULP are shown in **Table 135**. The parameters for the three-body SW potential used by GULP are shown in **Table 136**. Parameters for the SW potential used by LAMMPS are listed in **Table 137**. We note that 12 atom types have been introduced for the simulation of the single-layer 1H-WS₂ using LAMMPS, because the angles around atom W in **Figure 1** (with M = W and X = S) are not distinguishable in LAMMPS. We have suggested two options to differentiate these angles by implementing some additional constraints in LAMMPS, which can be accomplished by modifying the source file of LAMMPS [13, 14]. According to our experience, it is not so convenient for some users to implement these constraints and recompile the LAMMPS package. Hence, in the present work, we differentiate the angles by introducing more atom types, so it is not necessary to modify the LAMMPS package. **Figure 2** (with M = W and X = S) shows that, for 1H-WS₂, we can differentiate these angles around the W atom by assigning these six neighboring S atoms with different atom types. It can be found that 12 atom types are necessary for the purpose of differentiating all 6 neighbors around 1 W atom.

The parameters for the two-body SW potential used by GULP are shown in **Table 131**. The parameters for the three-body SW potential used by GULP are shown in **Table 132**. Some representative parameters for the SW potential used by LAMMPS are listed in **Table 133**. We note that 12 atom types have been introduced for the simulation of the single-layer 1H-WO₂

VFF type	Bond stretching	Angle bending		
Expression	$\frac{1}{2}K_{W-S}(\Delta r)^2$	$\frac{1}{2}K_{W-S-S}(\Delta\theta)^2$	$\frac{1}{2}K_{W-S-S}(\Delta\theta)^2$	$\frac{1}{2}K_{S-W-W}(\Delta\theta)^2$
Parameter	8.701	7.421	7.421	6.607
r_0 or θ_0	2.390	81.811	81.755	81.811

The second line gives an explicit expression for each VFF term. The third line is the force constant parameters. Parameters are in the unit of eV/ \AA^2 for the bond stretching interaction and in the unit of eV for the angle bending interaction. The fourth line gives the initial bond length (in the unit of \AA) for the bond stretching interaction and the initial angle (in the unit of degrees) for the angle bending interaction. The angle θ_{ijk} has atom *i* as the apex.

Table 134. The VFF model for single-layer 1H-WS₂.

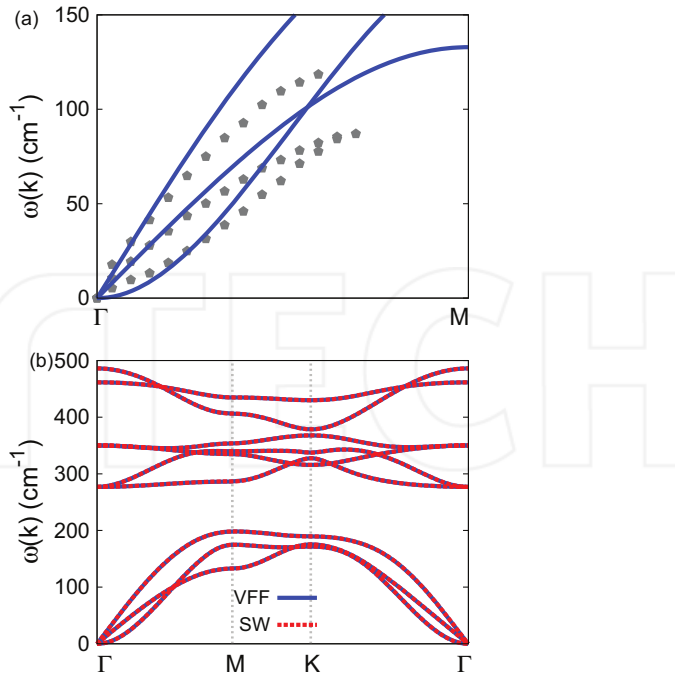


Figure 65. Phonon dispersion for single-layer 1H-WS₂. (a) The VFF model is fitted to three acoustic branches in the long wave limit along the Γ -M-K- Γ direction. The *ab initio* results (gray pentagons) are from Ref. [31]. (b) The VFF model (blue lines) and the SW potential (red lines) give the same phonon dispersion for single-layer 1H-WS₂ along $B = 0.5d^4$.

	A (eV)	ρ (\AA)	B (\AA^4)	r_{\min} (\AA)	r_{\max} (\AA)
W-S	5.664	0.889	15.335	0.0	3.164

Table 135. Two-body SW potential parameters for single-layer 1H-WS₂ used by GULP [8] as expressed in Eq. (3).

	K (eV)	θ_0 ($^\circ$)	ρ_1 (\AA)	ρ_2 (\AA)	$r_{\min 12}$ (\AA)	$r_{\max 12}$ (\AA)	$r_{\min 13}$ (\AA)	$r_{\max 13}$ (\AA)	$r_{\min 23}$ (\AA)	$r_{\max 23}$ (\AA)
θ_{W-S-S}	37.687	81.811	0.889	0.889	0.0	3.164	0.0	3.164	0.0	3.778
$\theta_{W-S-S'}$	37.697	81.755	0.889	0.889	0.0	3.164	0.0	3.164	0.0	3.778
θ_{S-W-W}	33.553	81.811	0.889	0.889	0.0	3.164	0.0	3.164	0.0	3.778

The angle θ_{ijk} in the first line indicates the bending energy for the angle with atom i as the apex.

Table 136. Three-body SW potential parameters for single-layer 1H-WS₂ used by GULP [8] as expressed in Eq. (4).

using LAMMPS, because the angles around atom W in **Figure 1** (with M = W and X = O) are not distinguishable in LAMMPS. We have suggested two options to differentiate these angles by implementing some additional constraints in LAMMPS, which can be accomplished by

	ϵ (eV)	$\sigma(\text{\AA})$	a	λ	γ	$\cos \theta_0$	A_L	B_L	p	q	Tol
W ₁ —S ₁ —S ₁	1.000	0.889	3.558	0.000	1.000	0.000	5.664	24.525	4	0	0.0
W ₁ —S ₁ —S ₃	1.000	0.000	0.000	37.687	1.000	0.142	0.000	0.000	4	0	0.0
W ₁ —S ₁ —S ₂	1.000	0.000	0.000	37.697	1.000	0.143	0.000	0.000	4	0	0.0
S ₁ —W ₁ —W ₃	1.000	0.000	0.000	33.553	1.000	0.142	0.000	0.000	4	0	0.0

Atom types in the first column are displayed in Figure 2 (with M = W and X = S).

Table 137. SW potential parameters for single-layer 1H-WS₂ used by LAMMPS [9] as expressed in Eqs. (9) and (10).

modifying the source file of LAMMPS [13, 14]. According to our experience, it is not so convenient for some users to implement these constraints and recompile the LAMMPS package. Hence, in the present work, we differentiate the angles by introducing more atom types, so it is not necessary to modify the LAMMPS package. Figure 2 (with M = W and X = O) shows that, for 1H-WO₂, we can differentiate these angles around the W atom by assigning these six neighboring O atoms with different atom types. It can be found that 12 atom types are necessary for the purpose of differentiating all 6 neighbors around 1 W atom.

We use LAMMPS to perform MD simulations for the mechanical behavior of the single-layer 1H-WS₂ under uniaxial tension at 1 and 300 K. Figure 66 shows the stress-strain curve for the tension of a single-layer 1H-WS₂ of dimension 100 × 100 Å. Periodic boundary conditions are applied in both armchair and zigzag directions. The single-layer 1H-WS₂ is stretched uniaxially along the armchair or zigzag direction. The stress is calculated without involving the actual thickness of the quasi-two-dimensional structure of the single-layer 1H-WS₂. The Young's modulus can be obtained by a linear fitting of the stress-strain relation in the small strain range of [0, 0.01]. The Young's modulus is 121.5 N/m along both armchair and zigzag directions. These values are in reasonable agreement with the *ab initio* results, e.g., 139.6 N/m

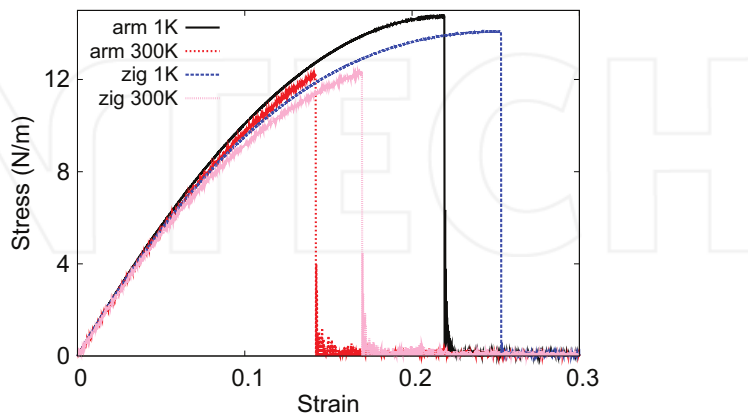


Figure 66. Stress-strain for single-layer 1H-WS₂ of dimension $\frac{1}{2}K_{W-S}(\Delta r)^2$ Å along the armchair and zigzag directions.

from Ref. [18], or 148.5 N/m from Ref. [35]. The Poisson's ratio from the VFF model and the SW potential is $\nu_{xy} = \nu_{yx} = 0.21$, which agrees with the *ab initio* value of 0.22 [18].

We have determined the nonlinear parameter to be $B = 0.47d^4$ in Eq. (5) by fitting to the third-order nonlinear elastic constant D from the *ab initio* calculations [35]. We have extracted the value of $D = -502.9$ N/m by fitting the stress-strain relation along the armchair direction in the *ab initio* calculations to the function $\sigma = E\epsilon + \frac{1}{2}D\epsilon^2$ with E as the Young's modulus. The values of D from the present SW potential are -472.8 and -529.6 N/m along the armchair and zigzag directions, respectively. The ultimate stress is about 14.7 N/m at the ultimate strain of 0.22 in the armchair direction at the low temperature of 1 K. The ultimate stress is about 14.1 N/m at the ultimate strain of 0.25 in the zigzag direction at the low temperature of 1 K.

35. 1H-WSe₂

Most existing theoretical studies on the single-layer 1H-WSe₂ are based on the first-principles calculations. Norouzzadeh and Singh provided one set of parameters for the SW potential for the single-layer 1H-WSe₂ [40]. In this section, we will develop both VFF model and the SW potential for the single-layer 1H-WSe₂.

The structure for the single-layer 1H-WSe₂ is shown in **Figure 1** (with M = W and X = Se). Each W atom is surrounded by six Se atoms. These Se atoms are categorized into the top group (e.g., atoms 1, 3, and 5) and bottom group (e.g., atoms 2, 4, and 6). Each Se atom is connected to three W atoms. The structural parameters are from [12], including the lattice constant $a = 3.25$ Å and the bond length $d_{W-Se} = 2.51$ Å. The resultant angles are $\theta_{WSeSe} = \theta_{SeWW} = 80.693^\circ$ and $\theta_{WSeSe'} = 83.240^\circ$, in which atoms Se and Se' are from different (top or bottom) groups.

Table 138 shows three VFF terms for the 1H-WSe₂; one of which is the bond stretching interaction shown by Eq. (1), while the other two terms are the angle bending interaction shown by Eq. (2). These force constant parameters are determined by fitting to the three acoustic branches in the phonon dispersion along the Γ M as shown in **Figure 67(a)**. The *ab initio* calculations for the phonon dispersion are from [31]. Similar phonon dispersion can also be found in other *ab initio* calculations [12, 33, 34, 39, 41]. **Figure 67(b)** shows that the VFF

VFF type	Bond stretching	Angle bending		
Expression	$\frac{1}{2}K_{W-Se}(\Delta r)^2$	$\frac{1}{2}K_{W-Se-Se}(\Delta\theta)^2$	$\frac{1}{2}K_{W-Se-Se'}(\Delta\theta)^2$	$\frac{1}{2}K_{Se-W-W}(\Delta\theta)^2$
Parameter	8.286	8.513	8.513	7.719
r_0 or θ_0	2.510	80.693	83.140	80.693

The second line gives an explicit expression for each VFF term. The third line is the force constant parameters. Parameters are in the unit of eV/Å² for the bond stretching interaction and in the unit of eV for the angle bending interaction. The fourth line gives the initial bond length (in the unit of Å) for the bond stretching interaction and the initial angle (in the unit of degrees) for the angle bending interaction. The angle θ_{ijk} has atom i as the apex.

Table 138. The VFF model for single-layer 1H-WSe₂.

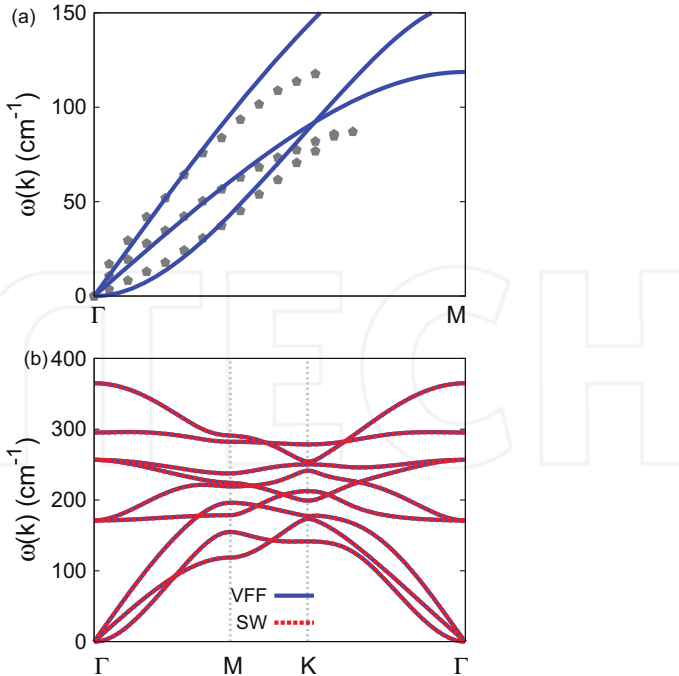


Figure 67. Phonon dispersion for single-layer 1H-WSe₂. (a) The VFF model is fitted to the three acoustic branches in the long wave limit along the Γ M direction. The *ab initio* results (gray pentagons) are from Ref. [31]. (b) The VFF model (blue lines) and the SW potential (red lines) give the same phonon dispersion for single-layer 1H-WSe₂ along Γ MK Γ .

model and the SW potential give exactly the same phonon dispersion, as the SW potential is derived from the VFF model.

The parameters for the two-body SW potential used by GULP are shown in **Table 139**. The parameters for the three-body SW potential used by GULP are shown in **Table 140**. Parameters for the SW potential used by LAMMPS are listed in **Table 141**. We note that 12 atom types have been introduced for the simulation of the single-layer 1H-WSe₂ using LAMMPS, because the angles around atom W in **Figure 1** (with M = W and X = Se) are not distinguishable in LAMMPS. We have suggested two options to differentiate these angles by implementing some additional constraints in LAMMPS, which can be accomplished by modifying the source file of LAMMPS [13, 14]. According to our experience, it is not so convenient for some users to implement these constraints and recompile the LAMMPS package. Hence, in the present work, we differentiate the angles by introducing more atom types, so it is not necessary to modify the

	A (eV)	ρ (Å)	B (Å ⁴)	r_{\min} (Å)	r_{\max} (Å)
W-Se	5.476	0.706	16.273	0.0	3.308

Table 139. Two-body SW potential parameters for single-layer 1H-WSe₂ used by GULP [8] as expressed in Eq. (3).

	K (eV)	θ_0 ($^\circ$)	ρ_1 (\AA)	ρ_2 (\AA)	$r_{\min 12}$ (\AA)	$r_{\max 12}$ (\AA)	$r_{\min 13}$ (\AA)	$r_{\max 13}$ (\AA)	$r_{\min 23}$ (\AA)	$r_{\max 23}$ (\AA)
$\theta_{W-\text{Se}-\text{Se}}$	25.607	80.693	0.706	0.706	0.0	3.308	0.0	3.308	0.0	3.953
$\theta_{W-\text{Se}-\text{Se}'}$	25.287	83.240	0.706	0.706	0.0	3.308	0.0	3.308	0.0	3.953
$\theta_{\text{Se}-\text{W}-\text{W}}$	23.218	80.693	0.706	0.706	0.0	3.308	0.0	3.308	0.0	3.953

The angle θ_{ijk} in the first line indicates the bending energy for the angle with atom i as the apex.

Table 140. Three-body SW potential parameters for single-layer 1H-WSe₂ used by GULP [8] as expressed in Eq. (4).

	ϵ (eV)	σ (\AA)	a	λ	γ	$\cos \theta_0$	A_L	B_L	p	q	Tol
W ₁ —Se ₁ —Se ₁	1.000	0.706	4.689	0.000	1.000	0.000	5.476	65.662	4	0	0.0
W ₁ —Se ₁ —Se ₃	1.000	0.000	0.000	25.607	1.000	0.162	0.000	0.000	4	0	0.0
W ₁ —Se ₁ —Se ₂	1.000	0.000	0.000	25.287	1.000	0.118	0.000	0.000	4	0	0.0
Se ₁ —W ₁ —W ₃	1.000	0.000	0.000	23.218	1.000	0.162	0.000	0.000	4	0	0.0

Atom types in the first column are displayed in Figure 2 (with M = W and X = Se).

Table 141. SW potential parameters for single-layer 1H-WSe₂ used by LAMMPS [9] as expressed in Eqs. (9) and (10).

LAMMPS package. **Figure 2** (with M = W and X = Se) shows that, for 1H-WSe₂, we can differentiate these angles around the W atom by assigning these six neighboring Se atoms with different atom types. It can be found that 12 atom types are necessary for the purpose of differentiating all 6 neighbors around 1 W atom.

We use LAMMPS to perform MD simulations for the mechanical behavior of the single-layer 1H-WSe₂ under uniaxial tension at 1 and 300 K. **Figure 68** shows the stress-strain curve for the tension of a single-layer 1H-WSe₂ of dimension 100 × 100 Å. Periodic boundary conditions are applied in both armchair and zigzag directions. The single-layer 1H-WSe₂ is stretched uniaxially along the armchair or zigzag direction. The stress is calculated without involving

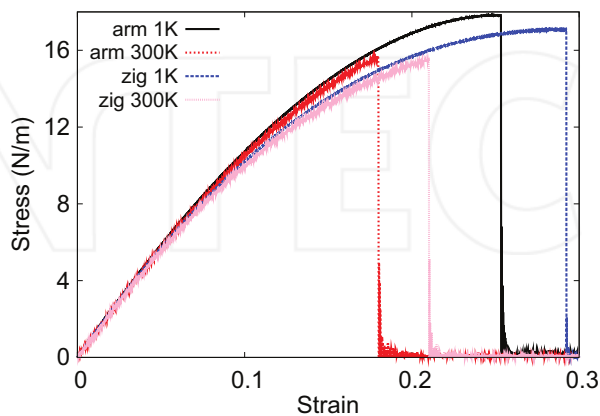


Figure 68. Stress-strain for single-layer 1H-WSe₂ of dimension 100 × 100 Å along the armchair and zigzag directions.

the actual thickness of the quasi-two-dimensional structure of the single-layer 1H-WSe₂. The Young's modulus can be obtained by a linear fitting of the stress-strain relation in the small strain range of [0, 0.01]. The Young's modulus is 124.1 and 123 N/m along the armchair and zigzag directions, respectively. The Young's modulus is essentially isotropic in the armchair and zigzag directions. These values are in reasonably agreement with the *ab initio* results, e.g., 116 N/m from [18], or 126.2 N/m from [35]. The Poisson's ratio from the VFF model and the SW potential is $\nu_{xy} = \nu_{yx} = 0.20$, which agrees with the *ab initio* value of 0.19 [18].

We have determined the nonlinear parameter to be $B = 0.41d^4$ in Eq. (5) by fitting to the third-order nonlinear elastic constant D from the *ab initio* calculations [17]. We have extracted the value of $D = -413.1$ N/m by fitting the stress-strain relation along the armchair direction in the *ab initio* calculations to the function $\sigma = E\epsilon + \frac{1}{2}D\epsilon^2$ with E as the Young's modulus. The values of D from the present SW potential are -400.4 and -444.3 N/m along the armchair and zigzag directions, respectively. The ultimate stress is about 17.8 N/m at the ultimate strain of 0.25 in the armchair direction at the low temperature of 1 K. The ultimate stress is about 17.1 N/m at the ultimate strain of 0.29 in the zigzag direction at the low temperature of 1 K.

36. 1H-WTe₂

Most existing theoretical studies on the single-layer 1H-WTe₂ are based on the first-principles calculations. In this section, we will develop both VFF model and the SW potential for the single-layer 1H-WTe₂.

The bulk WTe₂ has the trigonally coordinated H phase structure [43]. However, it has been predicted that the structure of the single-layer WTe₂ can be either the trigonally coordinated H phase [12] or the octahedrally coordinated T_d phase [44–47], with T_d phase as the more stable structure [42]. We will thus consider both phases in the present paper. This section is devoted to the H phase for the WTe₂ (1H-WTe₂), while the SW potential for the T_d -WTe₂ (1T-WTe₂) is presented in another section.

The structure for the single-layer 1H-WTe₂ is shown in **Figure 1** (with M = W and X = Te). Each W atom is surrounded by six Te atoms. These Te atoms are categorized into the top group (e.g., atoms 1, 3, and 5) and bottom group (e.g., atoms 2, 4, and 6). Each Te atom is connected to three W atoms. The structural parameters are from [42], including the lattice constant $a = 3.55$ Å and the bond length $d_{W-Te} = 2.73$ Å. The resultant angles are $\theta_{WTeTe} = \theta_{TeWW} = 81.111^\circ$ and $\theta_{WTeTe'} = 82.686^\circ$, in which atoms Te and Te' are from different (top or bottom) groups.

Table 142 shows the VFF terms for the 1H-WTe₂; one of which is the bond stretching interaction shown by Eq. (1), while the other terms are the angle bending interaction shown by Eq. (2). These force constant parameters are determined by fitting to the three acoustic branches in the phonon dispersion along the Γ M as shown in **Figure 69(a)**. The *ab initio* calculations for the phonon dispersion are from [42]. Similar phonon dispersion can also be found in other *ab initio* calculations [12]. **Figure 69(b)** shows that the VFF model and the SW potential give exactly the same phonon dispersion, as the SW potential is derived from the VFF model.

VFF type	Bond stretching	Angle bending		
Expression	$\frac{1}{2}K_{W-Te}(\Delta r)^2$	$\frac{1}{2}K_{W-Te-Te}(\Delta\theta)^2$	$\frac{1}{2}K_{W-Te-Te'}(\Delta\theta')^2$	$\frac{1}{2}K_{Te-W-W}(\Delta\theta)^2$
Parameter	5.483	7.016	7.016	5.718
r_0 or θ_0	2.730	81.111	82.686	81.111

The second line gives an explicit expression for each VFF term. The third line is the force constant parameters. Parameters are in the unit of eV/Å² for the bond stretching interaction and in the unit of eV for the angle bending interaction. The fourth line gives the initial bond length (in the unit of Å) for the bond stretching interaction and the initial angle (in the unit of degrees) for the angle bending interaction. The angle θ_{ijk} has atom i as the apex.

Table 142. The VFF model for single-layer 1H-WTe₂.

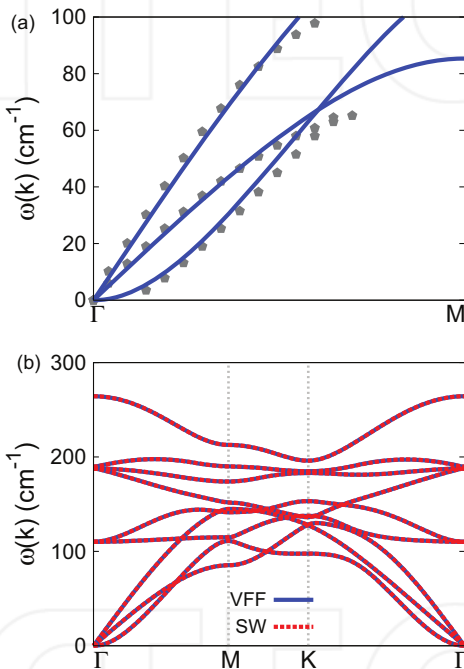


Figure 69. Phonon dispersion for single-layer 1H-WTe₂. (a) The VFF model is fitted to the three acoustic branches in the long wave limit along the Γ M direction. The *ab initio* results (gray pentagons) are from [42]. (b) The VFF model (blue lines) and the SW potential (red lines) give the same phonon dispersion for single-layer 1H-WTe₂ along Γ MK Γ .

The parameters for the two-body SW potential used by GULP are shown in **Table 143**. The parameters for the three-body SW potential used by GULP are shown in **Table 144**. Parameters for the SW potential used by LAMMPS are listed in **Table 145**. We note that 12 atom types have been introduced for the simulation of the single-layer 1H-WTe₂ using LAMMPS, because the angles around atom W in **Figure 1** (with M = W and X = Te) are not distinguishable in LAMMPS. We have suggested two options to differentiate these angles by implementing some additional constraints in LAMMPS, which can be accomplished by modifying the source file of

	A (eV)	ρ (Å)	B (Å ⁴)	r_{\min} (Å)	r_{\max} (Å)
W—Te	4.326	0.778	22.774	0.0	3.604

Table 143. Two-body SW potential parameters for single-layer 1H-WTe₂ used by GULP [8] as expressed in Eq. (3).

	K (eV)	θ_0 (°)	ρ_1 (Å)	ρ_2 (Å)	$r_{\min 12}$ (Å)	$r_{\max 12}$ (Å)	$r_{\min 13}$ (Å)	$r_{\max 13}$ (Å)	$r_{\min 23}$ (Å)	$r_{\max 23}$ (Å)
$\theta_{W-Te-Te}$	21.313	81.111	0.778	0.778	0.0	3.604	0.0	3.604	0.0	4.305
$\theta_{W-Te-Te'}$	21.147	82.686	0.778	0.778	0.0	3.604	0.0	3.604	0.0	4.305
θ_{Te-W-W}	17.370	81.111	0.778	0.778	0.0	3.604	0.0	3.604	0.0	4.305

The angle θ_{ijk} in the first line indicates the bending energy for the angle with atom i as the apex.

Table 144. Three-body SW potential parameters for single-layer 1H-WTe₂ used by GULP [8] as expressed in Eq. (4).

	ϵ (eV)	σ (Å)	a	λ	γ	$\cos \theta_0$	A_L	B_L	p	q	Tol
W ₁ —Te ₁ —Te ₁	1.000	0.778	4.632	0.000	1.000	0.000	4.326	62.148	4	0	0.0
W ₁ —Te ₁ —Te ₃	1.000	0.000	0.000	21.313	1.000	0.155	0.000	0.000	4	0	0.0
W ₁ —Te ₁ —Te ₂	1.000	0.000	0.000	21.147	1.000	0.127	0.000	0.000	4	0	0.0
Te ₁ —W ₁ —W ₃	1.000	0.000	0.000	17.370	1.000	0.155	0.000	0.000	4	0	0.0

Atom types in the first column are displayed in **Figure 2** (with M = W and X = Te).

Table 145. SW potential parameters for single-layer 1H-WTe₂ used by LAMMPS [9] as expressed in Eqs. (9) and (10).

LAMMPS [13, 14]. According to our experience, it is not so convenient for some users to implement these constraints and recompile the LAMMPS package. Hence, in the present work, we differentiate the angles by introducing more atom types, so it is not necessary to modify the LAMMPS package. **Figure 2** (with M = W and X = Te) shows that, for 1H-WTe₂, we can differentiate these angles around the W atom by assigning these six neighboring Te atoms with different atom types. It can be found that 12 atom types are necessary for the purpose of differentiating all 6 neighbors around 1 W atom.

We use LAMMPS to perform MD simulations for the mechanical behavior of the single-layer 1H-WTe₂ under uniaxial tension at 1 and 300 K. **Figure 70** shows the stress-strain curve for the tension of a single-layer 1H-WTe₂ of dimension 100 × 100 Å. Periodic boundary conditions are applied in both armchair and zigzag directions. The single-layer 1H-WTe₂ is stretched uniaxially along the armchair or zigzag direction. The stress is calculated without involving the actual thickness of the quasi-two-dimensional structure of the single-layer 1H-WTe₂. The Young's modulus can be obtained by a linear fitting of the stress-strain relation in the small strain range of [0, 0.01]. The Young's modulus is 82.7 and 81.9 N/m along the armchair and zigzag directions, respectively. The Young's modulus is essentially isotropic in the armchair and zigzag directions. These values are in reasonably agreement with the *ab initio* results, e.g., 86.4 N/m from [18] or 93.9 N/m from [35]. The Poisson's ratio from the VFF model and the SW potential is $\nu_{xy} = \nu_{yx} = 0.20$, which agrees with the *ab initio* value of 0.18 [18].

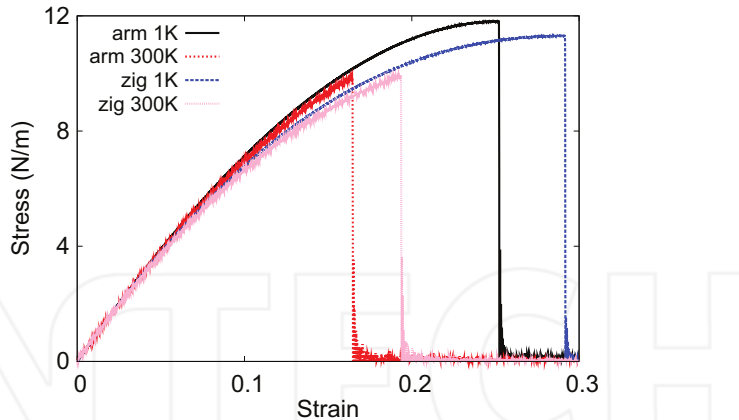


Figure 70. Stress-strain for single-layer 1H-WTe₂ of dimension 100 × 100 Å along the armchair and zigzag directions.

We have determined the nonlinear parameter to be $B = 0.41d^4$ in Eq. (5) by fitting to the third-order nonlinear elastic constant D from the *ab initio* calculations [35]. We have extracted the value of $D = -280.3$ N/m by fitting the stress-strain relation along the armchair direction in the *ab initio* calculations to the function $\sigma = E\epsilon + \frac{1}{2}D\epsilon^2$ with E as the Young's modulus. The values of D from the present SW potential are -269.4 and -297.9 N/m along the armchair and zigzag directions, respectively. The ultimate stress is about 11.8 N/m at the ultimate strain of 0.25 in the armchair direction at the low temperature of 1 K. The ultimate stress is about 11.3 N/m at the ultimate strain of 0.29 in the zigzag direction at the low temperature of 1 K.

37. 1T-ScO₂

Most existing theoretical studies on the single-layer 1T-ScO₂ are based on the first-principles calculations. In this section, we will develop the SW potential for the single-layer 1T-ScO₂.

The structure for the single-layer 1T-ScO₂ is shown in **Figure 71** (with M = Sc and X = O). Each Ni atom is surrounded by six O atoms. These O atoms are categorized into the top group (e.g., atoms 1, 3, and 5) and bottom group (e.g., atoms 2, 4, and 6). Each O atom is connected to three Sc atoms. The structural parameters are from the first-principles calculations [12], including the lattice constant $a = 3.22$ Å and the bond length $d_{\text{Sc}-\text{O}} = 2.07$ Å. The resultant angles are $\theta_{\text{ScOO}} = 102.115^\circ$ with O atoms from the same (top or bottom) group and $\theta_{\text{OSCSc}} = 102.115^\circ$.

Table 146 shows three VFF terms for the single-layer 1T-ScO₂; one of which is the bond stretching interaction shown by Eq. (1), while the other two terms are the angle bending interaction shown by Eq. (2). We note that the angle bending term $K_{\text{Sc}-\text{O}-\text{O}}$ is for the angle $\theta_{\text{Sc}-\text{O}-\text{O}}$ with both O atoms from the same (top or bottom) group. These force constant parameters are determined by fitting to the two in-plane acoustic branches in the phonon dispersion along the ΓM as shown in **Figure 72(a)**. The *ab initio* calculations for the phonon

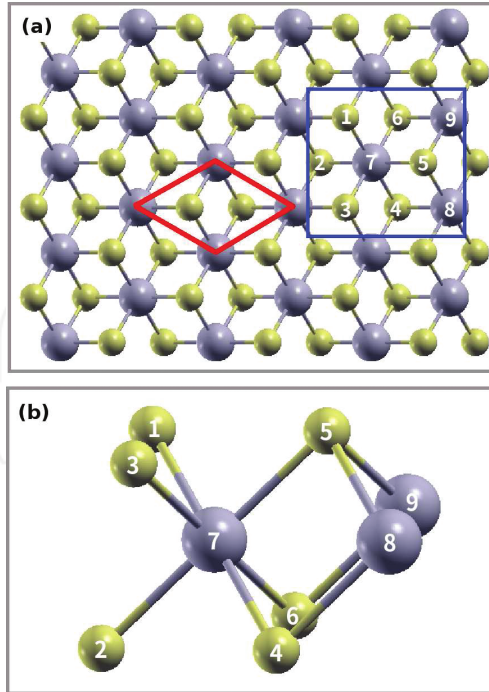


Figure 71. Configuration of the 1T-MX₂ in the 1T phase. (a) Top view. The unit cell is highlighted by a red parallelogram. The armchair direction is defined to be along the horizontal direction. The zigzag direction is along the vertical direction. (b) Enlarged view of atoms in the blue box in (a). Each M atom is surrounded by six X atoms, which are categorized into the top and bottom groups. Atoms X 1, 3, and 5 are from the top group, while atoms X 2, 4, and 6 are from the bottom group. M atoms are represented by larger gray balls. X atoms are represented by smaller yellow balls.

VFF type	Bond stretching	Angle bending	
Expression	$\frac{1}{2}K_{\text{Sc}-\text{O}}(\Delta r)^2$	$\frac{1}{2}K_{\text{Sc}-\text{O}-\text{O}}(\Delta\theta)^2$	$\frac{1}{2}K_{\text{O}-\text{Sc}-\text{Sc}}(\Delta\theta)^2$
Parameter	11.926	3.258	3.258
r ₀ or θ ₀	2.07	102.115	102.115

The second line gives an explicit expression for each VFF term. The third line is the force constant parameters. Parameters are in the unit of eV/Å² for the bond stretching interaction and in the unit of eV for the angle bending interaction. The fourth line gives the initial bond length (in the unit of Å) for the bond stretching interaction and the initial angle (in the unit of degrees) for the angle bending interaction. The angle θ_{ijk} has atom *i* as the apex.

Table 146. The VFF model for single-layer 1T-ScO₂.

dispersion are from [12]. **Figure 72(b)** shows that the VFF model and the SW potential give exactly the same phonon dispersion, as the SW potential is derived from the VFF model.

The parameters for the two-body SW potential used by GULP are shown in **Table 147**. The parameters for the three-body SW potential used by GULP are shown in **Table 148**. Some representative parameters for the SW potential used by LAMMPS are listed in **Table 149**.

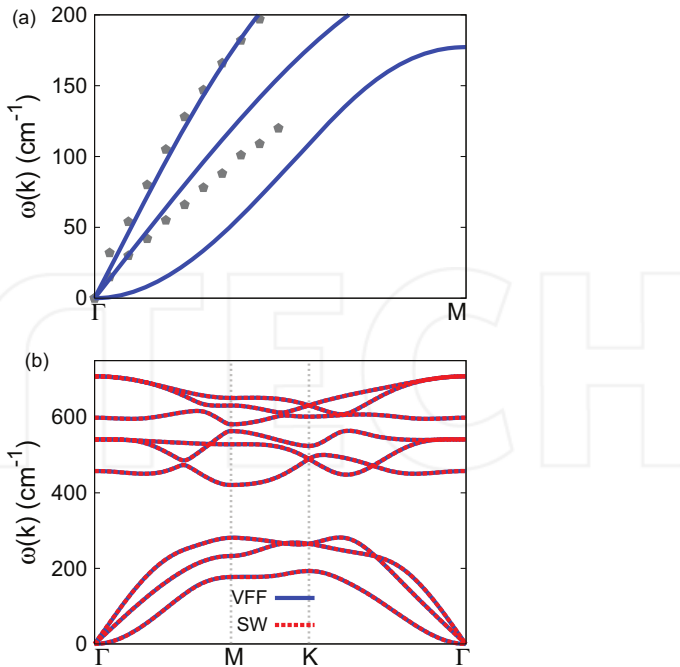


Figure 72. Phonon spectrum for single-layer 1T-ScO₂. (a) Phonon dispersion along the Γ M direction in the Brillouin zone. The results from the VFF model (lines) are comparable with the *ab initio* results (pentagons) from Ref. [12]. (b) The phonon dispersion from the SW potential is exactly the same as that from the VFF model.

	A (eV)	$\rho(\text{\AA})$	$B(\text{\AA}^4)$	r_{\min} (\text{\AA})	r_{\max} (\text{\AA})
Sc—O	10.187	1.493	9.180	0.0	2.949

Table 147. Two-body SW potential parameters for single-layer 1T-ScO₂ used by GULP [8] as expressed in Eq. (3).

	K (eV)	θ_0 (°)	ρ_1 (\text{\AA})	ρ_2 (\text{\AA})	$r_{\min 12}$ (\text{\AA})	$r_{\max 12}$ (\text{\AA})	$r_{\min 13}$ (\text{\AA})	$r_{\max 13}$ (\text{\AA})	$r_{\min 23}$ (\text{\AA})	$r_{\max 23}$ (\text{\AA})
$\theta_{\text{Sc}-\text{O}-\text{O}}$	50.913	102.115	1.493	1.493	0.0	2.949	0.0	2.949	0.0	4.399
$\theta_{\text{O}-\text{Sc}-\text{Sc}}$	50.913	102.115	1.493	1.493	0.0	2.949	0.0	2.949	0.0	4.399

The angle θ_{ijk} in the first line indicates the bending energy for the angle with atom i as the apex.

Table 148. Three-body SW potential parameters for single-layer 1T-ScO₂ used by GULP [8] as expressed in Eq. (4).

	ϵ (eV)	σ (\text{\AA})	a	λ	γ	$\cos \theta_0$	A_L	B_L	p	q	Tol
Sc—O ₁ —O ₁	1.000	1.493	1.975	50.913	1.000	-0.210	10.187	1.847	4	0	0.0

Table 149. SW potential parameters for single-layer 1T-ScO₂ used by LAMMPS [9] as expressed in Eqs. (9) and (10).

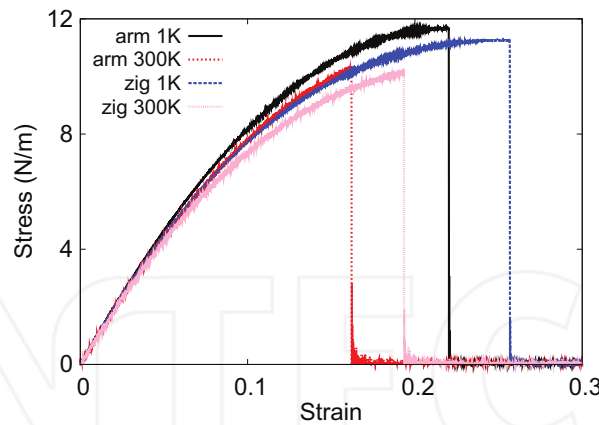


Figure 73. Stress-strain for single-layer 1T-ScO₂ of dimension 100 × 100 Å along the armchair and zigzag directions.

We use LAMMPS to perform MD simulations for the mechanical behavior of the single-layer 1T-ScO₂ under uniaxial tension at 1 and 300 K. **Figure 73** shows the stress-strain curve for the tension of a single-layer 1T-ScO₂ of dimension 100 × 100 Å. Periodic boundary conditions are applied in both armchair and zigzag directions. The single-layer 1T-ScO₂ is stretched uniaxially along the armchair or zigzag direction. The stress is calculated without involving the actual thickness of the quasi-two-dimensional structure of the single-layer 1T-ScO₂. The Young's modulus can be obtained by a linear fitting of the stress-strain relation in the small strain range of [0, 0.01]. The Young's modulus is 100.9 and 100.4 N/m along the armchair and zigzag directions, respectively. The Young's modulus is essentially isotropic in the armchair and zigzag directions. The Poisson's ratio from the VFF model and the SW potential is $\nu_{xy} = \nu_{yx} = 0.15$.

There is no available value for nonlinear quantities in the single-layer 1T-ScO₂. We have thus used the nonlinear parameter $B = 0.5d^4$ in Eq. (5), which is close to the value of B in most materials. The value of the third-order nonlinear elasticity D can be extracted by fitting the stress-strain relation to the function $\sigma = E\epsilon + \frac{1}{2}D\epsilon^2$ with E as the Young's modulus. The values of D from the present SW potential are -422.4 and -453.7 N/m along the armchair and zigzag directions, respectively. The ultimate stress is about 11.7 N/m at the ultimate strain of 0.22 in the armchair direction at the low temperature of 1 K. The ultimate stress is about 11.3 N/m at the ultimate strain of 0.25 in the zigzag direction at the low temperature of 1 K.

38. 1T-ScS₂

Most existing theoretical studies on the single-layer 1T-ScS₂ are based on the first-principles calculations. In this section, we will develop the SW potential for the single-layer 1T-ScS₂.

The structure for the single-layer 1T-ScS₂ is shown in **Figure 71** (with M = Sc and X = S). Each Sc atom is surrounded by six S atoms. These S atoms are categorized into the top group (e.g.,

atoms 1, 3, and 5) and bottom group (e.g., atoms 2, 4, and 6). Each S atom is connected to three Sc atoms. The structural parameters are from the first-principles calculations [12], including the lattice constant $a = 3.62 \text{ \AA}$ and the bond length $d_{\text{Sc-S}} = 2.50 \text{ \AA}$. The resultant angle is $\theta_{\text{SScSc}} = 92.771^\circ$ and $\theta_{\text{ScSS}} = 92.771^\circ$ with S atoms from the same (top or bottom) group.

Table 150 shows three VFF terms for the single-layer 1T-ScS₂, one of which is the bond stretching interaction shown by Eq. (1), while the other two terms are the angle bending interaction shown by Eq. (2). We note that the angle bending term $K_{\text{Sc-S-S}}$ is for the angle $\theta_{\text{Sc-S-S}}$ with both S atoms from the same (top or bottom) group. These force constant parameters are determined by fitting to the three acoustic branches in the phonon dispersion along the ΓM as shown in **Figure 74(a)**. The *ab initio* calculations for the phonon dispersion are from [12]. **Figure 74(b)** shows that the VFF model and the SW potential give exactly the same phonon dispersion, as the SW potential is derived from the VFF model.

The parameters for the two-body SW potential used by GULP are shown in **Table 151**. The parameters for the three-body SW potential used by GULP are shown in **Table 152**. Some representative parameters for the SW potential used by LAMMPS are listed in **Table 153**.

We use LAMMPS to perform MD simulations for the mechanical behavior of the single-layer 1T-ScS₂ under uniaxial tension at 1 and 300 K. **Figure 75** shows the stress-strain curve for the tension of a single-layer 1T-ScS₂ of dimension $100 \times 100 \text{ \AA}$. Periodic boundary conditions are applied in both armchair and zigzag directions. The single-layer 1T-ScS₂ is stretched uniaxially along the armchair or zigzag direction. The stress is calculated without involving the actual thickness of the quasi-two-dimensional structure of the single-layer 1T-ScS₂. The Young's modulus can be obtained by a linear fitting of the stress-strain relation in the small strain range of $[0, 0.01]$. The Young's modulus is 30 and 29.9 N/m along the armchair and zigzag directions, respectively. The Young's modulus is essentially isotropic in the armchair and zigzag directions. The Poisson's ratio from the VFF model and the SW potential is $\nu_{xy} = \nu_{yx} = 0.17$.

There is no available value for nonlinear quantities in the single-layer 1T-ScS₂. We have thus used the nonlinear parameter $B = 0.5d^4$ in Eq. (5), which is close to the value of B in most materials. The value of the third-order nonlinear elasticity D can be extracted by fitting the stress-strain relation to the function $\sigma = E\epsilon + \frac{1}{2}D\epsilon^2$ with E as the Young's modulus. The values of D from the present SW potential are -113.7 and -124.6 N/m along the armchair and zigzag

VFF type	Bond stretching	Angle bending	
Expression	$\frac{1}{2}K_{\text{Sc-S}}(\Delta r)^2$	$\frac{1}{2}K_{\text{Sc-S-S}}(\Delta\theta)^2$	$\frac{1}{2}K_{\text{S-Sc-Sc}}(\Delta\theta)^2$
Parameter	3.512	1.593	1.593
r_0 or θ_0	2.50	92.771	92.771

The second line gives an explicit expression for each VFF term. The third line is the force constant parameters. Parameters are in the unit of eV/ \AA^2 for the bond stretching interaction and in the unit of eV for the angle bending interaction. The fourth line gives the initial bond length (in the unit of \AA) for the bond stretching interaction and the initial angle (in the unit of degrees) for the angle bending interaction. The angle θ_{ijk} has atom i as the apex.

Table 150. The VFF model for single-layer 1T-ScS₂.

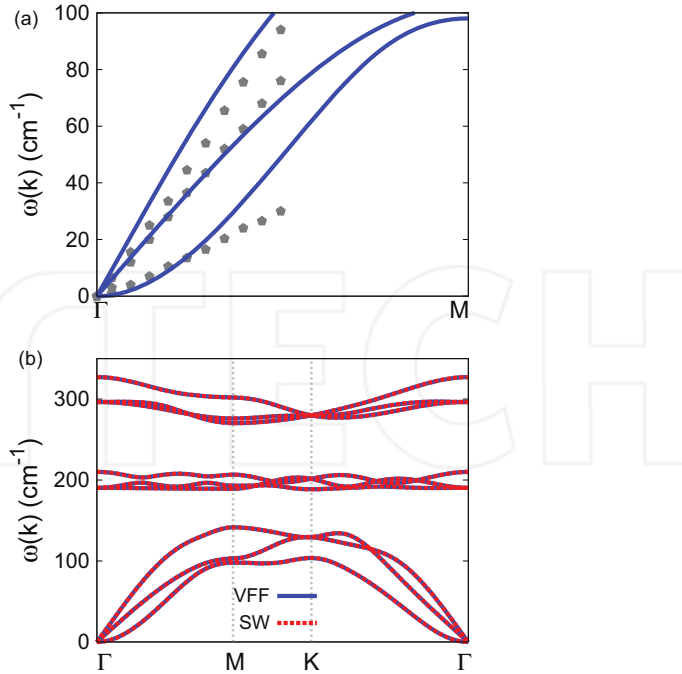


Figure 74. Phonon spectrum for single-layer 1T-ScS₂. (a) Phonon dispersion along the Γ M direction in the Brillouin zone. The results from the VFF model (lines) are comparable with the *ab initio* results (pentagons) from [12]. (b) The phonon dispersion from the SW potential is exactly the same as that from the VFF model.

	A (eV)	ρ (\AA)	B (\AA^4)	r_{\min} (\AA)	r_{\max} (\AA)
Sc—S	3.516	1.443	19.531	0.0	3.450

Table 151. Two-body SW potential parameters for single-layer 1T-ScS₂ used by GULP [8] as expressed in Eq. (3).

	K (eV)	θ_0 ($^\circ$)	ρ_1 (\AA)	ρ_2 (\AA)	$r_{\min 12}$ (\AA)	$r_{\max 12}$ (\AA)	$r_{\min 13}$ (\AA)	$r_{\max 13}$ (\AA)	$r_{\min 23}$ (\AA)	$r_{\max 23}$ (\AA)
$\theta_{\text{Sc-S-S}}$	16.674	92.771	1.443	1.443	0.0	3.450	0.0	3.450	0.0	4.945
$\theta_{\text{S-Sc-Sc}}$	16.674	92.771	1.443	1.443	0.0	3.450	0.0	3.450	0.0	4.945

The angle θ_{ijk} in the first line indicates the bending energy for the angle with atom i as the apex.

Table 152. Three-body SW potential parameters for single-layer 1T-ScS₂ used by GULP [8] as expressed in Eq. (4).

	ϵ (eV)	σ (\AA)	a	λ	γ	$\cos \theta_0$	A_L	B_L	p	q	Tol
Sc—S ₁ —S ₁	1.000	1.443	2.390	16.674	1.000	-0.048	3.516	4.504	4	0	0.0

Table 153. SW potential parameters for single-layer 1T-ScS₂ used by LAMMPS [9] as expressed in Eqs. (9) and (10).

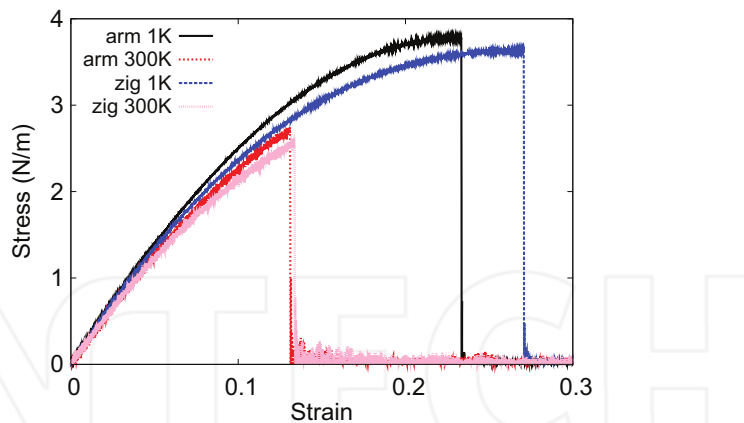


Figure 75. Stress-strain for single-layer 1T-ScS₂ of dimension 100 × 100 Å along the armchair and zigzag directions.

directions, respectively. The ultimate stress is about 3.8 N/m at the ultimate strain of 0.23 in the armchair direction at the low temperature of 1 K. The ultimate stress is about 3.6 N/m at the ultimate strain of 0.27 in the zigzag direction at the low temperature of 1 K.

39. 1T-ScSe₂

Most existing theoretical studies on the single-layer 1T-ScSe₂ are based on the first-principles calculations. In this section, we will develop the SW potential for the single-layer 1T-ScSe₂.

The structure for the single-layer 1T-ScSe₂ is shown in **Figure 71** (with M = Sc and X = Se). Each Sc atom is surrounded by six Se atoms. These Se atoms are categorized into the top group (e.g., atoms 1, 3, and 5) and bottom group (e.g., atoms 2, 4, and 6). Each Se atom is connected to three Sc atoms. The structural parameters are from the first-principles calculations [12], including the lattice constant $a = 3.52$ Å and the bond length $d_{\text{Sc-Se}} = 2.64$ Å. The resultant angle is $\theta_{\text{SeScSe}} = 83.621^\circ$ and $\theta_{\text{ScSeSe}} = 83.621^\circ$ with Se atoms from the same (top or bottom) group.

Table 154 shows three VFF terms for the single-layer 1T-ScSe₂, one of which is the bond stretching interaction shown by Eq. (1), while the other two terms are the angle bending interaction shown by Eq. (2). We note that the angle bending term $K_{\text{Sc-Se-Se}}$ is for the angle $\theta_{\text{Sc-Se-Se}}$ with both Se atoms from the same (top or bottom) group. These force constant parameters are determined by fitting to the three acoustic branches in the phonon dispersion along the Γ M as shown in **Figure 76(a)**. The *ab initio* calculations for the phonon dispersion are from [12]. We note that the lowest-frequency branch around the Γ point from the VFF model is lower than the *ab initio* results. This branch is the flexural branch, which should be a quadratic dispersion. However, the *ab initio* calculations give a linear dispersion for the flexural branch due to the violation of the rigid rotational invariance in the first-principles package [20], so *ab initio* calculations typically overestimate the frequency of this branch. **Figure 76(b)** shows that

VFF type	Bond stretching	Angle bending
Expression	$\frac{1}{2}K_{\text{Sc}-\text{Se}}(\Delta r)^2$	$\frac{1}{2}K_{\text{Sc}-\text{Se}-\text{Se}}(\Delta\theta)^2$
Parameter	4.407	2.399
r_0 or θ_0	2.64	83.621

The second line gives an explicit expression for each VFF term. The third line is the force constant parameters. Parameters are in the unit of eV/Å² for the bond stretching interaction and in the unit of eV for the angle bending interaction. The fourth line gives the initial bond length (in the unit of Å) for the bond stretching interaction and the initial angle (in the unit of degrees) for the angle bending interaction. The angle θ_{ijk} has atom i as the apex.

Table 154. The VFF model for single-layer 1T-ScSe₂.

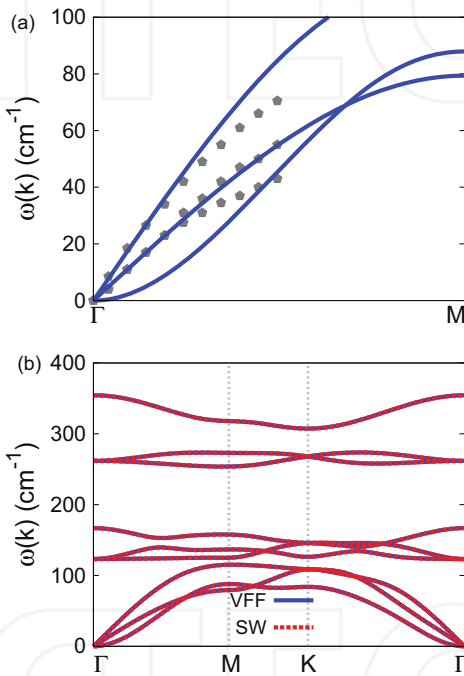


Figure 76. Phonon spectrum for single-layer 1T-ScSe₂. (a) Phonon dispersion along the Γ M direction in the Brillouin zone. The results from the VFF model (lines) are comparable with the *ab initio* results (pentagons) from [12]. (b) The phonon dispersion from the SW potential is exactly the same as that from the VFF model.

the VFF model and the SW potential give exactly the same phonon dispersion, as the SW potential is derived from the VFF model.

The parameters for the two-body SW potential used by GULP are shown in **Table 155**. The parameters for the three-body SW potential used by GULP are shown in **Table 156**. Some representative parameters for the SW potential used by LAMMPS are listed in **Table 157**.

	A (eV)	ρ (Å)	B (Å ⁴)	r_{\min} (Å)	r_{\max} (Å)
Sc—Se	3.884	1.173	24.288	0.0	3.520

Table 155. Two-body SW potential parameters for single-layer 1T-ScSe₂ used by GULP [8] as expressed in Eq. (3).

	K (eV)	θ_0 (°)	ρ_1 (Å)	ρ_2 (Å)	$r_{\min 12}$ (Å)	$r_{\max 12}$ (Å)	$r_{\min 13}$ (Å)	$r_{\max 13}$ (Å)	$r_{\min 23}$ (Å)	$r_{\max 23}$ (Å)
$\theta_{\text{Sc—Se—Se}}$	17.479	83.621	1.173	1.173	0.0	3.520	0.0	3.520	0.0	4.808
$\theta_{\text{Se—Sc—Sc}}$	17.479	83.621	1.173	1.173	0.0	3.520	0.0	3.520	0.0	4.808

The angle θ_{ijk} in the first line indicates the bending energy for the angle with atom i as the apex.

Table 156. Three-body SW potential parameters for single-layer 1T-ScSe₂ used by GULP [8] as expressed in Eq. (4).

	ϵ (eV)	σ (Å)	a	λ	γ	$\cos \theta_0$	A_L	B_L	p	q	Tol
Sc—Se ₁ —Se ₁	1.000	1.173	3.000	17.479	1.000	0.111	3.884	12.814	4	0	0.0

Table 157. SW potential parameters for single-layer 1T-ScSe₂ used by LAMMPS [9] as expressed in Eqs. (9) and (10).

We use LAMMPS to perform MD simulations for the mechanical behavior of the single-layer 1T-ScSe₂ under uniaxial tension at 1 and 300 K. **Figure 77** shows the stress-strain curve for the tension of a single-layer 1T-ScSe₂ of dimension 100 × 100 Å. Periodic boundary conditions are applied in both armchair and zigzag directions. The single-layer 1T-ScSe₂ is stretched uniaxially along the armchair or zigzag direction. The stress is calculated without involving the actual thickness of the quasi-two-dimensional structure of the single-layer 1T-ScSe₂. The Young's modulus can be obtained by a linear fitting of the stress-strain relation in the small strain range of [0, 0.01]. The Young's modulus is 36.4 and 36.3 N/m along the armchair and

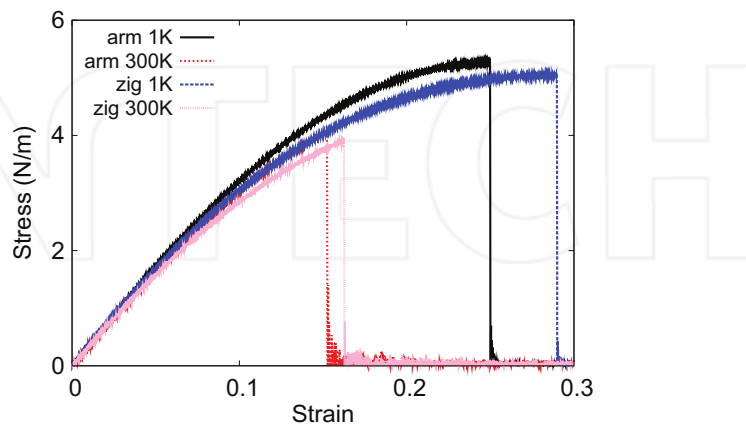


Figure 77. Stress-strain for single-layer 1T-ScSe₂ of dimension 100 × 100 Å along the armchair and zigzag directions.

zigzag directions, respectively. The Young's modulus is essentially isotropic in the armchair and zigzag directions. The Poisson's ratio from the VFF model and the SW potential is $\nu_{xy} = \nu_{yx} = 0.20$.

There is no available value for nonlinear quantities in the single-layer 1T-ScSe₂. We have thus used the nonlinear parameter $B = 0.5d^4$ in Eq. (5), which is close to the value of B in most materials. The value of the third-order nonlinear elasticity D can be extracted by fitting the stress-strain relation to the function $\sigma = E\epsilon + \frac{1}{2}D\epsilon^2$ with E as the Young's modulus. The values of D from the present SW potential are -113.7 and -130.3 N/m along the armchair and zigzag directions, respectively. The ultimate stress is about 5.3 N/m at the ultimate strain of 0.25 in the armchair direction at the low temperature of 1 K. The ultimate stress is about 5 N/m at the ultimate strain of 0.29 in the zigzag direction at the low temperature of 1 K.

40. 1T-ScTe₂

Most existing theoretical studies on the single-layer 1T-ScTe₂ are based on the first-principles calculations. In this section, we will develop the SW potential for the single-layer 1T-ScTe₂.

The structure for the single-layer 1T-ScTe₂ is shown in **Figure 71** (with M = Sc and X = Te). Each Sc atom is surrounded by six Te atoms. These Te atoms are categorized into the top group (e.g., atoms 1, 3, and 5) and bottom group (e.g., atoms 2, 4, and 6). Each Te atom is connected to three Sc atoms. The structural parameters are from the first-principles calculations [12], including the lattice constant $a = 3.72$ Å and the bond length $d_{\text{Sc-Te}} = 2.85$ Å. The resultant angle is $\theta_{\text{TeScSc}} = 81.481^\circ$ and $\theta_{\text{ScTeTe}} = 81.481^\circ$ with Se atoms from the same (top or bottom) group.

Table 158 shows three VFF terms for the single-layer 1T-ScTe₂; one of which is the bond stretching interaction shown by Eq. (1), while the other two terms are the angle bending interaction shown by Eq. (2). We note that the angle bending term $K_{\text{Sc-Te-Te}}$ is for the angle $\theta_{\text{Sc-Te-Te}}$ with both Te atoms from the same (top or bottom) group. These force constant parameters are determined by fitting to the two in-plane acoustic branches in the phonon dispersion along the ΓM as shown in **Figure 78(a)**. The *ab initio* calculations for the phonon dispersion are from [12]. **Figure 78(b)** shows that the VFF model and the SW potential give exactly the same phonon dispersion, as the SW potential is derived from the VFF model.

VFF type	Bond stretching	Angle bending	
Expression	$\frac{1}{2}K_{\text{Sc-Te}}(\Delta r)^2$	$\frac{1}{2}K_{\text{Sc-Te-Te}}(\Delta\theta)^2$	$\frac{1}{2}K_{\text{Te-Sc-Sc}}(\Delta\theta)^2$
Parameter	4.407	2.399	2.399
r_0 or θ_0	2.85	81.481	81.481

The second line gives an explicit expression for each VFF term. The third line is the force constant parameters. Parameters are in the unit of eV/Å² for the bond stretching interaction and in the unit of eV for the angle bending interaction. The fourth line gives the initial bond length (in the unit of Å) for the bond stretching interaction and the initial angle (in the unit of degrees) for the angle bending interaction. The angle θ_{ijk} has atom i as the apex.

Table 158. The VFF model for single-layer 1T-ScTe₂.

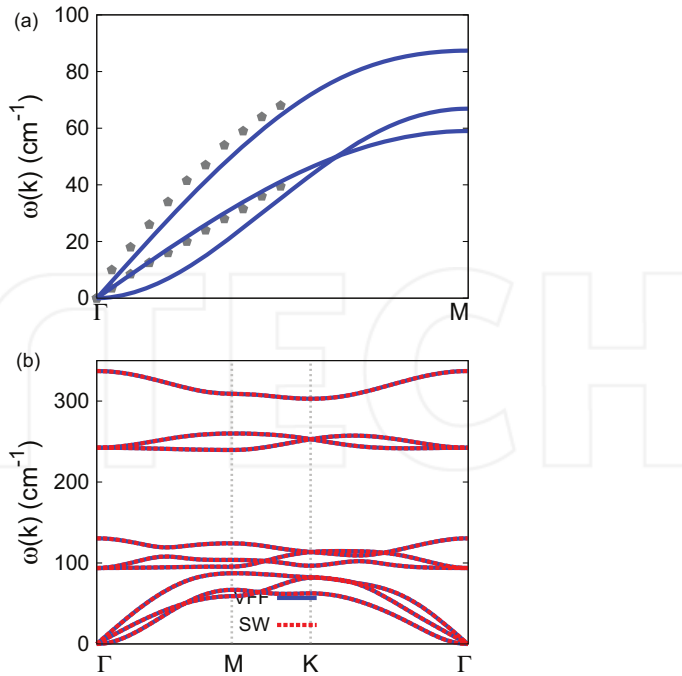


Figure 78. Phonon spectrum for single-layer 1T-ScTe₂. (a) Phonon dispersion along the Γ M direction in the Brillouin zone. The results from the VFF model (lines) are comparable with the *ab initio* results (pentagons) from [12]. (b) The phonon dispersion from the SW potential is exactly the same as that from the VFF model.

The parameters for the two-body SW potential used by GULP are shown in **Table 159**. The parameters for the three-body SW potential used by GULP are shown in **Table 160**. Some representative parameters for the SW potential used by LAMMPS are listed in **Table 161**.

	A (eV)	ρ (Å)	B (Å ⁴)	r_{\min} (Å)	r_{\max} (Å)
Sc—Te	4.269	1.183	32.988	0.0	3.768

Table 159. Two-body SW potential parameters for single-layer 1T-ScTe₂ used by GULP [8] as expressed in Eq. (3).

	K (eV)	θ_0 (°)	ρ_1 (Å)	ρ_2 (Å)	$r_{\min 12}$ (Å)	$r_{\max 12}$ (Å)	$r_{\min 13}$ (Å)	$r_{\max 13}$ (Å)	$r_{\min 23}$ (Å)	$r_{\max 23}$ (Å)
$\theta_{\text{Sc-Te-Te}}$	16.139	81.481	1.183	1.183	0.0	3.768	0.0	3.768	0.0	5.082
$\theta_{\text{Te-Sc-Sc}}$	16.139	81.481	1.183	1.183	0.0	3.768	0.0	3.768	0.0	5.082

The angle θ_{ijk} in the first line indicates the bending energy for the angle with atom i as the apex.

Table 160. Three-body SW potential parameters for single-layer 1T-ScTe₂ used by GULP [8] as expressed in Eq. (4).

	ϵ (eV)	σ (\AA)	a	λ	γ	$\cos \theta_0$	A_L	B_L	p	q	Tol
Sc—Te ₁ —Te ₁	1.000	1.183	3.185	16.139	1.000	0.148	4.269	16.841	4	0	0.0

Table 161. SW potential parameters for single-layer 1T-ScTe₂ used by LAMMPS [9] as expressed in Eqs. (9) and (10).

We use LAMMPS to perform MD simulations for the mechanical behavior of the single-layer 1T-ScTe₂ under uniaxial tension at 1 and 300 K. Figure 79 shows the stress-strain curve for the tension of a single-layer 1T-ScTe₂ of dimension 100 × 100 Å. Periodic boundary conditions are applied in both armchair and zigzag directions. The single-layer 1T-ScTe₂ is stretched uniaxially along the armchair or zigzag direction. The stress is calculated without involving the actual thickness of the quasi-two-dimensional structure of the single-layer 1T-ScTe₂. The Young's modulus can be obtained by a linear fitting of the stress-strain relation in the small strain range of [0, 0.01]. The Young's modulus is 31.4 and 31.3 N/m along the armchair and zigzag directions, respectively. The Young's modulus is essentially isotropic in the armchair and zigzag directions. The Poisson's ratio from the VFF model and the SW potential is $\nu_{xy} = \nu_{yx} = 0.22$.

There is no available value for nonlinear quantities in the single-layer 1T-ScTe₂. We have thus used the nonlinear parameter $B = 0.5d^4$ in Eq. (5), which is close to the value of B in most materials. The value of the third-order nonlinear elasticity D can be extracted by fitting the stress-strain relation to the function $\sigma = E\epsilon + \frac{1}{2}D\epsilon^2$ with E as the Young's modulus. The values of D from the present SW potential are -81.2 and -96.7 N/m along the armchair and zigzag directions, respectively. The ultimate stress is about 5.2 N/m at the ultimate strain of 0.27 in the armchair direction at the low temperature of 1 K. The ultimate stress is about 5 N/m at the ultimate strain of 0.31 in the zigzag direction at the low temperature of 1 K.

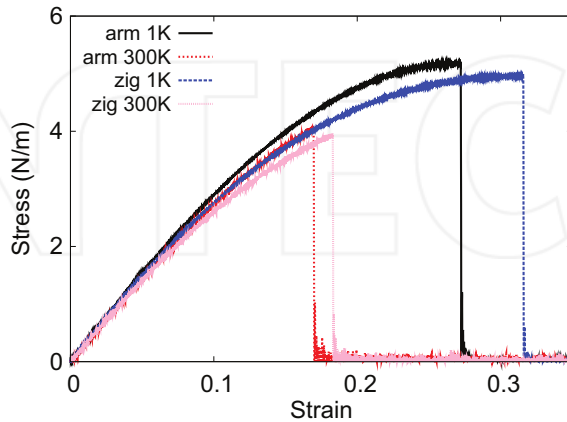


Figure 79. Stress-strain for single-layer 1T-ScTe₂ of dimension 100 × 100 Å along the armchair and zigzag directions.

41. 1T-TiS₂

Most existing theoretical studies on the single-layer 1T-TiS₂ are based on the first-principles calculations. In this section, we will develop the SW potential for the single-layer 1T-TiS₂.

The structure for the single-layer 1T-TiS₂ is shown in **Figure 71** (with M = Ti and X = S). Each Ti atom is surrounded by six S atoms. These S atoms are categorized into the top group (e.g., atoms 1, 3, and 5) and bottom group (e.g., atoms 2, 4, and 6). Each S atom is connected to three Ti atoms. The structural parameters are from the first-principles calculations [12], including the lattice constant $a = 3.32 \text{ \AA}$ and the bond length $d_{\text{Ti-S}} = 2.39 \text{ \AA}$. The resultant angles are $\theta_{\text{TiSS}} = 87.984^\circ$ with S atoms from the same (top or bottom) group and $\theta_{\text{STiTi}} = 87.984^\circ$.

Table 162 shows three VFF terms for the single-layer 1T-TiS₂; one of which is the bond stretching interaction shown by Eq. (1), while the other two terms are the angle bending interaction shown by Eq. (2). We note that the angle bending term $K_{\text{Ti-S-S}}$ is for the angle $\theta_{\text{Ti-S-S}}$ with both S atoms from the same (top or bottom) group. We find that there are actually only two parameters in the VFF model, so we can determine their value by fitting to the Young's modulus and the Poisson's ratio of the system. The *ab initio* calculations have predicted the Young's modulus to be 85 N/m and the Poisson's ratio as 0.20 [48].

The parameters for the two-body SW potential used by GULP are shown in **Table 163**. The parameters for the three-body SW potential used by GULP are shown in **Table 164**. Some representative parameters for the SW potential used by LAMMPS are listed in **Table 165**.

We use LAMMPS to perform MD simulations for the mechanical behavior of the single-layer 1T-TiS₂ under uniaxial tension at 1 and 300 K. **Figure 80** shows the stress-strain curve for the tension of a single-layer 1T-TiS₂ of dimension $100 \times 100 \text{ \AA}$. Periodic boundary conditions are applied in both armchair and zigzag directions. The single-layer 1T-TiS₂ is stretched uniaxially along the armchair or zigzag direction. The stress is calculated without involving the actual thickness of the quasi-two-dimensional structure of the single-layer 1T-TiS₂. The Young's modulus can be obtained by a linear fitting of the stress-strain relation in the small strain range of [0, 0.01]. The Young's modulus is 75 and 74.6 N/m along the armchair and zigzag directions, respectively. The Young's modulus is essentially isotropic in the armchair and zigzag directions. The Poisson's ratio from the VFF model and the SW potential is $\nu_{xy} = \nu_{yx} = 0.20$. The fitted Young's modulus

VFF type	Bond stretching	Angle bending	
Expression	$\frac{1}{2}K_{\text{Ti-S}}(\Delta r)^2$	$\frac{1}{2}K_{\text{Ti-S-S}}(\Delta\theta)^2$	$\frac{1}{2}K_{\text{S-Ti-Ti}}(\Delta\theta)^2$
Parameter	9.815	3.754	3.754
r_0 or θ_0	2.390	87.984	87.984

The second line gives an explicit expression for each VFF term. The third line is the force constant parameters. Parameters are in the unit of eV/ \AA^2 for the bond stretching interaction and in the unit of eV for the angle bending interaction. The fourth line gives the initial bond length (in the unit of \AA) for the bond stretching interaction and the initial angle (in the unit of degrees) for the angle bending interaction. The angle θ_{ijk} has atom i as the apex.

Table 162. The VFF model for single-layer 1T-TiS₂.

	A (eV)	ρ (Å)	B (Å 4)	r_{\min} (Å)	r_{\max} (Å)
Ti-S	7.958	1.210	16.314	0.0	3.240

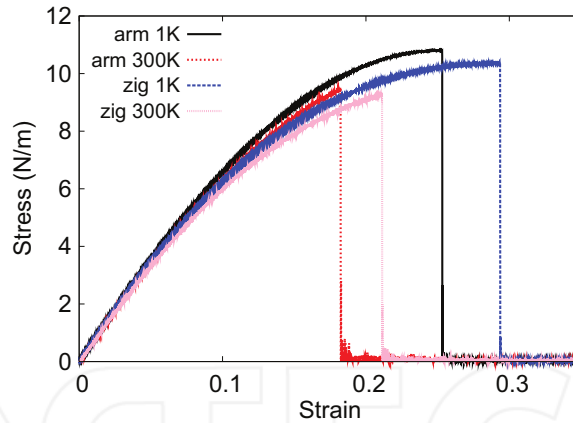
Table 163. Two-body SW potential parameters for single-layer 1T-TiS₂ used by GULP [8] as expressed in Eq. (3).

	K (eV)	θ_0 (°)	ρ_1 (Å)	ρ_2 (Å)	$r_{\min 12}$ (Å)	$r_{\max 12}$ (Å)	$r_{\min 13}$ (Å)	$r_{\max 13}$ (Å)	$r_{\min 23}$ (Å)	$r_{\max 23}$ (Å)
$\theta_{\text{Ti-S-S}}$	32.377	87.984	1.210	1.210	0.0	3.240	0.0	3.240	0.0	4.535
$\theta_{\text{S-Ti-Ti}}$	32.377	87.984	1.210	1.210	0.0	3.240	0.0	3.240	0.0	4.535

The angle θ_{ijk} in the first line indicates the bending energy for the angle with atom i as the apex.

Table 164. Three-body SW potential parameters for single-layer 1T-TiS₂ used by GULP [8] as expressed in Eq. (4).

	ϵ (eV)	σ (Å)	a	λ	γ	$\cos \theta_0$	A_L	B_L	p	q	Tol
Ti—S—S	1.000	1.210	2.677	32.377	1.000	0.035	7.958	7.602	4	0	0.0

Table 165. SW potential parameters for single-layer 1T-TiS₂ used by LAMMPS [9] as expressed in Eqs. (9) and (10).**Figure 80.** Stress-strain for single-layer 1T-TiS₂ of dimension 100 × 100 Å along the armchair and zigzag directions.

value is about 10% smaller than the *ab initio* result of 85 N/m [48], as only short-range interactions are considered in the present work. The long-range interactions are ignored, which typically leads to about 10% underestimation for the value of the Young's modulus.

There is no available value for nonlinear quantities in the single-layer 1T-TiS₂. We have thus used the nonlinear parameter $B = 0.5d^4$ in Eq. (5), which is close to the value of B in most materials. The value of the third-order nonlinear elasticity D can be extracted by fitting the stress-strain relation to the function $\sigma = E\epsilon + \frac{1}{2}D\epsilon^2$ with E as the Young's modulus. The values of D from the present SW potential are -220.8 and -264.4 N/m along the armchair and zigzag directions, respectively. The ultimate stress is about 10.8 N/m at the ultimate strain of 0.25 in

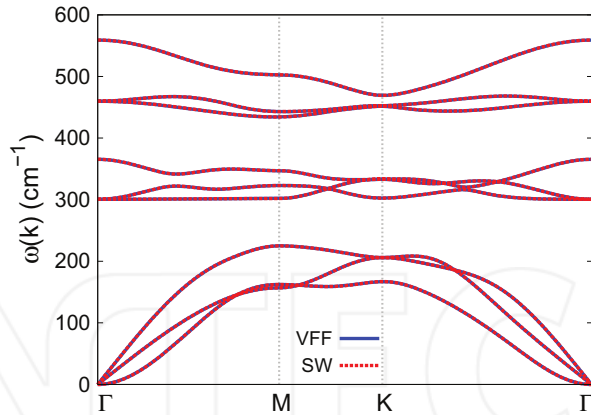


Figure 81. Phonon spectrum for single-layer 1T-TiS₂ along the Γ MK Γ direction in the Brillouin zone. The phonon dispersion from the SW potential is exactly the same as that from the VFF model.

the armchair direction at the low temperature of 1 K. The ultimate stress is about 10.4 N/m at the ultimate strain of 0.29 in the zigzag direction at the low temperature of 1 K.

Figure 81 shows that the VFF model and the SW potential give exactly the same phonon dispersion, as the SW potential is derived from the VFF model.

42. 1T-TiSe₂

Most existing theoretical studies on the single-layer 1T-TiSe₂ are based on the first-principles calculations. In this section, we will develop the SW potential for the single-layer 1T-TiSe₂.

The structure for the single-layer 1T-TiSe₂ is shown in **Figure 71** (with M = Ti and X = Se). Each Ti atom is surrounded by six Se atoms. These Se atoms are categorized into the top group (e.g., atoms 1, 3, and 5) and bottom group (e.g., atoms 2, 4, and 6). Each Se atom is connected to three Ti atoms. The structural parameters are from the first-principles calculations [12], including the lattice constant $a = 3.43 \text{ \AA}$ and the bond length $d_{\text{Ti-Se}} = 2.51 \text{ \AA}$. The resultant angles are $\theta_{\text{TiSeSe}} = 86.199^\circ$ with Se atoms from the same (top or bottom) group and $\theta_{\text{SeTiTi}} = 86.199^\circ$.

Table 166 shows three VFF terms for the single-layer 1T-TiSe₂; one of which is the bond stretching interaction shown by Eq. (1), while the other two terms are the angle bending interaction shown by Eq. (2). We note that the angle bending term $K_{\text{Ti-Se-Se}}$ is for the angle $\theta_{\text{Ti-Se-Se}}$ with both Se atoms from the same (top or bottom) group. We find that there are actually only two parameters in the VFF model, so we can determine their value by fitting to the Young's modulus and the Poisson's ratio of the system. The *ab initio* calculations have predicted the Young's modulus to be 70 N/m and the Poisson's ratio as 0.20 [48].

The parameters for the two-body SW potential used by GULP are shown in **Table 167**. The parameters for the three-body SW potential used by GULP are shown in **Table 168**. Some representative parameters for the SW potential used by LAMMPS are listed in **Table 169**.

VFF type	Bond stretching	Angle bending
Expression	$\frac{1}{2}K_{\text{Ti}-\text{Se}}(\Delta r)^2$	$\frac{1}{2}K_{\text{Ti}-\text{Se}-\text{Se}}(\Delta\theta)^2$
Parameter	7.712	3.363
r_0 or θ_0	2.510	86.199

The second line gives an explicit expression for each VFF term. The third line is the force constant parameters. Parameters are in the unit of eV/Å² for the bond stretching interaction and in the unit of eV for the angle bending interaction. The fourth line gives the initial bond length (in the unit of Å) for the bond stretching interaction and the initial angle (in the unit of degrees) for the angle bending interaction. The angle θ_{ijk} has atom i as the apex.

Table 166. The VFF model for single-layer 1T-TiSe₂.

	A (eV)	ρ (Å)	B (Å ⁴)	r_{\min} (Å)	r_{\max} (Å)
Ti—Se	6.582	1.207	19.846	0.0	3.380

Table 167. Two-body SW potential parameters for single-layer 1T-TiSe₂ used by GULP [8] as expressed in Eq. (3).

	K (eV)	θ_0 (°)	ρ_1 (Å)	ρ_2 (Å)	$r_{\min 12}$ (Å)	$r_{\max 12}$ (Å)	$r_{\min 13}$ (Å)	$r_{\max 13}$ (Å)	$r_{\min 23}$ (Å)	$r_{\max 23}$ (Å)
$\theta_{\text{Ti}-\text{Se}-\text{Se}}$	27.044	86.199	1.207	1.207	0.0	3.380	0.0	3.380	0.0	4.685
$\theta_{\text{Se}-\text{Ti}-\text{Ti}}$	27.044	86.199	1.207	1.207	0.0	3.380	0.0	3.380	0.0	4.685

The angle θ_{ijk} in the first line indicates the bending energy for the angle with atom i as the apex.

Table 168. Three-body SW potential parameters for single-layer 1T-TiSe₂ used by GULP [8] as expressed in Eq. (4).

	ϵ (eV)	σ (Å)	a	λ	γ	$\cos \theta_0$	A_L	B_L	p	q	Tol
Ti—Se—Se	1.000	1.207	2.801	27.044	1.000	0.066	6.582	9.362	4	0	0.0

Table 169. SW potential parameters for single-layer 1T-TiSe₂ used by LAMMPS [9] as expressed in Eqs. (9) and (10).

We use LAMMPS to perform MD simulations for the mechanical behavior of the single-layer 1T-TiSe₂ under uniaxial tension at 1 and 300 K. **Figure 82** shows the stress-strain curve for the tension of a single-layer 1T-TiSe₂ of dimension 100 × 100 Å. Periodic boundary conditions are applied in both armchair and zigzag directions. The single-layer 1T-TiSe₂ is stretched uniaxially along the armchair or zigzag direction. The stress is calculated without involving the actual thickness of the quasi-two-dimensional structure of the single-layer 1T-TiSe₂. The Young's modulus can be obtained by a linear fitting of the stress-strain relation in the small strain range of [0, 0.01]. The Young's modulus is 59.2 and 58.9 N/m along the armchair and zigzag directions, respectively. The Young's modulus is essentially isotropic in the armchair and zigzag directions. The Poisson's ratio from the VFF model and the SW potential is $\nu_{xy} = \nu_{yx} = 0.20$. The fitted Young's modulus value is about 10% smaller than the *ab initio* result of 70 N/m [48], as only short-range interactions are considered in the present work. The long-range interactions are ignored, which typically leads to about 10% underestimation for the value of the Young's modulus.

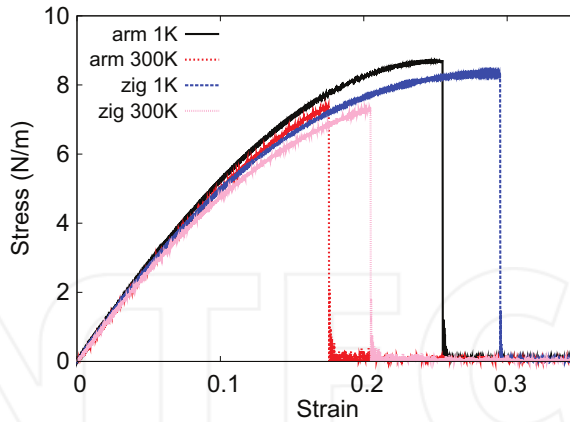


Figure 82. Stress-strain for single-layer 1T-TiSe₂ of dimension 100 × 100 Å along the armchair and zigzag directions.

There is no available value for nonlinear quantities in the single-layer 1T-TiSe₂. We have thus used the nonlinear parameter $B = 0.5d^4$ in Eq. (5), which is close to the value of B in most materials. The value of the third-order nonlinear elasticity D can be extracted by fitting the stress-strain relation to the function $\sigma = E\epsilon + \frac{1}{2}D\epsilon^2$ with E as the Young's modulus. The values of D from the present SW potential are -166.5 and -201.6 N/m along the armchair and zigzag directions, respectively. The ultimate stress is about 8.7 N/m at the ultimate strain of 0.25 in the armchair direction at the low temperature of 1 K. The ultimate stress is about 8.3 N/m at the ultimate strain of 0.29 in the zigzag direction at the low temperature of 1 K.

Figure 83 shows that the VFF model and the SW potential give exactly the same phonon dispersion, as the SW potential is derived from the VFF model.

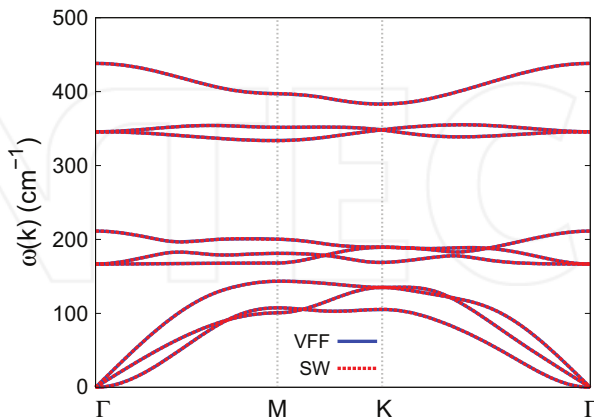


Figure 83. Phonon spectrum for single-layer 1T-TiSe₂ along the Γ MK Γ direction in the Brillouin zone. The phonon dispersion from the SW potential is exactly the same as that from the VFF model.

43. 1T-TiTe₂

Most existing theoretical studies on the single-layer 1T-TiTe₂ are based on the first-principles calculations. In this section, we will develop the SW potential for the single-layer 1T-TiTe₂.

The structure for the single-layer 1T-TiTe₂ is shown in **Figure 71** (with M = Ti and X = Te). Each Ti atom is surrounded by six Te atoms. These Te atoms are categorized into the top group (e.g., atoms 1, 3, and 5) and bottom group (e.g., atoms 2, 4, and 6). Each Te atom is connected to three Ti atoms. The structural parameters are from the first-principles calculations [12], including the lattice constant $a = 3.64 \text{ \AA}$ and the bond length $d_{\text{Ti}-\text{Te}} = 2.73 \text{ \AA}$. The resultant angles are $\theta_{\text{TiTeTe}} = 83.621^\circ$ with Te atoms from the same (top or bottom) group and $\theta_{\text{TeTTi}} = 83.621^\circ$.

Table 170 shows three VFF terms for the single-layer 1T-TiTe₂; one of which is the bond stretching interaction shown by Eq. (1), while the other two terms are the angle bending interaction shown by Eq. (2). We note that the angle bending term $K_{\text{Ti}-\text{Te}-\text{Te}}$ is for the angle $\theta_{\text{Ti}-\text{Te}-\text{Te}}$ with both Te atoms from the same (top or bottom) group. We find that there are actually only two parameters in the VFF model, so we can determine their value by fitting to the Young's modulus and the Poisson's ratio of the system. The *ab initio* calculations have predicted the Young's modulus to be 46 N/m and the Poisson's ratio as 0.15 [48].

The parameters for the two-body SW potential used by GULP are shown in **Table 171**. The parameters for the three-body SW potential used by GULP are shown in **Table 172**. Some representative parameters for the SW potential used by LAMMPS are listed in **Table 173**.

We use LAMMPS to perform MD simulations for the mechanical behavior of the single-layer 1T-TiTe₂ under uniaxial tension at 1 and 300 K. **Figure 84** shows the stress-strain curve for the tension of a single-layer 1T-TiTe₂ of dimension 100 × 100 Å. Periodic boundary conditions are applied in both armchair and zigzag directions. The single-layer 1T-TiTe₂ is stretched uniaxially along the armchair or zigzag direction. The stress is calculated without involving

VFF type	Bond stretching	Angle bending	
Expression	$\frac{1}{2}K_{\text{Ti}-\text{Te}}(\Delta r)^2$	$\frac{1}{2}K_{\text{Ti}-\text{Te}-\text{Te}}(\Delta\theta)^2$	$\frac{1}{2}K_{\text{Te}-\text{Ti}-\text{Ti}}(\Delta\theta)^2$
Parameter	3.758	3.217	3.217
r_0 or θ_0	2.730	83.621	83.621

The second line gives an explicit expression for each VFF term. The third line is the force constant parameters. Parameters are in the unit of eV/Å² for the bond stretching interaction and in the unit of eV for the angle bending interaction. The fourth line gives the initial bond length (in the unit of Å) for the bond stretching interaction and the initial angle (in the unit of degrees) for the angle bending interaction. The angle θ_{ijk} has atom i as the apex.

Table 170. The VFF model for single-layer 1T-TiTe₂.

	A (eV)	ρ (Å)	B (Å ⁴)	r_{\min} (Å)	r_{\max} (Å)
Ti–Te	3.542	1.213	27.773	0.0	3.640

Table 171. Two-body SW potential parameters for single-layer 1T-TiTe₂ used by GULP [8] as expressed in Eq. (3).

	K (eV)	θ_0 ($^\circ$)	ρ_1 (\AA)	ρ_2 (\AA)	$r_{\min 12}$ (\AA)	$r_{\max 12}$ (\AA)	$r_{\min 13}$ (\AA)	$r_{\max 13}$ (\AA)	$r_{\min 23}$ (\AA)	$r_{\max 23}$ (\AA)
$\theta_{\text{Ti}-\text{Te}-\text{Te}}$	23.439	83.621	1.213	1.213	0.0	3.640	0.0	3.640	0.0	4.972
$\theta_{\text{Te}-\text{Ti}-\text{Ti}}$	23.439	83.621	1.213	1.213	0.0	3.640	0.0	3.640	0.0	4.972

The angle θ_{ijk} in the first line indicates the bending energy for the angle with atom i as the apex.

Table 172. Three-body SW potential parameters for single-layer 1T-TiTe₂ used by GULP [8] as expressed in Eq. (4).

	ϵ (eV)	σ (\AA)	a	λ	γ	$\cos \theta_0$	A_L	B_L	p	q	Tol
Ti—Te—Te	1.000	1.213	3.000	23.439	1.000	0.111	3.542	12.814	4	0	0.0

Table 173. SW potential parameters for single-layer 1T-TiTe₂ used by LAMMPS [9] as expressed in Eqs. (9) and (10).

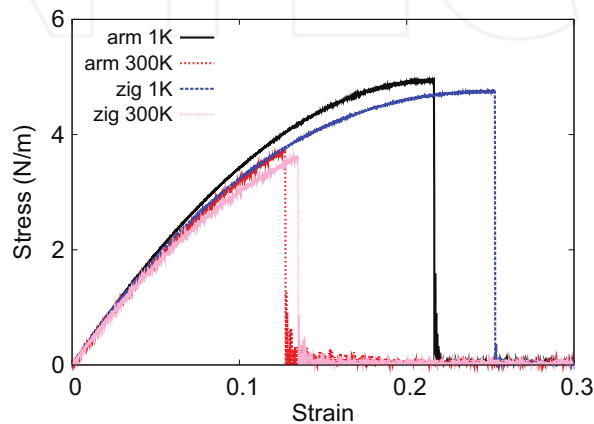


Figure 84. Stress-strain for single-layer 1T-TiTe₂ of dimension $100 \times 100 \text{ \AA}$ along the armchair and zigzag directions.

the actual thickness of the quasi-two-dimensional structure of the single-layer 1T-TiTe₂. The Young's modulus can be obtained by a linear fitting of the stress-strain relation in the small strain range of $[0, 0.01]$. The Young's modulus is 41.4 and 41.2 N/m along the armchair and zigzag directions, respectively. The Young's modulus is essentially isotropic in the armchair and zigzag directions. The Poisson's ratio from the VFF model and the SW potential is $\nu_{xy} = \nu_{yx} = 0.15$. The fitted Young's modulus value is about 10% smaller than the *ab initio* result of 46 N/m [48], as only short-range interactions are considered in the present work. The long-range interactions are ignored, which typically leads to about 10% underestimation for the value of the Young's modulus.

There is no available value for nonlinear quantities in the single-layer 1T-TiTe₂. We have thus used the nonlinear parameter $B = 0.5d^4$ in Eq. (5), which is close to the value of B in most materials. The value of the third-order nonlinear elasticity D can be extracted by fitting the stress-strain relation to the function $\sigma = E\epsilon + \frac{1}{2}D\epsilon^2$ with E as the Young's modulus. The values

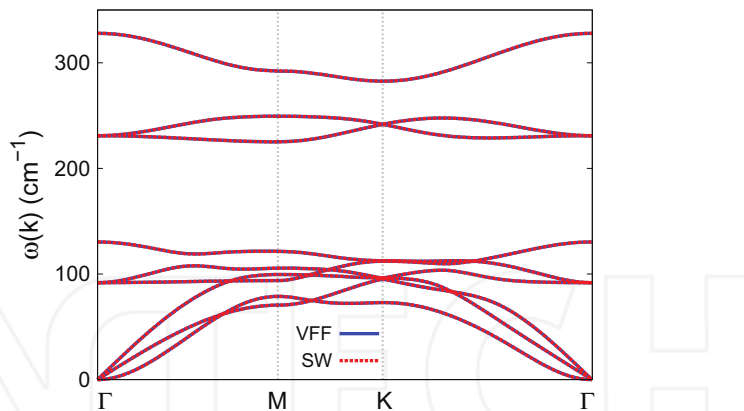


Figure 85. Phonon spectrum for single-layer 1T-TiTe₂ along the Γ MK Γ direction in the Brillouin zone. The phonon dispersion from the SW potential is exactly the same as that from the VFF model.

of D from the present SW potential are -161.3 and -181.4 N/m along the armchair and zigzag directions, respectively. The ultimate stress is about 4.9 N/m at the ultimate strain of 0.22 in the armchair direction at the low temperature of 1 K. The ultimate stress is about 4.7 N/m at the ultimate strain of 0.25 in the zigzag direction at the low temperature of 1 K.

Figure 85 shows that the VFF model and the SW potential give exactly the same phonon dispersion, as the SW potential is derived from the VFF model.

44. 1T-VS₂

Most existing theoretical studies on the single-layer 1T-VS₂ are based on the first-principles calculations. In this section, we will develop the SW potential for the single-layer 1T-VS₂.

The structure for the single-layer 1T-VS₂ is shown in **Figure 71** (with M = V and X = S). Each V atom is surrounded by six S atoms. These S atoms are categorized into the top group (e.g., atoms 1, 3, and 5) and bottom group (e.g., atoms 2, 4, and 6). Each S atom is connected to three V atoms. The structural parameters are from the first-principles calculations [12], including the lattice constant $a = 3.10$ Å and the bond length $d_{V-S} = 2.31$ Å. The resultant angles are $\theta_{VSS} = 84.288^\circ$ with S atoms from the same (top or bottom) group and $\theta_{SVV} = 84.288^\circ$.

Table 174 shows three VFF terms for the single-layer 1T-VS₂; one of which is the bond stretching interaction shown by Eq. (1), while the other two terms are the angle bending interaction shown by Eq. (2). We note that the angle bending term K_{V-S-S} is for the angle θ_{V-S-S} with both S atoms from the same (top or bottom) group. These force constant parameters are determined by fitting to the three acoustic branches in the phonon dispersion along the Γ M as shown in **Figure 86(a)**. The *ab initio* calculations for the phonon dispersion are from [12]. The lowest acoustic branch (flexural mode) is linear and very close to the in-plane

VFF type	Bond stretching	Angle bending
Expression	$\frac{1}{2}K_{V-S}(\Delta r)^2$	$\frac{1}{2}K_{V-S-S}(\Delta\theta)^2$
Parameter	11.562	4.237
r_0 or θ_0	2.310	84.288

The second line gives an explicit expression for each VFF term. The third line is the force constant parameters. Parameters are in the unit of eV/Å² for the bond stretching interaction and in the unit of eV for the angle bending interaction. The fourth line gives the initial bond length (in the unit of Å) for the bond stretching interaction and the initial angle (in the unit of degrees) for the angle bending interaction. The angle θ_{ijk} has atom i as the apex.

Table 174. The VFF model for single-layer 1T-VS₂.

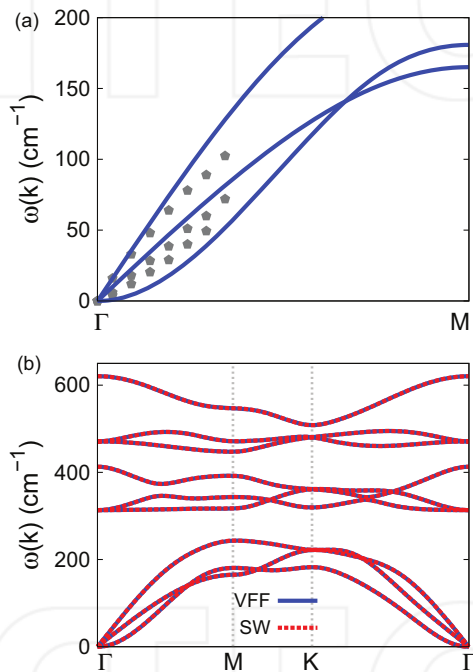


Figure 86. Phonon spectrum for single-layer 1T-VS₂. (a) Phonon dispersion along the ΓM direction in the Brillouin zone. The results from the VFF model (lines) are comparable with the *ab initio* results (pentagons) from [12]. (b) The phonon dispersion from the SW potential is exactly the same as that from the VFF model.

transverse acoustic branch in the *ab initio* calculations, which may be due to the violation of the rigid rotational invariance [20]. **Figure 86(b)** shows that the VFF model and the SW potential give exactly the same phonon dispersion, as the SW potential is derived from the VFF model.

The parameters for the two-body SW potential used by GULP are shown in **Table 175**. The parameters for the three-body SW potential used by GULP are shown in **Table 176**. Some representative parameters for the SW potential used by LAMMPS are listed in **Table 177**.

	A (eV)	ρ (Å)	B (Å ⁴)	r_{\min} (Å)	r_{\max} (Å)
V—S	7.943	1.048	14.237	0.0	3.088

Table 175. Two-body SW potential parameters for single-layer 1T-VS₂ used by GULP [8] as expressed in Eq. (3).

	K (eV)	θ_0 (°)	ρ_1 (Å)	ρ_2 (Å)	$r_{\min12}$ (Å)	$r_{\max12}$ (Å)	$r_{\min13}$ (Å)	$r_{\max13}$ (Å)	$r_{\min23}$ (Å)	$r_{\max23}$ (Å)
θ_{V-S-S}	31.659	84.288	1.048	1.048	0.0	3.088	0.0	3.088	0.0	4.235
θ_{S-V-V}	31.659	84.288	1.048	1.048	0.0	3.088	0.0	3.088	0.0	4.235

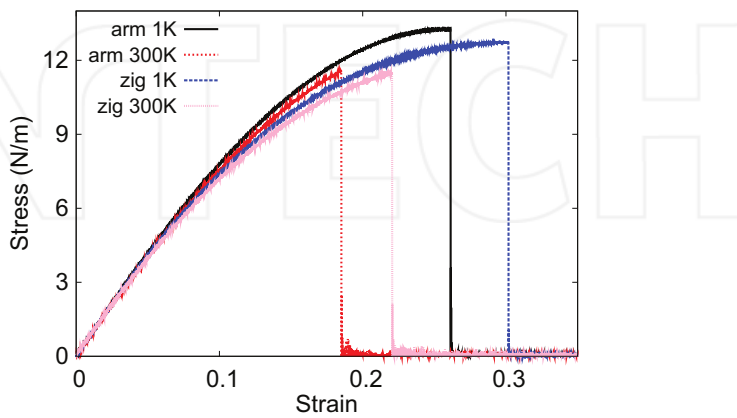
The angle θ_{ijk} in the first line indicates the bending energy for the angle with atom i as the apex.

Table 176. Three-body SW potential parameters for single-layer 1T-VS₂ used by GULP [8] as expressed in Eq. (4).

	ϵ (eV)	σ (Å)	a	λ	γ	$\cos \theta_0$	A_L	B_L	p	q	Tol
V—S ₁ —S ₁	1.000	1.048	2.946	31.659	1.000	0.100	7.943	11.797	4	0	0.0

Table 177. SW potential parameters for single-layer 1T-VS₂ used by LAMMPS [9] as expressed in Eqs. (9) and (10).

We use LAMMPS to perform MD simulations for the mechanical behavior of the single-layer 1T-VS₂ under uniaxial tension at 1 and 300 K. **Figure 87** shows the stress-strain curve for the tension of a single-layer 1T-VS₂ of dimension 100 × 100 Å. Periodic boundary conditions are applied in both armchair and zigzag directions. The single-layer 1T-VS₂ is stretched uniaxially along the armchair or zigzag direction. The stress is calculated without involving the actual thickness of the quasi-two-dimensional structure of the single-layer 1T-VS₂. The Young's modulus can be obtained by a linear fitting of the stress-strain relation in the small strain range of [0, 0.01]. The Young's modulus is 87.1 and 86.8 N/m along the armchair and zigzag directions, respectively. The Young's modulus is essentially isotropic in the armchair and zigzag directions. The Poisson's ratio from the VFF model and the SW potential is $\nu_{xy} = \nu_{yx} = 0.21$.

**Figure 87.** Stress-strain for single-layer 1T-VS₂ of dimension 100 × 100 Å along the armchair and zigzag directions.

There is no available value for nonlinear quantities in the single-layer 1T-VSe₂. We have thus used the nonlinear parameter $B = 0.5d^4$ in Eq. (5), which is close to the value of B in most materials. The value of the third-order nonlinear elasticity D can be extracted by fitting the stress-strain relation to the function $\sigma = E\epsilon + \frac{1}{2}D\epsilon^2$ with E as the Young's modulus. The values of D from the present SW potential are -230.5 and -283.6 N/m along the armchair and zigzag directions, respectively. The ultimate stress is about 13.3 N/m at the ultimate strain of 0.26 in the armchair direction at the low temperature of 1 K. The ultimate stress is about 12.7 N/m at the ultimate strain of 0.30 in the zigzag direction at the low temperature of 1 K.

45. 1T-VSe₂

Most existing theoretical studies on the single-layer 1T-VSe₂ are based on the first-principles calculations. In this section, we will develop the SW potential for the single-layer 1T-VSe₂.

The structure for the single-layer 1T-VSe₂ is shown in **Figure 71** (with M = V and X = Se). Each V atom is surrounded by six Se atoms. These Se atoms are categorized into the top group (e.g., atoms 1, 3, and 5) and bottom group (e.g., atoms 2, 4, and 6). Each Se atom is connected to three V atoms. The structural parameters are from the first-principles calculations [12], including the lattice constant $a = 3.24$ Å and the bond length $d_{V-Se} = 2.44$ Å. The resultant angles are $\theta_{VSeSe} = 83.201^\circ$ with Se atoms from the same (top or bottom) group and $\theta_{SeVV} = 83.201^\circ$.

Table 178 shows three VFF terms for the single-layer 1T-VSe₂; one of which is the bond stretching interaction shown by Eq. (1), while the other two terms are the angle bending interaction shown by Eq. (2). We note that the angle bending term $K_{V-Se-Se}$ is for the angle $\theta_{V-Se-Se}$ with both Se atoms from the same (top or bottom) group. These force constant parameters are determined by fitting to the three acoustic branches in the phonon dispersion along the Γ M as shown in **Figure 88(a)**. The *ab initio* calculations for the phonon dispersion are from [12]. The lowest acoustic branch (flexural mode) is almost linear in the *ab initio* calculations, which may be due to the violation of the rigid rotational invariance [20]. **Figure 88(b)** shows that the VFF model and the SW potential give exactly the same phonon dispersion, as the SW potential is derived from the VFF model.

VFF type	Bond stretching	Angle bending	
Expression	$\frac{1}{2}K_{V-Se}(\Delta r)^2$	$\frac{1}{2}K_{V-Se-Se}(\Delta\theta)^2$	$\frac{1}{2}K_{Se-V-V}(\Delta\theta)^2$
Parameter	11.562	4.237	4.237
r_0 or θ_0	2.440	83.201	83.201

The second line gives an explicit expression for each VFF term. The third line is the force constant parameters. Parameters are in the unit of eV/Å² for the bond stretching interaction and in the unit of eV for the angle bending interaction. The fourth line gives the initial bond length (in the unit of Å) for the bond stretching interaction and the initial angle (in the unit of degrees) for the angle bending interaction. The angle θ_{ijk} has atom i as the apex.

Table 178. The VFF model for single-layer 1T-VSe₂.

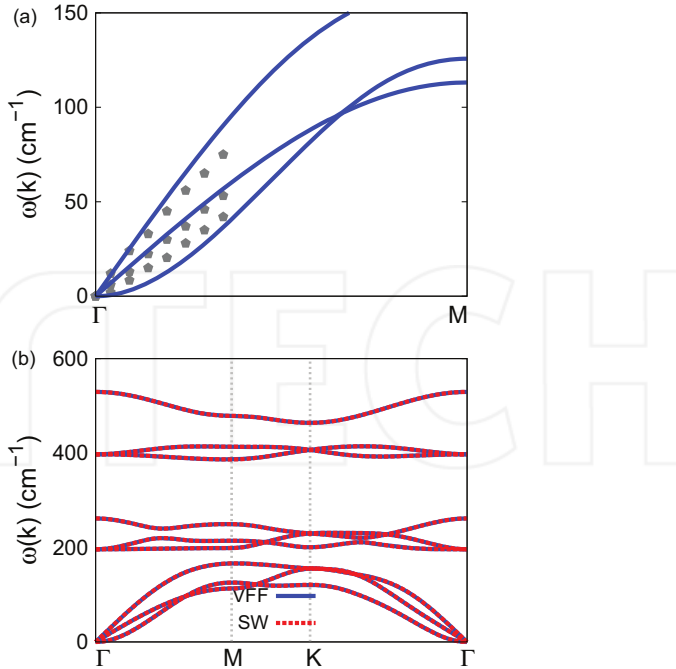


Figure 88. Phonon spectrum for single-layer 1T-VSe₂. (a) Phonon dispersion along the FM direction in the Brillouin zone. The results from the VFF model (lines) are comparable with the experiment data (pentagons) from [12]. (b) The phonon dispersion from the SW potential is exactly the same as that from the VFF model.

The parameters for the two-body SW potential used by GULP are shown in **Table 179**. The parameters for the three-body SW potential used by GULP are shown in **Table 180**. Some representative parameters for the SW potential used by LAMMPS are listed in **Table 181**.

We use LAMMPS to perform MD simulations for the mechanical behavior of the single-layer 1T-VSe₂ under uniaxial tension at 1 and 300 K. **Figure 89** shows the stress-strain curve for the tension of a single-layer 1T-VSe₂ of dimension 100 × 100 Å. Periodic boundary conditions are

	A (eV)	ρ (Å)	B (Å)	r_{\min} (Å)	r_{\max} (Å)
V—Se	8.606	1.070	17.723	0.0	3.248

Table 179. Two-body SW potential parameters for single-layer 1T-VSe₂ used by GULP [8] as expressed in Eq. (3).

	K (eV)	θ_0 (°)	ρ_1 (Å)	ρ_2 (Å)	$r_{\min12}$ (Å)	$r_{\max12}$ (Å)	$r_{\min13}$ (Å)	$r_{\max13}$ (Å)	$r_{\min23}$ (Å)	$r_{\max23}$ (Å)
$\theta_{\text{V}-\text{Se}-\text{Se}}$	30.387	83.201	1.070	1.070	0.0	3.248	0.0	3.248	0.0	4.426
$\theta_{\text{Se}-\text{V}-\text{V}}$	30.387	83.201	1.070	1.070	0.0	3.248	0.0	3.248	0.0	4.426

The angle θ_{ijk} in the first line indicates the bending energy for the angle with atom i as the apex.

Table 180. Three-body SW potential parameters for single-layer 1T-VSe₂ used by GULP [8] as expressed in Eq. (4).

	ϵ (eV)	σ (\AA)	a	λ	γ	$\cos \theta_0$	A_L	B_L	p	q	Tol
V—Se ₁ —Se ₁	1.000	1.070	3.035	30.387	1.000	0.118	8.606	13.507	4	0	0.0

Table 181. SW potential parameters for single-layer 1T-VSe₂ used by LAMMPS [9] as expressed in Eqs. (9) and (10).

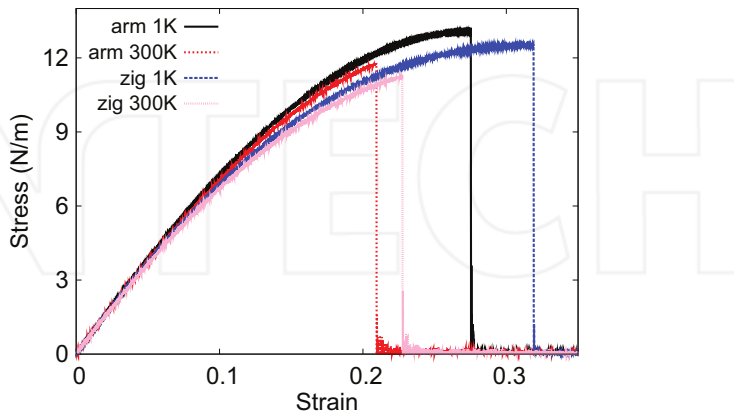


Figure 89. Stress-strain for single-layer 1T-VSe₂ of dimension $100 \times 100 \text{ \AA}$ along the armchair and zigzag directions.

applied in both armchair and zigzag directions. The single-layer 1T-VSe₂ is stretched uniaxially along the armchair or zigzag direction. The stress is calculated without involving the actual thickness of the quasi-two-dimensional structure of the single-layer 1T-VSe₂. The Young's modulus can be obtained by a linear fitting of the stress-strain relation in the small strain range of $[0, 0.01]$. The Young's modulus is 78.4 and 78.1 N/m along the armchair and zigzag directions, respectively. The Young's modulus is essentially isotropic in the armchair and zigzag directions. The Poisson's ratio from the VFF model and the SW potential is $\nu_{xy} = \nu_{yx} = 0.22$.

There is no available value for nonlinear quantities in the single-layer 1T-VSe₂. We have thus used the nonlinear parameter $B = 0.5d^4$ in Eq. (5), which is close to the value of B in most materials. The value of the third-order nonlinear elasticity D can be extracted by fitting the stress-strain relation to the function $\sigma = E\epsilon + \frac{1}{2}D\epsilon^2$ with E as the Young's modulus. The values of D from the present SW potential are -168.5 and -218.6 N/m along the armchair and zigzag directions, respectively. The ultimate stress is about 13.1 N/m at the ultimate strain of 0.27 in the armchair direction at the low temperature of 1 K. The ultimate stress is about 12.5 N/m at the ultimate strain of 0.32 in the zigzag direction at the low temperature of 1 K.

46. 1T-VTe₂

Most existing theoretical studies on the single-layer 1T-VTe₂ are based on the first-principles calculations. In this section, we will develop the SW potential for the single-layer 1T-VTe₂.

The structure for the single-layer 1T-VTe₂ is shown in **Figure 71** (with M = V and X = Te). Each V atom is surrounded by six Te atoms. These Te atoms are categorized into the top group (e.g., atoms 1, 3, and 5) and bottom group (e.g., atoms 2, 4, and 6). Each Te atom is connected to three V atoms. The structural parameters are from the first-principles calculations [12], including the lattice constant $a = 3.46 \text{ \AA}$ and the bond length $d_{V-Te} = 2.64 \text{ \AA}$. The resultant angles are $\theta_{VTeTe} = 81.885^\circ$ with Te atoms from the same (top or bottom) group and $\theta_{TeVV} = 81.885^\circ$.

Table 182 shows three VFF terms for the single-layer 1T-VTe₂; one of which is the bond stretching interaction shown by Eq. (1), while the other two terms are the angle bending interaction shown by Eq. (2). We note that the angle bending term $K_{V-Te-Te}$ is for the angle $\theta_{V-Te-Te}$ with both Te atoms from the same (top or bottom) group. We find that there are actually only two parameters in the VFF model, so we can determine their value by fitting to the Young's modulus and the Poisson's ratio of the system. The *ab initio* calculations have predicted the Young's modulus to be 67 N/m and the Poisson's ratio as 0.24 [48].

The parameters for the two-body SW potential used by GULP are shown in **Table 183**. The parameters for the three-body SW potential used by GULP are shown in **Table 184**. Some representative parameters for the SW potential used by LAMMPS are listed in **Table 185**.

VFF type	Bond stretching	Angle bending	
Expression	$\frac{1}{2}K_{V-Te}(\Delta r)^2$	$\frac{1}{2}K_{V-Te-Te}(\Delta\theta)^2$	$\frac{1}{2}K_{Te-V-V}(\Delta\theta)^2$
Parameter	10.476	3.814	3.814
r_0 or θ_0	2.640	81.885	81.885

The third line is the force constant parameters. Parameters are in the unit of eV/Å² for the bond stretching interaction and in the unit of eV for the angle bending interaction. The fourth line gives the initial bond length (in the unit of Å) for the bond stretching interaction and the initial angle (in the unit of degrees) for the angle bending interaction. The angle θ_{ijk} has atom i as the apex.

Table 182. The VFF model for single-layer 1T-VTe₂. The second line gives an explicit expression for each VFF term.

	A (eV)	ρ (Å)	B (Å ⁴)	r_{\min} (Å)	r_{\max} (Å)
V—Te	8.805	1.110	24.288	0.0	3.496

Table 183. Two-body SW potential parameters for single-layer 1T-VTe₂ used by GULP [8] as expressed in Eq. (3).

	K (eV)	θ_0 (°)	ρ_1 (Å)	ρ_2 (Å)	$r_{\min12}$ (Å)	$r_{\max12}$ (Å)	$r_{\min13}$ (Å)	$r_{\max13}$ (Å)	$r_{\min23}$ (Å)	$r_{\max23}$ (Å)
$\theta_{V-Te-Te}$	26.043	81.885	1.110	1.110	0.0	3.496	0.0	3.496	0.0	4.726
θ_{Te-V-V}	26.043	81.885	1.110	1.110	0.0	3.496	0.0	3.496	0.0	4.726

The angle θ_{ijk} in the first line indicates the bending energy for the angle with atom i as the apex.

Table 184. Three-body SW potential parameters for single-layer 1T-VTe₂ used by GULP [8] as expressed in Eq. (4).

	ϵ (eV)	σ (\AA)	a	λ	γ	$\cos \theta_0$	A_L	B_L	p	q	Tol
V—Te ₁ —Te ₁	1.000	1.110	3.149	26.043	1.000	0.141	8.805	15.980	4	0	0.0

Table 185. SW potential parameters for single-layer 1T-VTe₂ used by LAMMPS [9] as expressed in Eqs. (9) and (10).

We use LAMMPS to perform MD simulations for the mechanical behavior of the single-layer 1T-VTe₂ under uniaxial tension at 1 and 300 K. **Figure 90** shows the stress-strain curve for the tension of a single-layer 1T-VTe₂ of dimension 100 × 100 Å. Periodic boundary conditions are applied in both armchair and zigzag directions. The single-layer 1T-VTe₂ is stretched uniaxially along the armchair or zigzag direction. The stress is calculated without involving the actual thickness of the quasi-two-dimensional structure of the single-layer 1T-VTe₂. The Young's modulus can be obtained by a linear fitting of the stress-strain relation in the small strain range of [0, 0.01]. The Young's modulus is 61.2 and 61.0 N/m along the armchair and zigzag directions, respectively. The Young's modulus is essentially isotropic in the armchair and zigzag directions. The Poisson's ratio from the VFF model and the SW potential is $\nu_{xy} = \nu_{yx} = 0.24$. The fitted Young's modulus value is about 10% smaller than the *ab initio* result of 67 N/m [48], as only short-range interactions are considered in the present work. The long-range interactions are ignored, which typically leads to about 10% underestimation for the value of the Young's modulus.

There is no available value for nonlinear quantities in the single-layer 1T-VTe₂. We have thus used the nonlinear parameter $B = 0.5d^4$ in Eq. (5), which is close to the value of B in most materials. The value of the third-order nonlinear elasticity D can be extracted by fitting the stress-strain relation to the function $\sigma = E\epsilon + \frac{1}{2}D\epsilon^2$ with E as the Young's modulus. The values of D from the present SW potential are -95.8 and -135.6 N/m along the armchair and zigzag directions, respectively. The ultimate stress is about 11.5 N/m at the ultimate strain of 0.30 in the armchair direction at the low temperature of 1 K. The ultimate stress is about 11.0 N/m at the ultimate strain of 0.34 in the zigzag direction at the low temperature of 1 K.

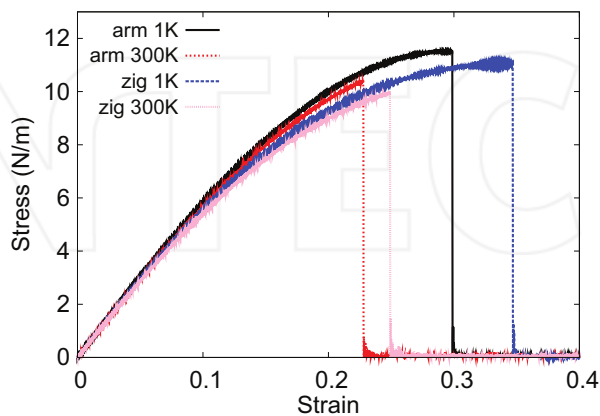


Figure 90. Stress-strain for single-layer 1T-VTe₂ of dimension 100 × 100 Å along the armchair and zigzag directions.

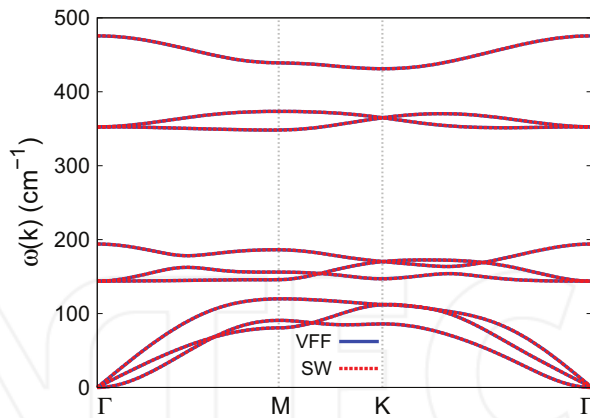


Figure 91. Phonon spectrum for single-layer 1T-VTe₂ along the Γ MK Γ direction in the Brillouin zone. The phonon dispersion from the SW potential is exactly the same as that from the VFF model.

Figure 91 shows that the VFF model and the SW potential give exactly the same phonon dispersion, as the SW potential is derived from the VFF model.

47. 1T-MnO₂

Most existing theoretical studies on the single-layer 1T-MnO₂ are based on the first-principles calculations. In this section, we will develop the SW potential for the single-layer 1T-MnO₂.

The structure for the single-layer 1T-MnO₂ is shown in **Figure 71** (with M = Mn and X = O). Each Mn atom is surrounded by six O atoms. These O atoms are categorized into the top group (e.g., atoms 1, 3, and 5) and bottom group (e.g., atoms 2, 4, and 6). Each O atom is connected to three Mn atoms. The structural parameters are from the first-principles calculations [12], including the lattice constant $a = 2.82 \text{ \AA}$ and the bond length $d_{\text{Mn-O}} = 1.88 \text{ \AA}$. The resultant angles are $\theta_{\text{MnOO}} = 97.181^\circ$ with O atoms from the same (top or bottom) group and $\theta_{\text{OMnMn}} = 97.181^\circ$.

Table 186 shows three VFF terms for the single-layer 1T-MnO₂; one of which is the bond stretching interaction shown by Eq. (1), while the other two terms are the angle bending interaction shown by Eq. (2). We note that the angle bending term $K_{\text{Mn-O-O}}$ is for the angle $\theta_{\text{Mn-O-O}}$ with both O atoms from the same (top or bottom) group. These force constant parameters are determined by fitting to the two in-plane acoustic branches in the phonon dispersion along the Γ M as shown in **Figure 92(a)**. The *ab initio* calculations for the phonon dispersion are from [12]. **Figure 92(b)** shows that the VFF model and the SW potential give exactly the same phonon dispersion, as the SW potential is derived from the VFF model.

The parameters for the two-body SW potential used by GULP are shown in **Table 187**. The parameters for the three-body SW potential used by GULP are shown in **Table 188**. Some representative parameters for the SW potential used by LAMMPS are listed in **Table 189**.

VFF type	Bond stretching	Angle bending
Expression	$\frac{1}{2}K_{\text{Mn-O}}(\Delta r)^2$	$\frac{1}{2}K_{\text{Mn-O-O}}(\Delta\theta)^2$
Parameter	15.371	4.822
r_0 or θ_0	1.88	97.181

The second line gives an explicit expression for each VFF term. The third line is the force constant parameters. Parameters are in the unit of eV/Å² for the bond stretching interaction and in the unit of eV for the angle bending interaction. The fourth line gives the initial bond length (in the unit of Å) for the bond stretching interaction and the initial angle (in the unit of degrees) for the angle bending interaction. The angle θ_{ijk} has atom i as the apex.

Table 186. The VFF model for single-layer 1T-MnO₂.

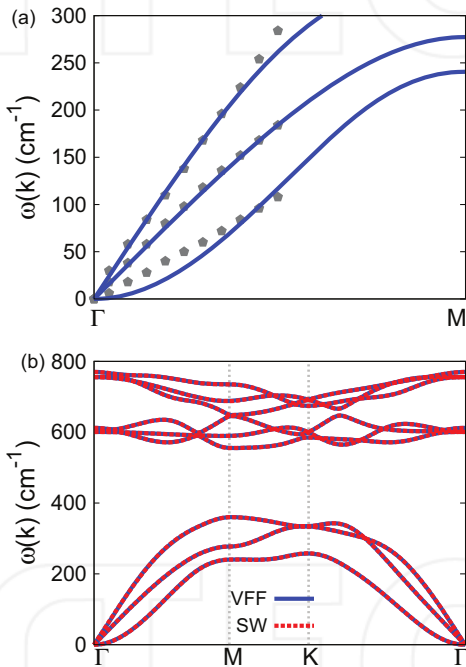


Figure 92. Phonon spectrum for single-layer 1T-MnO₂. (a) Phonon dispersion along the Γ M direction in the Brillouin zone. The results from the VFF model (lines) are comparable with the *ab initio* results (pentagons) from [12]. (b) The phonon dispersion from the SW potential is exactly the same as that from the VFF model.

	A (eV)	ρ (Å)	B (Å ⁴)	r_{\min} (Å)	r_{\max} (Å)
Mn—O	9.675	1.212	6.246	0.0	2.635

Table 187. Two-body SW potential parameters for single-layer 1T-MnO₂ used by GULP [8] as expressed in Eq. (3).

	K (eV)	θ_0 ($^\circ$)	ρ_1 (\AA)	ρ_2 (\AA)	$r_{\min 12}$ (\AA)	$r_{\max 12}$ (\AA)	$r_{\min 13}$ (\AA)	$r_{\max 13}$ (\AA)	$r_{\min 23}$ (\AA)	$r_{\max 23}$ (\AA)
$\theta_{\text{Mn-O-O}}$	60.755	97.181	1.212	1.212	0.0	2.635	0.0	2.635	0.0	3.852
$\theta_{\text{O-Mn-Mn}}$	60.755	97.181	1.212	1.212	0.0	2.635	0.0	2.635	0.0	3.852

The angle θ_{ijk} in the first line indicates the bending energy for the angle with atom i as the apex.

Table 188. Three-body SW potential parameters for single-layer 1T-MnO₂ used by GULP [8] as expressed in Eq. (4).

	ϵ (eV)	σ (\AA)	a	λ	γ	$\cos \theta_0$	A_L	B_L	p	q	Tol
Mn—O ₁ —O ₁	1.000	1.212	2.175	60.755	1.000	-0.125	9.675	2.899	4	0	0.0

Table 189. SW potential parameters for single-layer 1T-MnO₂ used by LAMMPS [9] as expressed in Eqs. (9) and (10).

We use LAMMPS to perform MD simulations for the mechanical behavior of the single-layer 1T-MnO₂ under uniaxial tension at 1 and 300 K. **Figure 93** shows the stress-strain curve for the tension of a single-layer 1T-MnO₂ of dimension 100 × 100 Å. Periodic boundary conditions are applied in both armchair and zigzag directions. The single-layer 1T-MnO₂ is stretched uniaxially along the armchair or zigzag direction. The stress is calculated without involving the actual thickness of the quasi-two-dimensional structure of the single-layer 1T-MnO₂. The Young's modulus can be obtained by a linear fitting of the stress-strain relation in the small strain range of [0, 0.01]. The Young's modulus is 156.3 and 155.4 N/m along the armchair and zigzag directions, respectively. The Young's modulus is essentially isotropic in the armchair and zigzag directions. The Poisson's ratio from the VFF model and the SW potential is $\nu_{xy} = \nu_{yx} = 0.12$.

There is no available value for nonlinear quantities in the single-layer 1T-MnO₂. We have thus used the nonlinear parameter $B = 0.5d^4$ in Eq. (5), which is close to the value of B in most materials. The value of the third-order nonlinear elasticity D can be extracted by fitting the

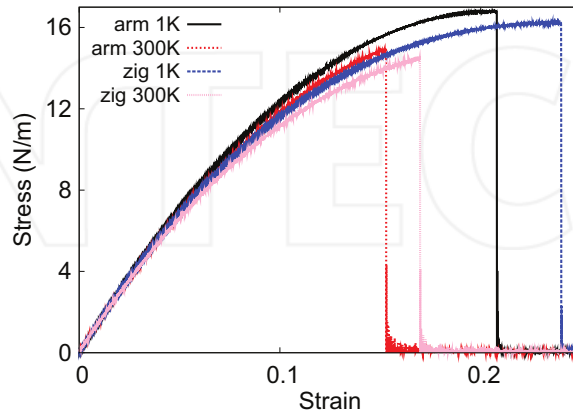


Figure 93. Stress-strain for single-layer 1T-MnO₂ of dimension 100 × 100 Å along the armchair and zigzag directions.

stress-strain relation to the function $\sigma = E\epsilon + \frac{1}{2}D\epsilon^2$ with E as the Young's modulus. The values of D from the present SW potential are -711.7 and -756.1 N/m along the armchair and zigzag directions, respectively. The ultimate stress is about 16.8 N/m at the ultimate strain of 0.21 in the armchair direction at the low temperature of 1 K. The ultimate stress is about 16.2 N/m at the ultimate strain of 0.24 in the zigzag direction at the low temperature of 1 K.

48. 1T-MnS₂

Most existing theoretical studies on the single-layer 1T-MnS₂ are based on the first-principles calculations. In this section, we will develop the SW potential for the single-layer 1T-MnS₂.

The structure for the single-layer 1T-MnS₂ is shown in **Figure 71** (with M = Mn and X = S). Each Mn atom is surrounded by six S atoms. These S atoms are categorized into the top group (e.g., atoms 1, 3, and 5) and bottom group (e.g., atoms 2, 4, and 6). Each S atom is connected to three Mn atoms. The structural parameters are from the first-principles calculations [12], including the lattice constant $a = 3.12$ Å and the bond length $d_{\text{Mn-S}} = 2.27$ Å. The resultant angles are $\theta_{\text{MnSS}} = 86.822^\circ$ with S atoms from the same (top or bottom) group and $\theta_{\text{SMnMn}} = 86.822^\circ$.

Table 190 shows three VFF terms for the single-layer 1T-MnS₂; one of which is the bond stretching interaction shown by Eq. (1), while the other two terms are the angle bending interaction shown by Eq. (2). We note that the angle bending term $K_{\text{Mn-S-S}}$ is for the angle $\theta_{\text{Mn-S-S}}$ with both S atoms from the same (top or bottom) group. These force constant parameters are determined by fitting to the acoustic branches in the phonon dispersion along the ΓM as shown in **Figure 94(a)**. The *ab initio* calculations for the phonon dispersion are from [12]. **Figure 94(b)** shows that the VFF model and the SW potential give exactly the same phonon dispersion, as the SW potential is derived from the VFF model.

The parameters for the two-body SW potential used by GULP are shown in **Table 191**. The parameters for the three-body SW potential used by GULP are shown in **Table 192**. Some representative parameters for the SW potential used by LAMMPS are listed in **Table 193**.

We use LAMMPS to perform MD simulations for the mechanical behavior of the single-layer 1T-MnS₂ under uniaxial tension at 1 and 300 K. **Figure 95** shows the stress-strain curve for the

VFF type	Bond stretching	Angle bending	
Expression	$\frac{1}{2}K_{\text{Mn-S}}(\Delta r)^2$	$\frac{1}{2}K_{\text{Mn-S-S}}(\Delta\theta)^2$	$\frac{1}{2}K_{\text{S-Mn-Mn}}(\Delta\theta)^2$
Parameter	4.407	2.399	2.399
r_0 or θ_0	2.27	86.822	86.822

The second line gives an explicit expression for each VFF term. The third line is the force constant parameters. Parameters are in the unit of eV/Å² for the bond stretching interaction and in the unit of eV for the angle bending interaction. The fourth line gives the initial bond length (in the unit of Å) for the bond stretching interaction and the initial angle (in the unit of degrees) for the angle bending interaction. The angle θ_{ijk} has atom i as the apex.

Table 190. The VFF model for single-layer 1T-MnS₂.

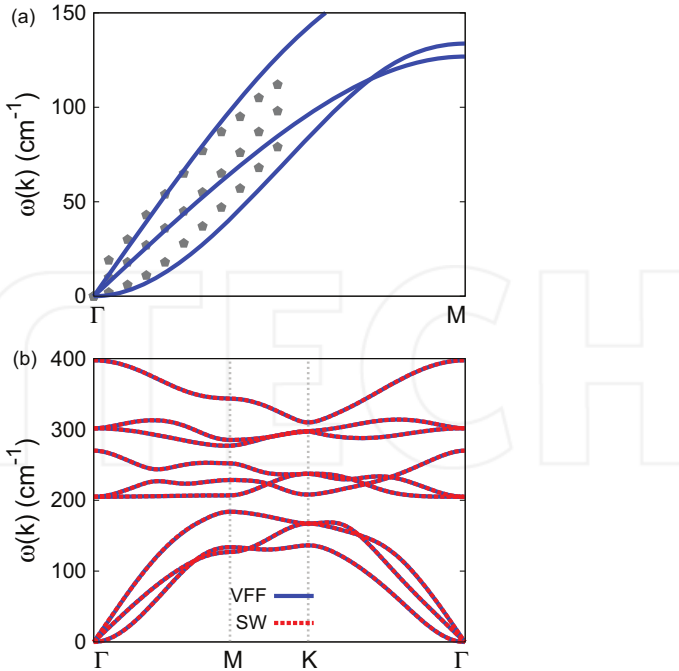


Figure 94. Phonon spectrum for single-layer 1T-MnS₂. (a) Phonon dispersion along the Γ M direction in the Brillouin zone. The results from the VFF model (lines) are comparable with the *ab initio* results (pentagons) from [12]. (b) The phonon dispersion from the SW potential is exactly the same as that from the VFF model.

	A (eV)	ρ (Å)	B (Å ⁴)	r_{\min} (Å)	r_{\max} (Å)
Mn—S	3.127	1.111	13.276	0.0	3.064

Table 191. Two-body SW potential parameters for single-layer 1T-MnS₂ used by GULP [8] as expressed in Eq. (3).

	K (eV)	θ_0 (°)	ρ_1 (Å)	ρ_2 (Å)	$r_{\min 12}$ (Å)	$r_{\max 12}$ (Å)	$r_{\min 13}$ (Å)	$r_{\max 13}$ (Å)	$r_{\min 23}$ (Å)	$r_{\max 23}$ (Å)
$\theta_{\text{Mn-S-S}}$	19.765	86.822	1.111	1.111	0.0	3.064	0.0	3.064	0.0	4.262
$\theta_{\text{S-Mn-Mn}}$	19.765	86.822	1.111	1.111	0.0	3.064	0.0	3.064	0.0	4.262

The angle θ_{ijk} in the first line indicates the bending energy for the angle with atom i as the apex.

Table 192. Three-body SW potential parameters for single-layer 1T-MnS₂ used by GULP [8] as expressed in Eq. (4).

	ϵ (eV)	σ (Å)	a	λ	γ	$\cos \theta_0$	A_L	B_L	p	q	Tol
Mn—S ₁ —S ₁	1.000	1.111	2.757	19.765	1.000	0.055	3.127	8.700	4	0	0.0

Table 193. SW potential parameters for single-layer 1T-MnS₂ used by LAMMPS [9] as expressed in Eqs. (9) and (10).

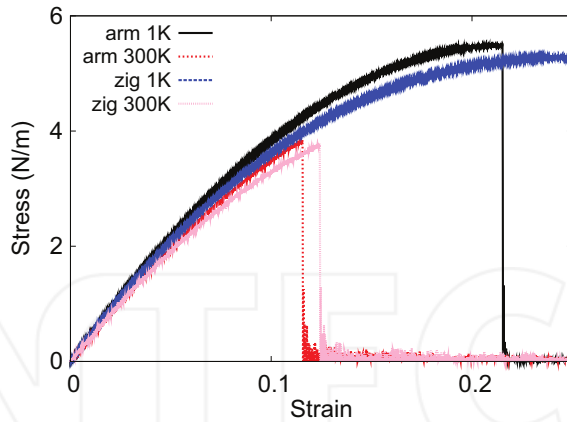


Figure 95. Stress-strain for single-layer 1T-MnS₂ of dimension 100 × 100 Å along the armchair and zigzag directions.

tension of a single-layer 1T-MnS₂ of dimension 100 × 100 Å. Periodic boundary conditions are applied in both armchair and zigzag directions. The single-layer 1T-MnS₂ is stretched uniaxially along the armchair or zigzag direction. The stress is calculated without involving the actual thickness of the quasi-two-dimensional structure of the single-layer 1T-MnS₂. The Young's modulus can be obtained by a linear fitting of the stress-strain relation in the small strain range of [0, 0.01]. The Young's modulus is 47.1 and 46.8 N/m along the armchair and zigzag directions, respectively. The Young's modulus is essentially isotropic in the armchair and zigzag directions. The Poisson's ratio from the VFF model and the SW potential is $\nu_{xy} = \nu_{yx} = 0.15$.

There is no available value for nonlinear quantities in the single-layer 1T-MnS₂. We have thus used the nonlinear parameter $B = 0.5d^4$ in Eq. (5), which is close to the value of B in most materials. The value of the third-order nonlinear elasticity D can be extracted by fitting the stress-strain relation to the function $\sigma = E\epsilon + \frac{1}{2}D\epsilon^2$ with E as the Young's modulus. The values of D from the present SW potential are -193.8 and -210.1 N/m along the armchair and zigzag directions, respectively. The ultimate stress is about 5.5 N/m at the ultimate strain of 0.21 in the armchair direction at the low temperature of 1 K. The ultimate stress is about 5.3 N/m at the ultimate strain of 0.25 in the zigzag direction at the low temperature of 1 K.

49. 1T-MnSe₂

Most existing theoretical studies on the single-layer 1T-MnSe₂ are based on the first-principles calculations. In this section, we will develop the SW potential for the single-layer 1T-MnSe₂.

The structure for the single-layer 1T-MnSe₂ is shown in **Figure 71** (with M = Mn and X = Se). Each Mn atom is surrounded by six Se atoms. These Se atoms are categorized into the top group (e.g., atoms 1, 3, and 5) and bottom group (e.g., atoms 2, 4, and 6). Each Se atom is

connected to three Mn atoms. The structural parameters are from the first-principles calculations [12], including the lattice constant $a = 3.27 \text{ \AA}$ and the bond length $d_{\text{Mn-Se}} = 2.39 \text{ \AA}$. The resultant angles are $\theta_{\text{MnSeSe}} = 86.330^\circ$ with Se atoms from the same (top or bottom) group and $\theta_{\text{SeMnMn}} = 86.330^\circ$.

Table 194 shows three VFF terms for the single-layer 1T-MnSe₂; one of which is the bond stretching interaction shown by Eq. (1), while the other two terms are the angle bending interaction shown by Eq. (2). We note that the angle bending term $K_{\text{Mn-Se-Se}}$ is for the angle $\theta_{\text{Mn-Se-Se}}$ with both Se atoms from the same (top or bottom) group. These force constant parameters are determined by fitting to the acoustic branches in the phonon dispersion along the ΓM as shown in **Figure 96(a)**. The *ab initio* calculations for the phonon dispersion are from [12]. **Figure 96(b)** shows that the VFF model and the SW potential give exactly the same phonon dispersion, as the SW potential is derived from the VFF model.

The parameters for the two-body SW potential used by GULP are shown in **Table 195**. The parameters for the three-body SW potential used by GULP are shown in **Table 196**. Some representative parameters for the SW potential used by LAMMPS are listed in **Table 197**.

We use LAMMPS to perform MD simulations for the mechanical behavior of the single-layer 1T-MnSe₂ under uniaxial tension at 1 and 300 K. **Figure 97** shows the stress-strain curve for the tension of a single-layer 1T-MnSe₂ of dimension $100 \times 100 \text{ \AA}$. Periodic boundary conditions are applied in both armchair and zigzag directions. The single-layer 1T-MnSe₂ is stretched uniaxially along the armchair or zigzag direction. The stress is calculated without involving the actual thickness of the quasi-two-dimensional structure of the single-layer 1T-MnSe₂. The Young's modulus can be obtained by a linear fitting of the stress-strain relation in the small strain range of $[0, 0.01]$. The Young's modulus is 43.2 and 42.9 N/m along the armchair and zigzag directions, respectively. The Young's modulus is essentially isotropic in the armchair and zigzag directions. The Poisson's ratio from the VFF model and the SW potential is $\nu_{xy} = \nu_{yx} = 0.17$.

There is no available value for nonlinear quantities in the single-layer 1T-MnSe₂. We have thus used the nonlinear parameter $B = 0.5d^4$ in Eq. (5), which is close to the value of B in most materials. The value of the third-order nonlinear elasticity D can be extracted by fitting the stress-strain relation to the function $\sigma = E\epsilon + \frac{1}{2}D\epsilon^2$ with E as the Young's modulus. The values

VFF type	Bond stretching	Angle bending	
Expression	$\frac{1}{2}K_{\text{Mn-Se}}(\Delta r)^2$	$\frac{1}{2}K_{\text{Mn-Se-Se}}(\Delta\theta)^2$	$\frac{1}{2}K_{\text{Se-Mn-Mn}}(\Delta\theta)^2$
Parameter	4.407	2.399	2.399
r_0 or θ_0	2.39	86.330	86.330

The second line gives an explicit expression for each VFF term. The third line is the force constant parameters. Parameters are in the unit of eV/ \AA^2 for the bond stretching interaction and in the unit of eV for the angle bending interaction. The fourth line gives the initial bond length (in the unit of \AA) for the bond stretching interaction and the initial angle (in the unit of degrees) for the angle bending interaction. The angle θ_{ijk} has atom i as the apex.

Table 194. The VFF model for single-layer 1T-MnSe₂.

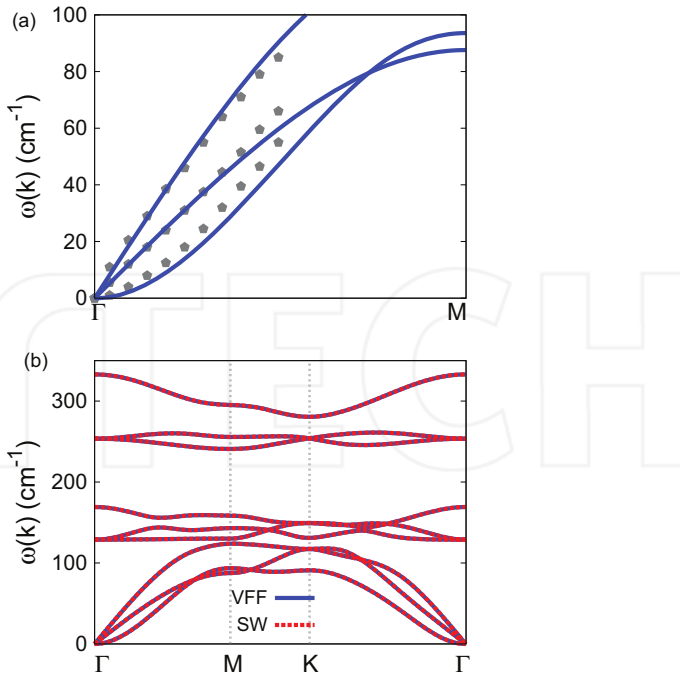


Figure 96. Phonon spectrum for single-layer 1T-MnSe₂. (a) Phonon dispersion along the TM direction in the Brillouin zone. The results from the VFF model (lines) are comparable with the *ab initio* results (pentagons) from [12]. (b) The phonon dispersion from the SW potential is exactly the same as that from the VFF model.

	A (eV)	ρ (Å)	B (Å ⁴)	r_{\min} (Å)	r_{\max} (Å)
Mn—Se	3.422	1.153	16.314	0.0	3.220

Table 195. Two-body SW potential parameters for single-layer 1T-MnSe₂ used by GULP [8] as expressed in Eq. (3).

	K (eV)	θ_0 (°)	ρ_1 (Å)	ρ_2 (Å)	$r_{\min 12}$ (Å)	$r_{\max 12}$ (Å)	$r_{\min 13}$ (Å)	$r_{\max 13}$ (Å)	$r_{\min 23}$ (Å)	$r_{\max 23}$ (Å)
$\theta_{\text{Mn—Se—Se}}$	19.390	86.330	1.153	1.153	0.0	3.220	0.0	3.220	0.0	4.467
$\theta_{\text{Se—Mn—Mn}}$	19.390	86.330	1.153	1.153	0.0	3.220	0.0	3.220	0.0	4.467

The angle θ_{ijk} in the first line indicates the bending energy for the angle with atom *i* as the apex.

Table 196. Three-body SW potential parameters for single-layer 1T-MnSe₂ used by GULP [8] as expressed in Eq. (4).

	ϵ (eV)	σ (Å)	a	λ	γ	$\cos \theta_0$	A_L	B_L	p	q	Tol
Mn—Se ₁ —Se ₁	1.000	1.153	2.792	19.390	1.000	0.064	3.422	9.219	4	0	0.0

Table 197. SW potential parameters for single-layer 1T-MnSe₂ used by LAMMPS [9] as expressed in Eqs. (9) and (10).

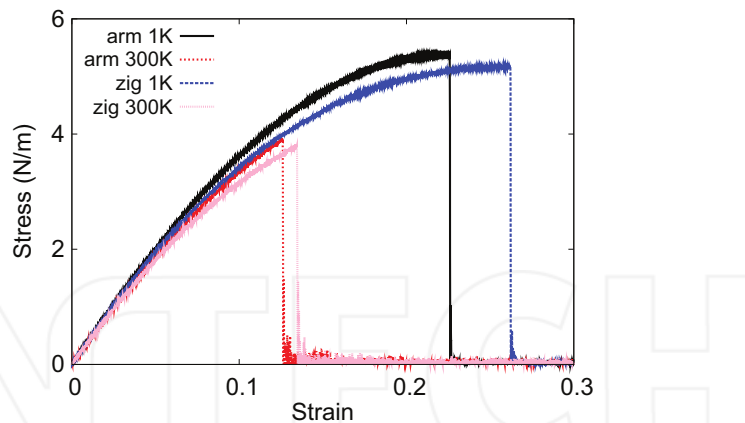


Figure 97. Stress-strain for single-layer 1T-MnSe₂ of dimension 100 × 100 Å along the armchair and zigzag directions.

of D from the present SW potential are -163.4 and -179.4 N/m along the armchair and zigzag directions, respectively. The ultimate stress is about 5.4 N/m at the ultimate strain of 0.22 in the armchair direction at the low temperature of 1 K. The ultimate stress is about 5.2 N/m at the ultimate strain of 0.26 in the zigzag direction at the low temperature of 1 K.

50. 1T-MnTe₂

Most existing theoretical studies on the single-layer 1T-MnTe₂ are based on the first-principles calculations. In this section, we will develop the SW potential for the single-layer 1T-MnTe₂.

The structure for the single-layer 1T-MnTe₂ is shown in **Figure 71** (with M = Mn and X = Te). Each Mn atom is surrounded by six Te atoms. These Te atoms are categorized into the top group (e.g., atoms 1, 3, and 5) and bottom group (e.g., atoms 2, 4, and 6). Each Te atom is connected to three Mn atoms. The structural parameters are from the first-principles calculations [12], including the lattice constant $a = 3.54$ Å and the bond length $d_{\text{Mn}-\text{Te}} = 2.59$ Å. The resultant angles are $\theta_{\text{MnTeTe}} = 86.219^\circ$ with Te atoms from the same (top or bottom) group and $\theta_{\text{TeMnMn}} = 86.219^\circ$.

Table 198 shows three VFF terms for the single-layer 1T-MnTe₂; one of which is the bond stretching interaction shown by Eq. (1), while the other two terms are the angle bending interaction shown by Eq. (2). We note that the angle bending term $K_{\text{Mn}-\text{Te}-\text{Te}}$ is for the angle $\theta_{\text{Mn}-\text{Te}-\text{Te}}$ with both Se atoms from the same (top or bottom) group. These force constant parameters are determined by fitting to the acoustic branches in the phonon dispersion along the ΓM as shown in **Figure 98(a)**. The *ab initio* calculations for the phonon dispersion are from [12]. **Figure 98(b)** shows that the VFF model and the SW potential give exactly the same phonon dispersion, as the SW potential is derived from the VFF model.

VFF type	Bond stretching	Angle bending
Expression	$\frac{1}{2} K_{\text{Mn}-\text{Te}}(\Delta r)^2$	$\frac{1}{2} K_{\text{Mn}-\text{Te}-\text{Te}}(\Delta\theta)^2$
Parameter	4.407	2.399
r_0 or θ_0	2.59	86.219

The second line gives an explicit expression for each VFF term. The third line is the force constant parameters. Parameters are in the unit of eV/Å² for the bond stretching interaction and in the unit of eV for the angle bending interaction. The fourth line gives the initial bond length (in the unit of Å) for the bond stretching interaction and the initial angle (in the unit of degrees) for the angle bending interaction. The angle θ_{ijk} has atom i as the apex.

Table 198. The VFF model for single-layer 1T-MnTe₂.

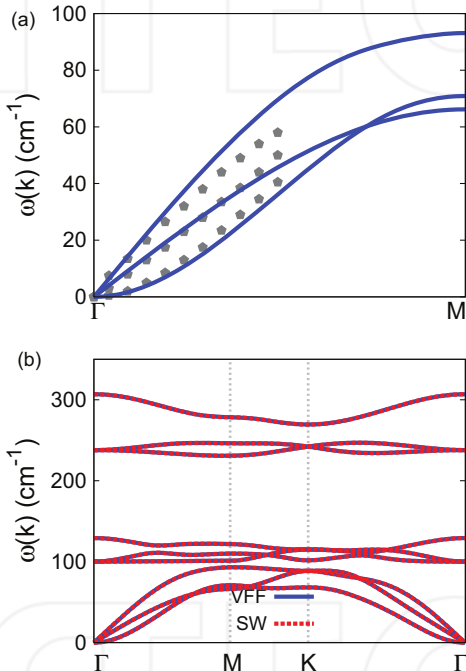


Figure 98. Phonon spectrum for single-layer 1T-MnTe₂. (a) Phonon dispersion along the Γ M direction in the Brillouin zone. The results from the VFF model (lines) are comparable with the *ab initio* results (pentagons) from [12]. (b) The phonon dispersion from the SW potential is exactly the same as that from the VFF model.

The parameters for the two-body SW potential used by GULP are shown in **Table 199**. The parameters for the three-body SW potential used by GULP are shown in **Table 200**. Some representative parameters for the SW potential used by LAMMPS are listed in **Table 201**.

We use LAMMPS to perform MD simulations for the mechanical behavior of the single-layer 1T-MnTe₂ under uniaxial tension at 1 and 300 K. **Figure 99** shows the stress-strain curve for the tension of a single-layer 1T-MnTe₂ of dimension 100 × 100 Å. Periodic boundary conditions are

	A (eV)	ρ (Å)	B (Å ⁴)	r_{\min} (Å)	r_{\max} (Å)
Mn—Te	4.007	1.246	22.499	0.0	3.488

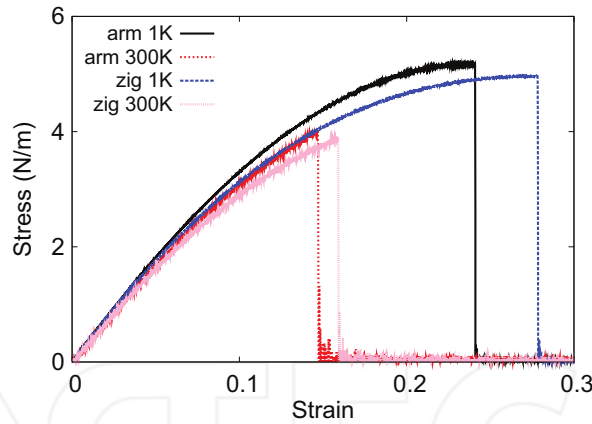
Table 199. Two-body SW potential parameters for single-layer 1T-MnTe₂ used by GULP [8] as expressed in Eq. (3).

	K (eV)	θ_0 (°)	ρ_1 (Å)	ρ_2 (Å)	$r_{\min 12}$ (Å)	$r_{\max 12}$ (Å)	$r_{\min 13}$ (Å)	$r_{\max 13}$ (Å)	$r_{\min 23}$ (Å)	$r_{\max 23}$ (Å)
$\theta_{\text{Mn—Te—Te}}$	19.307	86.219	1.246	1.246	0.0	3.488	0.0	3.488	0.0	4.836
$\theta_{\text{Te—Mn—Mn}}$	19.307	86.219	1.246	1.246	0.0	3.488	0.0	3.488	0.0	4.836

The angle θ_{ijk} in the first line indicates the bending energy for the angle with atom i as the apex.

Table 200. Three-body SW potential parameters for single-layer 1T-MnTe₂ used by GULP [8] as expressed in Eq. (4).

	ϵ (eV)	σ (Å)	a	λ	γ	$\cos \theta_0$	A_L	B_L	p	q	Tol
Mn—Te ₁ —Te ₁	1.000	1.246	2.800	19.307	1.000	0.066	4.007	9.340	4	0	0.0

Table 201. SW potential parameters for single-layer 1T-MnTe₂ used by LAMMPS [9] as expressed in Eqs. (9) and (10).**Figure 99.** Stress-strain for single-layer 1T-MnTe₂ of dimension 100 × 100 Å along the armchair and zigzag directions.

applied in both armchair and zigzag directions. The single-layer 1T-MnTe₂ is stretched uniaxially along the armchair or zigzag direction. The stress is calculated without involving the actual thickness of the quasi-two-dimensional structure of the single-layer 1T-MnTe₂. The Young's modulus can be obtained by a linear fitting of the stress-strain relation in the small strain range of [0, 0.01]. The Young's modulus is 38.5 and 38.4 N/m along the armchair and zigzag directions, respectively. The Young's modulus is essentially isotropic in the armchair and zigzag directions. The Poisson's ratio from the VFF model and the SW potential is $\nu_{xy} = \nu_{yx} = 0.19$.

There is no available value for nonlinear quantities in the single-layer 1T-MnTe₂. We have thus used the nonlinear parameter $B = 0.5d^4$ in Eq. (5), which is close to the value of B in most materials. The value of the third-order nonlinear elasticity D can be extracted by fitting the stress-strain relation to the function $\sigma = E\epsilon + \frac{1}{2}D\epsilon^2$ with E as the Young's modulus. The values of D from the present SW potential are -133.5 and -149.5 N/m along the armchair and zigzag directions, respectively. The ultimate stress is about 5.2 N/m at the ultimate strain of 0.24 in the armchair direction at the low temperature of 1 K. The ultimate stress is about 5.0 N/m at the ultimate strain of 0.28 in the zigzag direction at the low temperature of 1 K.

51. 1T-CoTe₂

Most existing theoretical studies on the single-layer 1T-CoTe₂ are based on the first-principles calculations. In this section, we will develop the SW potential for the single-layer 1T-CoTe₂.

The structure for the single-layer 1T-CoTe₂ is shown in **Figure 71** (with M = Co and X = Te). Each Co atom is surrounded by six Te atoms. These Te atoms are categorized into the top group (e.g., atoms 1, 3, and 5) and bottom group (e.g., atoms 2, 4, and 6). Each Te atom is connected to three Co atoms. The structural parameters are from the first-principles calculations [48], including the lattice constant $a = 3.5983$ Å and the bond length $d_{\text{Co}-\text{Te}} = 2.5117$ Å, which are derived from the angle $\theta_{\text{TeCoCo}} = 91.5^\circ$. The other angle is $\theta_{\text{CoTeTe}} = 91.5^\circ$ with Te atoms from the same (top or bottom) group.

Table 202 shows three VFF terms for the single-layer 1T-CoTe₂; one of which is the bond stretching interaction shown by Eq. (1), while the other two terms are the angle bending interaction shown by Eq. (2). We note that the angle bending term $K_{\text{Co}-\text{Te}-\text{Te}}$ is for the angle $\theta_{\text{Co}-\text{Te}-\text{Te}}$ with both Te atoms from the same (top or bottom) group. We find that there are actually only two parameters in the VFF model, so we can determine their value by fitting to the Young's modulus and the Poisson's ratio of the system. The *ab initio* calculations have predicted the Young's modulus to be 59 N/m and the Poisson's ratio as 0.14 [48].

The parameters for the two-body SW potential used by GULP are shown in **Table 203**. The parameters for the three-body SW potential used by GULP are shown in **Table 204**. Some representative parameters for the SW potential used by LAMMPS are listed in **Table 205**.

VFF type	Bond stretching	Angle bending	
Expression	$\frac{1}{2}K_{\text{Co}-\text{Te}}(\Delta r)^2$	$\frac{1}{2}K_{\text{Co}-\text{Te}-\text{Te}}(\Delta\theta)^2$	$\frac{1}{2}K_{\text{Te}-\text{Co}-\text{Co}}(\Delta\theta)^2$
Parameter	4.726	3.035	3.035
r_0 or θ_0	2.512	91.501	91.501

The second line gives an explicit expression for each VFF term. The third line is the force constant parameters. Parameters are in the unit of eV/Å² for the bond stretching interaction and in the unit of eV for the angle bending interaction. The fourth line gives the initial bond length (in the unit of Å) for the bond stretching interaction and the initial angle (in the unit of degrees) for the angle bending interaction. The angle θ_{ijk} has atom i as the apex.

Table 202. The VFF model for single-layer 1T-CoTe₂.

	A (eV)	ρ (Å)	B (Å ⁴)	r_{\min} (Å)	r_{\max} (Å)
Co—Te	4.628	1.402	19.899	0.0	3.450

Table 203. Two-body SW potential parameters for single-layer 1T-CoTe₂ used by GULP [8] as expressed in Eq. (3).

	K (eV)	θ_0 (°)	ρ_1 (Å)	ρ_2 (Å)	$r_{\min 12}$ (Å)	$r_{\max 12}$ (Å)	$r_{\min 13}$ (Å)	$r_{\max 13}$ (Å)	$r_{\min 23}$ (Å)	$r_{\max 23}$ (Å)
$\theta_{\text{Co}-\text{Te}-\text{Te}}$	30.149	91.501	1.402	1.402	0.0	3.450	0.0	3.450	0.0	4.915
$\theta_{\text{Te}-\text{Co}-\text{Co}}$	30.149	91.501	1.402	1.402	0.0	3.450	0.0	3.450	0.0	4.915

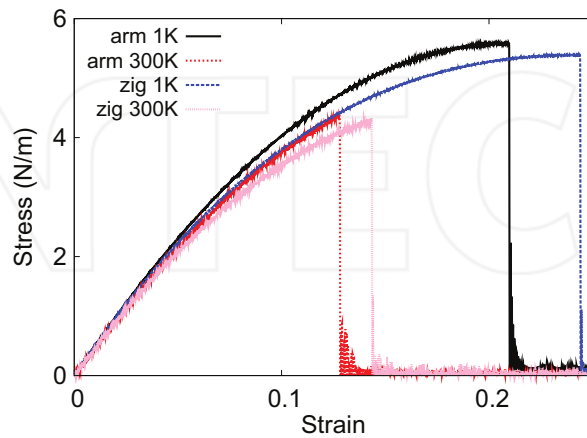
The angle θ_{ijk} in the first line indicates the bending energy for the angle with atom i as the apex.

Table 204. Three-body SW potential parameters for single-layer 1T-CoTe₂ used by GULP [8] as expressed in Eq. (4).

	ϵ (eV)	σ (Å)	a	λ	γ	$\cos \theta_0$	A_L	B_L	p	q	Tol
Co—Te ₁ —Te ₁	1.000	1.402	2.461	30.149	1.000	-0.026	4.628	5.151	4	0	0.0

Table 205. SW potential parameters for single-layer 1T-CoTe₂ used by LAMMPS [9] as expressed in Eqs. (9) and (10).

We use LAMMPS to perform MD simulations for the mechanical behavior of the single-layer 1T-CoTe₂ under uniaxial tension at 1 and 300 K. **Figure 100** shows the stress-strain curve for the tension of a single-layer 1T-CoTe₂ of dimension 100 × 100 Å. Periodic boundary conditions are applied in both armchair and zigzag directions. The single-layer 1T-CoTe₂ is stretched uniaxially along the armchair or zigzag direction. The stress is calculated without involving the actual thickness of the quasi-two-dimensional structure of the single-layer 1T-CoTe₂. The Young's modulus can be obtained by a linear fitting of the stress-strain relation in the small strain range of [0, 0.01]. The Young's modulus is 50.5 and 50.3 N/m along the armchair and zigzag directions, respectively. The Young's modulus is essentially isotropic in the armchair

**Figure 100.** Stress-strain for single-layer 1T-CoTe₂ of dimension 100 × 100 Å along the armchair and zigzag directions.

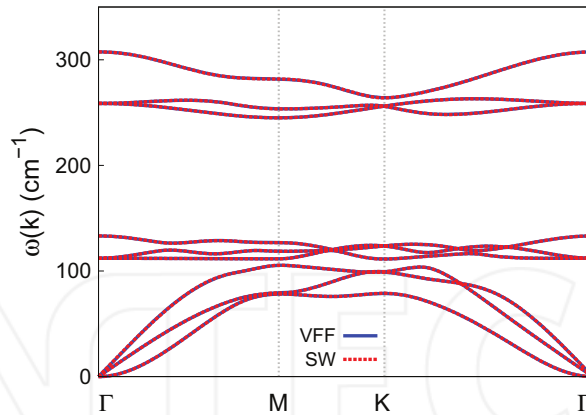


Figure 101. Phonon spectrum for single-layer 1T-CoTe₂ along the Γ MKG direction in the Brillouin zone. The phonon dispersion from the SW potential is exactly the same as that from the VFF model.

and zigzag directions. The Poisson's ratio from the VFF model and the SW potential is $\nu_{xy} = \nu_{yx} = 0.13$. The fitted Young's modulus value is about 10% smaller than the *ab initio* result of 59 N/m [48], as only short-range interactions are considered in the present work. The long-range interactions are ignored, which typically leads to about 10% underestimation for the value of the Young's modulus.

There is no available value for nonlinear quantities in the single-layer 1T-CoTe₂. We have thus used the nonlinear parameter $B = 0.5d^4$ in Eq. (5), which is close to the value of B in most materials. The value of the third-order nonlinear elasticity D can be extracted by fitting the stress-strain relation to the function $\sigma = E\epsilon + \frac{1}{2}D\epsilon^2$ with E as the Young's modulus. The values of D from the present SW potential are -221.5 and -238.3 N/m along the armchair and zigzag directions, respectively. The ultimate stress is about 5.6 N/m at the ultimate strain of 0.21 in the armchair direction at the low temperature of 1 K. The ultimate stress is about 5.4 N/m at the ultimate strain of 0.24 in the zigzag direction at the low temperature of 1 K.

Figure 101 shows that the VFF model and the SW potential give exactly the same phonon dispersion, as the SW potential is derived from the VFF model.

52. 1T-NiO₂

Most existing theoretical studies on the single-layer 1T-NiO₂ are based on the first-principles calculations. In this section, we will develop the SW potential for the single-layer 1T-NiO₂.

The structure for the single-layer 1T-NiO₂ is shown in **Figure 71** (with M = Ni and X = O). Each Ni atom is surrounded by six O atoms. These O atoms are categorized into the top group (e.g., atoms 1, 3, and 5) and bottom group (e.g., atoms 2, 4, and 6). Each O atom is connected to three

Ni atoms. The structural parameters are from the first-principles calculations [12], including the lattice constant $a = 2.77 \text{ \AA}$ and the bond length $d_{\text{Ni-O}} = 1.84 \text{ \AA}$. The resultant angles are $\theta_{\text{NiOO}} = 97.653^\circ$ with O atoms from the same (top or bottom) group and $\theta_{\text{ONiNi}} = 97.653^\circ$.

Table 206 shows three VFF terms for the single-layer 1T-NiO₂; one of which is the bond stretching interaction shown by Eq. (1), while the other two terms are the angle bending interaction shown by Eq. (2). We note that the angle bending term $K_{\text{Ni-O-O}}$ is for the angle $\theta_{\text{Ni-O-O}}$ with both O atoms from the same (top or bottom) group. These force constant parameters are determined by fitting to the two in-plane acoustic branches in the phonon dispersion along the ΓM as shown in **Figure 102(a)**. The *ab initio* calculations for the phonon dispersion are from [12]. **Figure 102(b)** shows that the VFF model and the SW potential give exactly the same phonon dispersion, as the SW potential is derived from the VFF model.

The parameters for the two-body SW potential used by GULP are shown in **Table 207**. The parameters for the three-body SW potential used by GULP are shown in **Table 208**. Some representative parameters for the SW potential used by LAMMPS are listed in **Table 209**.

We use LAMMPS to perform MD simulations for the mechanical behavior of the single-layer 1T-NiO₂ under uniaxial tension at 1 and 300 K. **Figure 103** shows the stress-strain curve for the tension of a single-layer 1T-NiO₂ of dimension $100 \times 100 \text{ \AA}$. Periodic boundary conditions are applied in both armchair and zigzag directions. The single-layer 1T-NiO₂ is stretched uniaxially along the armchair or zigzag direction. The stress is calculated without involving the actual thickness of the quasi-two-dimensional structure of the single-layer 1T-NiO₂. The Young's modulus can be obtained by a linear fitting of the stress-strain relation in the small strain range of [0, 0.01]. The Young's modulus is 163.3 and 162.4 N/m along the armchair and zigzag directions, respectively. The Young's modulus is essentially isotropic in the armchair and zigzag directions. The Poisson's ratio from the VFF model and the SW potential is $\nu_{xy} = \nu_{yx} = 0.12$.

There is no available value for nonlinear quantities in the single-layer 1T-NiO₂. We have thus used the nonlinear parameter $B = 0.5d^4$ in Eq. (5), which is close to the value of B in most materials. The value of the third-order nonlinear elasticity D can be extracted by fitting the stress-strain relation to the function $\sigma = E\epsilon + \frac{1}{2}D\epsilon^2$ with E as the Young's modulus. The values of D from the present SW potential are -748.7 and -796.0 N/m along the armchair and zigzag directions, respectively. The ultimate stress is about 17.4 N/m at the ultimate strain of 0.20 in

VFF type	Bond stretching	Angle bending	
Expression	$\frac{1}{2}K_{\text{Ni-O}}(\Delta r)^2$	$\frac{1}{2}K_{\text{Ni-O-O}}(\Delta\theta)^2$	$\frac{1}{2}K_{\text{O-Ni-Ni}}(\Delta\theta)^2$
Parameter	15.925	4.847	4.847
r_0 or θ_0		97.653	97.653

The third line is the force constant parameters. Parameters are in the unit of eV/ \AA^2 for the bond stretching interaction and in the unit of eV for the angle bending interaction. The fourth line gives the initial bond length (in the unit of \AA) for the bond stretching interaction and the initial angle (in the unit of degrees) for the angle bending interaction. The angle θ_{ijk} has atom i as the apex.

Table 206. The VFF model for single-layer 1T-NiO₂. The second line gives an explicit expression for each VFF term.

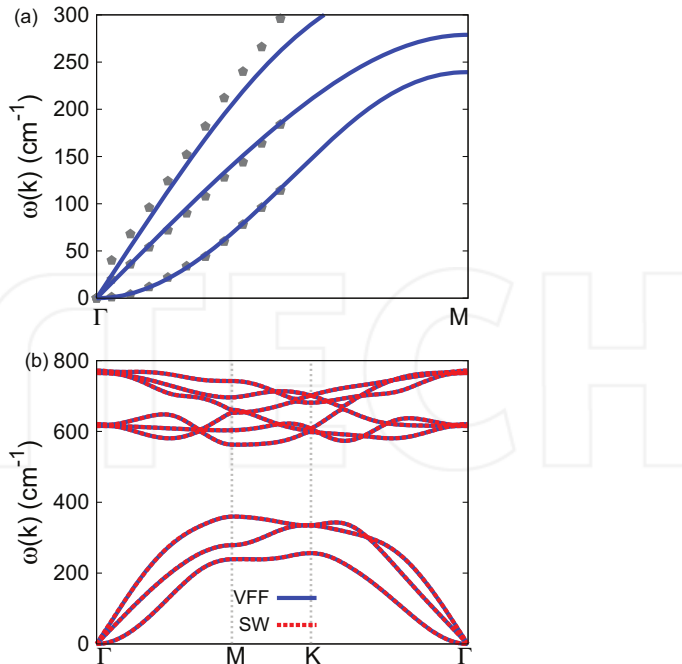


Figure 102. Phonon spectrum for single-layer 1T-NiO₂. (a) Phonon dispersion along the Γ M direction in the Brillouin zone. The results from the VFF model (lines) are comparable with the *ab initio* results (pentagons) from [12]. (b) The phonon dispersion from the SW potential is exactly the same as that from the VFF model.

	A (eV)	ρ Å	B Å ⁴	r_{\min} Å	r_{\max} Å
Ni-O	9.709	1.199	5.731	0.0	2.583

Table 207. Two-body SW potential parameters for single-layer 1T-NiO₂ used by GULP [8] as expressed in Eq. (3).

	K (eV)	θ_0 (°)	ρ_1 (Å)	ρ_2 (Å)	$r_{\min 12}$ (Å)	$r_{\max 12}$ (Å)	$r_{\min 13}$ (Å)	$r_{\max 13}$ (Å)	$r_{\min 23}$ (Å)	$r_{\max 23}$ (Å)
$\theta_{\text{Ni}-\text{O}-\text{O}}$	62.317	97.653	1.199	1.199	0.0	2.583	0.0	2.583	0.0	3.784
$\theta_{\text{O}-\text{Ni}-\text{Ni}}$	62.317	97.653	1.199	1.199	0.0	2.583	0.0	2.583	0.0	3.784

The angle θ_{ijk} in the first line indicates the bending energy for the angle with atom i as the apex.

Table 208. Three-body SW potential parameters for single-layer 1T-NiO₂ used by GULP [8] as expressed in Eq. (4).

	ϵ (eV)	σ (Å)	a	λ	γ	$\cos \theta_0$	A_L	B_L	p	q	Tol
Ni-O ₁ -O ₁	1.000	1.199	2.154	62.317	1.000	-0.133	9.709	2.772	4	0	0.0

Table 209. SW potential parameters for single-layer 1T-NiO₂ used by LAMMPS [9] as expressed in Eqs. (9) and (10).

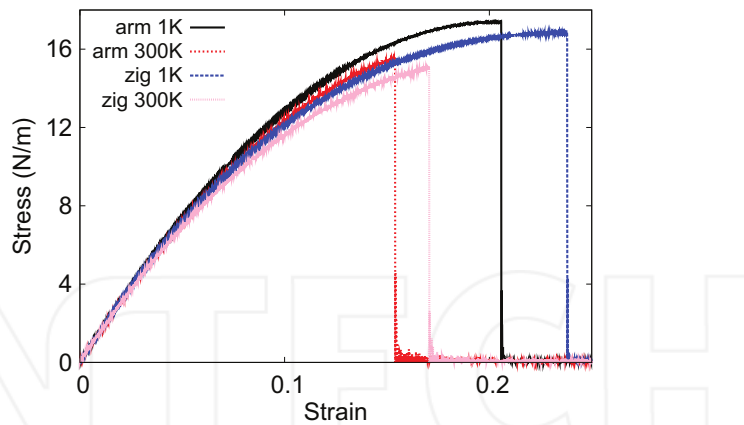


Figure 103. Stress-strain for single-layer 1T-NiO₂ of dimension 100 × 100 Å along the armchair and zigzag directions.

the armchair direction at the low temperature of 1 K. The ultimate stress is about 16.8 N/m at the ultimate strain of 0.24 in the zigzag direction at the low temperature of 1 K.

53. 1T-NiS₂

Most existing theoretical studies on the single-layer 1T-NiS₂ are based on the first-principles calculations. In this section, we will develop the SW potential for the single-layer 1T-NiS₂.

The structure for the single-layer 1T-NiS₂ is shown in **Figure 71** (with M = Ni and X = S). Each Ni atom is surrounded by six S atoms. These S atoms are categorized into the top group (e.g., atoms 1, 3, and 5) and bottom group (e.g., atoms 2, 4, and 6). Each S atom is connected to three Ni atoms. The structural parameters are from the first-principles calculations [48], including the lattice constant $a = 3.3174 \text{ \AA}$ and the bond length $d_{\text{Ni-S}} = 2.2320 \text{ \AA}$, which are derived from the angle $\theta_{\text{SNI}i} = 96^\circ$. The other angle is $\theta_{\text{NiSS}} = 96^\circ$ with S atoms from the same (top or bottom) group.

Table 210 shows three VFF terms for the single-layer 1T-NiS₂; one of which is the bond stretching interaction shown by Eq. (1), while the other two terms are the angle bending

VFF type	Bond stretching	Angle bending	
Expression	$\frac{1}{2}K_{\text{Ni-S}}(\Delta r)^2$	$\frac{1}{2}K_{\text{Ni-S-S}}(\Delta\theta)^2$	$\frac{1}{2}K_{\text{S-Ni-Ni}}(\Delta\theta)^2$
Parameter	9.385	2.952	2.952
r_0 or θ_0	2.232	96.000	96.000

The third line is the force constant parameters. Parameters are in the unit of eV/Å² for the bond stretching interaction and in the unit of eV for the angle bending interaction. The fourth line gives the initial bond length (in the unit of Å) for the bond stretching interaction and the initial angle (in the unit of degrees) for the angle bending interaction. The angle θ_{ijk} has atom *i* as the apex.

Table 210. The VFF model for single-layer 1T-NiS₂. The second line gives an explicit expression for each VFF term.

interaction shown by Eq. (2). We note that the angle bending term $K_{\text{Ni-S-S}}$ is for the angle $\theta_{\text{Ni-S-S}}$ with both S atoms from the same (top or bottom) group. These force constant parameters are determined by fitting to the two in-plane acoustic branches in the phonon dispersion along the $\Gamma\text{-M}$ as shown in **Figure 104(a)**. The *ab initio* calculations for the phonon dispersion are from [12]. **Figure 104(b)** shows that the VFF model and the SW potential give exactly the same phonon dispersion, as the SW potential is derived from the VFF model.

The parameters for the two-body SW potential used by GULP are shown in **Table 211**. The parameters for the three-body SW potential used by GULP are shown in **Table 212**. Some representative parameters for the SW potential used by LAMMPS are listed in **Table 213**.

We use LAMMPS to perform MD simulations for the mechanical behavior of the single-layer 1T-NiS₂ under uniaxial tension at 1 and 300 K. **Figure 105** shows the stress-strain curve for the tension of a single-layer 1T-NiS₂ of dimension 100 × 100 Å. Periodic boundary conditions are

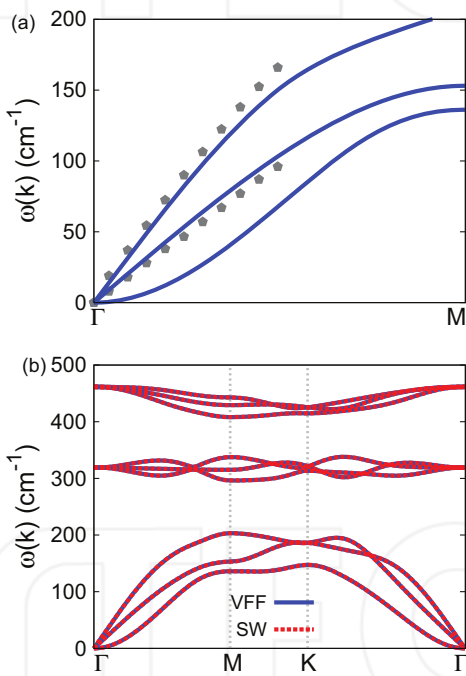


Figure 104. Phonon spectrum for single-layer 1T-NiS₂. (a) Phonon dispersion along the $\Gamma\text{-M}$ direction in the Brillouin zone. The results from the VFF model (lines) are comparable with the *ab initio* results (pentagons) from [12]. (b) The phonon dispersion from the SW potential is exactly the same as that from the VFF model.

	A (eV)	$\rho(\text{\AA})$	B (\AA^4)	$r_{\min} (\text{\AA})$	$r_{\max} (\text{\AA})$
Ni-S	8.098	1.398	12.409	0.0	3.115

Table 211. Two-body SW potential parameters for single-layer 1T-NiS₂ used by GULP [8] as expressed in Eq. (3).

	K (eV)	θ_0 ($^\circ$)	ρ_1 (\AA)	ρ_2 (\AA)	$r_{\min 12}$ (\AA)	$r_{\max 12}$ (\AA)	$r_{\min 13}$ (\AA)	$r_{\max 13}$ (\AA)	$r_{\min 23}$ (\AA)	$r_{\max 23}$ (\AA)
$\theta_{\text{Ni-S-S}}$	35.372	96.000	1.398	1.398	0.0	3.115	0.0	3.115	0.0	4.532
$\theta_{\text{S-Ni-Ni}}$	35.372	96.000	1.398	1.398	0.0	3.115	0.0	3.115	0.0	4.532

The angle θ_{ijk} in the first line indicates the bending energy for the angle with atom i as the apex.

Table 212. Three-body SW potential parameters for single-layer 1T-NiS₂ used by GULP [8] as expressed in Eq. (4).

	ϵ (eV)	σ (\AA)	a	λ	γ	$\cos \theta_0$	A_L	B_L	p	q	Tol
Ni—S ₁ —S ₁	1.000	1.398	2.228	35.372	1.000	-0.105	8.098	3.249	4	0	0.0

Table 213. SW potential parameters for single-layer 1T-NiS₂ used by LAMMPS [9] as expressed in Eqs. (9) and (10).

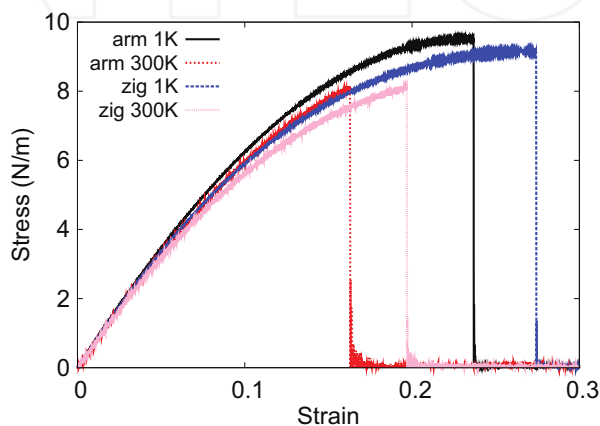


Figure 105. Stress-strain for single-layer 1T-NiS₂ of dimension $100 \times 100 \text{ \AA}$ along the armchair and zigzag directions.

applied in both armchair and zigzag directions. The single-layer 1T-NiS₂ is stretched uniaxially along the armchair or zigzag direction. The stress is calculated without involving the actual thickness of the quasi-two-dimensional structure of the single-layer 1T-NiS₂. The Young's modulus can be obtained by a linear fitting of the stress-strain relation in the small strain range of [0, 0.01]. The Young's modulus is 74.2 and 73.9 N/m along the armchair and zigzag directions, respectively. The Young's modulus is essentially isotropic in the armchair and zigzag directions. The Poisson's ratio from the VFF model and the SW potential is $\nu_{xy} = \nu_{yx} = 0.17$.

There is no available value for nonlinear quantities in the single-layer 1T-NiS₂. We have thus used the nonlinear parameter $B = 0.5d^4$ in Eq. (5), which is close to the value of B in most materials. The value of the third-order nonlinear elasticity D can be extracted by fitting the stress-strain relation to the function $\sigma = E\epsilon + \frac{1}{2}D\epsilon^2$ with E as the Young's modulus. The values of D from the present SW potential are -274.5 and -301.4 N/m along the armchair and zigzag directions, respectively. The ultimate stress is about 9.5 N/m at the ultimate strain of 0.23 in the

armchair direction at the low temperature of 1 K. The ultimate stress is about 9.2 N/m at the ultimate strain of 0.27 in the zigzag direction at the low temperature of 1 K.

54. 1T-NiSe₂

Most existing theoretical studies on the single-layer 1T-NiSe₂ are based on the first-principles calculations. In this section, we will develop the SW potential for the single-layer 1T-NiSe₂.

The structure for the single-layer 1T-NiSe₂ is shown in **Figure 71** (with M = Ni and X = Se). Each Ni atom is surrounded by six Se atoms. These Se atoms are categorized into the top group (e.g., atoms 1, 3, and 5) and bottom group (e.g., atoms 2, 4, and 6). Each Se atom is connected to three Ni atoms. The structural parameters are from the first-principles calculations [48], including the lattice constant $a = 3.4712 \text{ \AA}$ and the bond length $d_{\text{Ni-Se}} = 2.3392 \text{ \AA}$, which are derived from the angle $\theta_{\text{SeNiNi}} = 95.8^\circ$. The other angle is $\theta_{\text{NiSeSe}} = 95.8^\circ$ with Se atoms from the same (top or bottom) group.

Table 214 shows three VFF terms for the single-layer 1T-NiSe₂; one of which is the bond stretching interaction shown by Eq. (1), while the other two terms are the angle bending interaction shown by Eq. (2). We note that the angle bending term $K_{\text{Ni-Se-Se}}$ is for the angle $\theta_{\text{Ni-Se-Se}}$ with both Se atoms from the same (top or bottom) group. These force constant parameters are determined by fitting to the two in-plane acoustic branches in the phonon dispersion along the ΓM as shown in **Figure 106(a)**. The *ab initio* calculations for the phonon dispersion are from [12]. **Figure 106(b)** shows that the VFF model and the SW potential give exactly the same phonon dispersion, as the SW potential is derived from the VFF model.

The parameters for the two-body SW potential used by GULP are shown in **Table 215**. The parameters for the three-body SW potential used by GULP are shown in **Table 216**. Some representative parameters for the SW potential used by LAMMPS are listed in **Table 217**.

We use LAMMPS to perform MD simulations for the mechanical behavior of the single-layer 1T-NiSe₂ under uniaxial tension at 1 and 300 K. **Figure 107** shows the stress-strain curve for the tension of a single-layer 1T-NiSe₂ of dimension $100 \times 100 \text{ \AA}$. Periodic boundary conditions are applied in both armchair and zigzag directions. The single-layer 1T-NiSe₂ is stretched uniaxially along the armchair or zigzag direction. The stress is calculated without involving

VFF type	Bond stretching	Angle bending	
Expression	$\frac{1}{2} K_{\text{Ni-Se}} (\Delta r)^2$	$\frac{1}{2} K_{\text{Ni-Se-Se}} (\Delta \theta)^2$	$\frac{1}{2} K_{\text{Se-Ni-Ni}} (\Delta \theta)^2$
Parameter	8.814	3.149	3.149
r_0 or θ_0	2.339	95.798	95.798

The second line gives an explicit expression for each VFF term. The third line is the force constant parameters. Parameters are in the unit of eV/ \AA^2 for the bond stretching interaction and in the unit of eV for the angle bending interaction. The fourth line gives the initial bond length (in the unit of \AA) for the bond stretching interaction and the initial angle (in the unit of degrees) for the angle bending interaction. The angle θ_{ijk} has atom i as the apex.

Table 214. The VFF model for single-layer 1T-NiSe₂.

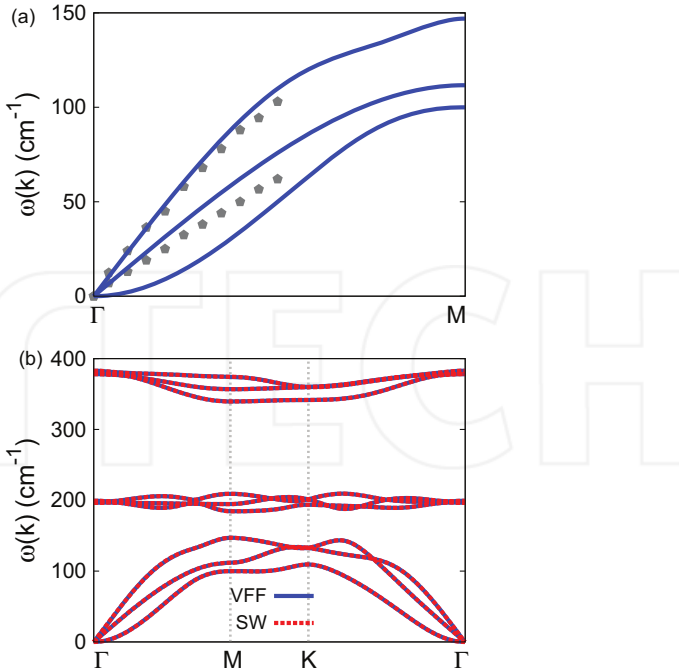


Figure 106. Phonon spectrum for single-layer 1T-NiSe₂. (a) Phonon dispersion along the Γ M direction in the Brillouin zone. The results from the VFF model (lines) are comparable with the *ab initio* results (pentagons) from [12]. (b) The phonon dispersion from the SW potential is exactly the same as that from the VFF model.

	A (eV)	ρ (Å)	B (Å ⁴)	r_{\min} (Å)	r_{\max} (Å)
Ni—Se	8.313	1.458	14.971	0.0	3.263

Table 215. Two-body SW potential parameters for single-layer 1T-NiSe₂ used by GULP [8] as expressed in Eq. (3).

	K (eV)	θ_0 (°)	ρ_1 (Å)	ρ_2 (Å)	$r_{\min 12}$ (Å)	$r_{\max 12}$ (Å)	$r_{\min 13}$ (Å)	$r_{\max 13}$ (Å)	$r_{\min 23}$ (Å)	$r_{\max 23}$ (Å)
$\theta_{\text{Ni—Se—Se}}$	37.407	95.798	1.458	1.458	0.0	3.263	0.0	3.263	0.0	4.742
$\theta_{\text{Se—Ni—Ni}}$	37.407	95.798	1.458	1.458	0.0	3.263	0.0	3.263	0.0	4.742

The angle θ_{ijk} in the first line indicates the bending energy for the angle with atom i as the apex.

Table 216. Three-body SW potential parameters for single-layer 1T-NiSe₂ used by GULP [8] as expressed in Eq. (4).

	ϵ (eV)	σ (Å)	a	λ	γ	$\cos \theta_0$	A_L	B_L	p	q	Tol
Ni—Se ₁ —Se ₁	1.000	1.458	2.238	37.407	1.000	-0.101	8.313	3.315	4	0	0.0

Table 217. SW potential parameters for single-layer 1T-NiSe₂ used by LAMMPS [9] as expressed in Eqs. (9) and (10).

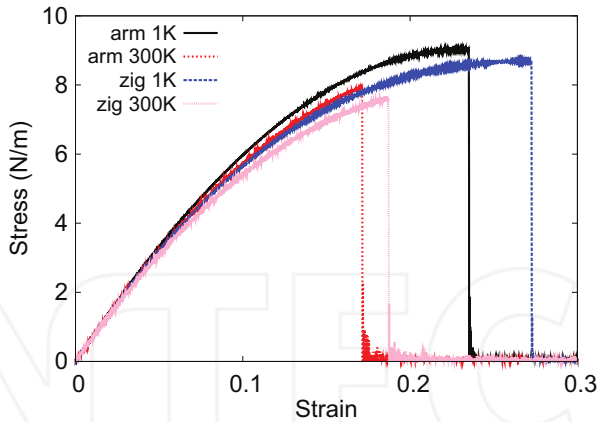


Figure 107. Stress-strain for single-layer 1T-NiSe₂ of dimension 100 × 100 Å along the armchair and zigzag directions.

the actual thickness of the quasi-two-dimensional structure of the single-layer 1T-NiSe₂. The Young's modulus can be obtained by a linear fitting of the stress-strain relation in the small strain range of [0, 0.01]. The Young's modulus is 70.9 and 70.6 N/m along the armchair and zigzag directions, respectively. The Young's modulus is essentially isotropic in the armchair and zigzag directions. The Poisson's ratio from the VFF model and the SW potential is $\nu_{xy} = \nu_{yx} = 0.17$.

There is no available value for nonlinear quantities in the single-layer 1T-NiSe₂. We have thus used the nonlinear parameter $B = 0.5d^4$ in Eq. (5), which is close to the value of B in most materials. The value of the third-order nonlinear elasticity D can be extracted by fitting the stress-strain relation to the function $\sigma = E\epsilon + \frac{1}{2}D\epsilon^2$ with E as the Young's modulus. The values of D from the present SW potential are -263.7 and -289.5 N/m along the armchair and zigzag directions, respectively. The ultimate stress is about 9.0 N/m at the ultimate strain of 0.23 in the armchair direction at the low temperature of 1 K. The ultimate stress is about 8.7 N/m at the ultimate strain of 0.27 in the zigzag direction at the low temperature of 1 K.

55. 1T-NiTe₂

Most existing theoretical studies on the single-layer 1T-NiTe₂ are based on the first-principles calculations. In this section, we will develop the SW potential for the single-layer 1T-NiTe₂.

The structure for the single-layer 1T-NiTe₂ is shown in **Figure 71** (with M = Ni and X = Te). Each Ni atom is surrounded by six Te atoms. These Te atoms are categorized into the top group (e.g., atoms 1, 3, and 5) and bottom group (e.g., atoms 2, 4, and 6). Each Te atom is connected to three Ni atoms. The structural parameters are from the first-principles calculations [48], including the lattice constant $a = 3.7248$ Å and the bond length $d_{Ni-Te} = 2.5321$ Å,

which are derived from the angle $\theta_{\text{TeNiNi}} = 94.7^\circ$. The other angle is $\theta_{\text{NiTeTe}} = 94.7^\circ$ with Te atoms from the same (top or bottom) group.

Table 218 shows three VFF terms for the single-layer 1T-NiTe₂; one of which is the bond stretching interaction shown by Eq. (1), while the other two terms are the angle bending interaction shown by Eq. (2). We note that the angle bending term $K_{\text{Ni}-\text{Te}-\text{Te}}$ is for the angle $\theta_{\text{Ni}-\text{Te}-\text{Te}}$ with both Te atoms from the same (top or bottom) group. We find that there are actually only two parameters in the VFF model, so we can determine their value by fitting to the Young's modulus and the Poisson's ratio of the system. The *ab initio* calculations have predicted the Young's modulus to be 44 N/m and the Poisson's ratio as 0.14 [48].

The parameters for the two-body SW potential used by GULP are shown in **Table 219**. The parameters for the three-body SW potential used by GULP are shown in **Table 220**. Some representative parameters for the SW potential used by LAMMPS are listed in **Table 221**.

VFF type	Bond stretching	Angle bending
Expression	$\frac{1}{2} K_{\text{Ni}-\text{Te}}(\Delta r)^2$	$\frac{1}{2} K_{\text{Ni}-\text{Te}-\text{Te}}(\Delta\theta)^2$
Parameter	4.230	2.429
r_0 or θ_0	2.532	94.702
or θ_0	2.635	95.999

The second line gives an explicit expression for each VFF term. The third line is the force constant parameters. Parameters are in the unit of eV/Å² for the bond stretching interaction and in the unit of eV for the angle bending interaction. The fourth line gives the initial bond length (in the unit of Å) for the bond stretching interaction and the initial angle (in the unit of degrees) for the angle bending interaction. The angle θ_{ijk} has atom *i* as the apex.

Table 218. The VFF model for single-layer 1T-NiTe₂.

	<i>A</i> (eV)	<i>p</i> (Å)	<i>B</i> (Å ⁴)	<i>r</i> _{min} (Å)	<i>r</i> _{max} (Å)
Ni—Te	4.554	1.536	20.554	0.0	3.518

Table 219. Two-body SW potential parameters for single-layer 1T-NiTe₂ used by GULP [8] as expressed in Eq. (3).

	<i>K</i> (eV)	θ_0 (°)	ρ_1 (Å)	ρ_2 (Å)	$r_{\min 12}$ (Å)	$r_{\max 12}$ (Å)	$r_{\min 13}$ (Å)	$r_{\max 13}$ (Å)	$r_{\min 23}$ (Å)	$r_{\max 23}$ (Å)
$\theta_{\text{Ni}-\text{Te}-\text{Te}}$	27.553	94.702	1.536	1.536	0.0	3.518	0.0	3.518	0.0	5.088
$\theta_{\text{Te}-\text{Ni}-\text{Ni}}$	27.553	94.702	1.536	1.536	0.0	3.518	0.0	3.518	0.0	5.088

The angle θ_{ijk} in the first line indicates the bending energy for the angle with atom *i* as the apex.

Table 220. Three-body SW potential parameters for single-layer 1T-NiTe₂ used by GULP [8] as expressed in Eq. (4).

	ϵ (eV)	σ (Å)	a	λ	γ	$\cos \theta_0$	A_L	B_L	p	q	Tol
Ni—Te ₁ —Te ₁	1.000	1.536	2.291	27.553	1.000	-0.082	4.554	3.696	4	0	0.0

Table 221. SW potential parameters for single-layer 1T-NiTe₂ used by LAMMPS [9] as expressed in Eqs. (9) and (10).

We use LAMMPS to perform MD simulations for the mechanical behavior of the single-layer 1T-NiTe₂ under uniaxial tension at 1 and 300 K. **Figure 108** shows the stress-strain curve for the tension of a single-layer 1T-NiTe₂ of dimension 100 × 100 Å. Periodic boundary conditions are applied in both armchair and zigzag directions. The single-layer 1T-NiTe₂ is stretched uniaxially along the armchair or zigzag direction. The stress is calculated without involving the actual thickness of the quasi-two-dimensional structure of the single-layer 1T-NiTe₂. The Young's modulus can be obtained by a linear fitting of the stress-strain relation in the small strain range of [0, 0.01]. The Young's modulus is 42.6 and 42.4 N/m along the armchair and zigzag directions, respectively. The Young's modulus is essentially isotropic in the armchair

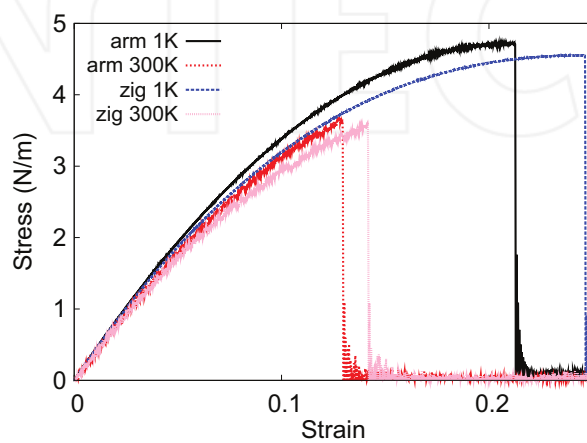


Figure 108. Stress-strain for single-layer 1T-NiTe₂ of dimension 100 × 100 Å along the armchair and zigzag directions.

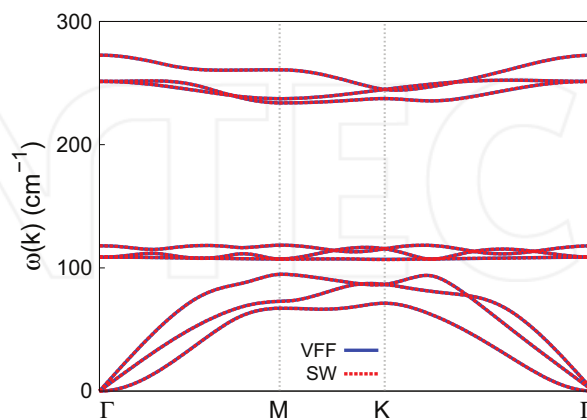


Figure 109. Phonon spectrum for single-layer 1T-NiTe₂ along the Γ -M-K- Γ direction in the Brillouin zone. The phonon dispersion from the SW potential is exactly the same as that from the VFF model.

and zigzag directions. The Poisson's ratio from the VFF model and the SW potential is $\nu_{xy} = \nu_{yx} = 0.14$.

There is no available value for nonlinear quantities in the single-layer 1T-NiTe₂. We have thus used the nonlinear parameter $B = 0.5d^4$ in Eq. (5), which is close to the value of B in most materials. The value of the third-order nonlinear elasticity D can be extracted by fitting the stress-strain relation to the function $\sigma = E\epsilon + \frac{1}{2}D\epsilon^2$ with E as the Young's modulus. The values of D from the present SW potential are -187.6 and -200.6 N/m along the armchair and zigzag directions, respectively. The ultimate stress is about 4.7 N/m at the ultimate strain of 0.21 in the armchair direction at the low temperature of 1 K. The ultimate stress is about 4.6 N/m at the ultimate strain of 0.24 in the zigzag direction at the low temperature of 1 K.

Figure 109 shows that the VFF model and the SW potential give exactly the same phonon dispersion, as the SW potential is derived from the VFF model.

56. 1T-ZrS₂

Most existing theoretical studies on the single-layer 1T-ZrS₂ are based on the first-principles calculations. In this section, we will develop the SW potential for the single-layer 1T-ZrS₂.

The structure for the single-layer 1T-ZrS₂ is shown in **Figure 71** (with M = Zr and X = S). Each Zr atom is surrounded by six S atoms. These S atoms are categorized into the top group (e.g., atoms 1, 3, and 5) and bottom group (e.g., atoms 2, 4, and 6). Each S atom is connected to three Zr atoms. The structural parameters are from the first-principles calculations [49], including the lattice constant $a = 3.690$ Å and the bond length $d_{Zr-S} = 2.58$ Å. The resultant angles are $\theta_{ZrSS} = 91.305^\circ$ with S atoms from the same (top or bottom) group and $\theta_{S Zr Zr} = 91.305^\circ$.

Table 222 shows three VFF terms for the single-layer 1T-ZrS₂; one of which is the bond stretching interaction shown by Eq. (1), while the other two terms are the angle bending interaction shown by Eq. (2). We note that the angle bending term K_{Zr-S-S} is for the angle θ_{Zr-S-S} with both S atoms from the same (top or bottom) group. These force constant parameters are determined by fitting to the three acoustic branches in the phonon dispersion along the Γ M as shown in **Figure 110(a)**. The *ab initio* calculations for the phonon dispersion are

VFF type	Bond stretching	Angle bending	
Expression	$\frac{1}{2}K_{Zr-S}(\Delta r)^2$	$\frac{1}{2}K_{Zr-S-S}(\Delta\theta)^2$	$\frac{1}{2}K_{S-Zr-Zr}(\Delta\theta)^2$
Parameter	7.930	4.283	4.283
r_0 or θ_0	2.580	91.305	91.305

The second line gives an explicit expression for each VFF term. The third line is the force constant parameters. Parameters are in the unit of eV/Å² for the bond stretching interaction and in the unit of eV for the angle bending interaction. The fourth line gives the initial bond length (in the unit of Å) for the bond stretching interaction and the initial angle (in the unit of degrees) for the angle bending interaction. The angle θ_{ijk} has atom i as the apex.

Table 222. The VFF model for single-layer 1T-ZrS₂.

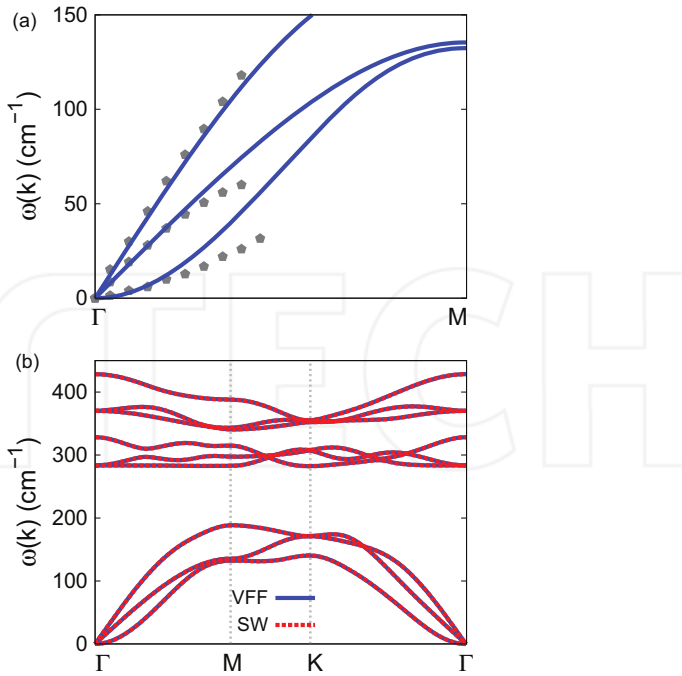


Figure 110. Phonon spectrum for single-layer 1T-ZrS₂. (a) Phonon dispersion along the TM direction in the Brillouin zone. The results from the VFF model (lines) are comparable with the experiment data (pentagons) from [38]. (b) The phonon dispersion from the SW potential is exactly the same as that from the VFF model.

from [38]. Similar phonon dispersion can also be found in other *ab initio* calculations [34]. **Figure 110(b)** shows that the VFF model and the SW potential give exactly the same phonon dispersion, as the SW potential is derived from the VFF model.

The parameters for the two-body SW potential used by GULP are shown in **Table 223**. The parameters for the three-body SW potential used by GULP are shown in **Table 224**. Some representative parameters for the SW potential used by LAMMPS are listed in **Table 225**.

We use LAMMPS to perform MD simulations for the mechanical behavior of the single-layer 1T-ZrS₂ under uniaxial tension at 1 and 300 K. **Figure 111** shows the stress-strain curve for the tension of a single-layer 1T-ZrS₂ of dimension 100 × 100 Å. Periodic boundary conditions are applied in both armchair and zigzag directions. The single-layer 1T-ZrS₂ is stretched uniaxially along the armchair or zigzag direction. The stress is calculated without involving the actual thickness of the quasi-two-dimensional structure of the single-layer 1T-ZrS₂. The Young's

	A (eV)	ρ (Å)	B (Å ⁴)	r_{\min} (Å)	r_{\max} (Å)
Zr-S	8.149	1.432	22.154	0.0	3.541

Table 223. Two-body SW potential parameters for single-layer 1T-ZrS₂ used by GULP [8] as expressed in Eq. (3).

	K (eV)	θ_0 ($^\circ$)	ρ_1 (\AA)	ρ_2 (\AA)	$r_{\min 12}$ (\AA)	$r_{\max 12}$ (\AA)	$r_{\min 13}$ (\AA)	$r_{\max 13}$ (\AA)	$r_{\min 23}$ (\AA)	$r_{\max 23}$ (\AA)
$\theta_{\text{Zr-S-S}}$	42.170	91.305	1.432	1.432	0.0	3.541	0.0	3.541	0.0	5.041
$\theta_{\text{S-Zr-Zr}}$	42.170	91.305	1.432	1.432	0.0	3.541	0.0	3.541	0.0	5.041

The angle θ_{ijk} in the first line indicates the bending energy for the angle with atom i as the apex.

Table 224. Three-body SW potential parameters for single-layer 1T-ZrS₂ used by GULP [8] as expressed in Eq. (4).

	ϵ (eV)	σ (\AA)	a	λ	γ	$\cos \theta_0$	A_L	B_L	p	q	Tol
Zr—S1—S1	1.000	1.432	2.473	42.177	1.000	-0.023	8.149	5.268	4	0	0.0
S1—Zr—Zr	1.000	1.432	2.473	42.177	1.000	-0.023	8.149	5.268	4	0	0.0

Table 225. SW potential parameters for single-layer 1T-ZrS₂ used by LAMMPS [9] as expressed in Eqs. (9) and (10).

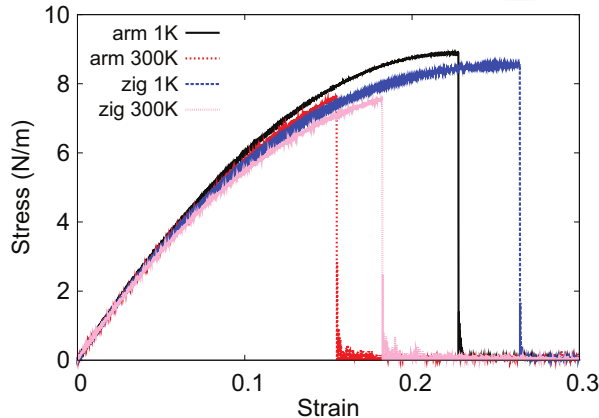


Figure 111. Stress-strain for single-layer 1T-ZrS₂ of dimension 100 \times 100 \AA along the armchair and zigzag directions.

modulus can be obtained by a linear fitting of the stress-strain relation in the small strain range of [0, 0.01]. The Young's modulus is 71.8 and 71.5 N/m along the armchair and zigzag directions, respectively. The Young's modulus is essentially isotropic in the armchair and zigzag directions. These values are close to the *ab initio* results at 0 K temperature, e.g., 75.74 N/m in [49]. The Poisson's ratio from the VFF model and the SW potential is $\nu_{xy} = \nu_{yx} = 0.16$, which are comparable with the *ab initio* result [49] of 0.22.

There is no available value for nonlinear quantities in the single-layer 1T-ZrS₂. We have thus used the nonlinear parameter $B = 0.5d^4$ in Eq. (5), which is close to the value of B in most materials. The value of the third-order nonlinear elasticity D can be extracted by fitting the stress-strain relation to the function $\sigma = E\epsilon + \frac{1}{2}D\epsilon^2$ with E as the Young's modulus. The values of D from the present SW potential are -268.9 and -305.2 N/m along the armchair and zigzag directions, respectively. The ultimate stress is about 8.9 N/m at the ultimate strain of 0.23 in the

armchair direction at the low temperature of 1 K. The ultimate stress is about 8.5 N/m at the ultimate strain of 0.26 in the zigzag direction at the low temperature of 1 K.

57. 1T-ZrSe₂

Most existing theoretical studies on the single-layer 1T-ZrSe₂ are based on the first-principles calculations. In this section, we will develop the SW potential for the single-layer 1T-ZrSe₂.

The structure for the single-layer 1T-ZrSe₂ is shown in **Figure 71** (with M = Zr and X = Se). Each Zr atom is surrounded by six Se atoms. These Se atoms are categorized into the top group (e.g., atoms 1, 3, and 5) and bottom group (e.g., atoms 2, 4, and 6). Each Se atom is connected to three Zr atoms. The structural parameters are from the first-principles calculations [51], including the lattice constant $a = 3.707 \text{ \AA}$ and the position of the Se atom with respect to the Zr atomic plane $h = 1.591 \text{ \AA}$. The resultant angles are $\theta_{\text{ZrSeSe}} = 88.058^\circ$ with Se atoms from the same (top or bottom) group and $\theta_{\text{SeZrZr}} = 88.058^\circ$.

Table 226 shows three VFF terms for the single-layer 1T-ZrSe₂; one of which is the bond stretching interaction shown by Eq. (1), while the other two terms are the angle bending interaction shown by Eq. (2). We note that the angle bending term $K_{\text{Zr-Se-Se}}$ is for the angle $\theta_{\text{Zr-Se-Se}}$ with both Se atoms from the same (top or bottom) group. These force constant parameters are determined by fitting to the three acoustic branches in the phonon dispersion along the ΓM as shown in **Figure 112(a)**. The *ab initio* calculations for the phonon dispersion are from [50]. Similar phonon dispersion can also be found in other *ab initio* calculations [34]. **Figure 112(b)** shows that the VFF model and the SW potential give exactly the same phonon dispersion, as the SW potential is derived from the VFF model.

The parameters for the two-body SW potential used by GULP are shown in **Table 227**. The parameters for the three-body SW potential used by GULP are shown in **Table 228**. Some representative parameters for the SW potential used by LAMMPS are listed in **Table 229**.

We use LAMMPS to perform MD simulations for the mechanical behavior of the single-layer 1T-ZrSe₂ under uniaxial tension at 1 and 300 K. **Figure 113** shows the stress-strain curve for the tension of a single-layer 1T-ZrSe₂ of dimension $100 \times 100 \text{ \AA}$. Periodic boundary conditions are applied in both armchair and zigzag directions. The single-layer 1T-ZrSe₂ is stretched

VFF type	Bond stretching	Angle bending	
Expression	$\frac{1}{2}K_{\text{Zr-Se}}(\Delta r)^2$	$\frac{1}{2}K_{\text{Zr-Se-Se}}(\Delta\theta)^2$	$\frac{1}{2}K_{\text{Se-Zr-Zr}}(\Delta\theta)^2$
Parameter	7.930	4.283	4.283
r_0 or θ_0	2.667	88.058	88.058

The second line gives an explicit expression for each VFF term. The third line is the force constant parameters. Parameters are in the unit of eV/ \AA^2 for the bond stretching interaction and in the unit of eV for the angle bending interaction. The fourth line gives the initial bond length (in the unit of \AA) for the bond stretching interaction and the initial angle (in the unit of degrees) for the angle bending interaction. The angle θ_{ijk} has atom i as the apex.

Table 226. The VFF model for single-layer 1T-ZrSe₂.

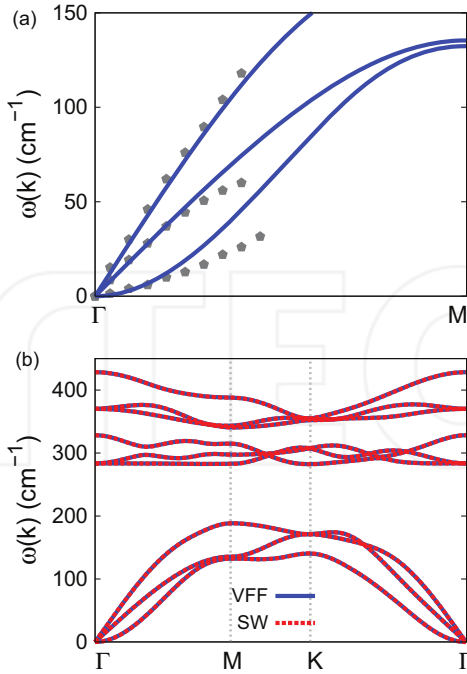


Figure 112. Phonon spectrum for single-layer 1T-ZrSe₂. (a) Phonon dispersion along the TM direction in the Brillouin zone. The results from the VFF model (lines) are comparable with the experiment data (pentagons) from [50]. (b) The phonon dispersion from the SW potential is exactly the same as that from the VFF model.

	<i>A</i> (eV)	ρ (Å)	<i>B</i> (Å ⁴)	<i>r</i> _{min} (Å)	<i>r</i> _{max} (Å)
Zr—Se	8.022	1.354	25.297	0.0	3.617

Table 227. Two-body SW potential parameters for single-layer 1T-ZrSe₂ used by GULP [8] as expressed in Eq. (3).

	<i>K</i> (eV)	θ_0 (°)	ρ_1 (Å)	ρ_2 (Å)	<i>r</i> _{min12} (Å)	<i>r</i> _{max12} (Å)	<i>r</i> _{min13} (Å)	<i>r</i> _{max13} (Å)	<i>r</i> _{min23} (Å)	<i>r</i> _{max23} (Å)
$\theta_{\text{Zr—Se—Se}}$	37.051	88.058	1.354	1.354	0.0	3.617	0.0	3.617	0.0	5.064
$\theta_{\text{Se—Zr—Zr}}$	37.051	88.058	1.354	1.354	0.0	3.617	0.0	3.617	0.0	5.064

The angle θ_{ijk} in the first line indicates the bending energy for the angle with atom *i* as the apex.

Table 228. Three-body SW potential parameters for single-layer 1T-ZrSe₂ used by GULP [8] as expressed in Eq. (4).

	ϵ (eV)	σ (Å)	α	λ	γ	$\cos \theta_0$	<i>A</i> _L	<i>B</i> _L	<i>p</i>	<i>q</i>	Tol
Zr—Se—Se	1.000	1.354	2.671	37.051	1.000	0.034	8.022	7.527	4	0	0.0
Se—Zr—Zr	1.000	1.354	2.671	37.051	1.000	0.034	8.022	7.527	4	0	0.0

Table 229. SW potential parameters for single-layer 1T-ZrSe₂ used by LAMMPS⁹ as expressed in Eqs. (9) and (10).

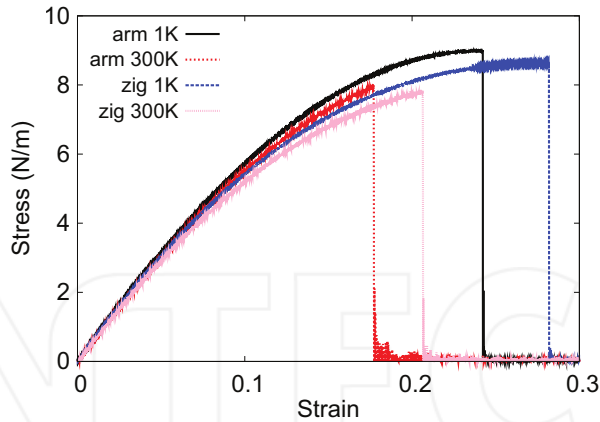


Figure 113. Stress-strain for single-layer 1T-ZrSe₂ of dimension 100 × 100 Å along the armchair and zigzag directions.

uniaxially along the armchair or zigzag direction. The stress is calculated without involving the actual thickness of the quasi-two-dimensional structure of the single-layer 1T-ZrSe₂. The Young's modulus can be obtained by a linear fitting of the stress-strain relation in the small strain range of [0, 0.01]. The Young's modulus is 66.7 and 66.4 N/m along the armchair and zigzag directions, respectively. The Young's modulus is essentially isotropic in the armchair and zigzag directions. The Poisson's ratio from the VFF model and the SW potential is $\nu_{xy} = \nu_{yx} = 0.19$.

There is no available value for nonlinear quantities in the single-layer 1T-ZrSe₂. We have thus used the nonlinear parameter $B = 0.5d^4$ in Eq. (5), which is close to the value of B in most materials. The value of the third-order nonlinear elasticity D can be extracted by fitting the stress-strain relation to the function $\sigma = E\epsilon + \frac{1}{2}D\epsilon^2$ with E as the Young's modulus. The values of D from the present SW potential are -219.6 and -256.6 N/m along the armchair and zigzag directions, respectively. The ultimate stress is about 9.0 N/m at the ultimate strain of 0.24 in the armchair direction at the low temperature of 1 K. The ultimate stress is about 8.6 N/m at the ultimate strain of 0.28 in the zigzag direction at the low temperature of 1 K.

58. 1T-ZrTe₂

Most existing theoretical studies on the single-layer 1T-ZrTe₂ are based on the first-principles calculations. In this section, we will develop the SW potential for the single-layer 1T-ZrTe₂.

The structure for the single-layer 1T-ZrTe₂ is shown in **Figure 71** (with M=Zr and X=Te). Each Zr atom is surrounded by six Te atoms. These Te atoms are categorized into the top group (e.g., atoms 1, 3, and 5) and bottom group (e.g., atoms 2, 4, and 6). Each Te atom is connected to three Zr atoms. The structural parameters are from the first-principles calculations [48], including the lattice constant $a = 4.0064$ Å and the bond length $d_{Zr-Te} = 2.9021$ Å, which are derived

from the angle $\theta_{\text{TeZrZr}} = 87.3^\circ$. The other angle is $\theta_{\text{ZrTeTe}} = 87.3^\circ$ with Te atoms from the same (top or bottom) group.

Table 230 shows three VFF terms for the single-layer 1T-ZrTe₂; one of which is the bond stretching interaction shown by Eq. (1), while the other two terms are the angle bending interaction shown by Eq. (2). We note that the angle bending term $K_{\text{Zr-Te-Te}}$ is for the angle $\theta_{\text{Zr-Te-Te}}$ with both Te atoms from the same (top or bottom) group. We find that there are actually only two parameters in the VFF model, so we can determine their value by fitting to the Young's modulus and the Poisson's ratio of the system. The *ab initio* calculations have predicted the Young's modulus to be 44 N/m and the Poisson's ratio as 0.13 [48].

The parameters for the two-body SW potential used by GULP are shown in **Table 231**. The parameters for the three-body SW potential used by GULP are shown in **Table 232**. Some representative parameters for the SW potential used by LAMMPS are listed in **Table 233**.

VFF type	Bond stretching	Angle bending	
Expression	$\frac{1}{2}K_{\text{Zr-Te}}(\Delta r)^2$	$\frac{1}{2}K_{\text{Zr-Te-Te}}(\Delta\theta)^2$	$\frac{1}{2}K_{\text{Te-Zr-Zr}}(\Delta\theta)^2$
Parameter	2.974	3.681	3.681
r_0 or θ_0	2.902	87.301	87.301

The second line gives an explicit expression for each VFF term. The third line is the force constant parameters. Parameters are in the unit of eV/Å² for the bond stretching interaction and in the unit of eV for the angle bending interaction. The fourth line gives the initial bond length (in the unit of Å) for the bond stretching interaction and the initial angle (in the unit of degrees) for the angle bending interaction. The angle θ_{ijk} has atom *i* as the apex.

Table 230. The VFF model for single-layer 1T-ZrTe₂.

	<i>A</i> (eV)	<i>ρ</i> (Å)	<i>B</i> (Å ⁴)	<i>r</i> _{min} (Å)	<i>r</i> _{max} (Å)
Zr—Te	3.493	1.441	35.467	0.0	3.925

Table 231. Two-body SW potential parameters for single-layer 1T-ZrTe₂ used by GULP [8] as expressed in Eq. (3).

	<i>K</i> (eV)	θ_0 (°)	ρ_1 (Å)	ρ_2 (Å)	$r_{\min 12}$ (Å)	$r_{\max 12}$ (Å)	$r_{\min 13}$ (Å)	$r_{\max 13}$ (Å)	$r_{\min 23}$ (Å)	$r_{\max 23}$ (Å)
$\theta_{\text{Zr-Te-Te}}$	30.905	87.301	1.441	1.441	0.0	3.925	0.0	3.925	0.0	5.473
$\theta_{\text{Te-Zr-Zr}}$	30.905	87.301	1.441	1.441	0.0	3.925	0.0	3.925	0.0	5.473

The angle θ_{ijk} in the first line indicates the bending energy for the angle with atom *i* as the apex.

Table 232. Three-body SW potential parameters for single-layer 1T-ZrTe₂ used by GULP [8] as expressed in Eq. (4).

	ϵ (eV)	σ (Å)	a	λ	γ	$\cos\theta_0$	A_L	B_L	p	q	Tol
Zr—Te ₁ —Te ₁	1.000	1.441	2.723	30.905	1.000	0.047	3.493	8.225	4	0	0.0

Table 233. SW potential parameters for single-layer 1T-ZrTe₂ used by LAMMPS [9] as expressed in Eqs. (9) and (10).

We use LAMMPS to perform MD simulations for the mechanical behavior of the single-layer 1T-ZrTe₂ under uniaxial tension at 1 and 300 K. **Figure 114** shows the stress-strain curve for the tension of a single-layer 1T-ZrTe₂ of dimension 100 × 100 Å. Periodic boundary conditions are applied in both armchair and zigzag directions. The single-layer 1T-ZrTe₂ is stretched uniaxially along the armchair or zigzag direction. The stress is calculated without involving the actual thickness of the quasi-two-dimensional structure of the single-layer 1T-ZrTe₂. The Young's modulus can be obtained by a linear fitting of the stress-strain relation in the small strain range of [0, 0.01]. The Young's modulus is 39.2 and 39.1 N/m along the armchair and zigzag directions, respectively. The Young's modulus is essentially isotropic in the armchair and zigzag directions. The Poisson's ratio from the VFF model and the SW potential is $\nu_{xy} = \nu_{yx} = 0.10$. The fitted Young's modulus value is about 10% smaller than the *ab initio* result of 44 N/m [48], as only short-range interactions are considered in the present work. The long-range interactions are ignored, which typically leads to about 10% underestimation for the value of the Young's modulus.

There is no available value for nonlinear quantities in the single-layer 1T-ZrTe₂. We have thus used the nonlinear parameter $B = 0.5d^4$ in Eq. (5), which is close to the value of B in most materials. The value of the third-order nonlinear elasticity D can be extracted by fitting the stress-strain relation to the function $\sigma = E\epsilon + \frac{1}{2}D\epsilon^2$ with E as the Young's modulus. The values of D from the present SW potential are -187.2 and -201.1 N/m along the armchair and zigzag directions, respectively. The ultimate stress is about 4.0 N/m at the ultimate strain of 0.19 in the armchair direction at the low temperature of 1 K. The ultimate stress is about 3.9 N/m at the ultimate strain of 0.22 in the zigzag direction at the low temperature of 1 K.

Figure 115 shows that the VFF model and the SW potential give exactly the same phonon dispersion, as the SW potential is derived from the VFF model.

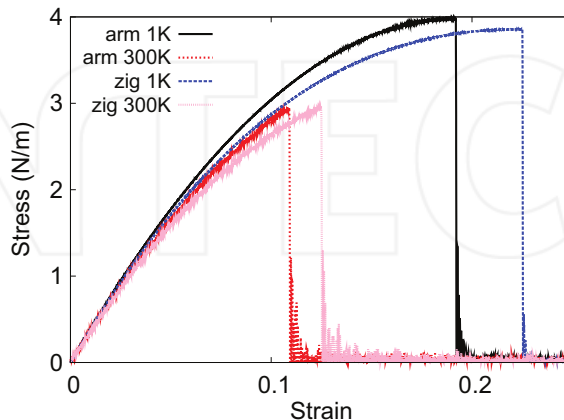


Figure 114. Stress-strain for single-layer 1T-ZrTe₂ of dimension 100 × 100 Å along the armchair and zigzag directions.

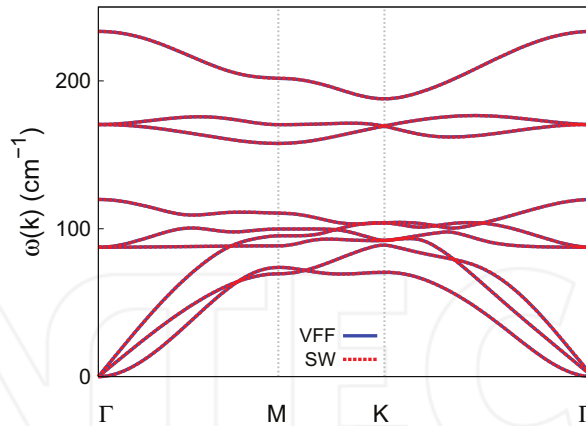


Figure 115. Phonon spectrum for single-layer 1T-ZrTe₂ along the ΓMΚΓ direction in the Brillouin zone. The phonon dispersion from the SW potential is exactly the same as that from the VFF model.

59. 1T-NbS₂

Most existing theoretical studies on the single-layer 1T-NbS₂ are based on the first-principles calculations. In this section, we will develop the SW potential for the single-layer 1T-NbS₂.

The structure for the single-layer 1T-NbS₂ is shown in **Figure 71** (with M=Nb and X=S). Each Nb atom is surrounded by six S atoms. These S atoms are categorized into the top group (e.g., atoms 1, 3, and 5) and bottom group (e.g., atoms 2, 4, and 6). Each S atom is connected to three Nb atoms. The structural parameters are from the first-principles calculations [12], including the lattice constant $a = 3.30 \text{ \AA}$ and the bond length $d_{\text{Nb-S}} = 2.45 \text{ \AA}$. The resultant angles are $\theta_{\text{NbSS}} = 84.671^\circ$ with S atoms from the same (top or bottom) group and $\theta_{\text{SNbNb}} = 84.671^\circ$.

Table 234 shows three VFF terms for the single-layer 1T-NbS₂; one of which is the bond stretching interaction shown by Eq. (1), while the other two terms are the angle bending interaction shown by Eq. (2). We note that the angle bending term $K_{\text{Nb-S-S}}$ is for the angle $\theta_{\text{Nb-S-S}}$ with both S atoms from the same (top or bottom) group. These force constant

VFF type	Bond stretching	Angle bending	
Expression	$\frac{1}{2} K_{\text{Nb-S}} (\Delta r)^2$	$\frac{1}{2} K_{\text{Nb-S-S}} (\Delta \theta)^2$	$\frac{1}{2} K_{\text{S-Nb-Nb}} (\Delta \theta)^2$
Parameter	7.930	4.283	4.283
r_0 or θ_0	2.450	84.671	84.671

The second line gives an explicit expression for each VFF term. The third line is the force constant parameters. Parameters are in the unit of eV/Å² for the bond stretching interaction and in the unit of eV for the angle bending interaction. The fourth line gives the initial bond length (in the unit of Å) for the bond stretching interaction and the initial angle (in the unit of degrees) for the angle bending interaction. The angle θ_{ijk} has atom i as the apex.

Table 234. The VFF model for single-layer 1T-NbS₂.

parameters are determined by fitting to the three acoustic branches in the phonon dispersion along the Γ M as shown in **Figure 116(a)**. The *ab initio* calculations for the phonon dispersion are from [12]. The lowest acoustic branch (flexural mode) is linear and very close to the in-plane transverse acoustic branch in the *ab initio* calculations, which may be due to the violation of the rigid rotational invariance [20]. **Figure 116(b)** shows that the VFF model and the SW potential give exactly the same phonon dispersion, as the SW potential is derived from the VFF model.

The parameters for the two-body SW potential used by GULP are shown in **Table 235**. The parameters for the three-body SW potential used by GULP are shown in **Table 236**. Some representative parameters for the SW potential used by LAMMPS are listed in **Table 237**.

We use LAMMPS to perform MD simulations for the mechanical behavior of the single-layer 1T-NbS₂ under uniaxial tension at 1 and 300 K. **Figure 117** shows the stress-strain curve for the

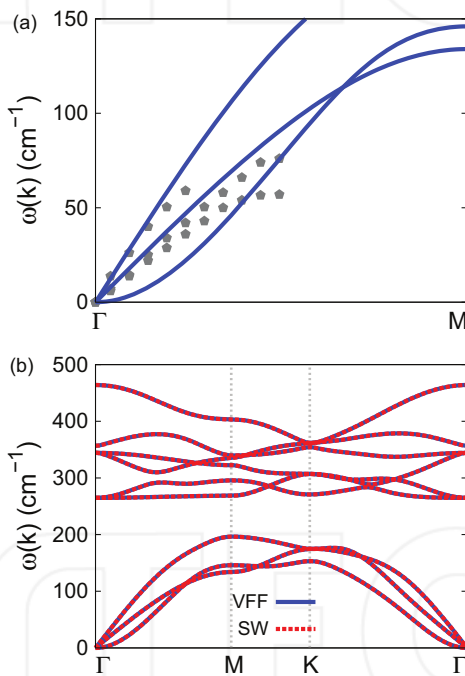


Figure 116. Phonon spectrum for single-layer 1T-NbS₂. (a) Phonon dispersion along the Γ M direction in the Brillouin zone. The results from the VFF model (lines) are comparable with the experiment data (pentagons) from [12]. (b) The phonon dispersion from the SW potential is exactly the same as that from the VFF model.

	A (eV)	ρ (\AA)	B (\AA^4)	r_{\min} (\AA)	r_{\max} (\AA)
Nb—S	6.192	1.125	18.015	0.0	3.280

Table 235. Two-body SW potential parameters for single-layer 1T-NbS₂ used by GULP [8] as expressed in Eq. (3).

	K (eV)	θ_0 ($^\circ$)	ρ_1 (\AA)	ρ_2 (\AA)	$r_{\min 12}$ (\AA)	$r_{\max 12}$ (\AA)	$r_{\min 13}$ (\AA)	$r_{\max 13}$ (\AA)	$r_{\min 23}$ (\AA)	$r_{\max 23}$ (\AA)
$\theta_{\text{Nb-S-S}}$	32.472	84.671	1.125	1.125	0.0	3.280	0.0	3.280	0.0	4.508
$\theta_{\text{S-Nb-Nb}}$	32.472	84.671	1.125	1.125	0.0	3.280	0.0	3.280	0.0	4.508

The angle θ_{ijk} in the first line indicates the bending energy for the angle with atom i as the apex.

Table 236. Three-body SW potential parameters for single-layer 1T-NbS₂ used by GULP [8] as expressed in Eq. (4).

	ϵ (eV)	σ (\AA)	a	λ	γ	$\cos \theta_0$	A_L	B_L	p	q	Tol
Nb—S ₁ —S ₁	1.000	1.125	2.916	32.472	1.000	0.093	6.192	11.247	4	0	0.0
S ₁ —Nb—Nb	1.000	1.125	2.916	32.472	1.000	0.093	6.192	11.247	4	0	0.0

Table 237. SW potential parameters for single-layer 1T-NbS₂ used by LAMMPS [9] as expressed in Eqs. (9) and (10).

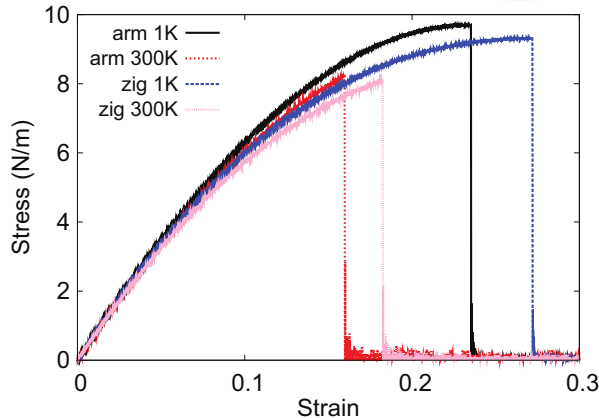


Figure 117. Stress-strain for single-layer 1T-NbS₂ of dimension $100 \times 100 \text{ \AA}$ along the armchair and zigzag directions.

tension of a single-layer 1T-NbS₂ of dimension $100 \times 100 \text{ \AA}$. Periodic boundary conditions are applied in both armchair and zigzag directions. The single-layer 1T-NbS₂ is stretched uniaxially along the armchair or zigzag direction. The stress is calculated without involving the actual thickness of the quasi-two-dimensional structure of the single-layer 1T-NbS₂. The Young's modulus can be obtained by a linear fitting of the stress-strain relation in the small strain range of [0, 0.01]. The Young's modulus is 73.8 and 73.4 N/m along the armchair and zigzag directions, respectively. The Young's modulus is essentially isotropic in the armchair and zigzag directions. The Poisson's ratio from the VFF model and the SW potential is $\nu_{xy} = \nu_{yx} = 0.18$.

There is no available value for nonlinear quantities in the single-layer 1T-NbS₂. We have thus used the nonlinear parameter $B = 0.5d^4$ in Eq. (5), which is close to the value of B in most materials. The value of the third-order nonlinear elasticity D can be extracted by fitting the stress-strain relation to the function $\sigma = E\epsilon + \frac{1}{2}D\epsilon^2$ with E as the Young's modulus. The values

of D from the present SW potential are -250.5 and -290.4 N/m along the armchair and zigzag directions, respectively. The ultimate stress is about 9.7 N/m at the ultimate strain of 0.23 in the armchair direction at the low temperature of 1 K. The ultimate stress is about 9.4 N/m at the ultimate strain of 0.27 in the zigzag direction at the low temperature of 1 K.

60. 1T-NbSe₂

Most existing theoretical studies on the single-layer 1T-NbSe₂ are based on the first-principles calculations. In this section, we will develop the SW potential for the single-layer 1T-NbSe₂.

The structure for the single-layer 1T-NbSe₂ is shown in **Figure 71** (with M=Nb and X=Se). Each Nb atom is surrounded by six Se atoms. These Se atoms are categorized into the top group (e.g., atoms 1, 3, and 5) and bottom group (e.g., atoms 2, 4, and 6). Each Se atom is connected to three Nb atoms. The structural parameters are from the first-principles calculations [12], including the lattice constant $a = 3.39$ Å and the bond length $d_{\text{Nb-Se}} = 2.57$ Å. The resultant angles are $\theta_{\text{NbSeSe}} = 82.529^\circ$ with Se atoms from the same (top or bottom) group and $\theta_{\text{SeNbNb}} = 82.529^\circ$.

Table 238 shows three VFF terms for the single-layer 1T-NbSe₂; one of which is the bond stretching interaction shown by Eq. (1), while the other two terms are the angle bending interaction shown by Eq. (2). We note that the angle bending term $K_{\text{Nb-Se-Se}}$ is for the angle $\theta_{\text{Nb-Se-Se}}$ with both Se atoms from the same (top or bottom) group. We find that there are actually only two parameters in the VFF model, so we can determine their value by fitting to the Young's modulus and the Poisson's ratio of the system. The *ab initio* calculations have predicted the Young's modulus to be 73 N/m and the Poisson's ratio as 0.20 [48].

The parameters for the two-body SW potential used by GULP are shown in **Table 239**. The parameters for the three-body SW potential used by GULP are shown in **Table 240**. Some representative parameters for the SW potential used by LAMMPS are listed in **Table 241**.

VFF type	Bond stretching	Angle bending	
Expression	$\frac{1}{2} K_{\text{Nb-Se}} (\Delta r)^2$	$\frac{1}{2} K_{\text{Nb-Se-Se}} (\Delta \theta)^2$	$\frac{1}{2} K_{\text{Se-Nb-Nb}} (\Delta \theta)^2$
Parameter	7.930	4.283	4.283
r_0 or θ_0	2.570	82.529	82.529

The second line gives an explicit expression for each VFF term. The third line is the force constant parameters. Parameters are in the unit of eV/Å² for the bond stretching interaction and in the unit of eV for the angle bending interaction. The fourth line gives the initial bond length (in the unit of Å) for the bond stretching interaction and the initial angle (in the unit of degrees) for the angle bending interaction. The angle θ_{ijk} has atom i as the apex.

Table 238. The VFF model for single-layer 1T-NbSe₂.

	A (eV)	ρ (Å)	B (Å ⁴)	r_{\min} (Å)	r_{\max} (Å)
Nb—Se	6.430	1.104	21.812	0.0	3.412

Table 239. Two-body SW potential parameters for single-layer 1T-NbSe₂ used by GULP [8] as expressed in Eq. (3).

	K (eV)	θ_0 ($^\circ$)	ρ_1 (\AA)	ρ_2 (\AA)	$r_{\min 12}$ (\AA)	$r_{\max 12}$ (\AA)	$r_{\min 13}$ (\AA)	$r_{\max 13}$ (\AA)	$r_{\min 23}$ (\AA)	$r_{\max 23}$ (\AA)
$\theta_{\text{Nb}-\text{Se}-\text{Se}}$	29.956	82.528	1.104	1.104	0.0	3.412	0.0	3.412	0.0	4.631
$\theta_{\text{Se}-\text{Nb}-\text{Nb}}$	29.956	82.528	1.104	1.104	0.0	3.412	0.0	3.412	0.0	4.631

The angle θ_{ijk} in the first line indicates the bending energy for the angle with atom i as the apex.

Table 240. Three-body SW potential parameters for single-layer 1T-NbSe₂ used by GULP [8] as expressed in Eq. (4).

	ϵ (eV)	σ (\AA)	a	λ	γ	$\cos \theta_0$	A_L	B_L	p	q	Tol
Nb—Se ₁ —Se ₁	1.000	1.104	3.092	29.956	1.000	0.130	6.430	14.706	4	0	0.0

Table 241. SW potential parameters for single-layer 1T-NbSe₂ used by LAMMPS [9] as expressed in Eqs. (9) and (10).

We use LAMMPS to perform MD simulations for the mechanical behavior of the single-layer 1T-NbSe₂ under uniaxial tension at 1 and 300 K. **Figure 118** shows the stress-strain curve for the tension of a single-layer 1T-NbSe₂ of dimension 100 × 100 Å. Periodic boundary conditions are applied in both armchair and zigzag directions. The single-layer 1T-NbSe₂ is stretched uniaxially along the armchair or zigzag direction. The stress is calculated without involving the actual thickness of the quasi-two-dimensional structure of the single-layer 1T-NbSe₂. The Young's modulus can be obtained by a linear fitting of the stress-strain relation in the small strain range of [0, 0.01]. The Young's modulus is 67.1 and 66.8 N/m along the armchair and zigzag directions, respectively. The Young's modulus is essentially isotropic in the armchair and zigzag directions. The Poisson's ratio from the VFF model and the SW potential is $\nu_{xy} = \nu_{yx} = 0.20$. The fitted Young's modulus value is about 10% smaller than the *ab initio* result of 73 N/m [48], as only short-range interactions are considered in the present work. The long-range interactions are ignored, which typically lead to about 10% underestimation for the Young's modulus value.

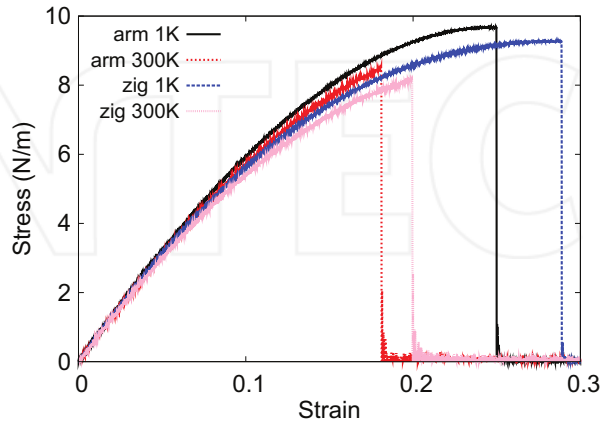


Figure 118. Stress-strain for single-layer 1T-NbSe₂ of dimension 100 × 100 Å along the armchair and zigzag directions.

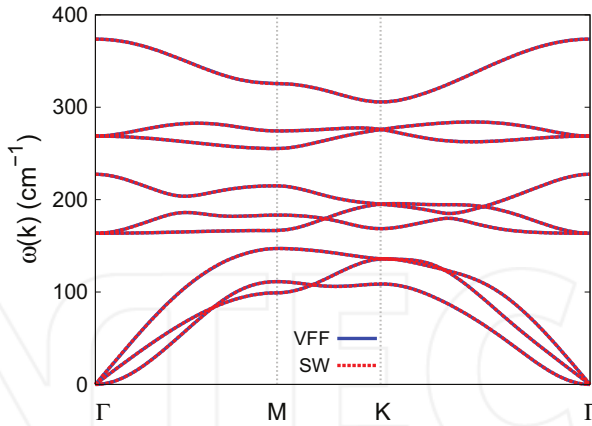


Figure 119. Phonon spectrum for single-layer 1T-NbSe₂ along the ΓMKT direction in the Brillouin zone. The phonon dispersion from the SW potential is exactly the same as that from the VFF model.

There is no available value for nonlinear quantities in the single-layer 1T-NbSe₂. We have thus used the nonlinear parameter $B = 0.5d^4$ in Eq. (5), which is close to the value of B in most materials. The value of the third-order nonlinear elasticity D can be extracted by fitting the stress-strain relation to the function $\sigma = E\epsilon + \frac{1}{2}D\epsilon^2$ with E as the Young's modulus. The values of D from the present SW potential are -193.5 N/m and -233.4 N/m along the armchair and zigzag directions, respectively. The ultimate stress is about 9.7 N/m at the ultimate strain of 0.25 in the armchair direction at the low temperature of 1 K. The ultimate stress is about 9.3 N/m at the ultimate strain of 0.29 in the zigzag direction at the low temperature of 1 K.

Figure 119 shows that the VFF model and the SW potential give exactly the same phonon dispersion, as the SW potential is derived from the VFF model.

61. 1T-NbTe₂

Most existing theoretical studies on the single-layer 1T-NbTe₂ are based on the first-principles calculations. In this section, we will develop the SW potential for the single-layer 1T-NbTe₂.

The structure for the single-layer 1T-NbTe₂ is shown in **Figure 71** (with M=Nb and X=Te). Each Nb atom is surrounded by six Te atoms. These Te atoms are categorized into the top group (e.g., atoms 1, 3, and 5) and bottom group (e.g., atoms 2, 4, and 6). Each Te atom is connected to three Nb atoms. The structural parameters are from the first-principles calculations [12], including the lattice constant $a = 3.56$ Å and the bond length $d_{Nb-Te} = 2.77$ Å. The resultant angles are $\theta_{NbTeTe} = 79.972^\circ$ with Te atoms from the same (top or bottom) group and $\theta_{TeNbNb} = 79.972^\circ$.

Table 242 shows three VFF terms for the single-layer 1T-NbTe₂; one of which is the bond stretching interaction shown by Eq. (1), while the other two terms are the angle bending

VFF type	Bond stretching	Angle bending
Expression	$\frac{1}{2}K_{\text{Nb}-\text{Te}}(\Delta r)^2$	$\frac{1}{2}K_{\text{Nb}-\text{Te}-\text{Te}}(\Delta\theta)^2$
Parameter	3.559	4.863
r_0 or θ_0	2.770	79.972

The second line gives an explicit expression for each VFF term. The third line is the force constant parameters. Parameters are in the unit of eV/Å² for the bond stretching interaction and in the unit of eV for the angle bending interaction. The fourth line gives the initial bond length (in the unit of Å) for the bond stretching interaction and the initial angle (in the unit of degrees) for the angle bending interaction. The angle θ_{ijk} has atom i as the apex.

Table 242. The VFF model for single-layer 1T-NbTe₂.

interaction shown by Eq. (2). We note that the angle bending term $K_{\text{Nb}-\text{Te}-\text{Te}}$ is for the angle $\theta_{\text{Nb}-\text{Te}-\text{Te}}$ with both Te atoms from the same (top or bottom) group. We find that there are actually only two parameters in the VFF model, so we can determine their value by fitting to the Young's modulus and the Poisson's ratio of the system. The *ab initio* calculations have predicted the Young's modulus to be 56 N/m and the Poisson's ratio as 0.11 [48].

The parameters for the two-body SW potential used by GULP are shown in **Table 243**. The parameters for the three-body SW potential used by GULP are shown in **Table 244**. Some representative parameters for the SW potential used by LAMMPS are listed in **Table 245**.

We use LAMMPS to perform MD simulations for the mechanical behavior of the single-layer 1T-NbTe₂ under uniaxial tension at 1 and 300 K. **Figure 120** shows the stress-strain curve for the tension of a single-layer 1T-NbTe₂ of dimension 100 × 100 Å. Periodic boundary conditions are applied in both armchair and zigzag directions. The single-layer 1T-NbTe₂ is stretched uniaxially along the armchair or zigzag direction. The stress is calculated without involving

	A (eV)	ρ (Å)	B (Å ⁴)	r_{\min} (Å)	r_{\max} (Å)
Nb—Te	3.123	1.094	29.437	0.0	3.640

Table 243. Two-body SW potential parameters for single-layer 1T-NbTe₂ used by GULP [8] as expressed in Eq. (3).

	K (eV)	θ_0 (°)	ρ_1 (Å)	ρ_2 (Å)	$r_{\min 12}$ (Å)	$r_{\max 12}$ (Å)	$r_{\min 13}$ (Å)	$r_{\max 13}$ (Å)	$r_{\min 23}$ (Å)	$r_{\max 23}$ (Å)
$\theta_{\text{Nb}-\text{Te}-\text{Te}}$	30.968	79.972	1.094	1.094	0.0	3.640	0.0	3.640	0.0	4.863
$\theta_{\text{Te}-\text{Nb}-\text{Nb}}$	30.968	79.972	1.094	1.094	0.0	3.640	0.0	3.640	0.0	4.863

The angle θ_{ijk} in the first line indicates the bending energy for the angle with atom i as the apex.

Table 244. Three-body SW potential parameters for single-layer 1T-NbTe₂ used by GULP [8] as expressed in Eq. (4).

	ϵ (eV)	σ (Å)	a	λ	γ	$\cos \theta_0$	A_L	B_L	p	q	Tol
Nb—Te ₁ —Te ₁	1.000	1.094	3.328	30.968	1.000	0.174	3.123	20.560	4	0	0.0

Table 245. SW potential parameters for single-layer 1T-NbTe₂ used by LAMMPS [9] as expressed in Eqs. (9) and (10).

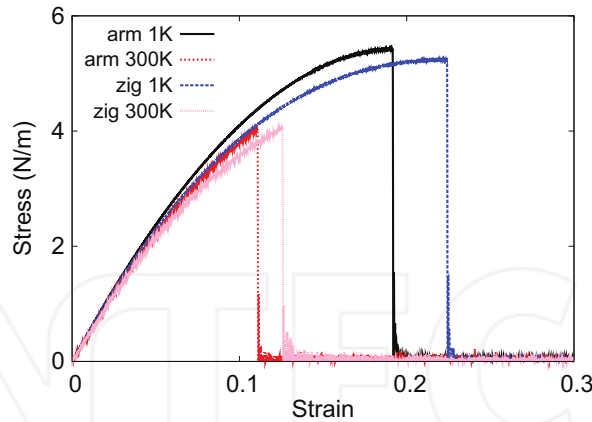


Figure 120. Stress-strain for single-layer 1T-NbTe₂ of dimension 100 × 100 Å along the armchair and zigzag directions.

the actual thickness of the quasi-two-dimensional structure of the single-layer 1T-NbTe₂. The Young's modulus can be obtained by a linear fitting of the stress-strain relation in the small strain range of [0, 0.01]. The Young's modulus is 52.2 and 51.9 N/m along the armchair and zigzag directions, respectively. The Young's modulus is essentially isotropic in the armchair and zigzag directions. The Poisson's ratio from the VFF model and the SW potential is $\nu_{xy} = \nu_{yx} = 0.11$. The fitted Young's modulus value is about 10% smaller than the *ab initio* result of 56 N/m [48], as only short-range interactions are considered in the present work. The long-range interactions are ignored, which typically leads to about 10% underestimation for the value of the Young's modulus.

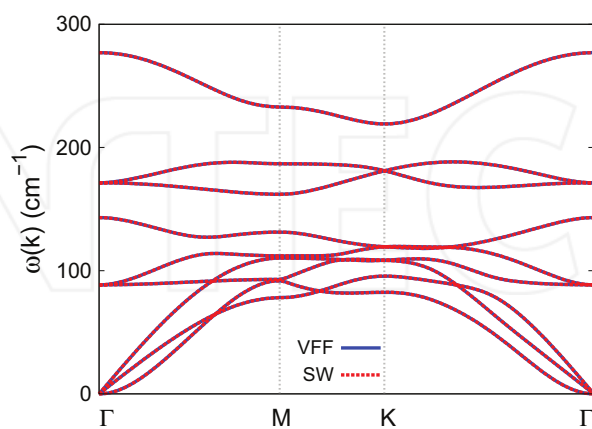


Figure 121. Phonon spectrum for single-layer 1T-NbTe₂ along the ΓMKΓ direction in the Brillouin zone. The phonon dispersion from the SW potential is exactly the same as that from the VFF model.

There is no available value for nonlinear quantities in the single-layer 1T-NbTe₂. We have thus used the nonlinear parameter $B = 0.5d^4$ in Eq. (5), which is close to the value of B in most materials. The value of the third-order nonlinear elasticity D can be extracted by fitting the stress-strain relation to the function $\sigma = E\epsilon + \frac{1}{2}D\epsilon^2$ with E as the Young's modulus. The values of D from the present SW potential are -237.7 and -265.0 N/m along the armchair and zigzag directions, respectively. The ultimate stress is about 5.4 N/m at the ultimate strain of 0.19 in the armchair direction at the low temperature of 1 K. The ultimate stress is about 5.2 N/m at the ultimate strain of 0.22 in the zigzag direction at the low temperature of 1 K.

Figure 121 shows that the VFF model and the SW potential give exactly the same phonon dispersion, as the SW potential is derived from the VFF model.

62. 1T-MoS₂

Most existing theoretical studies on the single-layer 1T-MoS₂ are based on the first-principles calculations. In this section, we will develop the SW potential for the single-layer 1T-MoS₂.

The structure for the single-layer 1T-MoS₂ is shown in **Figure 71** (with M=Mo and X=S). Each Mo atom is surrounded by six S atoms. These S atoms are categorized into the top group (e.g., atoms 1, 3, and 5) and bottom group (e.g., atoms 2, 4, and 6). Each S atom is connected to three Mo atoms. The structural parameters are from the first-principles calculations [48], including the lattice constant $a = 3.1998$ Å and the bond length $d_{\text{Mo-S}} = 2.4193$ Å, which are derived from the angle $\theta_{\text{SMoMo}} = 82.8^\circ$. The other angle is $\theta_{\text{MoSS}} = 82.8^\circ$ with S atoms from the same (top or bottom) group.

Table 246 shows three VFF terms for the single-layer 1T-MoS₂; one of which is the bond stretching interaction shown by Eq. (1), while the other two terms are the angle bending interaction shown by Eq. (2). We note that the angle bending term $K_{\text{Mo-S-S}}$ is for the angle $\theta_{\text{Mo-S-S}}$ with both S atoms from the same (top or bottom) group. We find that there are actually only two parameters in the VFF model, so we can determine their value by fitting to the Young's modulus and the Poisson's ratio of the system. The *ab initio* calculations have predicted the Young's modulus to be 103 N/m and the Poisson's ratio as -0.07 [48]. The *ab*

VFF type	Bond stretching	Angle bending	
Expression	$\frac{1}{2}K_{\text{Mo-S}}(\Delta r)^2$	$\frac{1}{2}K_{\text{Mo-S-S}}(\Delta\theta)^2$	$\frac{1}{2}K_{\text{S-Mo-Mo}}(\Delta\theta)^2$
Parameter	3.523	10.394	10.394
r_0 or θ_0	2.419	82.799	82.799

The second line gives an explicit expression for each VFF term. The third line is the force constant parameters. Parameters are in the unit of eV/Å² for the bond stretching interaction and in the unit of eV for the angle bending interaction. The fourth line gives the initial bond length (in the unit of Å) for the bond stretching interaction and the initial angle (in the unit of degrees) for the angle bending interaction. The angle θ_{ijk} has atom i as the apex.

Table 246. The VFF model for single-layer 1T-MoS₂.

initio calculations have predicted a negative Poisson's ratio in the 1T-MoS₂, which was attributed to the orbital coupling in this material. The orbital coupling enhances the angle bending interaction in the VFF model. As a result, the value of the angle bending parameter is much larger than the bond stretching force constant parameter, which is typical in auxetic materials with negative Poisson's ratio [52].

The parameters for the two-body SW potential used by GULP are shown in **Table 247**. The parameters for the three-body SW potential used by GULP are shown in **Table 248**. Some representative parameters for the SW potential used by LAMMPS are listed in **Table 249**.

We use LAMMPS to perform MD simulations for the mechanical behavior of the single-layer 1T-MoS₂ under uniaxial tension at 1 and 300 K. **Figure 122** shows the stress-strain curve for the tension of a single-layer 1T-MoS₂ of dimension 100 × 100 Å. Periodic boundary conditions are applied in both armchair and zigzag directions. The single-layer 1T-MoS₂ is stretched uniaxially along the armchair or zigzag direction. The stress is calculated without involving the actual thickness of the quasi-two-dimensional structure of the single-layer 1T-MoS₂. The Young's modulus can be obtained by a linear fitting of the stress-strain relation in the small strain range of [0, 0.01]. The Young's modulus is 88.7 and 88.3 N/m along the armchair and zigzag directions, respectively. The Young's modulus is essentially isotropic in the armchair and zigzag directions. The Poisson's ratio from the VFF model and the SW potential is $\nu_{xy} = \nu_{yx} = -0.07$. The fitted Young's modulus value is about 10% smaller than the *ab initio* result of 103 N/m [48], as only short-range interactions are considered in the present work. The long-range interactions are ignored, which typically leads to about 10% underestimation for the value of the Young's modulus.

	<i>A</i> (eV)	<i>ρ</i> (Å)	<i>B</i> (Å ⁴)	<i>r</i> _{min} (Å)	<i>r</i> _{max} (Å)
Mo—S	2.550	1.048	17.129	0.0	3.215

Table 247. Two-body SW potential parameters for single-layer 1T-MoS₂ used by GULP [8] as expressed in Eq. (3).

	<i>K</i> (eV)	θ_0 (degree)	<i>ρ</i> ₁ (Å)	<i>ρ</i> ₂ (Å)	<i>r</i> _{min 12} (Å)	<i>r</i> _{max 12} (Å)	<i>r</i> _{min 13} (Å)	<i>r</i> _{max 13} (Å)	<i>r</i> _{min 23} (Å)	<i>r</i> _{max 23} (Å)
$\theta_{\text{Mo-S-S}}$	73.436	82.799	1.048	1.048	0.0	3.215	0.0	3.215	0.0	4.371
$\theta_{\text{S-Mo-Mo}}$	73.436	82.799	1.048	1.048	0.0	3.215	0.0	3.215	0.0	4.371

The angle θ_{ijk} in the first line indicates the bending energy for the angle with atom *i* as the apex.

Table 248. Three-body SW potential parameters for single-layer 1T-MoS₂ used by GULP [8] as expressed in Eq. (4).

	<i>ε</i> (eV)	<i>σ</i> (Å)	<i>a</i>	<i>λ</i>	<i>γ</i>	$\cos \theta_0$	<i>A</i> _L	<i>B</i> _L	<i>p</i>	<i>q</i>	Tol
Mo—S ₁ —S ₁	1.000	1.048	3.069	73.436	1.000	0.125	2.550	14.207	4	0	0.0

Table 249. SW potential parameters for single-layer 1T-MoS₂ used by LAMMPS [9] as expressed in Eqs. (9) and (10).

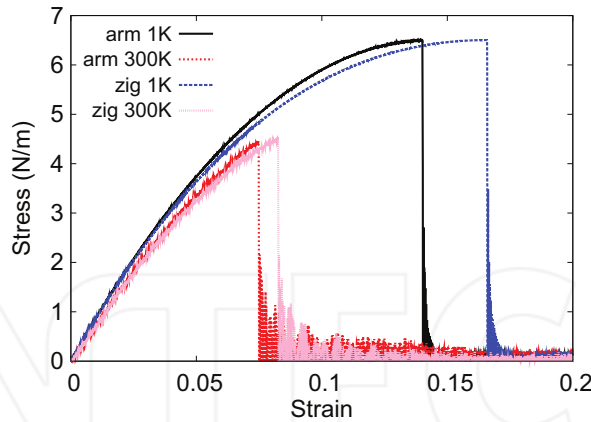


Figure 122. Stress-strain for single-layer 1T-MoS₂ of dimension 100 × 100 Å along the armchair and zigzag directions.

There is no available value for nonlinear quantities in the single-layer 1T-MoS₂. We have thus used the nonlinear parameter $B = 0.5d^4$ in Eq. (5), which is close to the value of B in most materials. The value of the third-order nonlinear elasticity D can be extracted by fitting the stress-strain relation to the function $\sigma = E\epsilon + \frac{1}{2}D\epsilon^2$ with E as the Young's modulus. The values of D from the present SW potential are -595.2 and -624.1 N/m along the armchair and zigzag directions, respectively. The ultimate stress is about 6.5 N/m at the ultimate strain of 0.14 in the armchair direction at the low temperature of 1 K. The ultimate stress is about 6.5 N/m at the ultimate strain of 0.16 in the zigzag direction at the low temperature of 1 K.

Figure 123 shows that the VFF model and the SW potential give exactly the same phonon dispersion, as the SW potential is derived from the VFF model.

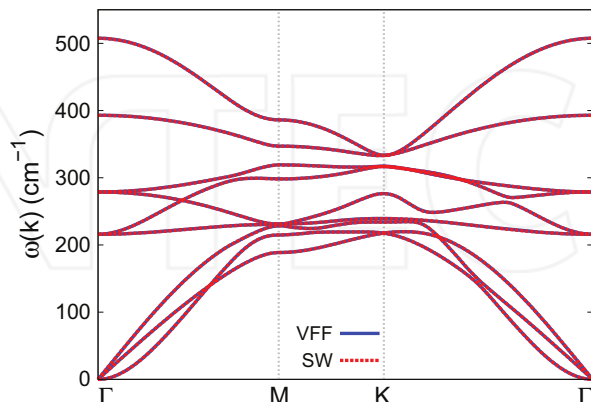


Figure 123. Phonon spectrum for single-layer 1T-MoS₂ along the Γ -M-K- Γ direction in the Brillouin zone. The phonon dispersion from the SW potential is exactly the same as that from the VFF model.

63. 1T-MoSe₂

Most existing theoretical studies on the single-layer 1T-MoSe₂ are based on the first-principles calculations. In this section, we will develop the SW potential for the single-layer 1T-MoSe₂.

The structure for the single-layer 1T-MoSe₂ is shown in **Figure 71** (with M=Mo and X=Se). Each Mo atom is surrounded by six Se atoms. These Se atoms are categorized into the top group (e.g., atoms 1, 3, and 5) and bottom group (e.g., atoms 2, 4, and 6). Each Se atom is connected to three Mo atoms. The structural parameters are from the first-principles calculations [48], including the lattice constant $a = 3.2685 \text{ \AA}$ and the bond length $d_{\text{Mo-Se}} = 2.5293 \text{ \AA}$, which are derived from the angle $\theta_{\text{SeMoMo}} = 80.5^\circ$. The other angle is $\theta_{\text{MoSeSe}} = 80.5^\circ$ with Se atoms from the same (top or bottom) group.

Table 250 shows three VFF terms for the single-layer 1T-MoSe₂; one of which is the bond stretching interaction shown by Eq. (1), while the other two terms are the angle bending interaction shown by Eq. (2). We note that the angle bending term $K_{\text{Mo-Se-Se}}$ is for the angle $\theta_{\text{Mo-Se-Se}}$ with both Se atoms from the same (top or bottom) group. We find that there are actually only two parameters in the VFF model, so we can determine their value by fitting to the Young's modulus and the Poisson's ratio of the system. The *ab initio* calculations have predicted the Young's modulus to be 104 N/m and the Poisson's ratio as -0.13 [48]. The *ab initio* calculations have predicted a negative Poisson's ratio in the 1T-MoSe₂, which was attributed to the orbital coupling in this material. The orbital coupling enhances the angle bending interaction in the VFF model. As a result, the value of the angle bending parameter is much larger than the bond stretching force constant parameter, which is typical in auxetic materials with negative Poisson's ratio [52].

The parameters for the two-body SW potential used by GULP are shown in **Table 251**. The parameters for the three-body SW potential used by GULP are shown in **Table 252**. Some representative parameters for the SW potential used by LAMMPS are listed in **Table 253**.

We use LAMMPS to perform MD simulations for the mechanical behavior of the single-layer 1T-MoSe₂ under uniaxial tension at 1 and 300 K. **Figure 124** shows the stress-strain curve for the tension of a single-layer 1T-MoSe₂ of dimension 100 × 100 Å. Periodic boundary conditions are applied in both armchair and zigzag directions. The single-layer 1T-MoSe₂ is stretched

VFF type	Bond stretching	Angle bending	
Expression	$\frac{1}{2}K_{\text{Mo-Se}}(\Delta r)^2$	$\frac{1}{2}K_{\text{Mo-Se-Se}}(\Delta\theta)^2$	$\frac{1}{2}K_{\text{Se-Mo-Mo}}(\Delta\theta)^2$
Parameter	2.964	14.753	14.753
r_0 or θ_0	2.529	80.501	80.501

The second line gives an explicit expression for each VFF term. The third line is the force constant parameters. Parameters are in the unit of eV/Å² for the bond stretching interaction and in the unit of eV for the angle bending interaction. The fourth line gives the initial bond length (in the unit of Å) for the bond stretching interaction and the initial angle (in the unit of degrees) for the angle bending interaction. The angle θ_{ijk} has atom *i* as the apex.

Table 250. The VFF model for single-layer 1T-MoSe₂.

	A (eV)	ρ (Å)	B (Å ⁴)	r_{\min} (Å)	r_{\max} (Å)
Mo—Se	2.201	1.017	20.463	0.0	3.331

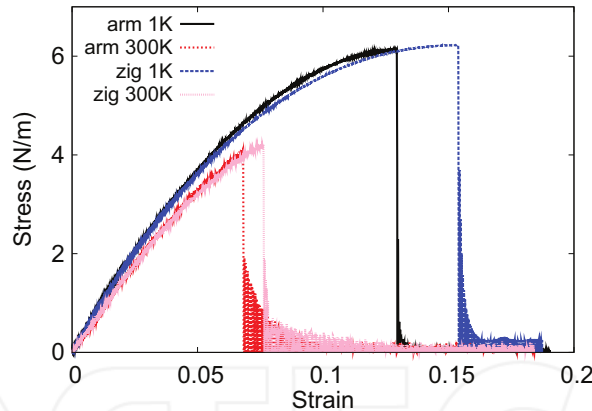
Table 251. Two-body SW potential parameters for single-layer 1T-MoSe₂ used by GULP [8] as expressed in Eq. (3).

	K (eV)	θ_0 (°)	ρ_1 (Å)	ρ_2 (Å)	$r_{\min 12}$ (Å)	$r_{\max 12}$ (Å)	$r_{\min 13}$ (Å)	$r_{\max 13}$ (Å)	$r_{\min 23}$ (Å)	$r_{\max 23}$ (Å)
$\theta_{\text{Mo—Se—Se}}$	95.770	80.501	1.017	1.017	0.0	3.331	0.0	3.331	0.0	4.465
$\theta_{\text{Se—Mo—Mo}}$	95.770	80.501	1.017	1.017	0.0	3.331	0.0	3.331	0.0	4.465

The angle θ_{ijk} in the first line indicates the bending energy for the angle with atom i as the apex.

Table 252. Three-body SW potential parameters for single-layer 1T-MoSe₂ used by GULP [8] as expressed in Eq. (4).

	ϵ (eV)	σ (Å)	a	λ	γ	$\cos \theta_0$	A_L	B_L	p	q	Tol
Mo—Se ₁ —Se ₁	1.000	1.017	3.276	95.770	1.000	0.165	2.201	19.152	4	0	0.0

Table 253. SW potential parameters for single-layer 1T-MoSe₂ used by LAMMPS [9] as expressed in Eqs. (9) and (10).**Figure 124.** Stress-strain for single-layer 1T-MoSe₂ of dimension 100 × 100 Å along the armchair and zigzag directions.

uniaxially along the armchair or zigzag direction. The stress is calculated without involving the actual thickness of the quasi-two-dimensional structure of the single-layer 1T-MoSe₂. The Young's modulus can be obtained by a linear fitting of the stress-strain relation in the small strain range of [0, 0.01]. The Young's modulus is 88.2 and 87.9 N/m along the armchair and zigzag directions, respectively. The Young's modulus is essentially isotropic in the armchair and zigzag directions. The Poisson's ratio from the VFF model and the SW potential is $\nu_{xy} = \nu_{yx} = -0.13$. The fitted Young's modulus value is about 10% smaller than the *ab initio* result of 104 N/m [48], as only short-range interactions are considered in the present work. The

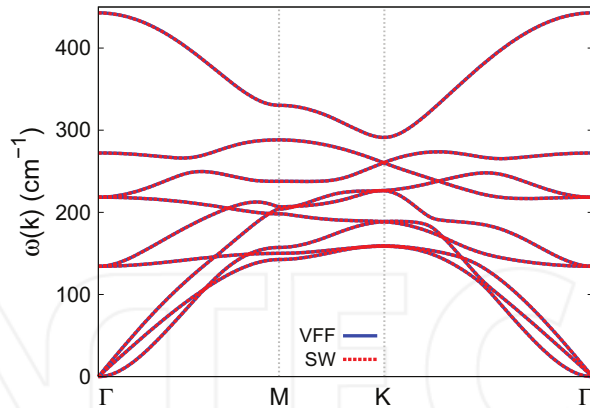


Figure 125. Phonon spectrum for single-layer 1T-MoSe₂ along the Γ MKT direction in the Brillouin zone. The phonon dispersion from the SW potential is exactly the same as that from the VFF model.

long-range interactions are ignored, which typically leads to about 10% underestimation for the value of the Young's modulus.

There is no available value for nonlinear quantities in the single-layer 1T-MoSe₂. We have thus used the nonlinear parameter $B = 0.5d^4$ in Eq. (5), which is close to the value of B in most materials. The value of the third-order nonlinear elasticity D can be extracted by fitting the stress-strain relation to the function $\sigma = E\epsilon + \frac{1}{2}D\epsilon^2$ with E as the Young's modulus. The values of D from the present SW potential are -632.6 and -629.7 N/m along the armchair and zigzag directions, respectively. The ultimate stress is about 6.1 N/m at the ultimate strain of 0.13 in the armchair direction at the low temperature of 1 K. The ultimate stress is about 6.2 N/m at the ultimate strain of 0.15 in the zigzag direction at the low temperature of 1 K.

Figure 125 shows that the VFF model and the SW potential give exactly the same phonon dispersion, as the SW potential is derived from the VFF model.

64. 1T-MoTe₂

Most existing theoretical studies on the single-layer 1T-MoTe₂ are based on the first-principles calculations. In this section, we will develop the SW potential for the single-layer 1T-MoTe₂.

The structure for the single-layer 1T-MoTe₂ is shown in **Figure 71** (with M=Mo and X=Te). Each Mo atom is surrounded by six Te atoms. These Te atoms are categorized into the top group (e.g., atoms 1, 3, and 5) and bottom group (e.g., atoms 2, 4, and 6). Each Te atom is connected to three Mo atoms. The structural parameters are from the first-principles calculations [48], including the lattice constant $a = 3.4970$ Å and the bond length $d_{\text{Mo}-\text{Te}} = 2.7287$ Å, which are derived from the angle $\theta_{\text{TeMoMo}} = 79.7^\circ$. The other angle is $\theta_{\text{MoTeTe}} = 79.7^\circ$ with Te atoms from the same (top or bottom) group.

Table 254 shows three VFF terms for the single-layer 1T-MoTe₂; one of which is the bond stretching interaction shown by Eq. (1), while the other two terms are the angle bending interaction shown by Eq. (2). We note that the angle bending term $K_{\text{Mo}-\text{Te}-\text{Te}}$ is for the angle $\theta_{\text{Mo}-\text{Te}-\text{Te}}$ with both Te atoms from the same (top or bottom) group. We find that there are actually only two parameters in the VFF model, so we can determine their value by fitting to the Young's modulus and the Poisson's ratio of the system. The *ab initio* calculations have predicted the Young's modulus to be 92 N/m and the Poisson's ratio as -0.07 [48]. The *ab initio* calculations have predicted a negative Poisson's ratio in the 1T-MoTe₂, which was attributed to the orbital coupling in this material. The orbital coupling enhances the angle bending interaction in the VFF model. As a result, the value of the angle bending parameter is much larger than the bond stretching force constant parameter, which is typical in auxetic materials with negative Poisson's ratio [52].

The parameters for the two-body SW potential used by GULP are shown in **Table 255**. The parameters for the three-body SW potential used by GULP are shown in **Table 256**. Some representative parameters for the SW potential used by LAMMPS are listed in **Table 257**.

We use LAMMPS to perform MD simulations for the mechanical behavior of the single-layer 1T-MoTe₂ under uniaxial tension at 1 and 300 K. **Figure 126** shows the stress-strain curve for the tension of a single-layer 1T-MoTe₂ of dimension 100 × 100 Å. Periodic boundary conditions

VFF type	Bond stretching	Angle bending
Expression	$\frac{1}{2}K_{\text{Mo}-\text{Te}}(\Delta r)^2$	$\frac{1}{2}K_{\text{Mo}-\text{Te}-\text{Te}}(\Delta\theta)^2$
Parameter	3.074	12.516
r_0 or θ_0	2.729	79.700

The second line gives an explicit expression for each VFF term. The third line is the force constant parameters. Parameters are in the unit of eV/Å² for the bond stretching interaction and in the unit of eV for the angle bending interaction. The fourth line gives the initial bond length (in the unit of Å) for the bond stretching interaction and the initial angle (in the unit of degrees) for the angle bending interaction. The angle θ_{ijk} has atom i as the apex.

Table 254. The VFF model for single-layer 1T-MoTe₂.

	A (eV)	ρ (Å)	B (Å ⁴)	r_{\min} (Å)	r_{\max} (Å)
Mo—Te	2.597	1.068	27.720	0.0	3.582

Table 255. Two-body SW potential parameters for single-layer 1T-MoTe₂ used by GULP [8] as expressed in Eq. (3).

	K (eV)	θ_0 (°)	ρ_1 (Å)	ρ_2 (Å)	$r_{\min 12}$ (Å)	$r_{\max 12}$ (Å)	$r_{\min 13}$ (Å)	$r_{\max 13}$ (Å)	$r_{\min 23}$ (Å)	$r_{\max 23}$ (Å)
$\theta_{\text{Mo}-\text{Te}-\text{Te}}$	78.925	79.700	1.068	1.068	0.0	3.582	0.0	3.582	0.0	4.777
$\theta_{\text{Te}-\text{Mo}-\text{Mo}}$	78.925	79.700	1.068	1.068	0.0	3.582	0.0	3.582	0.0	4.777

The angle θ_{ijk} in the first line indicates the bending energy for the angle with atom i as the apex.

Table 256. Three-body SW potential parameters for single-layer 1T-MoTe₂ used by GULP [8] as expressed in Eq. (4).

	ϵ (eV)	σ (\AA)	a	λ	γ	$\cos \theta_0$	A_L	B_L	p	q	Tol
Mo—Te ₁ —Te ₁	1.000	1.068	3.355	78.925	1.000	0.179	2.597	21.328	4	0	0.0

Table 257. SW potential parameters for single-layer 1T-MoTe₂ used by LAMMPS [9] as expressed in Eqs. (9) and (10).

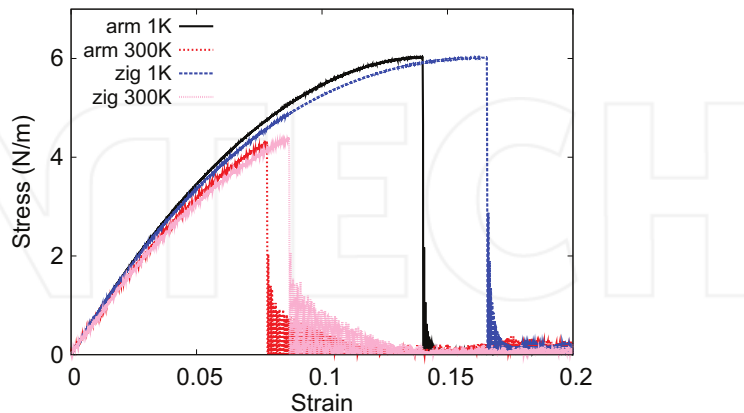


Figure 126. Stress-strain for single-layer 1T-MoTe₂ of dimension $100 \times 100 \text{ \AA}$ along the armchair and zigzag directions.

are applied in both armchair and zigzag directions. The single-layer 1T-MoTe₂ is stretched uniaxially along the armchair or zigzag direction. The stress is calculated without involving the actual thickness of the quasi-two-dimensional structure of the single-layer 1T-MoTe₂. The Young's modulus can be obtained by a linear fitting of the stress-strain relation in the small strain range of [0, 0.01]. The Young's modulus is 81.6 and 81.2 N/m along the armchair and zigzag directions, respectively. The Young's modulus is essentially isotropic in the armchair and zigzag directions. The Poisson's ratio from the VFF model and the SW potential is $\nu_{xy} = \nu_{yx} = -0.07$. The fitted Young's modulus value is about 10% smaller than the *ab initio* result of 92 N/m [48], as only short-range interactions are considered in the present work. The long-range interactions are ignored, which typically leads to about 10% underestimation for the value of the Young's modulus.

There is no available value for nonlinear quantities in the single-layer 1T-MoTe₂. We have thus used the nonlinear parameter $B = 0.5d^4$ in Eq. (5), which is close to the value of B in most materials. The value of the third-order nonlinear elasticity D can be extracted by fitting the stress-strain relation to the function $\sigma = E\epsilon + \frac{1}{2}D\epsilon^2$ with E as the Young's modulus. The values of D from the present SW potential are -543.1 and -558.6 N/m along the armchair and zigzag directions, respectively. The ultimate stress is about 6.0 N/m at the ultimate strain of 0.14 in the armchair direction at the low temperature of 1 K. The ultimate stress is about 6.0 N/m at the ultimate strain of 0.16 in the zigzag direction at the low temperature of 1 K.

Figure 127 shows that the VFF model and the SW potential give exactly the same phonon dispersion, as the SW potential is derived from the VFF model.

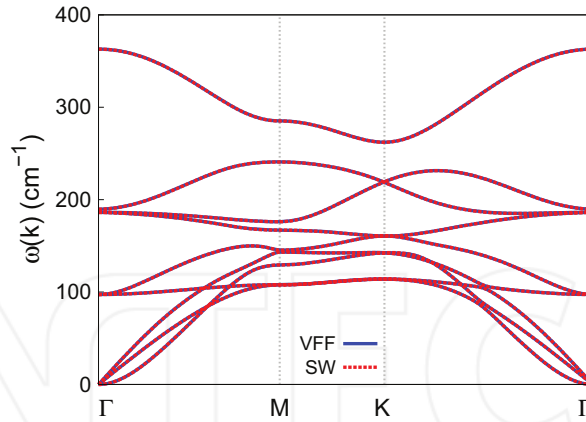


Figure 127. Phonon spectrum for single-layer 1T-MoTe₂ along the Γ MKG direction in the Brillouin zone. The phonon dispersion from the SW potential is exactly the same as that from the VFF model.

65. 1T-TcS₂

Most existing theoretical studies on the single-layer 1T-TcS₂ are based on the first-principles calculations. In this section, we will develop the SW potential for the single-layer 1T-TcS₂.

The structure for the single-layer 1T-TcS₂ is shown in **Figure 71** (with M = Tc and X = S). Each Tc atom is surrounded by six S atoms. These S atoms are categorized into the top group (e.g., atoms 1, 3, and 5) and bottom group (e.g., atoms 2, 4, and 6). Each S atom is connected to three Tc atoms. The structural parameters are from the first-principles calculations [48] including the lattice constant $a = 3.0692 \text{ \AA}$ and the bond length $d_{\text{Tc-S}} = 2.3924 \text{ \AA}$, which are derived from the angle $\theta_{\text{STcTc}} = 79.8^\circ$. The other angle is $\theta_{\text{TcSS}} = 79.8^\circ$ with S atoms from the same (top or bottom) group.

Table 258 shows three VFF terms for the single-layer 1T-TcS₂; one of which is the bond stretching interaction shown by Eq. (1), while the other two terms are the angle bending interaction shown by Eq. (2). We note that the angle bending term $K_{\text{Tc-S-S}}$ is for the angle $\theta_{\text{Tc-S-S}}$ with both S atoms from the same (top or bottom) group. We find that there are actually

VFF type	Bond stretching	Angle bending	
Expression	$\frac{1}{2}K_{\text{Tc-S}}(\Delta r)^2$	$\frac{1}{2}K_{\text{Tc-S-S}}(\Delta\theta)^2$	$\frac{1}{2}K_{\text{S-Tc-Tc}}(\Delta\theta)^2$
Parameter	2.986	11.141	11.141
r_0 or θ_0	2.392	79.800	79.800

The second line gives an explicit expression for each VFF term. The third line is the force constant parameters. Parameters are in the unit of eV/ \AA^2 for the bond stretching interaction and in the unit of eV for the angle bending interaction. The fourth line gives the initial bond length (in the unit of \AA) for the bond stretching interaction and the initial angle (in the unit of degrees) for the angle bending interaction. The angle θ_{ijk} has atom i as the apex.

Table 258. The VFF model for single-layer 1T-TcS₂.

only two parameters in the VFF model, so we can determine their value by fitting to the Young's modulus and the Poisson's ratio of the system. The *ab initio* calculations have predicted the Young's modulus to be 94 N/m and the Poisson's ratio as -0.10 [48]. The *ab initio* calculations have predicted a negative Poisson's ratio in the 1T-TcS₂, which was attributed to the orbital coupling in this material. The orbital coupling enhances the angle bending interaction in the VFF model. As a result, the value of the angle bending parameter is much larger than the bond stretching force constant parameter, which is typical in auxetic materials with negative Poisson's ratio [52].

The parameters for the two-body SW potential used by GULP are shown in **Table 259**. The parameters for the three-body SW potential used by GULP are shown in **Table 260**. Some representative parameters for the SW potential used by LAMMPS are listed in **Table 261**.

We use LAMMPS to perform MD simulations for the mechanical behavior of the single-layer 1T-TcS₂ under uniaxial tension at 1 and 300 K. **Figure 128** shows the stress-strain curve for the tension of a single-layer 1T-TcS₂ of dimension 100×100 Å. Periodic boundary conditions are applied in both armchair and zigzag directions. The single-layer 1T-TcS₂ is stretched uniaxially along the armchair or zigzag direction. The stress is calculated without involving the actual thickness of the quasi-two-dimensional structure of the single-layer 1T-TcS₂. The Young's modulus can be obtained by a linear fitting of the stress-strain relation in the small strain range of $[0, 0.01]$. The Young's modulus is 84.3 and 84.0 N/m along the armchair and zigzag directions, respectively. The Young's modulus is essentially isotropic in the armchair and zigzag directions. The Poisson's ratio from the VFF model and the SW potential is $\nu_{xy} = \nu_{yx} = -0.10$. The fitted Young's modulus value is about 10% smaller than the *ab initio* result of 94 N/m [48], as only short-range interactions are considered in the present work. The long-range interactions are ignored, which typically leads to about 10% underestimation for the value of the Young's modulus.

	<i>A</i> (eV)	ρ (Å)	<i>B</i> (Å ⁴)	<i>r</i> _{min} (Å)	<i>r</i> _{max} (Å)
Tc—S	1.945	0.939	16.380	0.0	3.142

Table 259. Two-body SW potential parameters for single-layer 1T-TcS₂ used by GULP [8] as expressed in Eq. (3).

	<i>K</i> (eV)	θ_0 (°)	ρ_1 (Å)	ρ_2 (Å)	<i>r</i> _{min 12} (Å)	<i>r</i> _{max 12} (Å)	<i>r</i> _{min 13} (Å)	<i>r</i> _{max 13} (Å)	<i>r</i> _{min 23} (Å)	<i>r</i> _{max 23} (Å)
Tc—S—S	70.512	79.800	0.939	0.939	0.0	3.142	0.0	3.142	0.0	4.193
θ _{S—Tc—Tc}	70.512	79.800	0.939	0.939	0.0	3.142	0.0	3.142	0.0	4.193

The angle θ_{ijk} in the first line indicates the bending energy for the angle with atom *i* as the apex.

Table 260. Three-body SW potential parameters for single-layer 1T-TcS₂ used by GULP [8] as expressed in Eq. (4).

	ϵ (eV)	σ (Å)	<i>a</i>	λ	γ	$\cos \theta_0$	<i>A</i> _L	<i>B</i> _L	<i>p</i>	<i>q</i>	Tol
Tc—S ₁ —S ₁	1.000	0.939	3.345	70.512	1.000	0.177	1.945	21.038	4	0	0.0

Table 261. SW potential parameters for single-layer 1T-TcS₂ used by LAMMPS [9] as expressed in Eqs. (9) and (10).

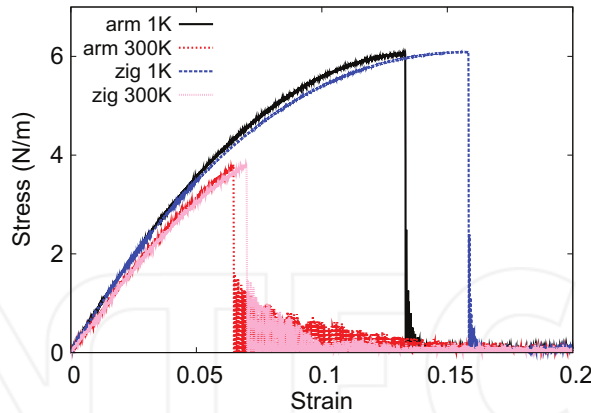


Figure 128. Stress-strain for single-layer 1T-TcS₂ of dimension 100 × 100 Å along the armchair and zigzag directions.

There is no available value for nonlinear quantities in the single-layer 1T-TcS₂. We have thus used the nonlinear parameter $B = 0.5d^4$ in Eq. (5), which is close to the value of B in most materials. The value of the third-order nonlinear elasticity D can be extracted by fitting the stress-strain relation to the function $\sigma = E\epsilon + \frac{1}{2}D\epsilon^2$ with E as the Young's modulus. The values of D from the present SW potential are -572.0 and -588.6 N/m along the armchair and zigzag directions, respectively. The ultimate stress is about 6.0 N/m at the ultimate strain of 0.13 in the armchair direction at the low temperature of 1 K. The ultimate stress is about 6.1 N/m at the ultimate strain of 0.16 in the zigzag direction at the low temperature of 1 K.

Figure 129 shows that the VFF model and the SW potential give exactly the same phonon dispersion, as the SW potential is derived from the VFF model.

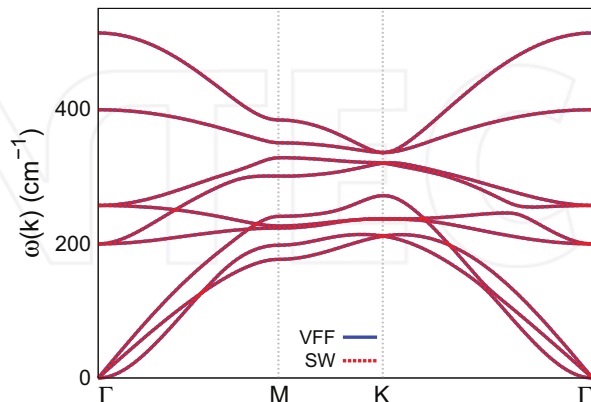


Figure 129. Phonon spectrum for single-layer 1T-TcS₂ along the ΓMKT direction in the Brillouin zone. The phonon dispersion from the SW potential is exactly the same as that from the VFF model.

66. 1T-TcSe₂

Most existing theoretical studies on the single-layer 1T-TcSe₂ are based on the first-principles calculations. In this section, we will develop the SW potential for the single-layer 1T-TcSe₂.

The structure for the single-layer 1T-TcSe₂ is shown in **Figure 71** (with M=Tc and X=Se). Each Tc atom is surrounded by six Se atoms. These Se atoms are categorized into the top group (e.g., atoms 1, 3, and 5) and bottom group (e.g., atoms 2, 4, and 6). Each Se atom is connected to three Tc atoms. The structural parameters are from the first-principles calculations [48], including the lattice constant $a = 3.1543 \text{ \AA}$ and the bond length $d_{\text{Tc-Se}} = 2.5061 \text{ \AA}$, which are derived from the angle $\theta_{\text{SeTcTc}} = 78^\circ$. The other angle is $\theta_{\text{TcSeSe}} = 78^\circ$ with Se atoms from the same (top or bottom) group.

Table 262 shows three VFF terms for the single-layer 1T-TcSe₂; one of which is the bond stretching interaction shown by Eq. (1), while the other two terms are the angle bending interaction shown by Eq. (2). We note that the angle bending term $K_{\text{Tc-Se-Se}}$ is for the angle $\theta_{\text{Tc-Se-Se}}$ with both Se atoms from the same (top or bottom) group. We find that there are actually only two parameters in the VFF model, so we can determine their value by fitting to the Young's modulus and the Poisson's ratio of the system. The *ab initio* calculations have predicted the Young's modulus to be 104 N/m and the Poisson's ratio as -0.04 [48]. The *ab initio* calculations have predicted a negative Poisson's ratio in the 1T-TcSe₂, which was attributed to the orbital coupling in this material. The orbital coupling enhances the angle bending interaction in the VFF model. As a result, the value of the angle bending parameter is much larger than the bond stretching force constant parameter, which is typical in auxetic materials with negative Poisson's ratio [52].

The parameters for the two-body SW potential used by GULP are shown in **Table 263**. The parameters for the three-body SW potential used by GULP are shown in **Table 264**. Some representative parameters for the SW potential used by LAMMPS are listed in **Table 265**.

VFF type	Bond stretching	Angle bending	
Expression	$\frac{1}{2} K_{\text{Tc-Se}}(\Delta r)^2$	$\frac{1}{2} K_{\text{Tc-Se-Se}}(\Delta\theta)^2$	$\frac{1}{2} K_{\text{Se-Tc-Tc}}(\Delta\theta)^2$
Parameter	3.467	10.636	10.636
r_0 or θ_0	2.506	78.001	78.001

The second line gives an explicit expression for each VFF term. The third line is the force constant parameters. Parameters are in the unit of ev/\text{\AA}^2 for the bond stretching interaction and in the unit of eV for the angle bending interaction. The fourth line gives the initial bond length (in the unit of \text{\AA}) for the bond stretching interaction and the initial angle (in the unit of degrees) for the angle bending interaction. The angle θ_{ijk} has atom i as the apex.

Table 262. The VFF model for single-layer 1T-TcSe₂.

	A (eV)	ρ (\text{\AA})	B (\text{\AA}^4)	r_{\min} (\text{\AA})	r_{\max} (\text{\AA})
Tc–Se	2.355	0.925	19.723	0.0	3.267

Table 263. Two-body SW potential parameters for single-layer 1T-TcSe₂ used by GULP [8] as expressed in Eq. (3).

	K (eV)	θ_0 ($^\circ$)	ρ_1 (\AA)	ρ_2 (\AA)	$r_{\min 12}$ (\AA)	$r_{\max 12}$ (\AA)	$r_{\min 13}$ (\AA)	$r_{\max 13}$ (\AA)	$r_{\min 23}$ (\AA)	$r_{\max 23}$ (\AA)
$\theta_{\text{Tc}-\text{Se}-\text{Se}}$	63.150	78.001	0.925	0.925	0.0	3.267	0.0	3.267	0.0	4.309
$\theta_{\text{Se}-\text{Tc}-\text{Tc}}$	63.150	78.001	0.925	0.925	0.0	3.267	0.0	3.267	0.0	4.309

The angle θ_{ijk} in the first line indicates the bending energy for the angle with atom i as the apex.

Table 264. Three-body SW potential parameters for single-layer 1T-TcSe₂ used by GULP [8] as expressed in Eq. (4).

	ϵ (eV)	σ (\AA)	a	λ	γ	$\cos \theta_0$	A_L	B_L	p	q	Tol
Tc—Se ₁ —Se ₁	1.000	0.925	3.532	63.150	1.000	0.208	2.355	26.932	4	0	0.0

Table 265. SW potential parameters for single-layer 1T-TcSe₂ used by LAMMPS [9] as expressed in Eqs. (9) and (10).

We use LAMMPS to perform MD simulations for the mechanical behavior of the single-layer 1T-TcSe₂ under uniaxial tension at 1 and 300 K. **Figure 130** shows the stress-strain curve for the tension of a single-layer 1T-TcSe₂ of dimension 100 × 100 Å. Periodic boundary conditions are applied in both armchair and zigzag directions. The single-layer 1T-TcSe₂ is stretched uniaxially along the armchair or zigzag direction. The stress is calculated without involving the actual thickness of the quasi-two-dimensional structure of the single-layer 1T-TcSe₂. The Young's modulus can be obtained by a linear fitting of the stress-strain relation in the small strain range of [0, 0.01]. The Young's modulus is 88.8 and 88.3 N/m along the armchair and zigzag directions, respectively. The Young's modulus is essentially isotropic in the armchair and zigzag directions. The Poisson's ratio from the VFF model and the SW potential is $\nu_{xy} = \nu_{yx} = -0.04$. The fitted Young's modulus value is about 10% smaller than the *ab initio* result of 104 N/m [48], as only short-range interactions are considered in the present work. The long-range interactions are ignored, which typically leads to about 10% underestimation for the value of the Young's modulus.

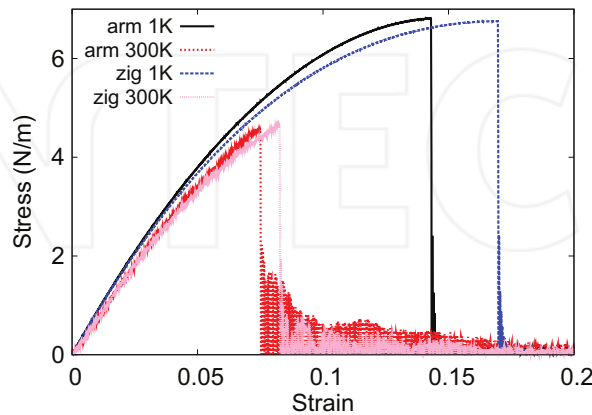


Figure 130. Stress-strain for single-layer 1T-TcSe₂ of dimension 100 × 100 Å along the armchair and zigzag directions.

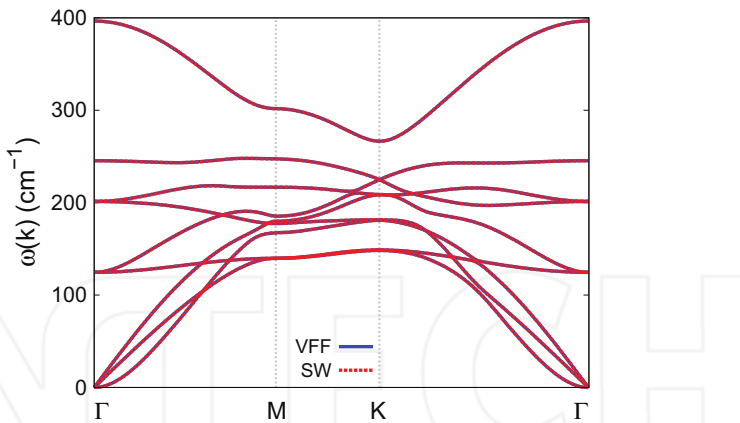


Figure 131. Phonon spectrum for single-layer 1T-TcSe₂ along the ΓMKΓ direction in the Brillouin zone. The phonon dispersion from the SW potential is exactly the same as that from the VFF model.

There is no available value for nonlinear quantities in the single-layer 1T-TcSe₂. We have thus used the nonlinear parameter $B = 0.5d^4$ in Eq. (5), which is close to the value of B in most materials. The value of the third-order nonlinear elasticity D can be extracted by fitting the stress-strain relation to the function $\sigma = E\epsilon + \frac{1}{2}D\epsilon^2$ with E as the Young's modulus. The values of D from the present SW potential are -565.7 and -587.3 N/m along the armchair and zigzag directions, respectively. The ultimate stress is about 6.8 N/m at the ultimate strain of 0.14 in the armchair direction at the low temperature of 1 K. The ultimate stress is about 6.8 N/m at the ultimate strain of 0.17 in the zigzag direction at the low temperature of 1 K.

Figure 131 shows that the VFF model and the SW potential give exactly the same phonon dispersion, as the SW potential is derived from the VFF model.

67. 1T-TcTe₂

Most existing theoretical studies on the single-layer 1T-TcTe₂ are based on the first-principles calculations. In this section, we will develop the SW potential for the single-layer 1T-TcTe₂.

The structure for the single-layer 1T-TcTe₂ is shown in **Figure 71** (with M=Tc and X=Te). Each Tc atom is surrounded by six Te atoms. These Te atoms are categorized into the top group (e.g., atoms 1, 3, and 5) and bottom group (e.g., atoms 2, 4, and 6). Each Te atom is connected to three Tc atoms. The structural parameters are from the first-principles calculations [48], including the lattice constant $a = 3.4149$ Å and the bond length $d_{\text{Tc}-\text{Te}} = 2.6900$ Å, which are derived from the angle $\theta_{\text{TeTcTc}} = 78.8^\circ$. The other angle is $\theta_{\text{TcTeTe}} = 78.8^\circ$ with Te atoms from the same (top or bottom) group.

Table 266 shows three VFF terms for the single-layer 1T-TcTe₂; one of which is the bond stretching interaction shown by Eq. (1), while the other two terms are the angle bending

VFF type	Bond stretching	Angle bending	
Expression	$\frac{1}{2}K_{\text{Tc}-\text{Te}}(\Delta r)^2$	$\frac{1}{2}K_{\text{Tc}-\text{Te}-\text{Te}}(\Delta\theta)^2$	$\frac{1}{2}K_{\text{Te}-\text{Tc}-\text{Tc}}(\Delta\theta)^2$
Parameter	0.785	8.894	8.894
r_0 or θ_0	2.690	78.801	78.801

The second line gives an explicit expression for each VFF term. The third line is the force constant parameters. Parameters are in the unit of $\text{eV}/\text{\AA}^2$ for the bond stretching interaction and in the unit of eV for the angle bending interaction. The fourth line gives the initial bond length (in the unit of \AA) for the bond stretching interaction and the initial angle (in the unit of degrees) for the angle bending interaction. The angle θ_{ijk} has atom i as the apex.

Table 266. The VFF model for single-layer 1T-TcTe₂.

interaction shown by Eq. (2). We note that the angle bending term $K_{\text{Tc}-\text{Te}-\text{Te}}$ is for the angle $\theta_{\text{Tc}-\text{Te}-\text{Te}}$ with both Te atoms from the same (top or bottom) group. We find that there are actually only two parameters in the VFF model, so we can determine their value by fitting to the Young's modulus and the Poisson's ratio of the system. The *ab initio* calculations have predicted the Young's modulus to be 34 N/m and the Poisson's ratio as -0.36 [48]. The *ab initio* calculations have predicted a negative Poisson's ratio in the 1T-TcTe₂, which was attributed to the orbital coupling in this material. The orbital coupling enhances the angle bending interaction in the VFF model. As a result, the value of the angle bending parameter is much larger than the bond stretching force constant parameter, which is typical in auxetic materials with negative Poisson's ratio [52].

The parameters for the two-body SW potential used by GULP are shown in **Table 267**. The parameters for the three-body SW potential used by GULP are shown in **Table 268**. Some representative parameters for the SW potential used by LAMMPS are listed in **Table 269**.

	A (eV)	ρ (\text{\AA})	B (\text{\AA}⁴)	r_{\min} (\text{\AA})	r_{\max} (\text{\AA})
Tc—Te	0.628	1.021	26.181	0.0	3.519

Table 267. Two-body SW potential parameters for single-layer 1T-TcTe₂ used by GULP [8] as expressed in Eq. (3).

	K (eV)	θ_0 (°)	ρ_1 (\text{\AA})	ρ_2 (\text{\AA})	$r_{\min 12}$ (\text{\AA})	$r_{\max 12}$ (\text{\AA})	$r_{\min 13}$ (\text{\AA})	$r_{\max 13}$ (\text{\AA})	$r_{\min 23}$ (\text{\AA})	$r_{\max 23}$ (\text{\AA})
$\theta_{\text{Tc}-\text{Te}-\text{Te}}$	54.313	78.801	1.021	1.021	0.0	3.519	0.0	3.519	0.0	4.665
$\theta_{\text{Te}-\text{Tc}-\text{Tc}}$	54.313	78.801	1.021	1.021	0.0	3.519	0.0	3.519	0.0	4.665

The angle θ_{ijk} in the first line indicates the bending energy for the angle with atom i as the apex.

Table 268. Three-body SW potential parameters for single-layer 1T-TcTe₂ used by GULP [8] as expressed in Eq. (4).

	ϵ (eV)	σ (\text{\AA})	a	λ	γ	$\cos\theta_0$	A_L	B_L	p	q	Tol
Tc—Te ₁ —Te ₁	1.000	1.021	3.447	54.313	1.000	0.194	0.628	24.110	4	0	0.0

Table 269. SW potential parameters for single-layer 1T-TcTe₂ used by LAMMPS [9] as expressed in Eqs. (9) and (10).

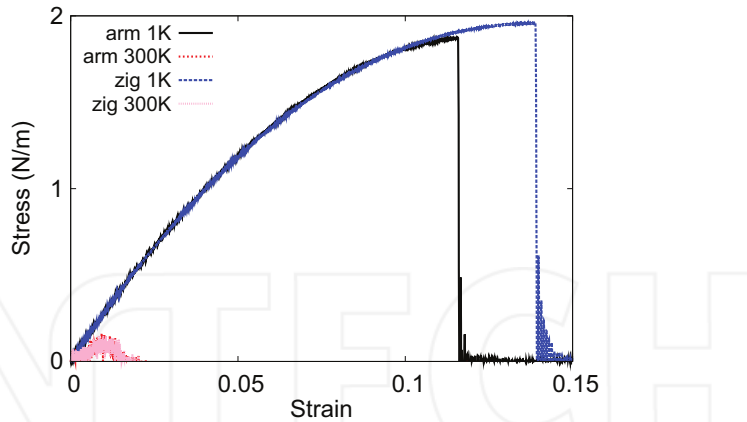


Figure 132. Stress-strain for single-layer 1T-TcTe₂ of dimension 100 × 100 Å along the armchair and zigzag directions.

We use LAMMPS to perform MD simulations for the mechanical behavior of the single-layer 1T-TcTe₂ under uniaxial tension at 1 and 300 K. **Figure 132** shows the stress-strain curve for the tension of a single-layer 1T-TcTe₂ of dimension 100 × 100 Å. Periodic boundary conditions are applied in both armchair and zigzag directions. The single-layer 1T-TcTe₂ is stretched uniaxially along the armchair or zigzag direction. The stress is calculated without involving the actual thickness of the quasi-two-dimensional structure of the single-layer 1T-TcTe₂. The Young's modulus can be obtained by a linear fitting of the stress-strain relation in the small strain range of [0, 0.01]. The Young's modulus is 28.6 N/m along the armchair and zigzag directions. The Poisson's ratio from the VFF model and the SW potential is $\nu_{xy} = \nu_{yx} = -0.21$. The fitted Young's modulus value is about 10% smaller than the *ab initio* result of 34 N/m [48], as only short-range interactions are considered in the present work. The long-range interactions are ignored, which typically leads to about 10% underestimation for the value of the Young's modulus.

There is no available value for nonlinear quantities in the single-layer 1T-TcTe₂. We have thus used the nonlinear parameter $B = 0.5d^4$ in Eq. (5), which is close to the value of B in most materials. The value of the third-order nonlinear elasticity D can be extracted by fitting the stress-strain relation to the function $\sigma = E\epsilon + \frac{1}{2}D\epsilon^2$ with E as the Young's modulus. The values of D from the present SW potential are -207.8 and -208.7 N/m along the armchair and zigzag directions, respectively. The ultimate stress is about 1.9 N/m at the ultimate strain of 0.11 in the armchair direction at the low temperature of 1 K. The ultimate stress is about 2.0 N/m at the ultimate strain of 0.14 in the zigzag direction at the low temperature of 1 K. The ultimate strain decreases to be about 0.01 at 300 K, so the single-layer 1T-TcTe₂ is not very stable at higher temperature. It is because this material is very soft and the Poisson's ratio is very small (negative value).

Figure 133 shows that the VFF model and the SW potential give exactly the same phonon dispersion, as the SW potential is derived from the VFF model.

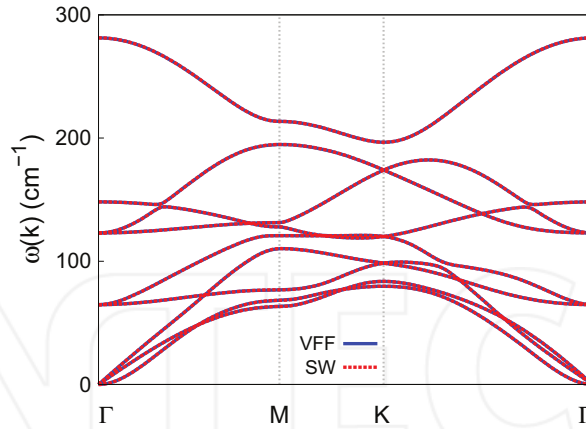


Figure 133. Phonon spectrum for single-layer 1T-TcTe₂ along the Γ -M-K- Γ direction in the Brillouin zone. The phonon dispersion from the SW potential is exactly the same as that from the VFF model.

68. 1T-RhTe₂

Most existing theoretical studies on the single-layer 1T-RhTe₂ are based on the first-principles calculations. In this section, we will develop the SW potential for the single-layer 1T-RhTe₂.

The structure for the single-layer 1T-RhTe₂ is shown in **Figure 71** (with M=Rh and X=Te). Each Rh atom is surrounded by six Te atoms. These Te atoms are categorized into the top group (e.g., atoms 1, 3, and 5) and bottom group (e.g., atoms 2, 4, and 6). Each Te atom is connected to three Rh atoms. The structural parameters are from the first-principles calculations [48], including the lattice constant $a = 3.7563 \text{ \AA}$ and the bond length $d_{\text{Rh}-\text{Te}} = 2.6332 \text{ \AA}$, which are derived from the angle $\theta_{\text{TeRhRh}} = 91^\circ$. The other angle is $\theta_{\text{RhTeTe}} = 91^\circ$ with Te atoms from the same (top or bottom) group.

Table 270 shows three VFF terms for the single-layer 1T-RhTe₂; one of which is the bond stretching interaction shown by Eq. (1), while the other two terms are the angle bending

VFF type	Bond stretching	Angle bending	
Expression	$\frac{1}{2} K_{\text{Rh}-\text{Te}} (\Delta r)^2$	$\frac{1}{2} K_{\text{Rh}-\text{Te}-\text{Te}} (\Delta\theta)^2$	$\frac{1}{2} K_{\text{Te}-\text{Rh}-\text{Rh}} (\Delta\theta)^2$
Parameter	4.366	1.869	1.869
r_0 or θ_0	2.633	91.001	91.001

The second line gives an explicit expression for each VFF term. The third line is the force constant parameters. Parameters are in the unit of eV/ \AA^2 for the bond stretching interaction and in the unit of eV for the angle bending interaction. The fourth line gives the initial bond length (in the unit of \AA) for the bond stretching interaction and the initial angle (in the unit of degrees) for the angle bending interaction. The angle θ_{ijk} has atom i as the apex.

Table 270. The VFF model for single-layer 1T-RhTe₂.

interaction shown by Eq. (2). We note that the angle bending term $K_{\text{Rh}-\text{Te}-\text{Te}}$ is for the angle $\theta_{\text{Rh}-\text{Te}-\text{Te}}$ with both Te atoms from the same (top or bottom) group. We find that there are actually only two parameters in the VFF model, so we can determine their value by fitting to the Young's modulus and the Poisson's ratio of the system. The *ab initio* calculations have predicted the Young's modulus to be 37 N/m and the Poisson's ratio as 0.20 [48].

The parameters for the two-body SW potential used by GULP are shown in **Table 271**. The parameters for the three-body SW potential used by GULP are shown in **Table 272**. Some representative parameters for the SW potential used by LAMMPS are listed in **Table 273**.

We use LAMMPS to perform MD simulations for the mechanical behavior of the single-layer 1T-RhTe₂ under uniaxial tension at 1 and 300 K. **Figure 134** shows the stress-strain curve for the tension of a single-layer 1T-RhTe₂ of dimension 100 × 100 Å. Periodic boundary conditions are applied in both armchair and zigzag directions. The single-layer 1T-RhTe₂ is stretched uniaxially along the armchair or zigzag direction. The stress is calculated without involving the actual thickness of the quasi-two-dimensional structure of the single-layer 1T-RhTe₂. The Young's modulus can be obtained by a linear fitting of the stress-strain relation in the small strain range of [0, 0.01]. The Young's modulus is 32.1 and 32.0 N/m along the armchair and zigzag directions, respectively. The Young's modulus is essentially isotropic in the armchair and zigzag directions. The Poisson's ratio from the VFF model and the SW potential is $\nu_{xy} = \nu_{yx} = 0.20$. The fitted Young's modulus value is about 10% smaller than the *ab initio* result of 37 N/m [48], as only short-range interactions are considered in the present work. The long-range interactions are ignored, which typically leads to about 10% underestimation for the value of the Young's modulus.

	A (eV)	ρ (Å)	B (Å ⁴)	r_{\min} (Å)	r_{\max} (Å)
Rh—Te	4.640	1.450	24.038	0.0	3.610

Table 271. Two-body SW potential parameters for single-layer 1T-RhTe₂ used by GULP [8] as expressed in Eq. (3).

	K (eV)	θ_0 (°)	ρ_1 (Å)	ρ_2 (Å)	$r_{\min 12}$ (Å)	$r_{\max 12}$ (Å)	$r_{\min 13}$ (Å)	$r_{\max 13}$ (Å)	$r_{\min 23}$ (Å)	$r_{\max 23}$ (Å)	
$\theta_{\text{Rh}-\text{Te}-\text{Te}}$	18.192	18.192	91.001	1.450	1.450	0.0	3.610	0.0	3.610	0.0	5.131
$\theta_{\text{Te}-\text{Rh}-\text{Rh}}$	18.192	18.192	91.001	1.450	1.450	0.0	3.610	0.0	3.610	0.0	5.131

The angle θ_{ijk} in the first line indicates the bending energy for the angle with atom i as the apex.

Table 272. Three-body SW potential parameters for single-layer 1T-RhTe₂ used by GULP [8] as expressed in Eq. (4).

	ϵ (eV)	σ (Å)	a	λ	γ	$\cos \theta_0$	A_L	B_L	p	q	Tol
Rh—Te ₁ —Te ₁	1.000	1.450	2.490	18.192	1.000	-0.017	4.640	5.436	4	0	0.0

Table 273. SW potential parameters for single-layer 1T-RhTe₂ used by LAMMPS [9] as expressed in Eqs. (9) and (10).

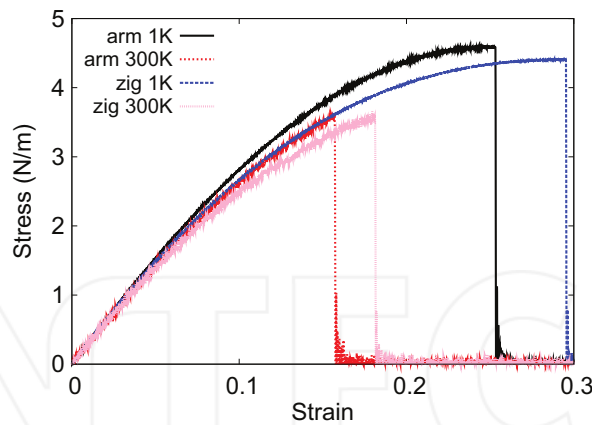


Figure 134. Stress-strain for single-layer 1T-RhTe₂ of dimension 100 × 100 Å along the armchair and zigzag directions.

There is no available value for nonlinear quantities in the single-layer 1T-RhTe₂. We have thus used the nonlinear parameter $B = 0.5d^4$ in Eq. (5), which is close to the value of B in most materials. The value of the third-order nonlinear elasticity D can be extracted by fitting the stress-strain relation to the function $\sigma = E\epsilon + \frac{1}{2}D\epsilon^2$ with E as the Young's modulus. The values of D from the present SW potential are -103.1 and -116.5 N/m along the armchair and zigzag directions, respectively. The ultimate stress is about 4.6 N/m at the ultimate strain of 0.25 in the armchair direction at the low temperature of 1 K. The ultimate stress is about 4.4 N/m at the ultimate strain of 0.29 in the zigzag direction at the low temperature of 1 K.

Figure 135 shows that the VFF model and the SW potential give exactly the same phonon dispersion, as the SW potential is derived from the VFF model.

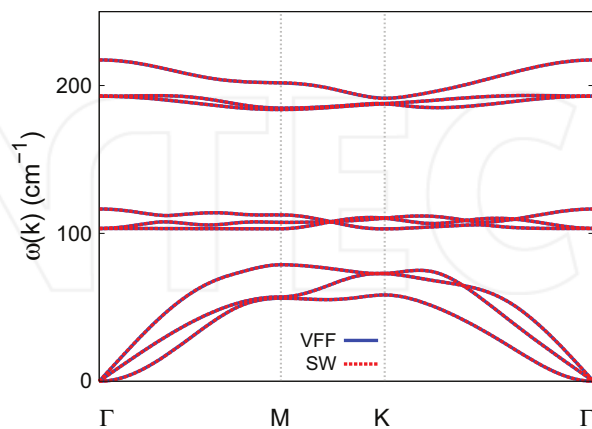


Figure 135. Phonon spectrum for single-layer 1T-RhTe₂ along the Γ -M-K- Γ direction in the Brillouin zone. The phonon dispersion from the SW potential is exactly the same as that from the VFF model.

69. 1T-PdS₂

Most existing theoretical studies on the single-layer 1T-PdS₂ are based on the first-principles calculations. In this section, we will develop the SW potential for the single-layer 1T-PdS₂.

The structure for the single-layer 1T-PdS₂ is shown in **Figure 71** (with M=Pd and X=S). Each Pd atom is surrounded by six S atoms. These S atoms are categorized into the top group (e.g., atoms 1, 3, and 5) and bottom group (e.g., atoms 2, 4, and 6). Each S atom is connected to three Pd atoms. The structural parameters are from the first-principles calculations [48], including the lattice constant $a = 3.5408 \text{ \AA}$ and the bond length $d_{\text{Pd-S}} = 2.4013 \text{ \AA}$, which are derived from the angle $\theta_{\text{SPdPd}} = 95^\circ$. The other angle is $\theta_{\text{PdSS}} = 95^\circ$ with S atoms from the same (top or bottom) group.

Table 274 shows three VFF terms for the single-layer 1T-PdS₂; one of which is the bond stretching interaction shown by Eq. (1), while the other two terms are the angle bending interaction shown by Eq. (2). We note that the angle bending term $K_{\text{Pd-S-S}}$ is for the angle $\theta_{\text{Pd-S-S}}$ with both S atoms from the same (top or bottom) group. We find that there are actually only two parameters in the VFF model, so we can determine their value by fitting to the Young's modulus and the Poisson's ratio of the system. The *ab initio* calculations have predicted the Young's modulus to be 77 N/m and the Poisson's ratio as 0.53 [48].

The parameters for the two-body SW potential used by GULP are shown in **Table 275**. The parameters for the three-body SW potential used by GULP are shown in **Table 276**. Some representative parameters for the SW potential used by LAMMPS are listed in **Table 277**.

We use LAMMPS to perform MD simulations for the mechanical behavior of the single-layer 1T-PdS₂ under uniaxial tension at 1 and 300 K. **Figure 136** shows the stress-strain curve for the tension of a single-layer 1T-PdS₂ of dimension $100 \times 100 \text{ \AA}$. Periodic boundary conditions are applied in both armchair and zigzag directions. The single-layer 1T-PdS₂ is stretched

VFF type	Bond stretching	Angle bending
Expression	$\frac{1}{2}K_{\text{Pd-S}}(\Delta r)^2$	$\frac{1}{2}K_{\text{Pd-S-S}}(\Delta\theta)^2$
Parameter	10.374	3.122
r_0 or θ_0	2.401	94.998

The second line gives an explicit expression for each VFF term. The third line is the force constant parameters. Parameters are in the unit of eV/Å² for the bond stretching interaction and in the unit of eV for the angle bending interaction. The fourth line gives the initial bond length (in the unit of Å) for the bond stretching interaction and the initial angle (in the unit of degrees) for the angle bending interaction. The angle θ_{ijk} has atom *i* as the apex.

Table 274. The VFF model for single-layer 1T-PdS₂.

	A (eV)	ρ (Å)	B (Å ⁴)	r_{\min} (Å)	r_{\max} (Å)
Pd—S	10.116	1.467	16.625	0.0	3.340

Table 275. Two-body SW potential parameters for single-layer 1T-PdS₂ used by GULP [8] as expressed in Eq. (3).

	K (eV)	θ_0 ($^\circ$)	ρ_1 (\AA)	ρ_2 (\AA)	$r_{\min 12}$ (\AA)	$r_{\max 12}$ (\AA)	$r_{\min 13}$ (\AA)	$r_{\max 13}$ (\AA)	$r_{\min 23}$ (\AA)	$r_{\max 23}$ (\AA)
$\theta_{\text{Pd-S-S}}$	35.859	94.998	1.467	1.467	0.0	3.340	0.0	3.340	0.0	4.837
$\theta_{\text{S-Pd-Pd}}$	35.859	94.998	1.467	1.467	0.0	3.340	0.0	3.340	0.0	4.837

The angle θ_{ijk} in the first line indicates the bending energy for the angle with atom i as the apex.

Table 276. Three-body SW potential parameters for single-layer 1T-PdS₂ used by GULP [8] as expressed in Eq. (4).

	ϵ (eV)	σ (\AA)	a	λ	γ	$\cos \theta_0$	A_L	B_L	p	q	Tol
Pd—S ₁ —S ₁	1.000	1.467	2.276	35.859	1.000	-0.087	10.116	3.588	4	0	0.0

Table 277. SW potential parameters for single-layer 1T-PdS₂ used by LAMMPS [9] as expressed in Eqs. (9) and (10).

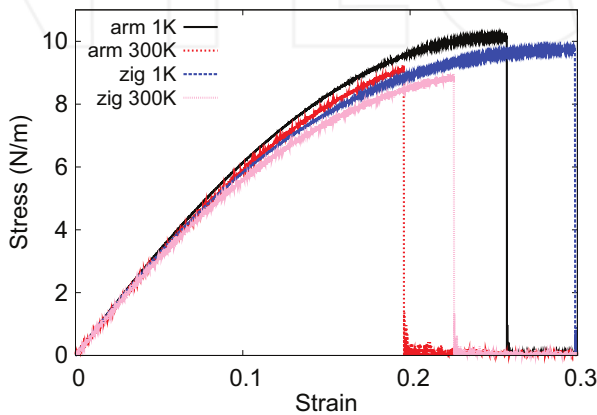


Figure 136. Stress-strain for single-layer 1T-PdS₂ of dimension $100 \times 100 \text{\AA}$ along the armchair and zigzag directions.

uniaxially along the armchair or zigzag direction. The stress is calculated without involving the actual thickness of the quasi-two-dimensional structure of the single-layer 1T-PdS₂. The Young's modulus can be obtained by a linear fitting of the stress-strain relation in the small strain range of $[0, 0.01]$. The Young's modulus is 69.9 and 69.5 N/m along the armchair and zigzag directions, respectively. The Young's modulus is essentially isotropic in the armchair and zigzag directions. The Poisson's ratio from the VFF model and the SW potential is $\nu_{xy} = \nu_{yx} = 0.20$. The fitted Young's modulus value is about 10% smaller than the *ab initio* result of 77 N/m [48], as only short-range interactions are considered in the present work. The long-range interactions are ignored, which typically leads to about 10% underestimation for the value of the Young's modulus.

There is no available value for nonlinear quantities in the single-layer 1T-PdS₂. We have thus used the nonlinear parameter $B = 0.5d^4$ in Eq. (5), which is close to the value of B in most materials. The value of the third-order nonlinear elasticity D can be extracted by fitting the stress-strain relation to the function $\sigma = E\epsilon + \frac{1}{2}D\epsilon^2$ with E as the Young's modulus. The values

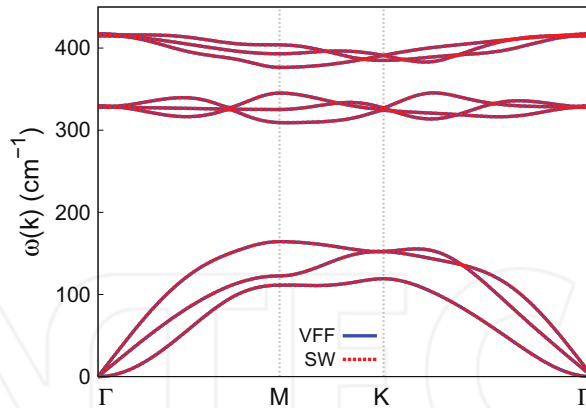


Figure 137. Phonon spectrum for single-layer 1T-PdS₂ along the Γ MKT direction in the Brillouin zone. The phonon dispersion from the SW potential is exactly the same as that from the VFF model.

of D from the present SW potential are -222.0 and -248.8 N/m along the armchair and zigzag directions, respectively. The ultimate stress is about 10.1 N/m at the ultimate strain of 0.25 in the armchair direction at the low temperature of 1 K. The ultimate stress is about 9.7 N/m at the ultimate strain of 0.30 in the zigzag direction at the low temperature of 1 K.

Figure 137 shows that the VFF model and the SW potential give exactly the same phonon dispersion, as the SW potential is derived from the VFF model.

70. 1T-PdSe₂

Most existing theoretical studies on the single-layer 1T-PdSe₂ are based on the first-principles calculations. In this section, we will develop the SW potential for the single-layer 1T-PdSe₂.

The structure for the single-layer 1T-PdSe₂ is shown in **Figure 71** (with M=Pd and X=Se). Each Pd atom is surrounded by six Se atoms. These Se atoms are categorized into the top group (e.g., atoms 1, 3, and 5) and bottom group (e.g., atoms 2, 4, and 6). Each Se atom is connected to three Pd atoms. The structural parameters are from the first-principles calculations [48], including the lattice constant $a = 3.6759$ Å and the bond length $d_{\text{Pd-Se}} = 2.4929$ Å, which are derived from the angle $\theta_{\text{SePdPd}} = 95^\circ$. The other angle is $\theta_{\text{PdSeSe}} = 95^\circ$ with Se atoms from the same (top or bottom) group.

Table 278 shows three VFF terms for the single-layer 1T-PdSe₂; one of which is the bond stretching interaction shown by Eq. (1), while the other two terms are the angle bending interaction shown by Eq. (2). We note that the angle bending term $K_{\text{Pd-Se-Se}}$ is for the angle $\theta_{\text{Pd-Se-Se}}$ with both Se atoms from the same (top or bottom) group. We find that there are actually only two parameters in the VFF model, so we can determine their value by fitting to the Young's modulus and the Poisson's ratio of the system. The *ab initio* calculations have predicted the Young's modulus to be 66 N/m and the Poisson's ratio as 0.45 [48].

VFF type	Bond stretching	Angle bending
Expression	$\frac{1}{2}K_{\text{Pd-Se}}(\Delta r)^2$	$\frac{1}{2}K_{\text{Pd-Se-Se}}(\Delta\theta)^2$
Parameter	10.374	3.122
r_0 or θ_0	2.493	94.999

The second line gives an explicit expression for each VFF term. The third line is the force constant parameters. Parameters are in the unit of $\text{eV}/\text{\AA}^2$ for the bond stretching interaction and in the unit of eV for the angle bending interaction. The fourth line gives the initial bond length (in the unit of \AA) for the bond stretching interaction and the initial angle (in the unit of degrees) for the angle bending interaction. The angle θ_{ijk} has atom i as the apex.

Table 278. The VFF model for single-layer 1T-PdSe₂.

The parameters for the two-body SW potential used by GULP are shown in **Table 279**. The parameters for the three-body SW potential used by GULP are shown in **Table 280**. Some representative parameters for the SW potential used by LAMMPS are listed in **Table 281**.

We use LAMMPS to perform MD simulations for the mechanical behavior of the single-layer 1T-PdSe₂ under uniaxial tension at 1 and 300 K. **Figure 138** shows the stress-strain curve for the tension of a single-layer 1T-PdSe₂ of dimension $100 \times 100 \text{\AA}$. Periodic boundary conditions are applied in both armchair and zigzag directions. The single-layer 1T-PdSe₂ is stretched uniaxially along the armchair or zigzag direction. The stress is calculated without involving the actual thickness of the quasi-two-dimensional structure of the single-layer 1T-PdSe₂. The Young's modulus can be obtained by a linear fitting of the stress-strain relation in the small strain range of [0, 0.01]. The Young's modulus is 65.5 and 65.3 N/m along the armchair and zigzag directions, respectively. The Young's modulus is essentially isotropic in the armchair and zigzag directions. The Poisson's ratio from the VFF model and the SW potential is $\nu_{xy} = \nu_{yx} = 0.21$.

	A (eV)	ρ (\AA)	B (\AA^4)	r_{\min} (\AA)	r_{\max} (\AA)
Pd—Se	10.902	1.523	19.310	0.0	3.467

Table 279. Two-body SW potential parameters for single-layer 1T-PdSe₂ used by GULP [8] as expressed in Eq. (3).

	K (eV)	θ_0 (°)	ρ_1 (\AA)	ρ_2 (\AA)	$r_{\min 12}$ (\AA)	$r_{\max 12}$ (\AA)	$r_{\min 13}$ (\AA)	$r_{\max 13}$ (\AA)	$r_{\min 23}$ (\AA)	$r_{\max 23}$ (\AA)
$\theta_{\text{Pd-Se-Se}}$	35.859	94.999	1.523	1.523	0.0	3.467	0.0	3.467	0.0	5.021
$\theta_{\text{Se-Pd-Pd}}$	35.859	94.999	1.523	1.523	0.0	3.467	0.0	3.467	0.0	5.021

The angle θ_{ijk} in the first line indicates the bending energy for the angle with atom i as the apex.

Table 280. Three-body SW potential parameters for single-layer 1T-PdSe₂ used by GULP [8] as expressed in Eq. (4).

	ϵ (eV)	σ (\AA)	a	λ	γ	$\cos\theta_0$	A_L	B_L	p	q	Tol
Pd—Se ₁ —Se ₁	1.000	1.523	2.276	35.859	1.000	-0.087	10.902	3.588	4	0	0.0

Table 281. SW potential parameters for single-layer 1T-PdSe₂ used by LAMMPS [9] as expressed in Eqs. (9) and (10).

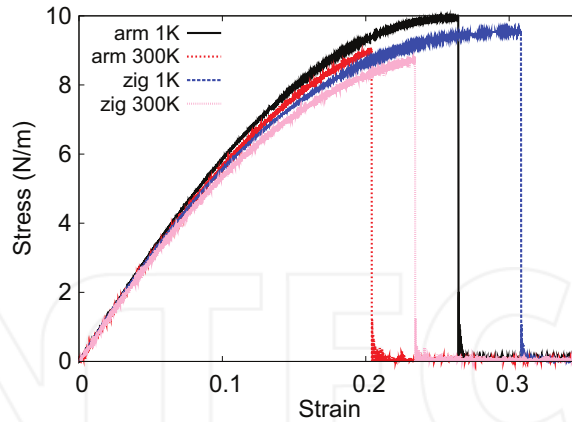


Figure 138. Stress-strain for single-layer 1T-PdSe₂ of dimension 100 × 100 Å along the armchair and zigzag directions.

There is no available value for nonlinear quantities in the single-layer 1T-PdSe₂. We have thus used the nonlinear parameter $B = 0.5d^4$ in Eq. (5), which is close to the value of B in most materials. The value of the third-order nonlinear elasticity D can be extracted by fitting the stress-strain relation to the function $\sigma = E\epsilon + \frac{1}{2}D\epsilon^2$ with E as the Young's modulus. The values of D from the present SW potential are -194.7 and -222.8 N/m along the armchair and zigzag directions, respectively. The ultimate stress is about 9.9 N/m at the ultimate strain of 0.26 in the armchair direction at the low temperature of 1 K. The ultimate stress is about 9.5 N/m at the ultimate strain of 0.31 in the zigzag direction at the low temperature of 1 K.

Figure 139 shows that the VFF model and the SW potential give exactly the same phonon dispersion, as the SW potential is derived from the VFF model.

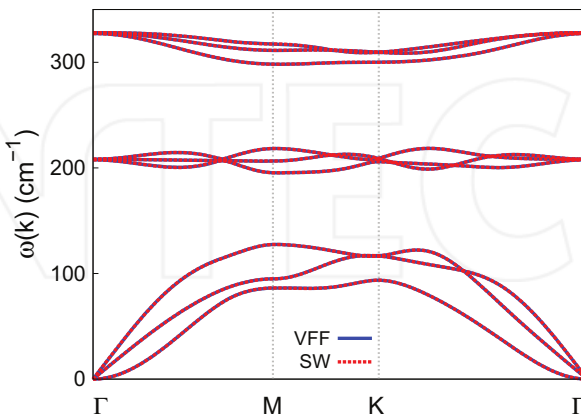


Figure 139. Phonon spectrum for single-layer 1T-PdSe₂ along the Γ -M-K- Γ direction in the Brillouin zone. The phonon dispersion from the SW potential is exactly the same as that from the VFF model.

71. 1T-PdTe₂

Most existing theoretical studies on the single-layer 1T-PdTe₂ are based on the first-principles calculations. In this section, we will develop the SW potential for the single-layer 1T-PdTe₂.

The structure for the single-layer 1T-PdTe₂ is shown in **Figure 71** (with M=Pd and X=Te). Each Pd atom is surrounded by six Te atoms. These Te atoms are categorized into the top group (e.g., atoms 1, 3, and 5) and bottom group (e.g., atoms 2, 4, and 6). Each Te atom is connected to three Pd atoms. The structural parameters are from the first-principles calculations [48], including the lattice constant $a = 3.9162 \text{ \AA}$ and the bond length $d_{\text{Pd}-\text{Te}} = 2.6349 \text{ \AA}$, which are derived from the angle $\theta_{\text{TePdPd}} = 96^\circ$. The other angle is $\theta_{\text{PdTeTe}} = 96^\circ$ with Te atoms from the same (top or bottom) group.

Table 282 shows three VFF terms for the single-layer 1T-PdTe₂; one of which is the bond stretching interaction shown by Eq. (1), while the other two terms are the angle bending interaction shown by Eq. (2). We note that the angle bending term $K_{\text{Pd}-\text{Te}-\text{Te}}$ is for the angle $\theta_{\text{Pd}-\text{Te}-\text{Te}}$ with both Te atoms from the same (top or bottom) group. We find that there are actually only two parameters in the VFF model, so we can determine their value by fitting to the Young's modulus and the Poisson's ratio of the system. The *ab initio* calculations have predicted the Young's modulus to be 63 N/m and the Poisson's ratio as 0.35 [48].

The parameters for the two-body SW potential used by GULP are shown in **Table 283**. The parameters for the three-body SW potential used by GULP are shown in **Table 284**. Some representative parameters for the SW potential used by LAMMPS are listed in **Table 285**.

We use LAMMPS to perform MD simulations for the mechanical behavior of the single-layer 1T-PdTe₂ under uniaxial tension at 1 and 300 K. **Figure 140** shows the stress-strain curve for the tension of a single-layer 1T-PdTe₂ of dimension 100 × 100 Å. Periodic boundary conditions are applied in both armchair and zigzag directions. The single-layer 1T-PdTe₂ is stretched

VFF type	Bond stretching	Angle bending	
Expression	$\frac{1}{2} K_{\text{Pd}-\text{Te}} (\Delta r)^2$	$\frac{1}{2} K_{\text{Pd}-\text{Te}-\text{Te}} (\Delta \theta)^2$	$\frac{1}{2} K_{\text{Te}-\text{Pd}-\text{Pd}} (\Delta \theta)^2$
Parameter	10.374	3.122	3.122
r_0 or θ_0	2.635	95.999	95.999

The second line gives an explicit expression for each VFF term. The third line is the force constant parameters. Parameters are in the unit of ev/Å² for the bond stretching interaction and in the unit of eV for the angle bending interaction. The fourth line gives the initial bond length (in the unit of Å) for the bond stretching interaction and the initial angle (in the unit of degrees) for the angle bending interaction. The angle θ_{ijk} has atom i as the apex.

Table 282. The VFF model for single-layer 1T-PdTe₂.

	A (eV)	ρ (Å)	B (Å ⁴)	r_{\min} (Å)	r_{\max} (Å)
Pd—Te	12.474	1.650	24.101	0.0	3.678

Table 283. Two-body SW potential parameters for single-layer 1T-PdTe₂ used by GULP [8] as expressed in Eq. (3).

	K (eV)	θ_0 ($^\circ$)	ρ_1 (\AA)	ρ_2 (\AA)	$r_{\min 12}$ (\AA)	$r_{\max 12}$ (\AA)	$r_{\min 13}$ (\AA)	$r_{\max 13}$ (\AA)	$r_{\min 23}$ (\AA)	$r_{\max 23}$ (\AA)
$\theta_{\text{Pd}-\text{Te}-\text{Te}}$	37.406	95.999	1.650	1.650	0.0	3.678	0.0	3.678	0.0	5.350
$\theta_{\text{Te}-\text{Pd}-\text{Pd}}$	37.406	95.999	1.650	1.650	0.0	3.678	0.0	3.678	0.0	5.350

The angle θ_{ijk} in the first line indicates the bending energy for the angle with atom i as the apex.

Table 284. Three-body SW potential parameters for single-layer 1T-PdTe₂ used by GULP [8] as expressed in Eq. (4).

	ϵ (eV)	σ (\AA)	a	λ	γ	$\cos \theta_0$	A_L	B_L	p	q	Tol
Pd—Te ₁ —Te ₁	1.000	1.650	2.229	37.406	1.000	-0.105	12.474	3.250	4	0	0.0

Table 285. SW potential parameters for single-layer 1T-PdTe₂ used by LAMMPS [9] as expressed in Eqs. (9) and (10).

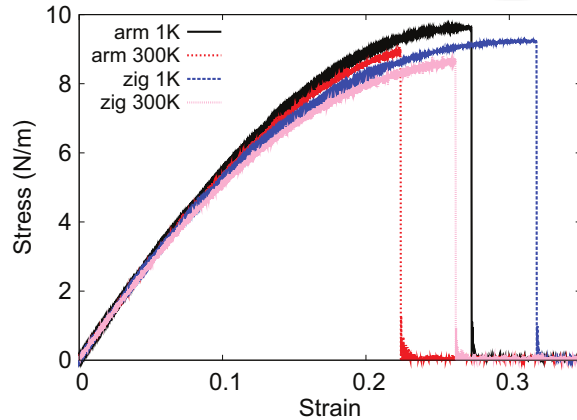


Figure 140. Stress-strain for single-layer 1T-PdTe₂ of dimension 100×100 \AA along the armchair and zigzag directions.

uniaxially along the armchair or zigzag direction. The stress is calculated without involving the actual thickness of the quasi-two-dimensional structure of the single-layer 1T-PdTe₂. The Young's modulus can be obtained by a linear fitting of the stress-strain relation in the small strain range of [0, 0.01]. The Young's modulus is 61.6 and 61.4 N/m along the armchair and zigzag directions, respectively. The Young's modulus is essentially isotropic in the armchair and zigzag directions. The Poisson's ratio from the VFF model and the SW potential is $\nu_{xy} = \nu_{yx} = 0.22$.

There is no available value for nonlinear quantities in the single-layer 1T-PdTe₂. We have thus used the nonlinear parameter $B = 0.5d^4$ in Eq. (5), which is close to the value of B in most materials. The value of the third-order nonlinear elasticity D can be extracted by fitting the stress-strain relation to the function $\sigma = E\epsilon + \frac{1}{2}D\epsilon^2$ with E as the Young's modulus. The values of D from the present SW potential are -178.8 and -203.8 N/m along the armchair and zigzag

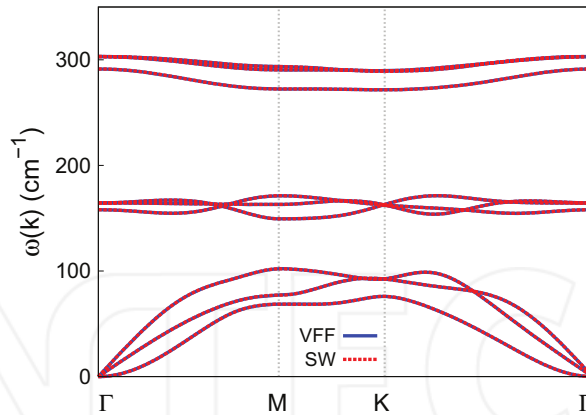


Figure 141. Phonon spectrum for single-layer 1T-PdTe₂ along the Γ M \mathbf{K} Γ direction in the Brillouin zone. The phonon dispersion from the SW potential is exactly the same as that from the VFF model.

directions, respectively. The ultimate stress is about 9.6 N/m at the ultimate strain of 0.27 in the armchair direction at the low temperature of 1 K. The ultimate stress is about 9.2 N/m at the ultimate strain of 0.32 in the zigzag direction at the low temperature of 1 K.

Figure 141 shows that the VFF model and the SW potential give exactly the same phonon dispersion, as the SW potential is derived from the VFF model.

72. 1T-SnS₂

Most existing theoretical studies on the single-layer 1T-SnS₂ are based on the first-principles calculations. In this section, we will develop the SW potential for the single-layer 1T-SnS₂.

The structure for the single-layer 1T-SnS₂ is shown in **Figure 71** (with M=Sn and X=S). Each Sn atom is surrounded by six S atoms. These S atoms are categorized into the top group (e.g., atoms 1, 3, and 5) and bottom group (e.g., atoms 2, 4, and 6). Each S atom is connected to three Sn atoms. The structural parameters are from the first-principles calculations [34], including the lattice constant $a = 3.640 \text{ \AA}$ and the bond length $d_{\text{Sn-S}} = 2.570 \text{ \AA}$. The resultant angles are $\theta_{\text{SSnSn}} = 90.173^\circ$ and $\theta_{\text{SnSS}} = 90.173^\circ$ with S atoms from the same (top or bottom) group.

Table 286 shows three VFF terms for the single-layer 1T-SnS₂; one of which is the bond stretching interaction shown by Eq. (1), while the other two terms are the angle bending interaction shown by Eq. (2). We note that the angle bending term $K_{\text{Sn-S-S}}$ is for the angle $\theta_{\text{Sn-S-S}}$ with both S atoms from the same (top or bottom) group. These force constant parameters are determined by fitting to the acoustic branches in the phonon dispersion along the Γ M as shown in **Figure 142(a)**. The *ab initio* calculations for the phonon dispersion are from Ref. [34]. The lowest acoustic branch (flexural mode) is almost linear in the *ab initio* calculations, which may be due to the violation of the rigid rotational invariance [20]. **Figure 142(b)** shows

VFF type	Bond stretching	Angle bending
Expression	$\frac{1}{2}K_{\text{Sn-S}}(\Delta r)^2$	$\frac{1}{2}K_{\text{Sn-S-S}}(\Delta\theta)^2$
Parameter	7.872	5.817
r_0 or θ_0	2.570	90.173

The second line gives an explicit expression for each VFF term. The third line is the force constant parameters. Parameters are in the unit of $\text{eV}/\text{\AA}^2$ for the bond stretching interaction and in the unit of eV for the angle bending interaction. The fourth line gives the initial bond length (in the unit of \AA) for the bond stretching interaction and the initial angle (in the unit of degrees) for the angle bending interaction. The angle θ_{ijk} has atom i as the apex.

Table 286. The VFF model for single-layer 1T-SnS₂.

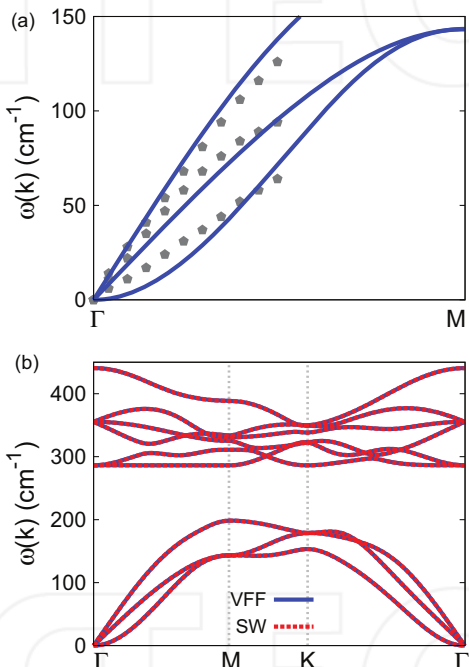


Figure 142. Phonon spectrum for single-layer 1T-SnS₂. (a) Phonon dispersion along the ΓM direction in the Brillouin zone. The results from the VFF model (lines) are comparable with the *ab initio* results (pentagons) from Ref. [34]. (b) The phonon dispersion from the SW potential is exactly the same as that from the VFF model.

that the VFF model and the SW potential give exactly the same phonon dispersion, as the SW potential is derived from the VFF model.

The parameters for the two-body SW potential used by GULP are shown in **Table 287**. The parameters for the three-body SW potential used by GULP are shown in **Table 288**. Some representative parameters for the SW potential used by LAMMPS are listed in **Table 289**.

	A (eV)	ρ (Å)	B (Å ⁴)	r_{\min} (Å)	r_{\max} (Å)
Sn—S	7.805	1.384	21.812	0.0	3.513

Table 287. Two-body SW potential parameters for single-layer 1T-SnS₂ used by GULP [8] as expressed in Eq. (3).

	K (eV)	θ_0 (°)	ρ_1 (Å)	ρ_2 (Å)	$r_{\min 12}$ (Å)	$r_{\max 12}$ (Å)	$r_{\min 13}$ (Å)	$r_{\max 13}$ (Å)	$r_{\min 23}$ (Å)	$r_{\max 23}$ (Å)
$\theta_{\text{Sn-S-S}}$	54.748	90.173	1.384	1.384	0.0	3.513	0.0	3.513	0.0	4.972
$\theta_{\text{S-Sn-Sn}}$	54.748	90.173	1.384	1.384	0.0	3.513	0.0	3.513	0.0	4.972

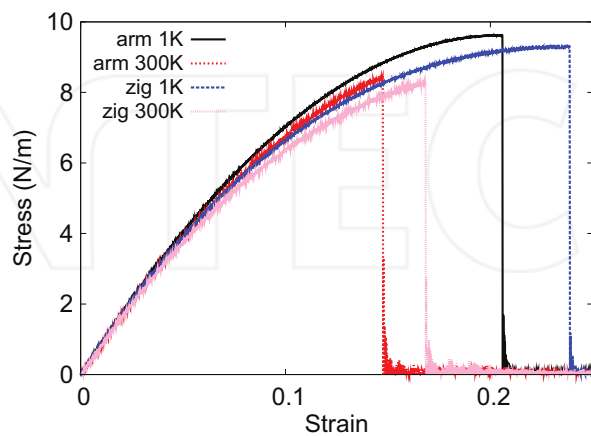
The angle θ_{ijk} in the first line indicates the bending energy for the angle with atom i as the apex.

Table 288. Three-body SW potential parameters for single-layer 1T-SnS₂ used by GULP [8] as expressed in Eq. (4).

	ϵ (eV)	σ (Å)	a	λ	γ	$\cos \theta_0$	A_L	B_L	p	q	Tol
Sn—S ₁ —S ₁	1.000	1.384	2.539	54.748	1.000	-0.003	7.805	5.949	4	0	0.0

Table 289. SW potential parameters for single-layer 1T-SnS₂ used by LAMMPS [9] as expressed in Eqs. (9) and (10).

We use LAMMPS to perform MD simulations for the mechanical behavior of the single-layer 1T-SnS₂ under uniaxial tension at 1 and 300 K. **Figure 143** shows the stress-strain curve for the tension of a single-layer 1T-SnS₂ of dimension 100 × 100 Å. Periodic boundary conditions are applied in both armchair and zigzag directions. The single-layer 1T-SnS₂ is stretched uniaxially along the armchair or zigzag direction. The stress is calculated without involving the actual thickness of the quasi-two-dimensional structure of the single-layer 1T-SnS₂. The Young's modulus can be obtained by a linear fitting of the stress-strain relation in the small strain range of [0, 0.01]. The Young's modulus is 88.4 and 87.9 N/m along the armchair and zigzag

**Figure 143.** Stress-strain for single-layer 1T-SnS₂ of dimension 100 × 100 Å along the armchair and zigzag directions.

directions, respectively. The Young's modulus is essentially isotropic in the armchair and zigzag directions. The Poisson's ratio from the VFF model and the SW potential is $\nu_{xy} = \nu_{yx} = 0.13$.

There is no available value for nonlinear quantities in the single-layer 1T-SnS₂. We have thus used the nonlinear parameter $B = 0.5d^4$ in Eq. (5), which is close to the value of B in most materials. The value of the third-order nonlinear elasticity D can be extracted by fitting the stress-strain relation to the function $\sigma = E\epsilon + \frac{1}{2}D\epsilon^2$ with E as the Young's modulus. The values of D from the present SW potential are -392.8 and -421.6 N/m along the armchair and zigzag directions, respectively. The ultimate stress is about 9.6 N/m at the ultimate strain of 0.20 in the armchair direction at the low temperature of 1 K. The ultimate stress is about 9.3 N/m at the ultimate strain of 0.24 in the zigzag direction at the low temperature of 1 K.

73. 1T-SnSe₂

Most existing theoretical studies on the single-layer 1T-SnSe₂ are based on the first-principles calculations. In this section, we will develop the SW potential for the single-layer 1T-SnSe₂.

The structure for the single-layer 1T-SnSe₂ is shown in **Figure 71** (with M=Sn and X=Se). Each Sn atom is surrounded by six Se atoms. These Se atoms are categorized into the top group (e.g., atoms 1, 3, and 5) and bottom group (e.g., atoms 2, 4, and 6). Each Se atom is connected to three Sn atoms. The structural parameters are from the first-principles calculations [34] including the lattice constant $a = 3.792$ Å and the bond length $d_{\text{Sn-Se}} = 2.704$ Å. The resultant angles are $\theta_{\text{SeSnSn}} = 89.044^\circ$ and $\theta_{\text{SnSeSe}} = 89.044^\circ$ with Se atoms from the same (top or bottom) group.

Table 290 shows three VFF terms for the single-layer 1T-SnSe₂; one of which is the bond stretching interaction shown by Eq. (1), while the other two terms are the angle bending interaction shown by Eq. (2). We note that the angle bending term $K_{\text{Sn-Se-Se}}$ is for the angle $\theta_{\text{Sn-Se-Se}}$ with both Se atoms from the same (top or bottom) group. These force constant parameters are determined by fitting to the acoustic branches in the phonon dispersion along the GM as shown in **Figure 144(a)**. The *ab initio* calculations for the phonon dispersion are from Ref. [34]. The lowest acoustic branch (flexural mode) is almost linear in the *ab initio*

VFF type	Bond stretching	Angle bending	
Expression	$\frac{1}{2}K_{\text{Sn-Se}}(\Delta r)^2$	$\frac{1}{2}K_{\text{Sn-Se-Se}}(\Delta\theta)^2$	$\frac{1}{2}K_{\text{Se-Sn-Sn}}(\Delta\theta)^2$
Parameter	7.872	5.817	5.817
r_0 or θ_0	2.704	89.044	89.044

The second line gives an explicit expression for each VFF term. The third line is the force constant parameters. Parameters are in the unit of eV/Å² for the bond stretching interaction and in the unit of eV for the angle bending interaction. The fourth line gives the initial bond length (in the unit of Å) for the bond stretching interaction and the initial angle (in the unit of degrees) for the angle bending interaction. The angle θ_{ijk} has atom i as the apex.

Table 290. The VFF model for single-layer 1T-SnSe₂.

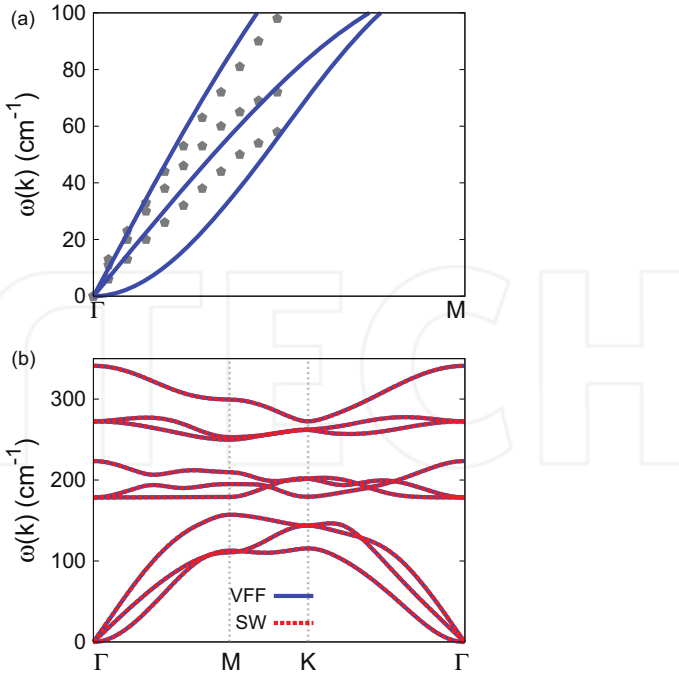


Figure 144. Phonon spectrum for single-layer 1T-SnSe₂. (a) Phonon dispersion along the TM direction in the Brillouin zone. The results from the VFF model (lines) are comparable with the *ab initio* results (pentagons) from Ref. [34]. (b) The phonon dispersion from the SW potential is exactly the same as that from the VFF model.

calculations, which may be due to the violation of the rigid rotational invariance [20]. **Figure 144(b)** shows that the VFF model and the SW potential give exactly the same phonon dispersion, as the SW potential is derived from the VFF model.

The parameters for the two-body SW potential used by GULP are shown in **Table 291**. The parameters for the three-body SW potential used by GULP are shown in **Table 292**. Some representative parameters for the SW potential used by LAMMPS are listed in **Table 293**.

We use LAMMPS to perform MD simulations for the mechanical behavior of the single-layer 1T-SnSe₂ under uniaxial tension at 1 and 300 K. **Figure 145** shows the stress-strain curve for the tension of a single-layer 1T-SnSe₂ of dimension 100 × 100 Å. Periodic boundary conditions are applied in both armchair and zigzag directions. The single-layer 1T-SnSe₂ is stretched uniaxially along the armchair or zigzag direction. The stress is calculated without involving the actual thickness of the quasi-two-dimensional structure of the single-layer 1T-SnSe₂. The

	A (eV)	ρ (Å)	B (Å ⁴)	r_{\min} (Å)	r_{\max} (Å)
Sn–Se	8.395	1.411	26.730	0.0	3.681

Table 291. Two-body SW potential parameters for single-layer 1T-SnSe₂ used by GULP [8] as expressed in Eq. (3).

	K (eV)	θ_0 ($^\circ$)	ρ_1 (\AA)	ρ_2 (\AA)	$r_{\min 12}$ (\AA)	$r_{\max 12}$ (\AA)	$r_{\min 13}$ (\AA)	$r_{\max 13}$ (\AA)	$r_{\min 23}$ (\AA)	$r_{\max 23}$ (\AA)
$\theta_{\text{Sn}-\text{Se}-\text{Se}}$	52.322	89.044	1.411	1.411	0.0	3.681	0.0	3.681	0.0	5.180
$\theta_{\text{Se}-\text{Sn}-\text{Sn}}$	52.322	89.044	1.411	1.411	0.0	3.681	0.0	3.681	0.0	5.180

The angle θ_{ijk} in the first line indicates the bending energy for the angle with atom i as the apex.

Table 292. Three-body SW potential parameters for single-layer 1T-SnSe₂ used by GULP [8] as expressed in Eq. (4).

	ϵ (eV)	σ (\AA)	a	λ	γ	$\cos \theta_0$	A_L	B_L	p	q	Tol
Sn–Se ₁ –Se ₁	1.000	1.411	2.609	52.322	1.000	0.017	8.395	6.743	4	0	0.0

Table 293. SW potential parameters for single-layer 1T-SnSe₂ used by LAMMPS [9] as expressed in Eqs. (9) and (10).

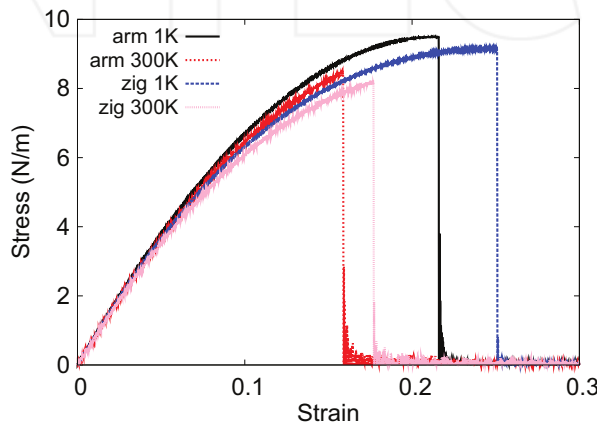


Figure 145. Stress-strain for single-layer 1T-SnSe₂ of dimension 100×100 \AA along the armchair and zigzag directions.

Young's modulus can be obtained by a linear fitting of the stress-strain relation in the small strain range of [0, 0.01]. The Young's modulus is 82.0 and 81.6 N/m along the armchair and zigzag directions, respectively. The Young's modulus is essentially isotropic in the armchair and zigzag directions. The Poisson's ratio from the VFF model and the SW potential is $\nu_{xy} = \nu_{yx} = 0.15$.

There is no available value for nonlinear quantities in the single-layer 1T-SnSe₂. We have thus used the nonlinear parameter $B = 0.5d^4$ in Eq. (5), which is close to the value of B in most materials. The value of the third-order nonlinear elasticity D can be extracted by fitting the stress-strain relation to the function $\sigma = E\epsilon + \frac{1}{2}D\epsilon^2$ with E as the Young's modulus. The values of D from the present SW potential are -339.2 and -368.3 N/m along the armchair and zigzag directions, respectively. The ultimate stress is about 9.5 N/m at the ultimate strain of 0.21 in the armchair direction at the low temperature of 1 K. The ultimate stress is about 9.1 N/m at the ultimate strain of 0.25 in the zigzag direction at the low temperature of 1 K.

74. 1T-HfS₂

Most existing theoretical studies on the single-layer 1T-HfS₂ are based on the first-principles calculations. In this section, we will develop the SW potential for the single-layer 1T-HfS₂.

The structure for the single-layer 1T-HfS₂ is shown in **Figure 71** (with M=Hf and X=S). Each Hf atom is surrounded by six S atoms. These S atoms are categorized into the top group (e.g., atoms 1, 3, and 5) and bottom group (e.g., atoms 2, 4, and 6). Each S atom is connected to three Hf atoms. The structural parameters are from the first-principles calculations [53], including the lattice constant $a = 3.64 \text{ \AA}$ and the bond length $d_{\text{Hf-S}} = 2.55 \text{ \AA}$. The resultant angles are $\theta_{\text{HfSS}} = 91.078^\circ$ with S atoms from the same (top or bottom) group and $\theta_{\text{SHfHF}} = 91.078^\circ$.

Table 294 shows three VFF terms for the single-layer 1T-HfS₂; one of which is the bond stretching interaction shown by Eq. (1), while the other two terms are the angle bending interaction shown by Eq. (2). We note that the angle bending term $K_{\text{Hf-S-S}}$ is for the angle $\theta_{\text{Hf-S-S}}$ with both S atoms from the same (top or bottom) group. These force constant parameters are determined by fitting to the three acoustic branches in the phonon dispersion along the ΓM as shown in **Figure 146(a)**. The *ab initio* calculations for the phonon dispersion are from Ref. [38]. Similar phonon dispersion can also be found in other *ab initio* calculations [34, 35]. **Figure 146(b)** shows that the VFF model and the SW potential give exactly the same phonon dispersion, as the SW potential is derived from the VFF model.

The parameters for the two-body SW potential used by GULP are shown in **Table 295**. The parameters for the three-body SW potential used by GULP are shown in **Table 296**. Some representative parameters for the SW potential used by LAMMPS are listed in **Table 297**.

We use LAMMPS to perform MD simulations for the mechanical behavior of the single-layer 1T-HfS₂ under uniaxial tension at 1 and 300 K. **Figure 147** shows the stress-strain curve for the tension of a single-layer 1T-HfS₂ of dimension $100 \times 100 \text{ \AA}$. Periodic boundary conditions are applied in both armchair and zigzag directions. The single-layer 1T-HfS₂ is stretched uniaxially along the armchair or zigzag direction. The stress is calculated without involving the actual thickness of the quasi-two-dimensional structure of the single-layer 1T-HfS₂. The Young's modulus can be obtained by a linear fitting of the stress-strain relation in the small strain range of [0, 0.01]. The Young's modulus is 73.3 and 72.9 N/m along the armchair and zigzag

VFF type	Bond stretching	Angle bending	
Expression	$\frac{1}{2}K_{\text{Hf-S}}(\Delta r)^2$	$\frac{1}{2}K_{\text{Hf-S-S}}(\Delta\theta)^2$	$\frac{1}{2}K_{\text{S-Hf-Hf}}(\Delta\theta)^2$
Parameter	7.930	4.283	4.283
r_0 or θ_0	2.550	91.078	91.078

The second line gives an explicit expression for each VFF term. The third line is the force constant parameters. Parameters are in the unit of eV/ \AA^2 for the bond stretching interaction and in the unit of eV for the angle bending interaction. The fourth line gives the initial bond length (in the unit of \AA) for the bond stretching interaction and the initial angle (in the unit of degrees) for the angle bending interaction. The angle θ_{ijk} has atom i as the apex.

Table 294. The VFF model for single-layer 1T-HfS₂.

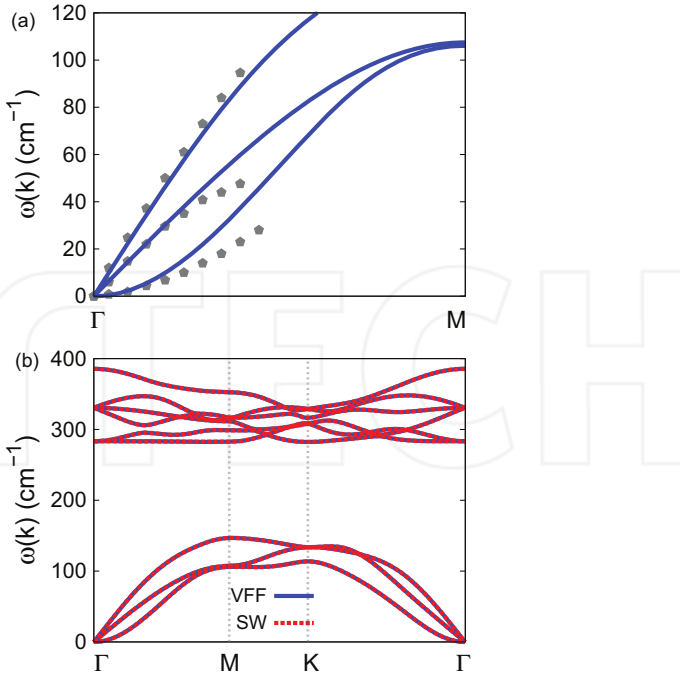


Figure 146. Phonon spectrum for single-layer 1T-HfS₂. (a) Phonon dispersion along the Γ M direction in the Brillouin zone. The results from the VFF model (lines) are comparable with the experiment data (pentagons) from Ref. [38]. (b) The phonon dispersion from the SW potential is exactly the same as that from the VFF model.

	A (eV)	ρ (Å)	B (Å ⁴)	r_{\min} (Å)	r_{\max} (Å)
Hf-S	7.917	1.407	21.141	0.0	3.497

Table 295. Two-body SW potential parameters for single-layer 1T-HfS₂ used by GULP [8] as expressed in Eq. (3).

	K (eV)	θ_0 (°)	ρ_1 (Å)	ρ_2 (Å)	$r_{\min 12}$ (Å)	$r_{\max 12}$ (Å)	$r_{\min 13}$ (Å)	$r_{\max 13}$ (Å)	$r_{\min 23}$ (Å)	$r_{\max 23}$ (Å)
$\theta_{\text{Hf-S-S}}$ (Å)	41.798	91.078	1.407	1.407	0.0	3.497	0.0	3.497	0.0	4.973
$\theta_{\text{S-Hf-Hf}}$ (Å)	41.798	91.078	1.407	1.407	0.0	3.497	0.0	3.497	0.0	4.973

The angle θ_{ijk} in the first line indicates the bending energy for the angle with atom i as the apex.

Table 296. Three-body SW potential parameters for single-layer 1T-HfS₂ used by GULP [8] as expressed in Eq. (4).

	ϵ (eV)	σ (Å)	a	λ	γ	$\cos \theta_0$	A_L	B_L	p	q	Tol
Hf-S-S	1.000	1.407	2.485	41.798	1.000	-0.019	7.917	5.394	4	0	0.0
S-Hf-Hf	1.000	1.407	2.485	41.798	1.000	-0.019	7.917	5.394	4	0	0.0

Table 297. SW potential parameters for single-layer 1T-HfS₂ used by LAMMPS [9] as expressed in Eqs. (9) and (10).

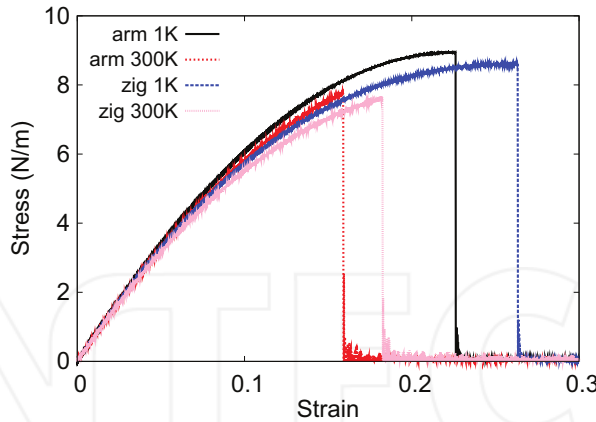


Figure 147. Stress-strain for single-layer 1T-HfS₂ of dimension 100 × 100 Å along the armchair and zigzag directions.

directions, respectively. The Young's modulus is essentially isotropic in the armchair and zigzag directions. These values are close to the *ab initio* results at 0 K temperature, e.g., 79.86 N/m in Ref. [53]. The Poisson's ratio from the VFF model and the SW potential is $\nu_{xy} = \nu_{yx} = 0.16$, which agrees reasonably with the *ab initio* result [54] of 0.19.

There is no available value for nonlinear quantities in the single-layer 1T-HfS₂. We have thus used the nonlinear parameter $B = 0.5d^4$ in Eq. (5), which is close to the value of B in most materials. The value of the third-order nonlinear elasticity D can be extracted by fitting the stress-strain relation to the function $\sigma = E\epsilon + \frac{1}{2}D\epsilon^2$ with E as the Young's modulus. The values of D from the present SW potential are -280.9 and -317.2 N/m along the armchair and zigzag directions, respectively. The ultimate stress is about 8.9 N/m at the ultimate strain of 0.22 in the armchair direction at the low temperature of 1 K. The ultimate stress is about 8.6 N/m at the ultimate strain of 0.26 in the zigzag direction at the low temperature of 1 K.

75. 1T-HfSe₂

Most existing theoretical studies on the single-layer 1T-HfSe₂ are based on the first-principles calculations. In this section, we will develop the SW potential for the single-layer 1T-HfSe₂.

The structure for the single-layer 1T-HfSe₂ is shown in **Figure 71** (with M=Hf and X=Se). Each Hf atom is surrounded by six Se atoms. These Se atoms are categorized into the top group (e.g., atoms 1, 3, and 5) and bottom group (e.g., atoms 2, 4, and 6). Each Se atom is connected to three Hf atoms. The structural parameters are from the first-principles calculations [51], including the lattice constant $a = 3.673$ Å and the position of the Se atom with respect to the Hf atomic plane $h = 1.575$ Å. The resultant angles are $\theta_{\text{HfSeSe}} = 88.093^\circ$ with S atoms from the same (top or bottom) group and $\theta_{\text{SeHfHf}} = 88.093^\circ$.

Table 298 shows three VFF terms for the single-layer 1T-HfSe₂; one of which is the bond stretching interaction shown by Eq. (1), while the other two terms are the angle bending interaction shown by Eq. (2). We note that the angle bending term $K_{\text{Hf}-\text{Se}-\text{Se}}$ is for the angle $\theta_{\text{Hf}-\text{Se}-\text{Se}}$ with both Se atoms from the same (top or bottom) group. These force constant parameters are determined by fitting to the three acoustic branches in the phonon dispersion along the Γ M as shown in **Figure 148(a)**. The *ab initio* calculations for the phonon dispersion are from Ref. [50]. Similar phonon dispersion can also be found in other *ab initio*

VFF type	Bond stretching	Angle bending	
Expression	$\frac{1}{2} K_{\text{Hf}-\text{Se}}(\Delta r)^2$	$\frac{1}{2} K_{\text{Hf}-\text{Se}-\text{Se}}(\Delta\theta)^2$	$\frac{1}{2} K_{\text{Se}-\text{Hf}-\text{Hf}}(\Delta\theta)^2$
Parameter	7.930	4.283	4.283
r_0 or θ_0	2.642	88.093	88.093

The second line gives an explicit expression for each VFF term. The third line is the force constant parameters. Parameters are in the unit of eV/Å² for the bond stretching interaction and in the unit of eV for the angle bending interaction. The fourth line gives the initial bond length (in the unit of Å) for the bond stretching interaction and the initial angle (in the unit of degrees) for the angle bending interaction. The angle θ_{ijk} has atom i as the apex.

Table 298. The VFF model for single-layer 1T-HfSe₂.

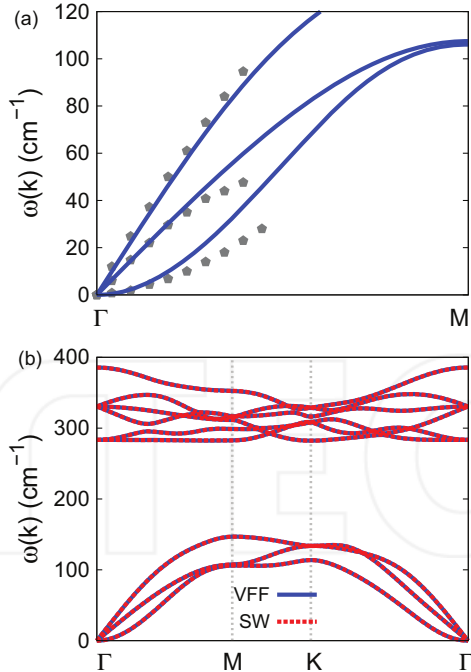


Figure 148. Phonon spectrum for single-layer 1T-HfSe₂. (a) Phonon dispersion along the Γ M direction in the Brillouin zone. The results from the VFF model (lines) are comparable with the experiment data (pentagons) from Ref. [50]. (b) The phonon dispersion from the SW potential is exactly the same as that from the VFF model.

calculations [34]. **Figure 148(b)** shows that the VFF model and the SW potential give exactly the same phonon dispersion, as the SW potential is derived from the VFF model.

The parameters for the two-body SW potential used by GULP are shown in **Table 299**. The parameters for the three-body SW potential used by GULP are shown in **Table 300**. Some representative parameters for the SW potential used by LAMMPS are listed in **Table 301**.

We use LAMMPS to perform MD simulations for the mechanical behavior of the single-layer 1T-HfSe₂ under uniaxial tension at 1 and 300 K. **Figure 149** shows the stress-strain curve for the tension of a single-layer 1T-HfSe₂ of dimension 100 × 100 Å. Periodic boundary conditions are applied in both armchair and zigzag directions. The single-layer 1T-HfSe₂ is stretched uniaxially along the armchair or zigzag direction. The stress is calculated without involving the actual thickness of the quasi-two-dimensional structure of the single-layer 1T-HfSe₂. The Young's modulus can be obtained by a linear fitting of the stress-strain relation in the small strain range of [0, 0.01]. The Young's modulus is 67.3 and 67.0 N/m along the armchair and zigzag directions, respectively. The Young's modulus is essentially isotropic in the armchair and zigzag directions. The Poisson's ratio from the VFF model and the SW potential is $\nu_{xy} = \nu_{yx} = 0.18$.

There is no available value for nonlinear quantities in the single-layer 1T-HfSe₂. We have thus used the nonlinear parameter $B = 0.5d^4$ in Eq. (5), which is close to the value of B in most materials. The value of the third-order nonlinear elasticity D can be extracted by fitting the stress-strain relation to the function $\sigma = E\epsilon + \frac{1}{2}D\epsilon^2$ with E as the Young's modulus. The values of D from the present SW potential are -221.5 and -258.6 N/m along the armchair and zigzag directions, respectively. The ultimate stress is about 9.0 N/m at the ultimate strain of 0.24 in the

	A (eV)	ρ (Å)	B (Å ⁴)	r_{\min} (Å)	r_{\max} (Å)
Hf—Se	7.871	1.341	24.361	0.0	3.583

Table 299. Two-body SW potential parameters for single-layer 1T-HfSe₂ used by GULP [8] as expressed in Eq. (3).

	K (eV)	θ_0 (°)	ρ_1 (Å)	ρ_2 (Å)	$r_{\min 12}$ (Å)	$r_{\max 12}$ (Å)	$r_{\min 13}$ (Å)	$r_{\max 13}$ (Å)	$r_{\min 23}$ (Å)	$r_{\max 23}$ (Å)
$\theta_{\text{Hf—Se—Se}}$	37.039	88.093	1.341	1.341	0.0	3.583	0.0	3.583	0.0	5.018
$\theta_{\text{Se—Hf—Hf}}$	37.039	88.093	1.341	1.341	0.0	3.583	0.0	3.583	0.0	5.018

The angle θ_{ijk} in the first line indicates the bending energy for the angle with atom i as the apex.

Table 300. Three-body SW potential parameters for single-layer 1T-HfSe₂ used by GULP [8] as expressed in Eq. (4).

	ϵ (eV)	σ (Å)	a	λ	γ	$\cos \theta_0$	A_L	B_L	p	q	Tol
Hf—Se—Se	1.000	1.341	2.672	37.039	1.000	0.033	7.871	7.533	4	0	0.0
Se—Hf—Hf	1.000	1.341	2.672	37.039	1.000	0.033	7.871	7.533	4	0	0.0

Table 301. SW potential parameters for single-layer 1T-HfSe₂ used by LAMMPS [9] as expressed in Eqs. (9) and (10).

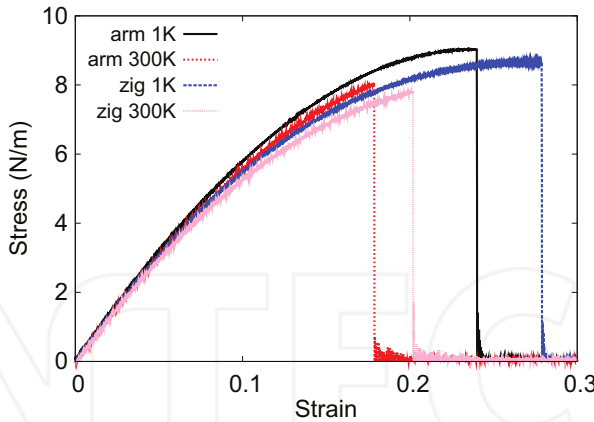


Figure 149. Stress-strain for single-layer 1T-HfSe₂ of dimension 100 × 100 Å along the armchair and zigzag directions.

armchair direction at the low temperature of 1 K. The ultimate stress is about 8.7 N/m at the ultimate strain of 0.28 in the zigzag direction at the low temperature of 1 K.

76. 1T-HfTe₂

Most existing theoretical studies on the single-layer 1T-HfTe₂ are based on the first-principles calculations. In this section, we will develop the SW potential for the single-layer 1T-HfTe₂.

The structure for the single-layer 1T-HfTe₂ is shown in **Figure 71** (with M = Hf and X = Te). Each Hf atom is surrounded by six Te atoms. These Te atoms are categorized into the top group (e.g., atoms 1, 3, and 5) and bottom group (e.g., atoms 2, 4, and 6). Each Te atom is connected to three Hf atoms. The structural parameters are from the first-principles calculations [48], including the lattice constant $a = 3.9606 \text{ \AA}$ and the bond length $d_{\text{Hf}-\text{Te}} = 2.8559 \text{ \AA}$, which are derived from the angle $\theta_{\text{TeHfHf}} = 87.8^\circ$. The other angle is $\theta_{\text{HfTeTe}} = 87.8^\circ$ with Te atoms from the same (top or bottom) group.

Table 302 shows three VFF terms for the single-layer 1T-HfTe₂; one of which is the bond stretching interaction shown by Eq. (1), while the other two terms are the angle bending interaction shown by Eq. (2). We note that the angle bending term $K_{\text{Hf}-\text{Te}-\text{Te}}$ is for the angle $\theta_{\text{Hf}-\text{Te}-\text{Te}}$ with both Te atoms from the same (top or bottom) group. We find that there are actually only two parameters in the VFF model, so we can determine their value by fitting to the Young's modulus and the Poisson's ratio of the system. The *ab initio* calculations have predicted the Young's modulus to be 50 N/m and the Poisson's ratio as 0.10 [48].

The parameters for the two-body SW potential used by GULP are shown in **Table 303**. The parameters for the three-body SW potential used by GULP are shown in **Table 304**. Some representative parameters for the SW potential used by LAMMPS are listed in **Table 305**.

VFF type	Bond stretching	Angle bending	
Expression	$\frac{1}{2} K_{\text{Hf}-\text{Te}}(\Delta r)^2$	$\frac{1}{2} K_{\text{Hf}-\text{Te}-\text{Te}}(\Delta \theta)^2$	$\frac{1}{2} K_{\text{Te}-\text{Hf}-\text{Hf}}(\Delta \theta)^2$
Parameter	3.328	3.877	3.877
r_0 or θ_0	2.856	87.801	87.801

The second line gives an explicit expression for each VFF term. The third line is the force constant parameters. Parameters are in the unit of $\text{eV}/\text{\AA}^2$ for the bond stretching interaction and in the unit of eV for the angle bending interaction. The fourth line gives the initial bond length (in the unit of \AA) for the bond stretching interaction and the initial angle (in the unit of degrees) for the angle bending interaction. The angle θ_{ijk} has atom i as the apex.

Table 302. The VFF model for single-layer 1T-HfTe₂.

	A (eV)	ρ (\AA)	B (\AA^4)	r_{\min} (\AA)	r_{\max} (\AA)
Hf—Te	3.835	1.439	33.262	0.0	3.869

Table 303. Two-body SW potential parameters for single-layer 1T-HfTe₂ used by GULP [8] as expressed in Eq. (3).

	K (eV)	θ_0 (°)	ρ_1 (\AA)	ρ_2 (\AA)	$r_{\min 12}$ (\AA)	$r_{\max 12}$ (\AA)	$r_{\min 13}$ (\AA)	$r_{\max 13}$ (\AA)	$r_{\min 23}$ (\AA)	$r_{\max 23}$ (\AA)
$\theta_{\text{Hf}-\text{Te}-\text{Te}}$	33.196	87.801	1.439	1.439	0.0	3.869	0.0	3.869	0.0	5.410
$\theta_{\text{Te}-\text{Hf}-\text{Hf}}$	33.196	87.801	1.439	1.439	0.0	3.869	0.0	3.869	0.0	5.410

The angle θ_{ijk} in the first line indicates the bending energy for the angle with atom i as the apex.

Table 304. Three-body SW potential parameters for single-layer 1T-HfTe₂ used by GULP [8] as expressed in Eq. (4).

	ϵ (eV)	σ (\AA)	a	λ	γ	$\cos \theta_0$	A_L	B_L	p	q	Tol
Hf—Te ₁ —Te ₁	1.000	1.439	2.690	33.196	1.000	0.038	3.835	7.764	4	0	0.0

Table 305. SW potential parameters for single-layer 1T-HfTe₂ used by LAMMPS [9] as expressed in Eqs. (9) and (10).

We use LAMMPS to perform MD simulations for the mechanical behavior of the single-layer 1T-HfTe₂ under uniaxial tension at 1 and 300 K. **Figure 150** shows the stress-strain curve for the tension of a single-layer 1T-HfTe₂ of dimension $100 \times 100 \text{\AA}$. Periodic boundary conditions are applied in both armchair and zigzag directions. The single-layer 1T-HfTe₂ is stretched uniaxially along the armchair or zigzag direction. The stress is calculated without involving the actual thickness of the quasi-two-dimensional structure of the single-layer 1T-HfTe₂. The Young's modulus can be obtained by a linear fitting of the stress-strain relation in the small strain range of [0, 0.01]. The Young's modulus is 43.1 N/m along the armchair and zigzag directions. The Poisson's ratio from the VFF model and the SW potential is $\nu_{xy} = \nu_{yx} = 0.10$. The fitted Young's modulus value is about 10% smaller than the *ab initio* result of 50 N/m [48], as only short-range interactions are considered in the present work. The long-range interactions are ignored, which typically lead to about 10% underestimation for the value of the Young's modulus.

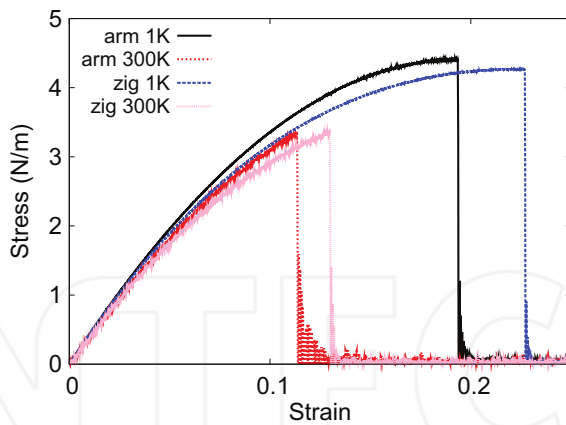


Figure 150. Stress-strain for single-layer 1T-HfTe₂ of dimension 100 × 100 Å along the armchair and zigzag directions.

There is no available value for nonlinear quantities in the single-layer 1T-HfTe₂. We have thus used the nonlinear parameter $B = 0.5d^4$ in Eq. (5), which is close to the value of B in most materials. The value of the third-order nonlinear elasticity D can be extracted by fitting the stress-strain relation to the function $\sigma = E\epsilon + \frac{1}{2}D\epsilon^2$ with E as the Young's modulus. The values of D from the present SW potential are -204.3 and -220.7 N/m along the armchair and zigzag directions, respectively. The ultimate stress is about 4.4 N/m at the ultimate strain of 0.19 in the armchair direction at the low temperature of 1 K. The ultimate stress is about 4.3 N/m at the ultimate strain of 0.22 in the zigzag direction at the low temperature of 1 K.

Figure 151 shows that the VFF model and the SW potential give exactly the same phonon dispersion, as the SW potential is derived from the VFF model.

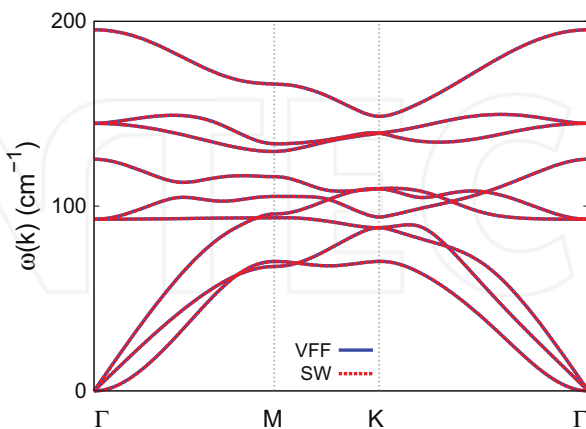


Figure 151. Phonon spectrum for single-layer 1T-HfTe₂ along the Γ -M-K- Γ direction in the Brillouin zone. The phonon dispersion from the SW potential is exactly the same as that from the VFF model.

77. 1T-TaS₂

Most existing theoretical studies on the single-layer 1T-TaS₂ are based on the first-principles calculations. In this section, we will develop the SW potential for the single-layer 1T-TaS₂.

The structure for the single-layer 1T-TaS₂ is shown in **Figure 71** (with M=Ta and X=S). Each Ta atom is surrounded by six S atoms. These S atoms are categorized into the top group (e.g., atoms 1, 3, and 5) and bottom group (e.g., atoms 2, 4, and 6). Each S atom is connected to three Ta atoms. The structural parameters are from the first-principles calculations [48], including the lattice constant $a = 3.3524 \text{ \AA}$ and the bond length $d_{\text{Ta-S}} = 2.4578 \text{ \AA}$, which are derived from the angle $\theta_{\text{STA} \text{Ta}} = 86^\circ$. The other angle is $\theta_{\text{TASS}} = 86^\circ$ with S atoms from the same (top or bottom) group.

Table 306 shows three VFF terms for the single-layer 1T-TaS₂; one of which is the bond stretching interaction shown by Eq. (1), while the other two terms are the angle bending interaction shown by Eq. (2). We note that the angle bending term $K_{\text{Ta-S-S}}$ is for the angle $\theta_{\text{Ta-S-S}}$ with both S atoms from the same (top or bottom) group. We find that there are actually only two parameters in the VFF model, so we can determine their value by fitting to the Young's modulus and the Poisson's ratio of the system. The *ab initio* calculations have predicted the Young's modulus to be 101 N/m and the Poisson's ratio as 0.20 [48].

The parameters for the two-body SW potential used by GULP are shown in **Table 307**. The parameters for the three-body SW potential used by GULP are shown in **Table 308**. Some representative parameters for the SW potential used by LAMMPS are listed in **Table 309**.

We use LAMMPS to perform MD simulations for the mechanical behavior of the single-layer 1T-TaS₂ under uniaxial tension at 1 and 300 K. **Figure 152** shows the stress-strain curve for the tension of a single-layer 1T-TaS₂ of dimension 100 × 100 Å. Periodic boundary conditions are applied in both armchair and zigzag directions. The single-layer 1T-TaS₂ is stretched uniaxially

VFF type	Bond stretching	Angle bending	
Expression	$\frac{1}{2}K_{\text{Ta-S}}(\Delta r)^2$	$\frac{1}{2}K_{\text{Ta-S-S}}(\Delta\theta)^2$	$\frac{1}{2}K_{\text{S-Ta-Ta}}(\Delta\theta)^2$
Parameter	11.192	4.774	4.774
r_0 or θ_0	2.458	85.999	85.999

The second line gives an explicit expression for each VFF term. The third line is the force constant parameters. Parameters are in the unit of eV/Å² for the bond stretching interaction and in the unit of eV for the angle bending interaction. The fourth line gives the initial bond length (in the unit of Å) for the bond stretching interaction and the initial angle (in the unit of degrees) for the angle bending interaction. The angle θ_{ijk} has atom *i* as the apex.

Table 306. The VFF model for single-layer 1T-TaS₂.

	A (eV)	ρ (Å)	B (Å ⁴)	r_{\min} (Å)	r_{\max} (Å)
Ta-S	9.110	1.174	18.246	0.0	3.307

Table 307. Two-body SW potential parameters for single-layer 1T-TaS₂ used by GULP [8] as expressed in Eq. (3).

	K (eV)	θ_0 ($^\circ$)	ρ_1 (\AA)	ρ_2 (\AA)	$r_{\min 12}$ (\AA)	$r_{\max 12}$ (\AA)	$r_{\min 13}$ (\AA)	$r_{\max 13}$ (\AA)	$r_{\min 23}$ (\AA)	$r_{\max 23}$ (\AA)
$\theta_{\text{Ta-S-S}}$	38.092	85.999	1.174	1.174	0.0	3.307	0.0	3.307	0.0	4.579
$\theta_{\text{S-Ta-Ta}}$	38.092	85.999	1.174	1.174	0.0	3.307	0.0	3.307	0.0	4.579

The angle θ_{ijk} in the first line indicates the bending energy for the angle with atom i as the apex.

Table 308. Three-body SW potential parameters for single-layer 1T-TaS₂ used by GULP [8] as expressed in Eq. (4).

	ϵ (eV)	σ (\AA)	a	λ	γ	$\cos \theta_0$	A_L	B_L	p	q	Tol
Ta—S ₁ —S ₁	1.000	1.174	2.816	38.092	1.000	0.070	9.110	9.589	4	0	0.0

Table 309. SW potential parameters for single-layer 1T-TaS₂ used by LAMMPS [9] as expressed in Eqs. (9) and (10).

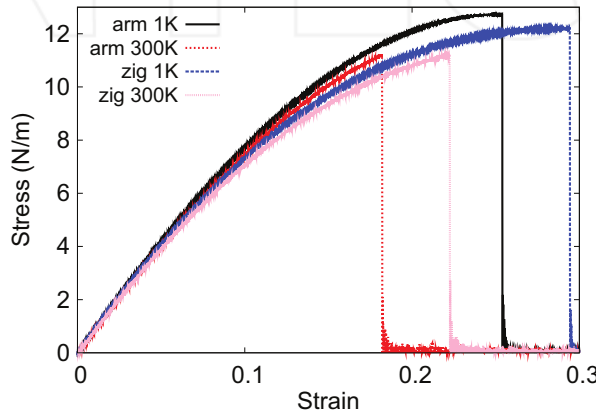


Figure 152. Stress-strain for single-layer 1T-TaS₂ of dimension $100 \times 100 \text{ \AA}$ along the armchair and zigzag directions.

along the armchair or zigzag direction. The stress is calculated without involving the actual thickness of the quasi-two-dimensional structure of the single-layer 1T-TaS₂. The Young's modulus can be obtained by a linear fitting of the stress-strain relation in the small strain range of [0, 0.01]. The Young's modulus is 87.8 and 87.4 N/m along the armchair and zigzag directions, respectively. The Young's modulus is essentially isotropic in the armchair and zigzag directions. The Poisson's ratio from the VFF model and the SW potential is $\nu_{xy} = \nu_{yz} = 0.20$. The fitted Young's modulus value is about 10% smaller than the *ab initio* result of 101 N/m [48], as only short-range interactions are considered in the present work. The long-range interactions are ignored, which typically lead to about 10% underestimation for the value of the Young's modulus.

There is no available value for nonlinear quantities in the single-layer 1T-TaS₂. We have thus used the nonlinear parameter $B = 0.5d^4$ in Eq. (5), which is close to the value of B in most materials. The value of the third-order nonlinear elasticity D can be extracted by fitting the